DESIGN AND SYNTHESIS OF TRIAZENE AND INDOLE-SUBSTITUTED PUSH–PULL CHROMOPHORES VIA CLICK-TYPE TRANSFORMATIONS: EFFECTS OF DONOR GROUPS ON THE OPTOELECTRONIC PROPERTIES

A THESIS SUBMITTED TO
THE GRADUATE SCHOOL OF NATURAL AND APPLIED SCIENCES
OF
MIDDLE EAST TECHNICAL UNIVERSITY

BY

KÜBRA ERDEN

IN PARTIAL FULFILLMENT OF THE REQUIREMENTS
FOR
THE DEGREE OF MASTER OF SCIENCE
IN
CHEMISTRY

JULY 2021

ABSTRACT

DESIGN AND SYNTHESIS OF TRIAZENE AND INDOLE-SUBSTITUTED PUSH–PULL CHROMOPHORES VIA CLICK-TYPE TRANSFORMATIONS: EFFECTS OF DONOR GROUPS ON THE OPTOELECTRONIC PROPERTIES

Erden, Kübra
Master of Science, Chemistry
Supervisor : Assist. Prof. Dr. Çağatay Dengiz

July 2021, 181 pages

Conjugated materials play an indispensable role in daily life due to their extraordinary properties and applications. Of particular interest are the donor–acceptor-type push–pull chromophores since they have already been utilized in many advanced applications such as organic light emitting diodes (OLEDs), organic field effect transistors (OFETs), dye-synthesized solar cells (DSSCs), and non-linear optical (NLO) devices. The thermal [2+2] cycloaddition reactions are chemical transformations that we will study in detail in this thesis to access triazene-substituted homoconjugated push–pull chromophores. Moreover, the formal [2+2] cycloaddition-retroelectrocyclization transformations were utilized for the preparation of the indole-substituted push–pull systems. The optoelectronic properties of the chromophores will be explored by UV/Vis spectroscopy and computational analysis.

Keywords: [2+2] CA-RE, Push–Pull Chromophores, Triazene, Indole

ÖZ

TRİAZEN VE İNDOL GRUPLARI İÇEREN İT–ÇEK-TİPİ KROMOFORLARIN KLİK-TİPİ DÖNÜŞÜMLER İLE TASARIMI VE SENTEZİ: DONÖR GRUPLARININ OPTOELEKTRONİK ÖZELLİKLER ÜZERİNE ETKİLERİ

Erden, Kübra
Yüksek Lisans, Kimya
Tez Yöneticisi: Assist. Prof. Dr. Çağatay Dengiz

Temmuz 2021, 181 sayfa

Konjuge malzemeler olağanüstü özellikleri ve uygulamaları nedeniyle günlük hayatta vazgeçilmez bir rol oynamaktadır. Özellikle ilgi çekici olan donör–akseptör-tipi it–çek kromoforları organik ışık yayan diyotlar (OLEDler), organik alan etkili transistörler (OFETler), boyaya duyarlı güneş pilleri (DSSCler) ve doğrusal olmayan optik (NLO) cihazlar gibi birçok gelişmiş uygulamada kullanılmaktadır. Termal [2+2] siklokatılma tepkimeleri, bu tezde triazen grupları içeren homokonjüge it–çek kromoforlara erişmek için detaylı olarak inceleyeceğimiz kimyasal dönüşümlerdir. Ayrıca, [2+2] siklokatılma-retroelektrosiklizasyon dönüşümleri, indol içeren it–çek sistemlerinin hazırlanmasında kullanıldı. Kromoforların optoelektronik özellikleri UV/Vis spektroskopisi ve hesaplamalı kimya kullanılarak araştırılacaktır.

Anahtar Kelimeler: [2+2] CA-RE, İt-Çek Kromofor, Triazen, İndol

To my mother and people who stand against injustice and oppression

ACKNOWLEDGMENTS

I would like to express my deepest gratitude, Assist. Prof. Dr. Çağatay Dengiz, for his guidance and invaluable advice during my research. I am also truly grateful for his moral support and for enlightening my professional and academic vision throughout my work.

I would like to thank my labmates; A. Semin Özsinan, Aslıcan Şimşek, Fevzi Can İnyurt, F. Melih Günay, İpek Öktem, Hazal Kayaş for their friendship. It was a real pleasure working with each of you.

I special thank my labmate İpek Savaş for her friendship from the beginning. We had a great time together and shared so many memories.

I would also like to thank my friends Başak Karagöllü and Flora Mammadova for their contributions during my thesis writing process.

I would like to thank my friends Berrin Ayyıldız, Deniz Şen Kardelen, Gülsüm Güneş for their precious friendship.

I cannot thank enough my sisters, Dr. Emine Erden and Dr. Özlem Erden Başaran, for encouraging me whenever I need and for believing in me when I did not even believe in myself.

This thesis study is funded by Scientific and Technological Research Council of Turkey under grant number TUBITAK 119C005 and TUBITAK 218Z126 and also supported by Scientific Research Projects Coordination (BAP -TEZ-YL 103-2021-10598).

Last but certainly not the least, I would like to give the biggest thanks my family for their endless and unconditional love, throughout my whole life. I could not have done this without them.

TABLE OF CONTENTS

LIST OF TABLES

TABLES

LIST OF FIGURES

FIGURES

LIST OF ABBREVIATIONS

ABBREVIATIONS

CA:	Cycloaddition
CA-RE:	Cycloaddition–Retroelectrocyclization
CPCM:	Conductor-like Polarizable Continuum Model
DFT:	Density functional theory
DDQ:	2,3-Dichloro-5,6-dicyano-1,4-benzoquinone
EDG:	Electron donating group
ICT:	Intramolecular charge-transfer
IR:	Infrared spectroscopy
J:	Coupling constant
MHz:	Megahertz
M.p.:	Melting point
NMR:	Nuclear magnetic resonance
TD-DFT:	Time-dependent density functional theory
THF:	Tetrahydrofuran
TCNE:	Tetracyanoethylene
TCNQ:	7,7,8,8-Tetracyanoquinodimethane

LIST OF SCHEMES

SCHEMES

CHAPTER 1

INTRODUCTION

Organic electronics, which can be defined as the field dealing with the design, synthesis, characterization, and application of electroactive materials based on conjugated organic compounds, have received considerable attention for the last 50 years.[1,2] Interest in organic electronics stems from conjugated materials' remarkable properties such as high flexibility, easy processing, low fabrication cost, and large-area fabrication.[3] Moreover, organic electronics is highly promising for future resource management. For example, materials used in the organic electronics field can fulfill many commercial product design requirements such as low-energy consumption, replacement of toxic materials, utilization of sustainable resources, and recycling potential.[4] With these all desired features, conjugated organic materials find applications in organic solar cells (OSCs), organic light-emitting diodes (OLEDs), organic photodetectors, and organic sensors.[3] Interest in conjugated molecules have gradually increased in recent years because of their usage in optoelectronic devices.[5]

Organic chemistry plays a crucial role in the design of easily modified conjugated molecules with tailor-made properties. Especially with the developments in recent years, target conjugated structures with desired properties can be synthesized by inexpensive methods. One of the most prominent groups among all conjugated systems are named as π-conjugated donor–acceptor (D–A)-type chromophores. (D–A)-type chromophoric structures also possess high potential in electronic and optoelectronic areas such as fabrications of solar cells and nonlinear optical (NLO) devices.[6] The utilization of conjugated systems in such important areas requires the development of new synthetic methods. Most synthetic methods used to synthesize conjugated molecules and polymers include cross-coupling reactions (Stille, Suzuki, and Heck) that necessitates transition metal catalysts.[7]

Although there are many studies in the literature using these chemical transformations, several drawbacks such as synthetically demanding multi-step syntheses of monomers, instability of organometallic reagents, and low atom-economy have been reported. Moreover, these reactions require large quantities of toxic solvents, relatively long reaction times, and high-cost methods during the purification of the products from by-products and metals. All these negative aspects make such coupling reactions used to synthesize conjugated materials synthetically insufficient.[8] Therefore, it is very important to develop environmentally friendly, atom/cost effective, and short methods that can eliminate or minimize previously mentioned problems in the syntheses of (D–A)-type π-conjugated chromophores to overcome these deficiencies in the literature. At this point, click-type synthetic protocols are coming back to the fore as an alternative method to cross-coupling reactions. The fact that click-type reactions can meet the green chemistry requirements also increase the interest in this field. Even though concepts in green chemistry are not new, such transformations have recently become a hot topic in chemistry with increasing concerns related to environment. Such reactions can take place in environmentally friendly and temperate conditions.[9] All these positive aspects lead to the frequent use of click chemistry in organic chemistry, material science, and drug discovery.[10] The concept of click chemistry was first introduced by K. Barry Sharpless in 2001. [11] Sharpless and his group developed a new set of powerful and selective reactions called click chemistry to create new molecular architectures that can be utilized reliably in different application areas.[11] Click-type reactions are known as chemical transformations with a high thermodynamic driving force (>20 kcal.mol^{-1}), producing a single product with high efficiency from easily accessible starting materials, and reagents. In such reactions, product isolation is generally performed by simple non-chromatographic methods like crystallization since by-products can easily be removed. Click type reactions can be carried out under mild conditions, they are insensitive to oxygen and water and are also compatible with different kinds of benign solvents.[11] All these features gradually increase the importance of click-type reactions in organic syntheses.

1.1 Click type reaction

Increasing demand for the synthesis of new materials that can be used in the field of organic electronics leads scientists to develop easy and effective synthetic strategies. Therefore, several types of click type reactions have emerged.[12] According to the Sharpless and co-workers' classification, some of the click type reactions are:

- Cycloaddition reactions, especially Huisgen 1,3-dipolar cycloaddition and Diels-Alder reaction.[11]
- Nucleophilic substitution reactions like ring-opening reactions of heterocyclic electrophiles (epoxides, aziridines, and aziridinium ions) [11]
- Addition to carbon-carbon multiple bonds such as thiol-ene reaction, dihydroxylation, Michael additions. [11]
- Non-aldol type carbonyl chemistry such as oxime/hydrazone formations [11]

Among all, the most commonly utilized click-type reactions are Huisgen 1,3-dipolar cycloadditions (**3** from **1** and **2**), Diels-Alder cycloadditions (**6** from **4** and **5**), and thiol-ene reactions (**9** from **7** and **8**) since these reactions have high selectivity, fast reaction kinetics, high-yielding transformation, and wide application areas (Scheme 1).[12]

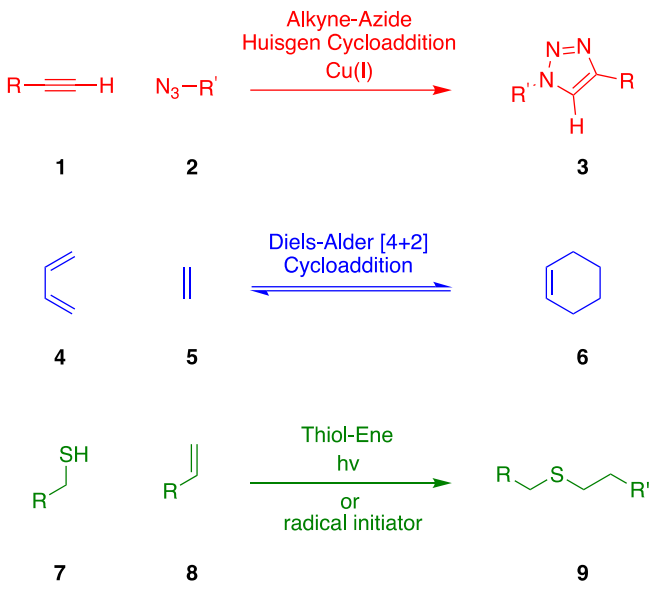

Scheme 1. General representations of click-type reactions.

1.1.1 Azide-Alkyne Huisgen Cycloadditions

Presumably the most well-known click-type reaction is the Huisgen 1.3-dipolar cycloaddition reactions which occur between azides and terminal alkynes to form 1,2,3-triazoles in the presence of copper catalysts. Huisgen introduced the 1,3-dipolar cycloaddition method in 1960 to synthesize a variety of structurally interesting 5-membered heterocyclic compounds.[13] Classical Huisgen 1,3-dipolar cycloadditions can also occur between alkyne **10** and azide **11** at high temperatures without a copper catalyst (Scheme 2).[13] However, these types of Huisgen reactions usually produce mixtures of 1,4 and 1,5-triazole regioisomers **12** and **13** when using asymmetric alkynes.

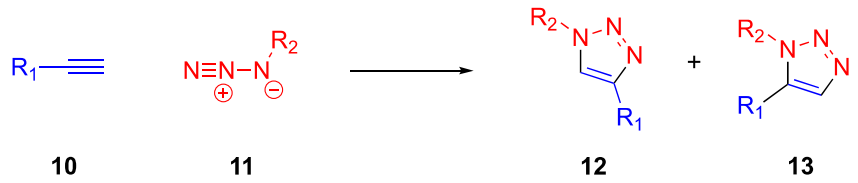

Scheme 2. General representation of Classical Huisgen 1,3-dipolar cycloaddition reactions.

Although the Sharpless' review mentions the 1,3-dipolar cycloadditions as a good candidate for click-type reactions, these reactions cannot fullfill the required conditions for click-type reactions in terms of selectivity.[14] To overcome this issue, Sharpless and co-workers published their first report on copper-catalyzed azide-alkyne cycloadditions (CuAACs) in 2002.[15] This report showed that copper-catalyzed 1,3-dipolar cycloaddition allowed for the formation of only 1,4-disubstituted regioisomer **12** with high efficiency under mild reaction medium (Scheme 3). Accordingly, copper-catalyzed azide-alkyne cycloadditions are accepted as the first catalyzed click-type reaction.[12] The reason behind this is that the copper catalyst is quite benign and inexpensive compared to most other organometallic compounds.[16]

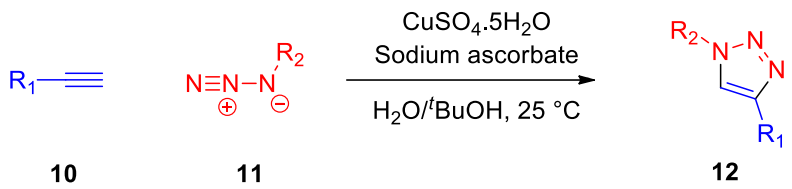

Scheme 3. General representation CuAAC reaction.

In 2005, Sharpless and his group synthesized 1,5-disubstituted 1,2,3-triazole by the same method using ruthenium catalyst instead of copper catalyst. By this way, they showed that ruthenium catalyst is also an effective catalyst to be used in Huisgen reactions.[17] Subsequently, less effective Ni^{2+}, Pd^{2+}, Pt^{2+}, and Au^{+} catalysts were also utilized in Huisgen-type reactions. It is worth noting that the CuAAC's popularity

among other click-type reactions are solvent tolerance and high selectivity.[18] Additionally, these reactions are compatible with several functional groups and can be carried out with different catalysts.[18] After the value of copper-catalyzed Huisgen reactions' recognition in click chemistry field, studies have been directed to understand the mechanism of this transformation. In 2005, mechanistical studies including kinetic studies and density functional theory (DFT) calculations have been reported by Fokin and Finn. Accordingly, a bimetallic reaction mechanism was proposed. While alkynyl group coordinated to the center of a copper(I), azide is attacking to another copper center.[19] Later, in another study of Finn and Fokin, which was reported in 2007, unlike the previous mechanism, a new mechanism was proposed in which the azide group and the alkynyl group are attached to the center of the same copper(I) center (Scheme 4). Experimental and theoretical studies are still ongoing to fully understand the mechanism.[18,20]

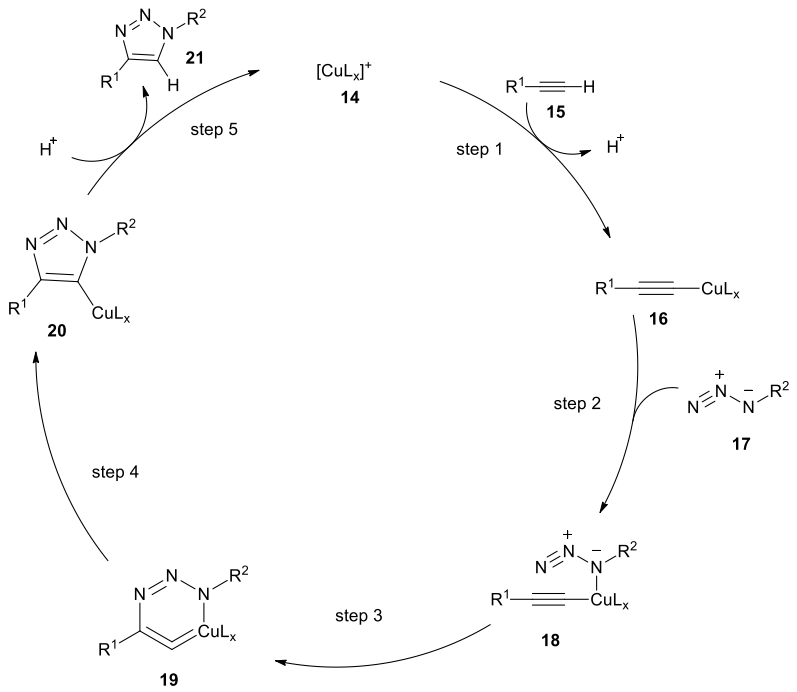

Scheme 4. Mechanism of the Copper-catalyzed azide-alkyne cycloaddition (CuAAC).

1.1.2 Diels-Alder Reactions

Diels-Alder reaction is another family that can be a good fit for click-type transformations according to Sharpless' description of click chemistry in 2001.[11] Unlike recently discovered Huisgen reactions, Diels-Alder reactions were invented by Otto Diels and Kurt Alder in 1928. Diels and Alder characterized the products **24** and **25** formed by the reaction of cyclopentadiene **22** and quinone **23** (Scheme 5).[21] This successful study earned Otto and Kurt the Nobel Prize in 1950.[21]

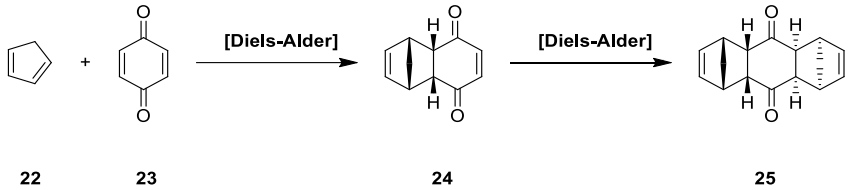

Scheme 5. Discovery of the Diels-Alder reaction

Diels-Alder reactions is now one of the most commonly used synthetic transformations in organic chemistry. These valuable reactions are straightforward [4+2] cycloadditions that occur between an electron-rich diene **26** (4π) and electron-poor dienophiles **27** (2π) to form stable cyclohexenes **28** (Scheme 6).[22]

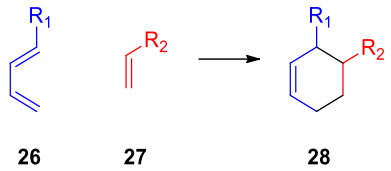

Scheme 6. General representation of Diels-Alder reactions.

In recent years, Diels-Alder reactions received the title of “click-type reaction” with its high efficiency under mild reaction conditions, high-selectivity, stability, and versatility. Similar to Huisgen 1,3-dipolar cycloaddition reactions, Diels-Alder reactions are now evaluated under the category of cycloaddition

reactions in click chemistry world. Diels-Alder reactions take precedence over copper-catalyzed Huisgen 1,3-dipolar cycloaddition reaction due to some of their positive features. The most important advantage of Diels-Alder cycloadditions in comparison to CuAACs is that no catalyst is required to facilitate these transformations.[22] High yields, exceptional selectivities, and short reaction time in water compared to other non-polar solvents make Diels-Alder cycloadditions more favorable compared to other click-type reactions. Another distinctive property of Diels-Alder reactions is thermoreversibility unlike other click reactions.[23] The other features such as biorthogonality, biocompatibility paves the way for use of these reactions in biology-related fields.[24]

1.1.3 Thiol-Ene Reactions

After initiation of click-chemistry concept with the triazole synthesis in 2002, researchers began to more closely investigate other reactions having potential click-type properties.[25] One of such reactions, thiol-ene reaction (also alkene hydrothiolation), was first reported in 1905.[26] However, thiol-ene chemistry started to gain popularity in the early 2000s after the advent of "click chemistry" concept.[25] Thiol-ene reactions are well-associated with click chemistry because they meet many requirements. Firstly, thiol-ene reactions are significantly rapid in environmentally benign solvents even at room temperature and atmospheric pressure. Secondly, thiol-ene reactions produce a single regioselective product in high yields under relatively mild conditions, making them suitable for applications in chemical, biological, physical, and engineering fields. The only negative aspect is requirement of a small amount of catalyst although it is a relatively benign one.[25,27] Thiol-ene reactions can be divided into two sub-groups: thiol-ene radical and thiol-Michael addition reactions.

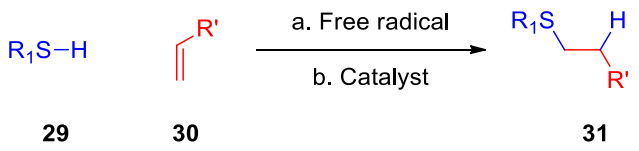

Scheme 7. General representation of thiol-ene reaction.

The first radical-mediated thiol-ene reaction was reported as a click reaction in 2007.[28] These types of thiol-ene reactions occur between electron-rich alkenes (enes) **30** and thiol groups **29** to yield **31** (Scheme 7). The mechanism of thiol-ene radical reactions consists of addition and chain transfer steps (Scheme 8a). Such radical reactions are initiated by heat, light, or radical initiators. After the initiation step, thiyl radical **32** attacks to the carbon-carbon double bond from the least substituted side to form carbon-centered radical. Then, the radical carbon **34** abstracts hydrogen from thiol group to form an anti-Markovnikov product and completes the cycle by regenerating thiyl radical by chain transfer step.[25,29] Radical-mediated thiol-ene reactions are mainly used for post-polymerization modifications.[25] There are several examples showing the utilization of thiol-ene chemistry in the optical and biological applications.[30]

As we mentioned before, thiol-ene click-type reactions are not just restricted to radical reactions, thiol-Michael additions are another group that will be discussed.[21] This efficient synthetic transformation occurs between electron-deficient alkenes and thiol groups. In thiol-Michael addition reactions, a variety of strong bases, metals, and organometallic reagents are required to initiate reactions. Another responsibility of these reagents is the activation of carbon-carbon double bond as catalyst. The mechanism of thiol-Michael reactions is based on nucleophilic addition reaction (Scheme 8b). In the first step, the proton of the thiol group is abstracted by a base (**B**), to form nucleophilic thiolate anion **37**, RS^-. Then, the thiolate anion attacks to the carbon-carbon double bond. Upon generation of a carbon-centered anion **40**, a proton is abstracted from conjugated acid formed in the first step to give a highly efficient thiol-Michael addition product **41**.[13]

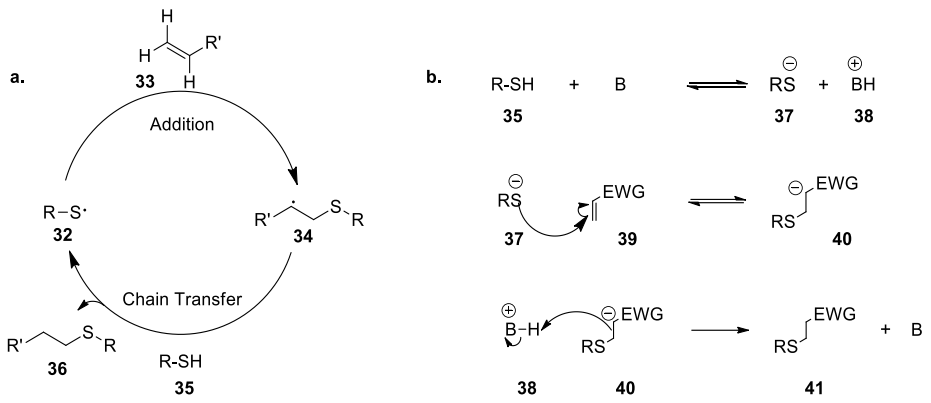

Scheme 8. **a)** Thiol-ene reaction mechanism, **b)** Thiol-Michael addition mechanism.

Similar to the earlier examples, high-yielding nature, high reaction rates under ambient conditions, and the presence of mild catalyst make thiol-Michael additions suitable click-type reactions. All these key properties led thiol-Michael additions to find application in several areas, such as organic synthesis, material chemistry, surface modification, biologically relevant polymer synthesis. [31, 32]

1.2 Click-Type Reactions in Polymer and Dendrimer Synthesis

With the recent advances in the field of click chemistry, several studies have been reported in dendrimer and polymer synthesis.[33] Polymers have intermolecular or interchain π–π interactions like conjugated small organic molecules. These interactions cause a change in the charge carrier mobility which affects the performance in fabricated devices.[34] Thus, structure of polymers has an important effect on determining charge carrying properties.[34] Accordingly, design and synthesis of desired polymer structures has gained great importance in the field of polymer chemistry. However, complex mechanism of polymerization techniques and limited number of substrates are some of the drawbacks of polymerization techniques. Although post-polymerizations have been introduced to the literature to solve these issues, highly efficient coupling reactions are required for successful

post-polymerization transformations. Another issue related to post polymerizations is the limited solubility of polymers. Reactants and polymers to be used in post-functionalizations cannot always be treated in homogenous reaction media. To overcome these issues, click chemistry is a very good alternative in polymer synthesis and modifications due to its high efficiency regardless of the ligand structure in non-homogeneous reaction systems. In recent years, the use of click reactions has increased significantly in material chemistry especially in polymer synthesis because of the above-mentioned advantages.[35] The most commonly used click reactions in polymer syntheses are CuAAC, the Diels–Alder cycloadditions, and the thiol-ene (or -yne) additions.[36] Stable azides and alkynes utilized in the CuAAC can easily be prepared by various simple techniques.[37] Therefore, CuAAC was the first reaction to be adapted widely and effectively in polymer synthesis.[36] Fokin, Finn, and co-workers reported the first example of linear polymer synthesis in 2004.[38] Diazide **42** and dialkyne **43** give polymerization reaction via copper-catalyzed Huisgen 1,3-dipolar cycloaddition (Scheme 9). [38]

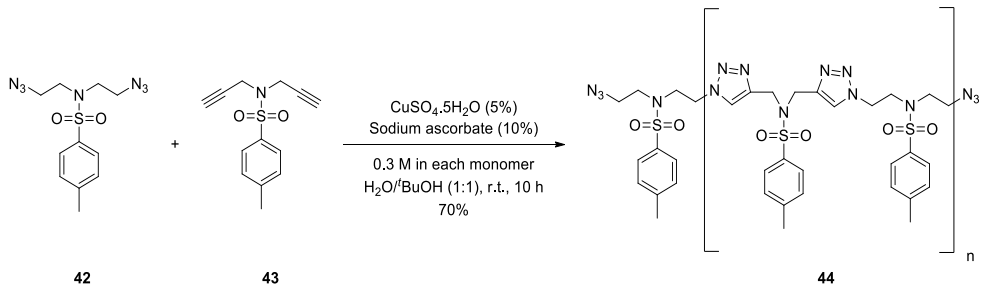

Scheme 9. Solution-phase polymerization by copper-catalyzed azide-alkyne cycloaddition.

As an alternative to CuAAC reactions, Diels-Alder in polymer synthesis also widely used in the literature.[39] Diels-Alder cycloadditions possess more advantages than copper-catalyzed Huisgen 1,3-dipolar cycloadditions in the polymer syntheses since these reactions are catalyst-free and relatively fast.[39] Moreover, Diels-Alder reactions do not require complex reaction conditions and generally provide desired

products without formation of by-products.[24] Thanks to all these features, Diels-Alder reactions have become one of the preferable click reactions in polymer syntheses. Therefore, synthesizing complex macromolecular structures became more convenient by using the Diels-Alder reaction. Recently, Kimura and co-workers synthesized anthracene–maleimide type copolymers **47** by a simple heating method (Scheme 10).[39]

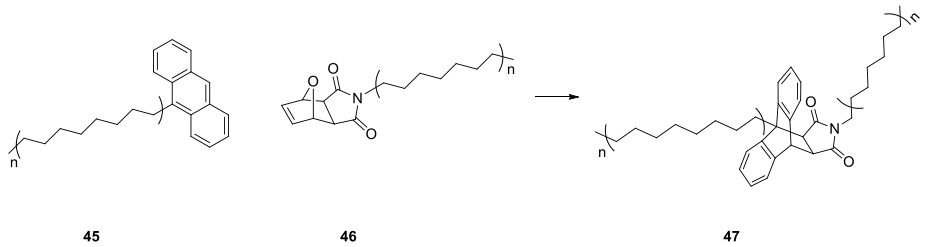

Scheme 10. Synthesis of copolymers via anthracene–maleimide type D-A click reaction.

Click reactions are widely used in dendrimer syntheses as well as in polymer syntheses. Dendrimers are mono disperse 3-dimensional molecules that consist of highly and regularly branched repeating units (Figure 1). Dendrimers generally have a spherical shape of nanometer sizes consisting of branching around the nucleus.[40] Besides common advantages of click-type reactions such as high efficiency and high tolerance to most functional groups, these transformations are very important in dendrimer synthesis because they also function well in sterically hindered environments.[35] Moreover, few reactions are known in dendrimer syntheses providing very high yields and good orthogonality.[16]

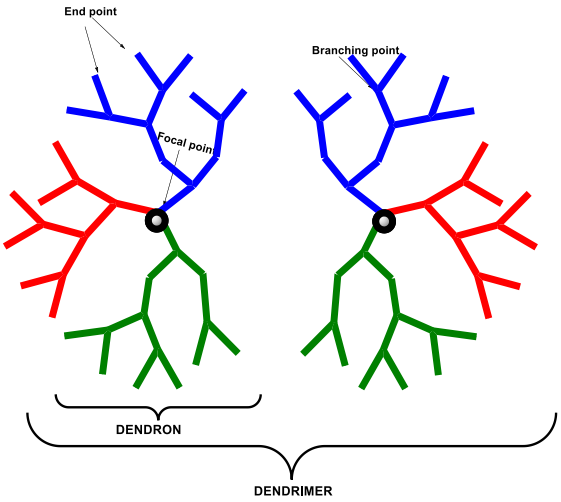

Figure 1. Anatomy of a dendrimer.

Dendrimer was initially discovered in 1978 by Fritz Vogtle using the method called cascade synthesis. In the 1980s, Tomalia's PAMAM dendrimers [41,42] and Newkome's "arborol" systems [43] have attracted great attention. In the 1990s, Frechet firstly reported convergent strategy and revealed its applicability in the nanochemistry field. [44,45] Thus, it has been shown that dendrimers can be utilized in many different fields such as nanotechnology, catalysis, biomedicine, and material science. All these application areas of dendrimers have encouraged scientists to find efficient, atom-economic, and simple synthetic pathways in dendrimer syntheses. At this point, click reactions have become an important concept in dendrimer syntheses as they can provide the desired properties. CuAACs, one of the click-type reactions, have recently been a preferred synthetic strategy in dendrimer synthesis due to short reaction time, versatility, water compatibility, and simple work-up properties.[45] The CuAAC click reaction was first utilized by Hawker and Fokin in the synthesis of triazole dendrimer in 2004 (Scheme 11).[37] Firstly, bistriazole **50** was synthesized in the presence of $CuSO_4$ and sodium carbonate in 1:1 mixture of water and *tert*-butyl alcohol at 25 ^{o}C. Then, primary alkyl chloride **49** was converted to an azide using NaN_3 in acetone/water mixture. Then, bistriazole azide **50** reacts with alkyne again

and the same conversion processes are applied to generate triazole dendrimer (G-2) with chain end groups (R) and internal repeating units (X) (Scheme 11).[46]

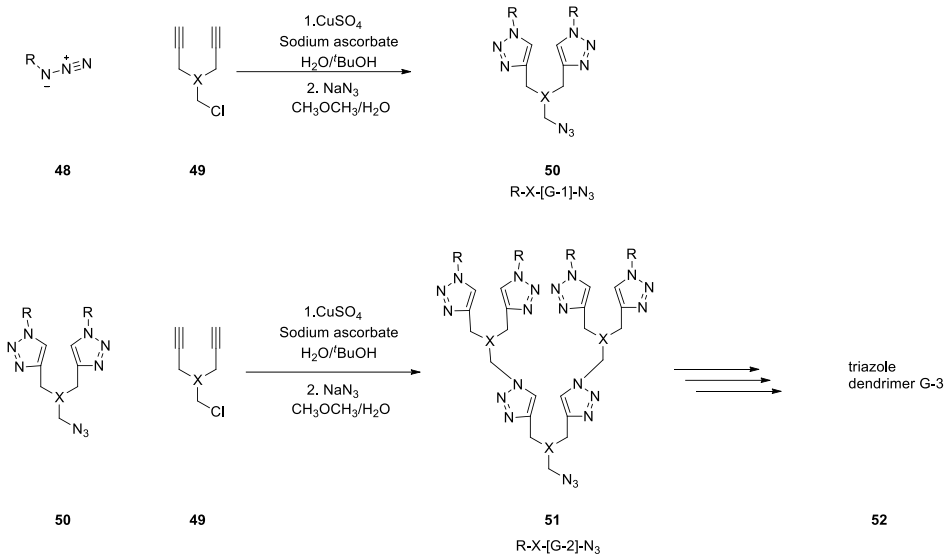

Scheme 11. Synthesis of triazole dendrimer **52**.

Another example, where the Cu-catalyzed Huisgen cycloaddition is used, is reaction between the polyalkynyl molecule **53** and azido sugar **54** in presence of copper catalyst in a homogeneous THF/water mixture (Scheme 12). Three generations of glycodendrimers were synthesized using click chemistry strategy. [45,47]

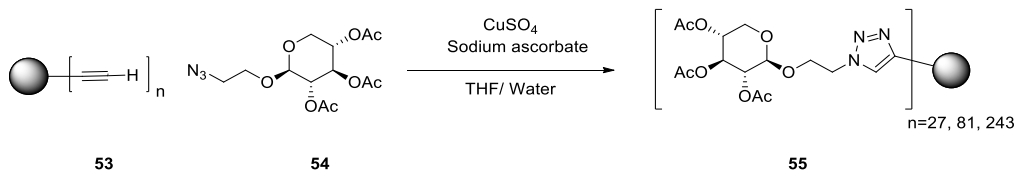

Scheme 12. Synthesis of different generations of glycodendrimer **55**.

Another preferred click reaction in dendrimer syntheses is the thiol-ene reaction. With its insensitivity to water and oxygen and no by-product formation, it has been found application in the dendrimer synthesis.[45] In 2008, Hawker reported

the synthesis of poly(thioether) dendrimers **59** by the reaction between tris-alkene triazine **56** and 1-thioglycerol in the presence of 2,2-dimethoxy-2-phenylacetophenone **57** as a photoinitiator. This reaction occurs in a solvent-free environment without requiring a metal catalyst (Scheme 13).[48]

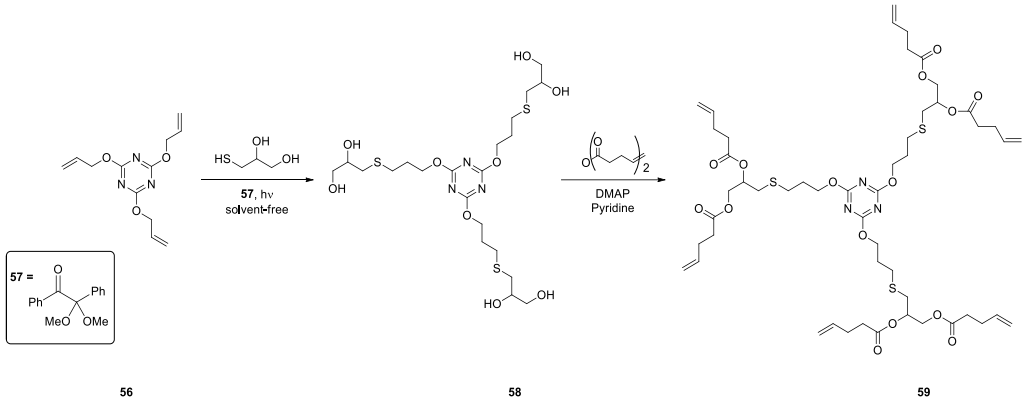

Scheme 13. Synthesis of poly(thioether) dendrimers **59**.

Diels-Alder cycloadditions are another important click-type reaction that has been used in the dendrimer synthesis.[45] In 1997, Diels-Alder reaction was first used in polyphenylene dendrimer synthesis by Müllen and co-workers. In this study, tetraphenylcyclopentadienone **60** and polyphenylacetylene **61** react in diphenyl ether/*a*-methylnaphthalene (l:l) at 180–200 ºC to create 3D rigid dendrimer structure (Scheme 14).[49]

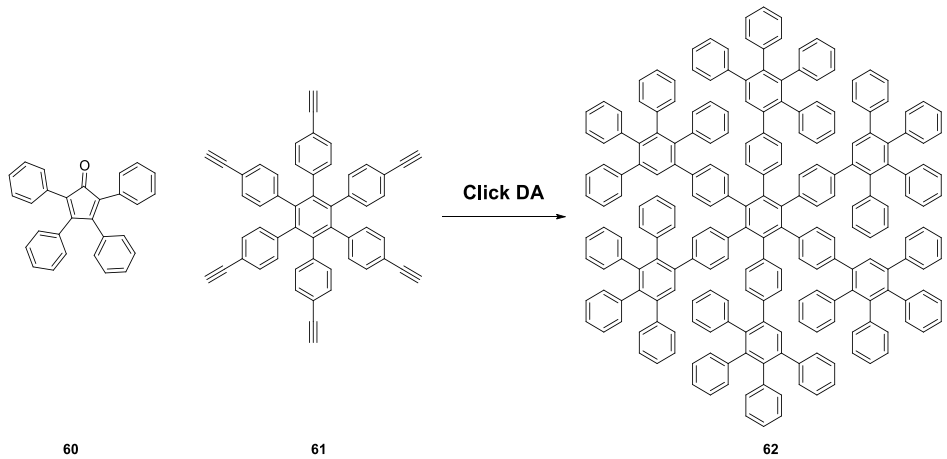

Scheme 14. Synthesis of polyphenylene dendrimer **62**.

In another study, Sanyal and his group successfully synthesized the structure **65** using dendrons **63** and **64** containing furan and maleimide groups respectively (Scheme 15).[50]

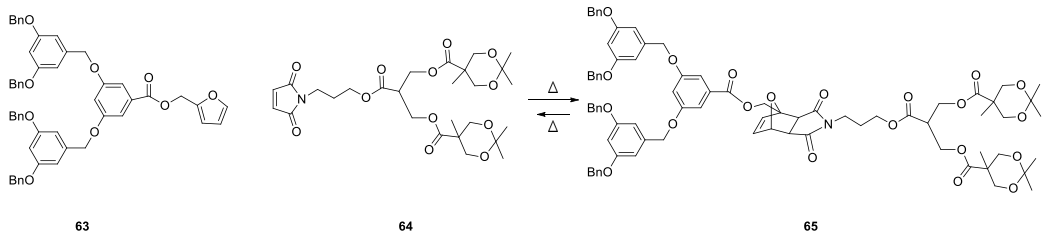

Scheme 15. Synthesis of structure **65** via Dials-Alder cycloadditions

1.3 Other Potential Click-type Transformations

1.3.1 [2+2] Cycloadditions

Studies on the development and the use of organic electronic devices are rapidly increasing worldwide. This increasing situation turns this area into a market that makes millions of profits annually. [51] Since conjugated organic molecules are used in organic electronic devices, the synthesis of conjugated structures gains importance.[52] However, there are few high-efficiency, low-step, environmentally friendly reactions in the synthesis of these complex π-conjugated structures in the literature. Although click-type reactions as mentioned above are some of the most preferred reactions in the organic electronics with their several advantages, some deficiencies of these reactions also draw attention. Forming non-π-conjugated products in thiol-ene reaction, explosive nature of the azide groups in 1,3-dipolar cycloaddition reactions and requirement of high temperatures in Diels-Alder reactions are some of the major concerns.[53] In addition, the substrate diversity of azide-alkyne 1,3-dipolar cycloaddition click-type reactions, which are constantly used in this field, has almost reached its limits.[53] Accordingly, two new click-type

reactions, [2+2] cycloadditions and [2+2] cycloaddition-retroelectrocyclizations, have attracted our attention to overcome aforementioned limitations.[54] These reactions have not found the sufficient value they deserve in the literature. [2+2] cycloaddition-retroelectrocyclizations and [2+2] cycloadditions are important click type reaction candidates that can be alternatives to the current synthetic methodologies in the syntheses of conjugated molecules.[55] It should also be noted that there are several limitations that need to be resolved before seeing these two click-type transformations as common strategies for the synthesis of conjugated molecules. Our discussion will begin with [2+2] cycloadditions then will be expanded to [2+2] cycloaddition-retroelectrocyclizations since both transformations are closely related to each other. Unlike Diels-Alder [4+2] cycloadditions, [2+2] cycloaddition reactions do not occur under thermal conditions. Starting materials that will be used in these reactions should be stimulated in ultraviolet or visible light.[56] When these transformations were first discovered, it was not fully understood how the cycloaddition step took place. However, in 1969, Woodward and Hoffmann's study suggested that preservation of orbital symmetry is an important factor determining the outcome of the pericyclic processes.[57] According to Woodward-Hoffmann rules, [4+2] cycloaddition reactions are thermally allowed whereas [2+2] cycloaddition reactions are thermally forbidden reactions.[57] The study that revealed the Woodward-Hoffmann rules explains why some reactions occur under thermal conditions and others prefer photochemical conditions via the HOMO and LUMO orbitals (Figure 2).

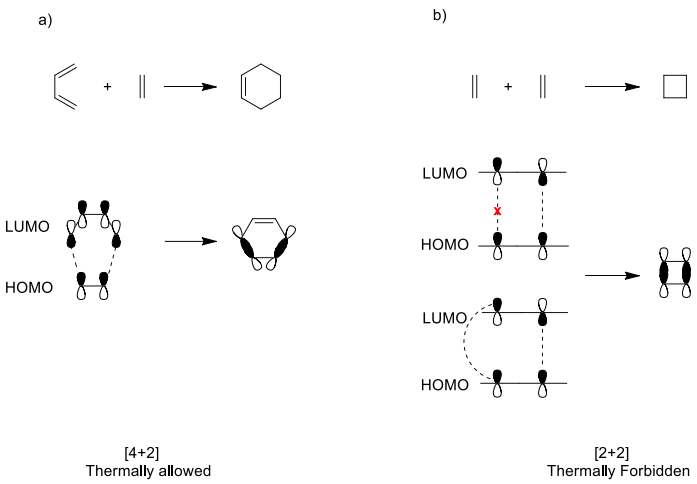

Figure 2. a) [4+2] and b) [2+2] cycloaddition reactions.

In Figure 2a, the phases of diene and dienophile frontier orbitals are overlapping with each other in [4+2] cycloadditions and they can easily form σ-bonds under thermal conditions. However, the same case is not valid for [2+2] cycloadditions (Figure 2b). It is clearly seen that the phase of HOMO does not overlap with the phase of LUMO in the [2+2] cycloadditions and this case is not suitable for bonding. To facilitate this transformation, one of the reactants should be excited photochemically to match the phases in [2+2] cycloaddition reactions.[58] Accordingly, [2+2] cycloadditions are known in the literature as [2+2] photochemical cycloadditions.[59] [2+2] photocycloaddition reactions are widely used cycloaddition reactions in organic chemistry to form cyclobutane-type compounds **68** from olefins **66** and **67** by UV light or visible light (Scheme 16).[60] Since cyclobutane ring can be used in fragmentation and ring expansion reactions in the syntheses of complex structures, [2+2] photocycloadditions play an important role in the synthesis of bioactive products.[61,62]

Moreover, [2+2] photocycloaddition reactions may take place between alkenes-alkynes and/or between alkenes-enones to form cyclobutene-type compounds **70** and/or cyclobutanes **73** and **74** respectively (Scheme 16).[56,60] The formation of head-to-tail isomer and head-to-head isomer depend on the R group in

the alkene molecule. When the electron-donating-substituents attached to the alkene, a head-to-tail **74** isomer is generated. Head-to-head isomer **73** is preferred with electron-withdrawing substituents.[63]

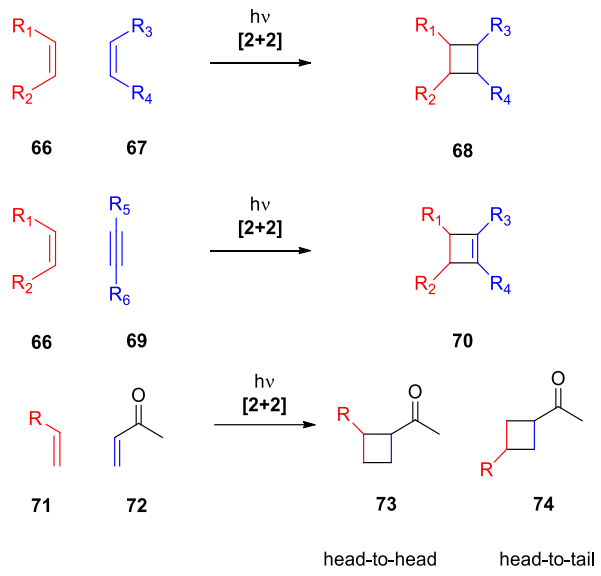

Scheme 16. General representation of [2+2] photochemical cycloadditions.

The first example of photoinitiated [2+2] enone cycloaddition reaction was reported by Ciamician and co-workers in 1908.[64] Ciamician and co-workers observed that the carvon molecule **75** transformed into the carvone camphor **76** under sunlight (Scheme 17). This reaction is also known as the intramolecular enone-olefin [2+2] photocycloaddition.[65]

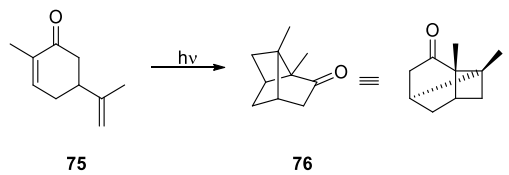

Scheme 17. Formation of carvone camphor **76** when exposing carvone to sunlight.

Later, Eaton discovered the photocyclodimerization of 2-cyclopentenone **77** and the intermolecular photocycloaddition between cyclopentenone and cyclopentene in 1962 (Scheme 18). Photocyclodimerization of 2-cyclopentenone generates a mixture of cyclobutene products **78** and **79**.[66] Subsequently, Corey reported the synthesis of the caryophyllene molecule **86** using a photocycloaddition strategy. 2-cyclohexenone **83** and an excess amount of isobutylene **82** react to form bicyclo[4.2.0]oct-anone derivative **84** as the major product (Scheme 19). In the next step, the five-membered ring fused into the six-membered ring to yield **85**, and then the 9-membered ring structure was formed by cleavage of the C-C bond.[60]

All these pioneering studies, once again, highlighted the importance of the [2+2] photocycloaddition reaction in the field of organic chemistry and they have also paved the way for many studies in recent years. This photochemical reaction is now widely used to synthesize complex molecules in synthetic organic chemistry.[60,66]

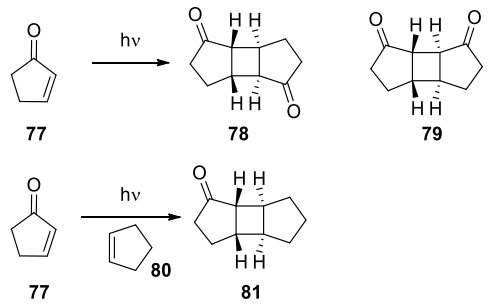

Scheme 18. Photodimerization of cyclopentenone and [2+2] photocycloaddition of cyclopentene to cyclopentenone.

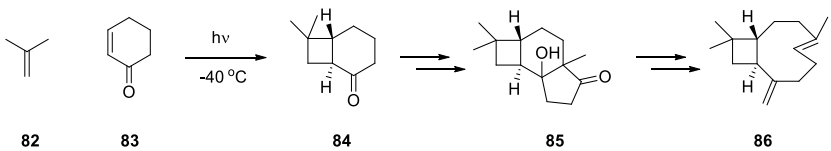

Scheme 19. Synthesis of Caryophyllene **86**.

1.3.2 Thermal [2+2] Cycloadditions

Although [2+2] cycloaddition reaction was considered thermally prohibited according to Woodward Hoffman rules,[57] Reinhoudt's study in 1974 revealed that these reactions could also occur under thermal conditions.[67] Reinhoudt stated in his study that alkyne and alkenes with opposite electron densities undergo thermal [2+2] cycloaddition under mild reaction conditions. Thiophene attached pyrrolidine at the 3-position **87** and electron-poor alkyne **88** formed cyclobutene **89**, a product of thermal [2+2] cycloaddition obtained at very low temperature (-30 ^{o}C). This intermediate **89** could be observed by IR and NMR studies (Scheme 20). However, this product rearranges into thiepine **90** spontaneously.[67]

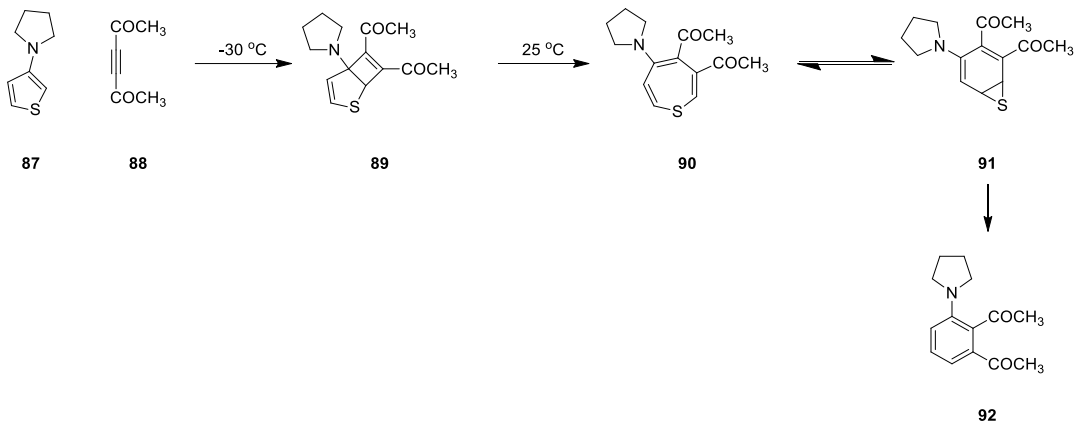

Scheme 20. Thermal [2+2] cycloaddition between electron-rich thiophene and electron-poor alkyne.

However, studies in this area did not receive sufficient attention at that time due to the limited variety of substrates, low yields, and the instability of the products.[68] In 2010, Trofimov and his group serendipitously discovered the [2+2] cycloaddition reaction instead of the anticipated aromatization reaction while using dichloro-5,6-dicyano-1,4-benzoquinone (DDQ).[69] Although DDQ is a powerful oxidizing agent for dehydrogenation reactions and an effective reagent for aromatization, Trofimov's work surprisingly reveals that DDQ reacts with the triple bond to form cycloadducts.[69] When compound 4,5,6,7-tetrahydroindole alkyne **93**

was treated with DDQ **94** at room temperature, compound **95** was synthesized in a very short time in 93% yield instead of aromatized indole derivative **96** (Scheme 21). This shows that the cyclobutene derivative is stable under ambient conditions. When Trofimov and co-workers repeated the reaction using different heterocycle-substituted alkynes, cycloaddition products were similarly obtained in high yields.[69]

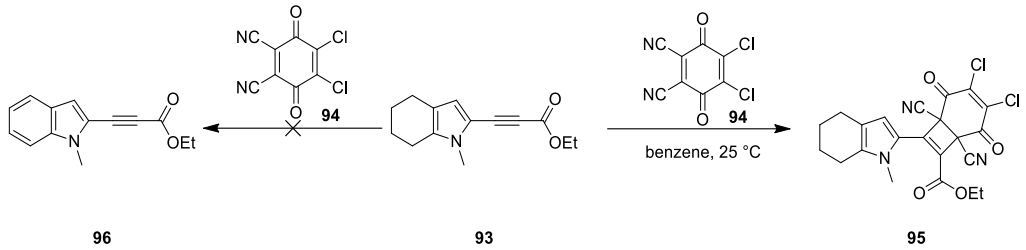

Scheme 21. Reactions of DDQ with electron-rich alkynes [2+2] cycloactive reactions.

At about the same time, Diederich and his group published a study on the reactions of DDQ with dialkylaniline-substituted alkynes.[70] The reaction of the terminal alkyne attached to dimethylaniline **97** with DDQ **94** at room temperature yielded highly stable cyclobutene derivative **98** (Scheme 22). As a contribution of this study, cyclobutene derivatives formed as highly colored chromophoric structures as a result of the reaction between donor-activated electron-rich alkynes and the electron-deficient C=C double bond in DDQ . It has also been reported that the synthesized cyclobutene structures possess properties that can be utilized in nonlinear optical applications. Another interesting point is to obtain π-conjugated spirocyclic D-A type systems by heating the synthesized cycloadducts to 80 °C.[70]

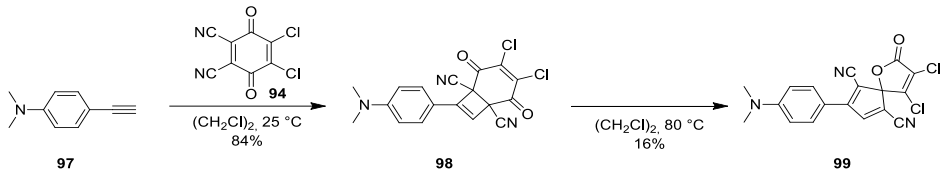

Scheme 22. Thermal [2 + 2] cycloaddition reaction of DDQ and dimethylanilino acetylene.

In addition to these pioneering studies, Shoji [71] and Diederich[72] published several studies on reactions between various alkyne derivatives and DDQ that can be used in thermal [2+2] cycloaddition reactions in the following years. Shoji and his group worked with the new alkyne derivative 2*H*-cyclohepta[*b*]furan-2-one, also known as heteroazulene, which can be used in thermal [2+2] cycloaddition reactions.[71] On the other hand, Diederich and his co-workers synthesized new homoconjugated push-pull chromophores with various *N*-substituted anilinoacetylenes.[72] Thus, new alkyne donor groups that can be used in thermal [2+2] cyclocation reactions were introduced to the literature. Common electron-rich alkynes used in thermal [2+2] cycloaddition reactions are shown in Figure 3.

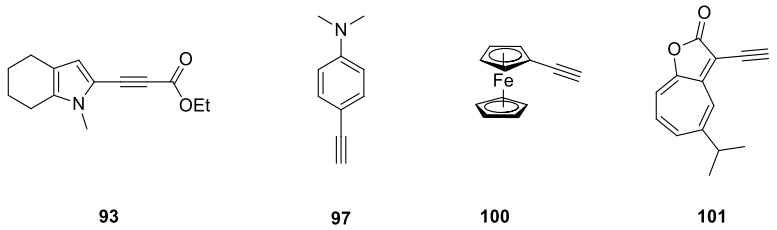

Figure 3. Electron-rich alkyne derivatives used in thermal [2+2] cycloadditions.

Despite all these important studies, the variety of alkynes used for thermal [2+2] cycloadditions is rather limited. Moreover, these alkynes could not be stored in ambient conditions for a long time due to stability issues. For all these reasons, thermal [2+2] cycloaddition reactions have not received enough attention. Another important problem is that post-modification reactions on cycloaddition products cannot be performed.

1.3.3 [2+2] Cycloaddition-Retroelectrocyclizations

Another important click-type reaction is [2+2] cycloaddition-retroelectrocyclization (CA-RE) reactions. These reactions occur between electron rich alkynes **102** and electron deficient olefin such as tetracyanoethene **103** (TCNE), 7,7,8,8-tetracyanoquinodimethane **106** (TCNQ) (Scheme 23).[54] The reaction starts

with cycloaddition to form unstable cyclobutene derivatives **104**, **107** and then spontaneous retroelectrocyclization of cyclobutene produces target donor-acceptor-type chromophores **105**, **108** under mild conditions. [2+2] CA-RE reactions are effective and robust methods used in the synthesis of nonplanar donor-acceptor (D-A) push-pull chromophores having low-energy and strong intramolecular charge-transfer (ICT) bands.[73] They also display second-order nonlinear optical properties as well as enhanced third-order nonlinear optical responses.[74] D-A-type push-pull chromophores have some advantages in terms of high thermal stability, solubility in organic solvents, less aggregation and easy sublimation for the formation high-optical-quality amorphous thin films because of nonplanar structures.[74] Nonplanar D-A push-pull chromophores are potential candidates for use in electronic and optoelectronic devices since these compounds possess features that are essential for device fabrications.[75] Successful utilization of these molecules in optoelectronic applications led to increasing demand for the discovery of effective atom-economic and simple methods. Accordingly, [2+2] CA-RE reactions have attracted significant attention in recent years as these transformations fulfill the aforementioned expectations.[76]

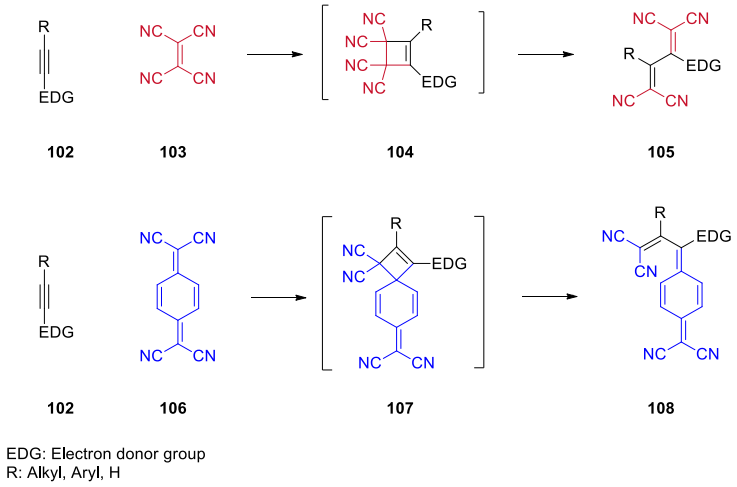

Scheme 23. General mechanism of [2+2] cycloaddition-retroelectrocyclization (CA-RE) reactions.

The first [2+2] CA-RE reaction was reported by Bruce and coworkers in 1981.[77] In this study, the first organometallic 1,1,4,4-tetracyanobuta-1,3-diene (TCBD) derivative **111** was synthesized using metal-substituted acetylide **109** and electron-deficient olefin TCNE **103** (Scheme 24). The chemical structures of these TCBD derivatives were confirmed by X-ray crystal structure analysis.[77] Later, TCBD derivatives **112**, **113**, **114** including different metals such as tungsten, nickel, and iron were synthesized.[78]

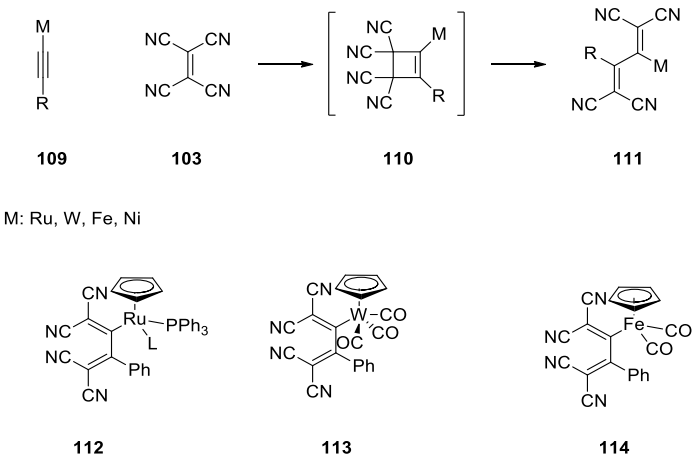

Scheme 24. Mechanism for the reaction between metal-substituted acetylides and TCNE and metal-substituted TCBD products.

In 1990, Takashi and coworkers reported the synthesis of s-cis or s-trans TCBD structures **115a**, **115b** using reaction of TCNE with Pt-acetylide (Figure 4).[79] Surprisingly, these studies have not received enough attention at that time due to the limited substrate scope.[76] There were only a few studies on [2+2] cycloaddition-retroelectrocyclization reactions in the literature between 1990-2005. One of them was the synthesis of pure organic tetracyanobutadiene structures **116a**, **116b** having nonlinear optical properties reported by the Jen and Suter groups.[80] Another study is by Yamashita and co-workers on the synthesis of D-A compounds **117a**, **117b** using 1,3-dithiol-2-ylidene and TCNE in 2004.[81] However, none of these studies investigated structure-reactivity relationship until 2005.[76]

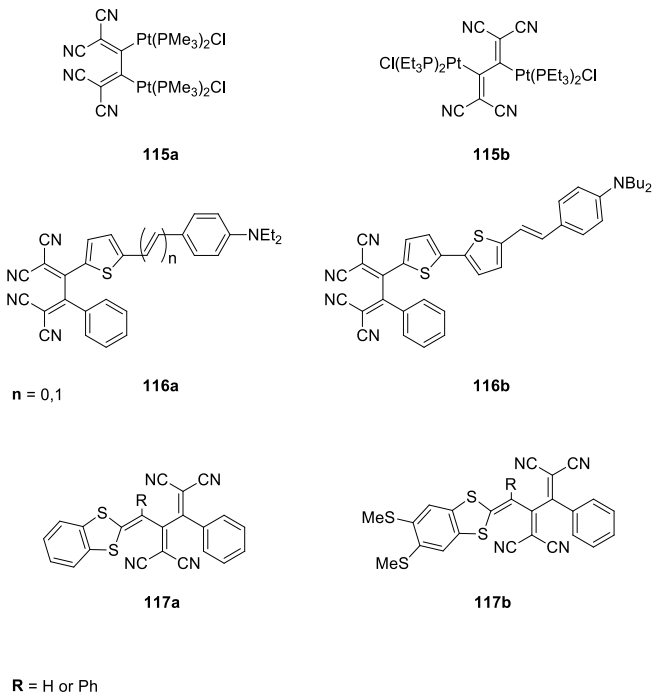

Figure 4. Some donor-substituted TCBD derivatives reported before 2005.

In 2005, Diederich and co-workers focused on controlling the reactivity of alkynes, accordingly dialkylaniline-substituted alkynes were proved to be efficient substrates in [2+2] CA-RE reactions.[82] Thus, this reaction came to the fore with great interest. In this study, alkyne derivatives **118** and TCNE **103** reacted in a very short time and yielded non-planar chromophores **119** in high yields (Scheme 25).

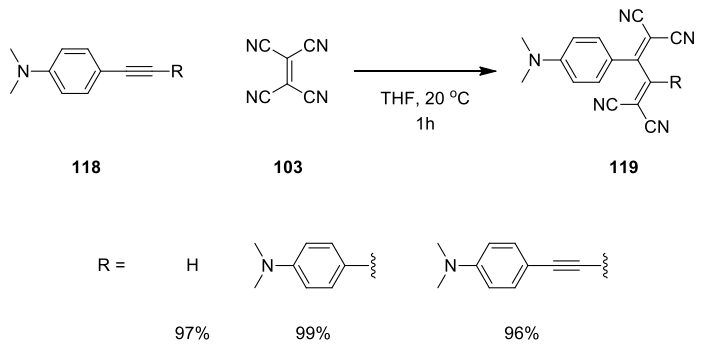

Scheme 25. The first study of dialkylaniline-substituted alkynes in [2+2] CA-RE.

In the following years, new alkyne substrates **120** having strong donor substituents such as thiophene and *p*-methoxy groups were used in [2+2] cycloaddition-retroelectrocyclization reactions (Scheme 26).[83] As a result of this study, it was revealed that these two groups did not perform well in [2+2] CA-RE reactions as dialkylaniline derivatives. While dialkylaniline-substituted alkynes reached full conversion within 1 hour at room temperature, thiophene and *p*-methoxy-substituted alkynes required higher temperatures and longer times. Despite these difficult conditions, target products could be synthesized successfully in 80% and 42% yields respectively. These reactions are considered as click-type reactions since there are no by-product formations.[76]

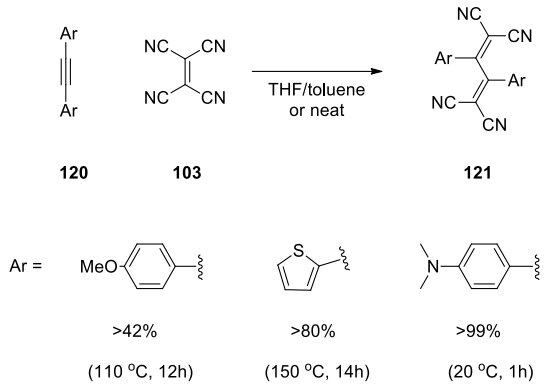

Scheme 26. Effect of donor groups in [2 + 2] CA-RE with TCNE.

Another aspect that makes this transformation important is reaction conditions. According to Woodward and Hoffmann rules, [2+2] cycloadditions was considered as thermally forbidden reactions.[57] This kind of reaction normally occur under photochemical conditions. As we mentioned earlier, Reinhoudt reported that when olefins and alkynes with highly polarized and opposing electron density are used, [2+2] cycloaddition reactions take place under mild thermal conditions.[67] Therefore, [2+2] cycloaddition-retroelectrocyclization reactions selectively produce target products in high yields even at room temperature in the dark if the proper substrates are chosen.

Mechanistic studies for [2+2] CA-RE are rather limited and the generally accepted mechanism for [2+2] CA-RE has not been presented so far. In a recent study, it was proposed via theoretical calculations that these reactions proceed through zwitterionic intermediates (Scheme 27).[84] However, this claim could not be proven since zwitterionic intermediates could not be isolated up to now.

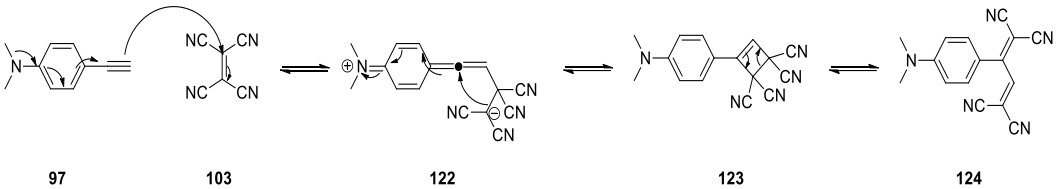

Scheme 27. The proposed zwitterionic mechanism for [2+2] CA-RE.

Upon realizing the significance of [2+2] CA-RE reactions in the synthesis of D-A type chromophores, donor alkyne groups were investigated in detail. In addition to alkynes reported in previous studies, triphenylamine derivatives **125,** [85a] BODIPY derivatives **126**,[85b] ynamide derivatives **127**,[85c] phenothiazine derivatives **128**,[85d] ferrocene derivatives **129**,[85e] azulene derivatives **130**,[85f] cyclopenta*[*b*]*furan-*2*-one derivatives **131**,[85g] tetrathiafulvalene derivatives **132**,[85h] carbazole derivatives **133**[85ı] are synthesized under different reaction conditions (Figure 5).

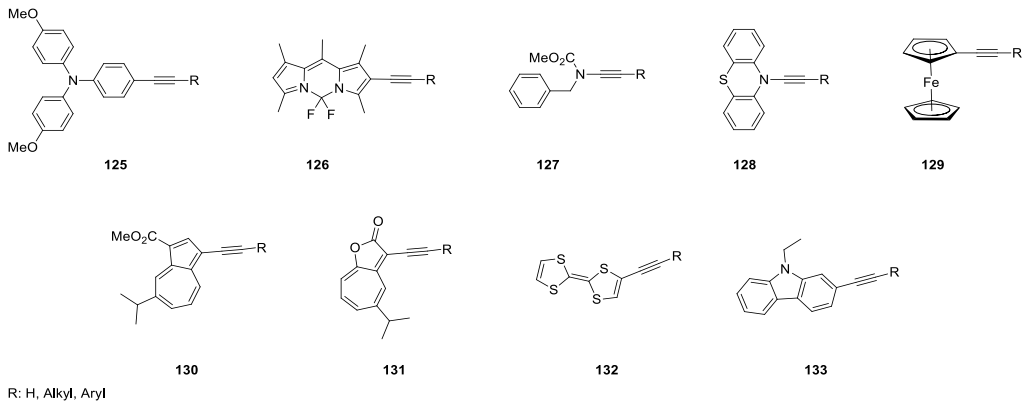

Figure 5. Alkynes used in [2+2] cycloaddition-retroelectrocyclization reactions.

At the same time, studies have been carried out on electron deficient alkenes to increase substrate diversity. For this purpose, commercially available acceptor groups are used as well as new electron deficient groups that have been synthesized in recent years.[86] Commercially available electron deficient alkenes used in [2+2] CA-RE reactions are tetracyanoethylene **103** (TCNE),[82] 7,7,8,8-tetracyanoquinodimethane **106** (TCNQ),[87a] 2,3,5,6-tetrafloro-TCNQ **134**[87b] (F_4-TCNQ) (Figure 6).

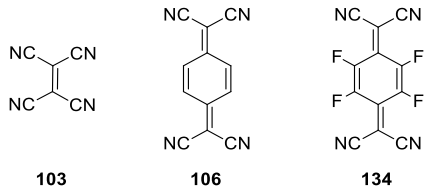

Figure 6. Commercially available electron deficient alkenes used in [2+2] CA-RE reactions.

The new synthesized electron deficient alkene derivatives used in [2+2] CA-RE reactions are *N*,*N*-dimethylanilino-substituted tricyanovinyl **135**,[88a] 2-(dicyanomethylene)indan-1,3-dione **136**,[88b] *N,N'*-dicyanoquinone diimide **137**,[88c] 6,6-dicyanopentafulvene **138**,[88d] adamantanylidene malononitrile **139**[88e] (Figure 7).

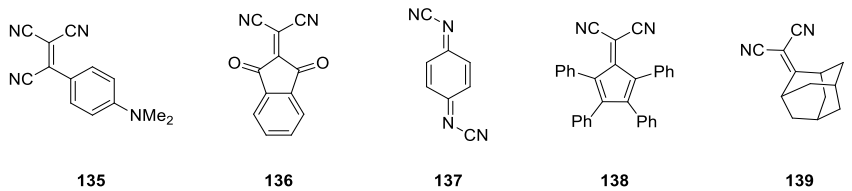

Figure 7. Synthesized electron deficient alkenes used in [2+2] CA-RE reactions.

Despite all these successful synthetic studies to expand substrate diversity, the most important problem in the literature is that electron-rich donor alkyne groups are still quite limited. Another issue is the difficulties of long-term storage of these donor alkyne groups under ambient conditions and isolation problems in the

purification step because of their instability. These limitations also reduce the diversity of π-conjugated systems that can be obtained by [2+2] CA-RE. It should also be noted that it is not possible to perform post-modification reactions on CA-RE products with the current substrate systems.

1.4 Aim of study

[2+2] cycloaddition and [2+2] cycloaddition-retroelectrocyclization reactions have attracted great attention in recent years due to their several crucial properties. However, there are still major drawbacks to be resolved. The alkyne donor groups used in these reactions are limited and they cannot be isolated under ambient conditions due to their instability. The second Chapter of this thesis focused on synthesizing new electron-rich alkyne substrates that are stable under ambient conditions in order to overcome all these synthetic limitations and to offer alternatives to donor alkyne groups for thermal [2+2] cycloaddition reactions in the literature. In addition, donor activities of these synthesized alkyne groups toward cycloadditions with electron deficient DDQ were discussed. Optoelectronic properties of synthesized chromophore structures were examined by experimental and theoretical studies.

In Chapter 3, to provide solutions to aforementioned problems related to donor alkynes, heterocycle (methyl indole)-substituted new donor alkynes were synthesized. Methyl indole-substituted alkynes have never been used in CA-RE transformations. Moreover, electron density on the nitrogen lone pair of the indole ring is relatively free to move mesomerically compared to other heterocycles like benzofuran and benzothiophene. Lastly, methyl indole can easily be modified to expand substrate scope. Besides synthesis of methyl-indole-substituted alkyne derivatives, their donor activities were tested toward [2+2] CA-RE by using TCNE and TCNQ. At the final step, the optoelectronic properties of the synthesized push-pull chromophores were studied both experimentally and theoretically.

CHAPTER 2

RESULTS AND DISCUSSION

2.1 Design and Synthesis of New Homoconjugated Push-Pull Chromophores

2.1.1 Synthesis of Triazene-Substituted Alkynes

Until now, the triazene group has been used to mask aryl iodide substrates for branched dendrimer synthesis in dendrimer chemistry.[89] Triazenes also find application areas in medicinal chemistry.[90] However, there are no studies about the donor-acceptor properties of triazenes in the literature. Therefore, our efforts mainly focused on synthesizing triazene-substituted alkyne derivatives in order to test their donor abilities.

Target alkyne substrates were designed regarding crucial properties like donor strength, reactivity, and solubility. The target triazene-functionalized substrates were synthesized in three steps according to the literature procedures (Scheme 28).[91] Firstly, starting with commercially available 4-iodoaniline **140**, iodo-triazene **141a-f** were prepared by trapping in situ formed diazonium salt with corresponding dialkylamines. Sonogashira cross-coupling of **141a-f** with an excess amount of ethynyl trimethylsilane afforded **142a-f** at room temperature. According to our strategy, the final step was deprotection to yield triazene-substituted alkyne derivatives **143a-f**. The alkyne products **143a-f** were obtained in 30–77% yields. To confirm synthesized structures, ^{1}H and ^{13}C NMR techniques were utilized. The NMR studies indicated that alkyl signals are relatively broad compared to the rest of the peaks due to restricted free rotation around the N-N bond. This result is consistent with earlier literature studies.[92]

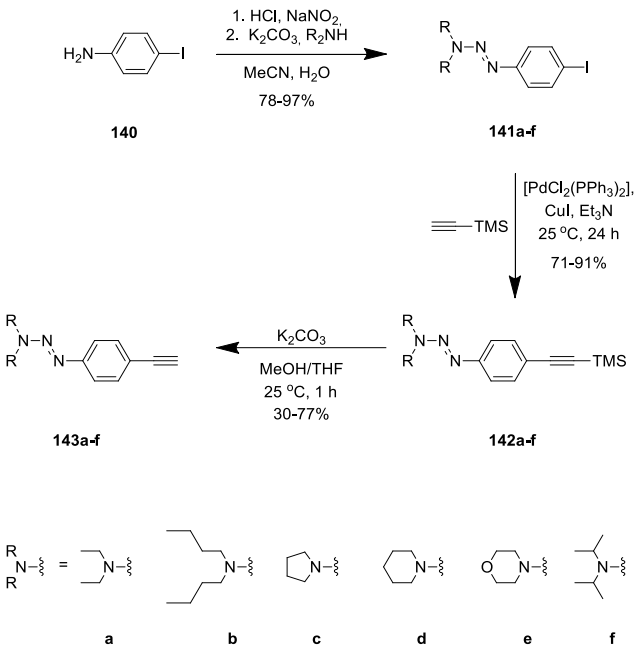

Scheme 28. Three-step synthesis of electron-rich alkynes **143a-f**.

2.1.2 Synthesis of Homoconjugated Push-Pull Chromophores

In this part, donor reactivities of triazene-substituted alkyne substrates **143a-f** were tested towards formal [2+2] cycloadditions by using DDQ **94** as an acceptor group. Therefore, the targeted push–pull homoconjugated chromophores (±)-**144a-f** were synthesized from electron-rich triazene alkynes in dichloromethane at room temperature by a one-step procedure (Scheme 29). All homoconjugated chromophore structures (±)-**144a-f** possess dark-orange color due to donor-acceptor interactions. Additionally, these chromophores are very stable under ambient conditions compared to earlier reported cyclobutene systems.

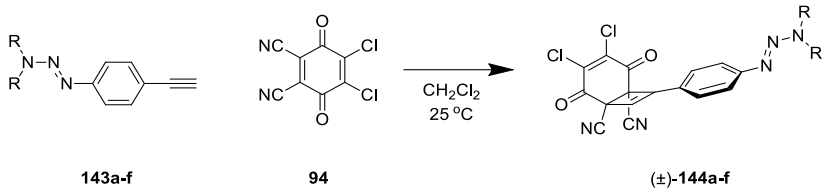

Scheme 29. Formal [2+2] cycloadditions of triazene-substituted electron-rich alkynes with DDQ.

The yield of homoconjugated dyes (±)-**144a-f** is changing from 19% to 73% (Table 1). In pyrrolidine substrate, yield is lower than the other substrates because of competing oxidation reactions as reported earlier for DDQ cycloadditions.[91] Moreover, we have not observed any correlation between the electron-donor strength of triazene-substituted alkyne and the yields of the homoconjugated chromophores (±)-**144a-f.**

Table 1. [2+2] Cycloaddition of electron-rich alkynes with DDQ.

Substrate		***Yield [%]***
(±)-**144a**		60%
(±)-**144b**	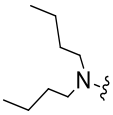	54%
(±)-**144c**		19%
(±)-**144d**		53%
(±)-**144e**		48%
(±)-**144f**		73%

2.2 UV/Vis Spectroscopy

UV/Vis spectroscopy display evidence for the intramolecular charge transfer (ICT) behavior of homoconjugated chromophores at room temperature in dichloromethane. The cycloadducts indicate intramolecular CT bands of moderate intensity with λ_{max}-values between 428 and 448 nm; 2.77-2.90 eV and ε-values between 3100-3800 M^{-1} cm^{-1} (Figure 8). When electron-donor strength increased, the CT bands are bathochromically shifted, commonly called red shift.[72] Compounds (±)-**144a-f** appear intramolecular charge-transfer bands of moderate intensity (ε values between 3100 and 3800 M^{-1} cm^{-1}): λ_{max} = 440 nm (2.82 eV, 3700 M^{-1} cm^{-1}, (±)-**144a**), 442 (2.81 eV, 3800 M^{-1} cm^{-1}, (±)-**144b**), 438 (2.83 eV, 3100 M^{-1} cm^{-1}, (±)-**144c**), 428 (2.90 eV, 3600 M^{-1} cm^{-1}, (±)-**144d**), 430 (2.88 eV, 3800 M^{-1} cm^{-1}, (±)-**144e**), and 448 (2.77 eV, 3500 M^{-1} cm^{-1}, (±)-**144f**).

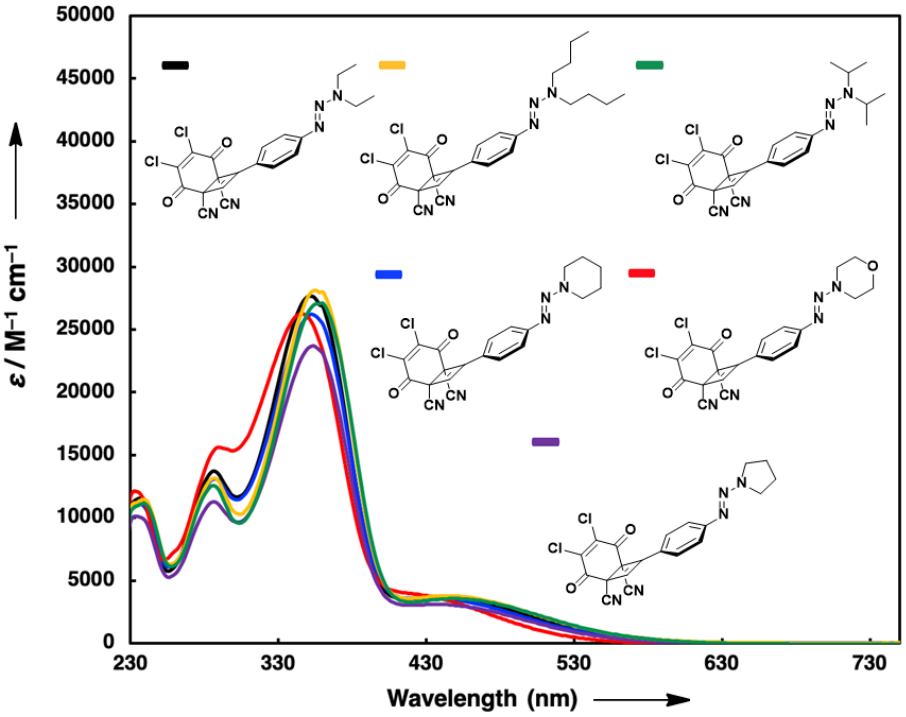

Figure 8. UV/Vis spectra of homoconjugate chromophores (±)-**144a** (black line), (±)-**144b** (yellow line), (±)-**144c** (purple line), (±)-144d (blue line), (±)-**144e** (red line), and (±)-**144f** (green line) in CH_2Cl_2 at 298 K.

Homoconjugated push–pull chromophores (±)-**144a-f** shows positive solvatochromism which also supports intramolecular CT interactions (Figure 9). Less polar (e.g. toluene) solutions of chromophores (±)-**144a-f** are yellow and more polar solutions (e.g. dichloromethane) are dark orange; with corresponding bathochromic shifts for low energy bands approximately 25 nm.

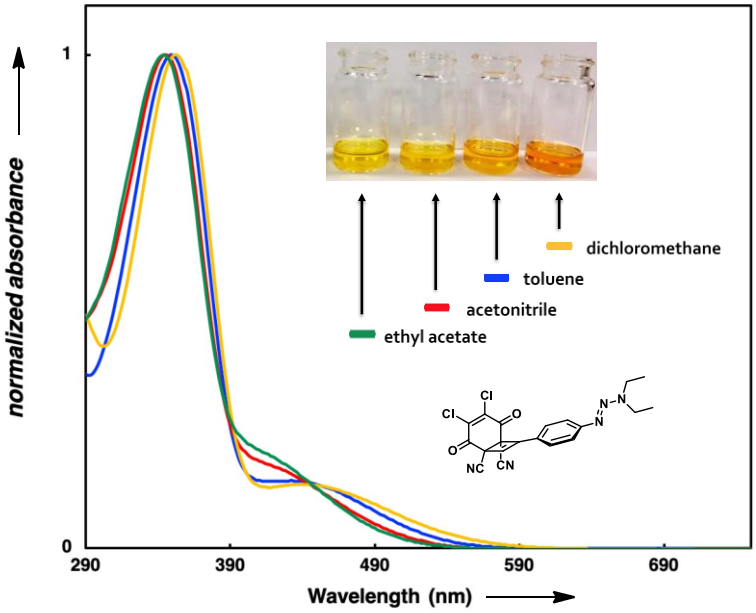

Figure 9. UV/Vis absorption spectra of chromophore (±)-**144a** in different solvents at 298 K.

2.3 Computational Studies

After analyzing charge-transfer bands of the non-planar chromophores using experimental UV/Vis studies, computational techniques were also used to investigate optoelectronic properties of these molecules (Figure 10). As we mentioned earlier, triazene groups were claimed to be electron-donor groups. According to the theoretical studies, it displays that the areas covered by the HOMO and LUMO orbitals are separated almost fully from each other. HOMO and LUMO

frontier orbital depictions support ICT process involving transfer of electron density from electron-rich triazene groups to the CN groups. The HOMO is localized on the triazene unit while the LUMO is concentrated on the CN groups and electron-deficient dichloro-dicyano-substituted cyclohexenedione structure. The representations of these orbitals support that the structures obtained in the structures show donor-acceptor characteristics.

a) b)

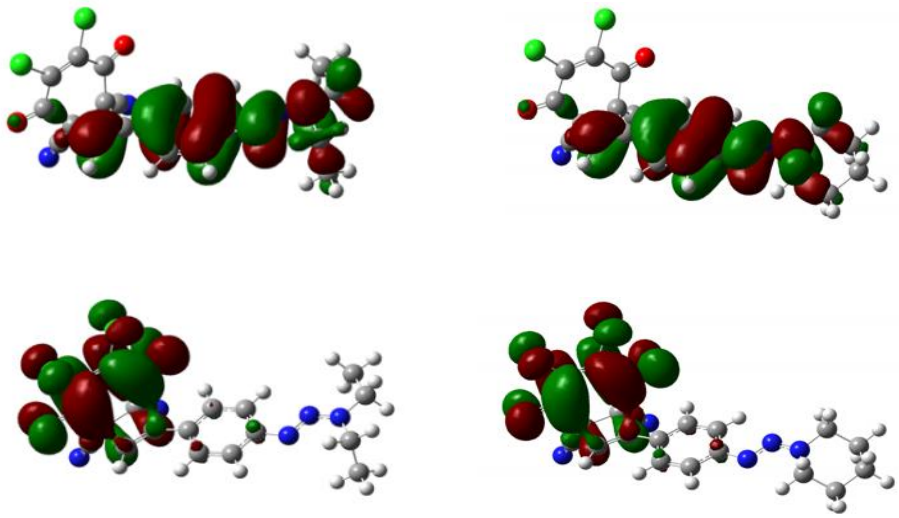

Figure 10. HOMO-LUMO orbital depiction of a) (±)-**144a** and b) (±)-**144d.** The upper plots represent the HOMOs, and the lower plots represent the LUMOs.

Target triazene-substituted molecules (±)-**144a-f** were optimized at the B3LYP/6-31G(d)[93] level of theory with the CPCM solvation model in CH_2Cl_2. The vertical optical transitions were calculated by time-dependent density functional theory (TD-DFT) at the CAM-B3LYP/6-31G(d) level of theory, again with the CPCM solvation model in CH_2Cl_2 using the software package Gaussian 09.[94] Accordingly, the lowest-energy bands are mostly composed of HOMO to LUMO excitations at around 500 nm. The computed transition energies and experimental values are in really good agreement (Figure 11). Figure 11 shows the calculated and

experimental UV/Vis spectra for the selected dye (±)-**144a**. Although the computational results are slightly off for the high energy absorption bands, the results for the low energy ICT band are fitting well with only 3 nm difference.

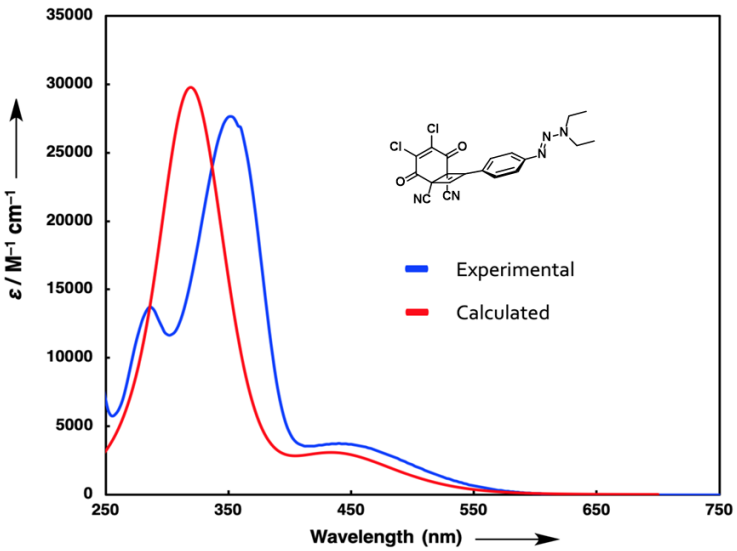

Figure 11. Calculated (not shifted, scaled by 0.6, red line) TD-DFT:CAM-B3LYP/6-31G* level of theory in CH_2Cl_2 and experimental (blue line) UV/Vis absorption spectrum of (±)-**144a**.

CHAPTER 3

RESULTS AND DISCUSSION

3.1 Design and Synthesis of New Heterocyclic Donor Group for [2+2] Cycloaddition-Retroelectrocyclization Transformation

3.1.1 Synthesis of Methyl-Indole-Substituted Alkynes

Since electron-rich alkynes are highly reactive molecules, they are difficult to store at ambient conditions. Therefore, studies with electron-rich donor alkynes are quite limited in the literature. Our investigations on new donor alkyne derivatives were initiated for the purpose of solving this problem in the literature. Considering several alkyne examples known in the literature, we realized that conjugated alkyne systems containing lone pair electrons are required to participate in the [2+2] CA-RE transformations. With this information, the indole molecule, a heterocyclic compound, was chosen as a donor group in this study. One of the crucial points in choosing this compound is that the indole-substituted alkynes has not been tested for [2+2] CA-RE chemistry. Moreover, compared to other heterocyclic structures such as benzofuran and benzothiophene, the lone pair on heteroatom is loosely bounded and activate alkyne group mesomerically. Additionally, the methyl indole group can easily be coupled with different alkynes to increase substrate scope.

In the first stage of the study, starting with indole **145**, the iodo indole compound **146** was synthesized to be used in the coupling reaction in next step (Scheme 30). Even if the Sonogashira cross-coupling reaction was tested at both room temperature and at high temperatures by using the iodo-indole compound **146,** the desired TMS-protected alkyne **147** could not be obtained.

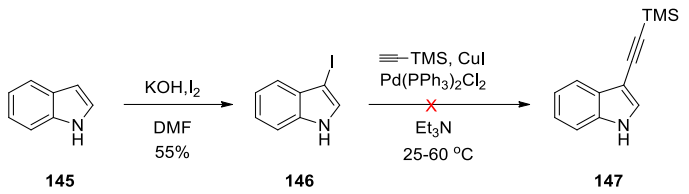

Scheme 30. Effect of acidic proton on coupling reactions.

Next, we decided to use the methyl group because of the possibility that the acidic proton attached to the indole nitrogen atom can prevent the coupling reaction. Accordingly, 1-methyl-1*H*-indole was selected as the target structure. First, indole **146** was treated with KOH and MeI to yield 1-metyl-1*H*-indole **148** in 98% yield (Scheme 31). [95] After the successful synthesis of compound **148**, we attempted to synthesize aryl halides as substrates for Sonogashira cross-coupling reactions. The target iodo compound **149**[96] was obtained in high yield. With aryl halide **149** in hand, TMS protected alkyne **150** was obtained via Sonogashira cross-coupling reaction. Unfortunately, we experienced a severe instability issue during the purification of compound **150**. After a detailed literature search, we realized that a very similar problem has also been reported before by Anderson group from Oxford University.[97] Although different purification techniques (SiO_2, Al_2O_3 acidic/basic column chromatography) were tried, the desired compound **150** could not be obtained in acceptable amounts. In anyway, we tested the following reaction with a small amount of isolated **150**. Compound **151** was successfully synthesized in 76% yield by the treatment of compound **150** with potassium carbonate in methanol. These results confirm that the protecting group is crucial to reach indole-substituted alkynes.

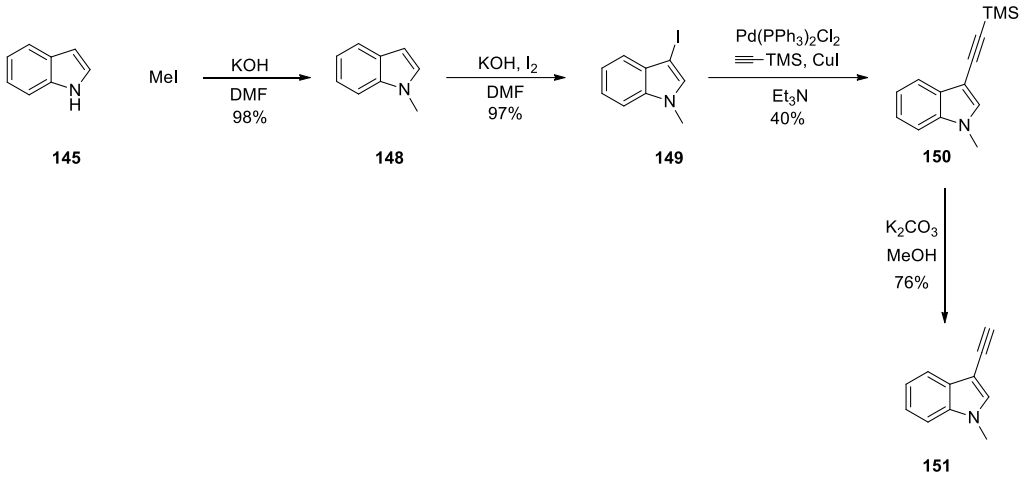

Scheme 31. Synthesis of metyl-indole-substituted alkyne **151**.

Since we could obtain **151** in extremely small amounts, target CA-RE reactions could not be studied as planned (Scheme 32).

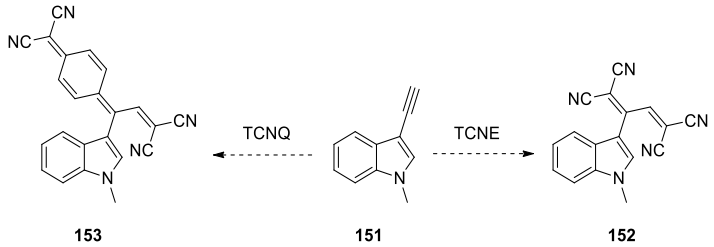

Scheme 32. Effect of methyl-indole-substituted alkyne reactivity in CA-RE reactions.

Later, [2+2] CA-RE was tested with TMS protected alkyne **150** to find a solution for stability problem. When compound **150** was treated with TCNE **103**, color of solution changed from light yellow to dark yellow-red color (Scheme 33). This observation was consistent with the literature results and supports the formation of a product between **150** and **103**. Moreover, TLC analysis supported the formation of dark colored product **154**.

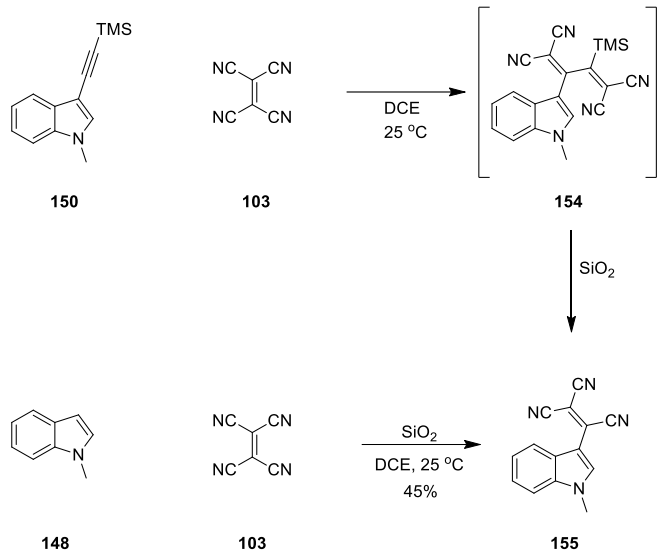

Scheme 33. Effect of TMS protecting alkyne reactivity with TCNE.

Interestingly, the dark colored product unexpectedly decomposed in the column chromatography stage and turned into a dark orange product during purification process. NMR and X-ray analysis revealed the structure of this compound as **155** (Figure 12 and Figure 13). On the other side, starting from **148**, compound **155** was synthesized by another method known in the literature. The results obtained by both methods are compatible with each other. With this information, we suggest that the target [2+2] CA-RE product **154** is formed but this product turned into compound **155** with the effect of the slightly acidic silica gel used in column packing material.

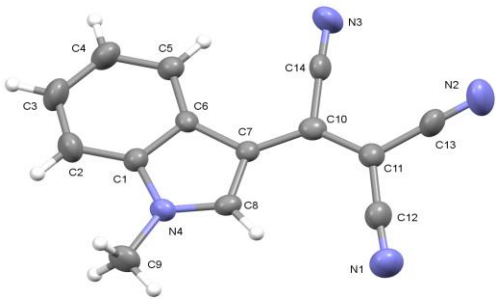

Figure 12. X-ray analysis of compound **155**.

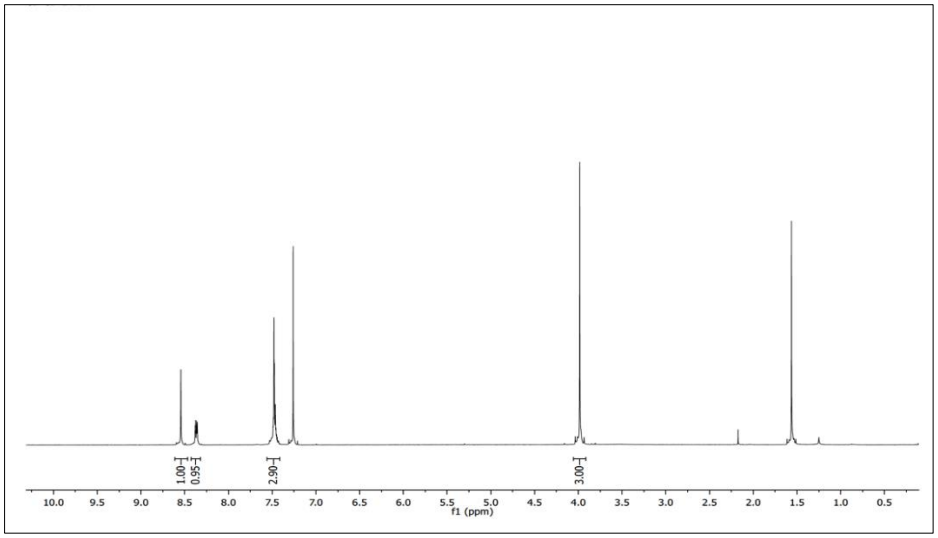

Figure 13. ^{1}H-NMR spectrum of compound **155**.

After these results, we proposed a mechanism for the formation of compound **155** (Scheme 34). According to the proposed mechanism, the reaction starts with the elimination of CN^- from compound number **154** catalyzed with the acidic environment provided by silica gel. Unstable allene compound **154a** is formed as an intermediate and alkyne derivative **154b** having TMS and CN groups. In this step, this alkyne derivative **154b** could not be isolated. In the last step, CN^- anions attacks the reactive center allene carbon, making the structure neutral and forming compound number **155.**

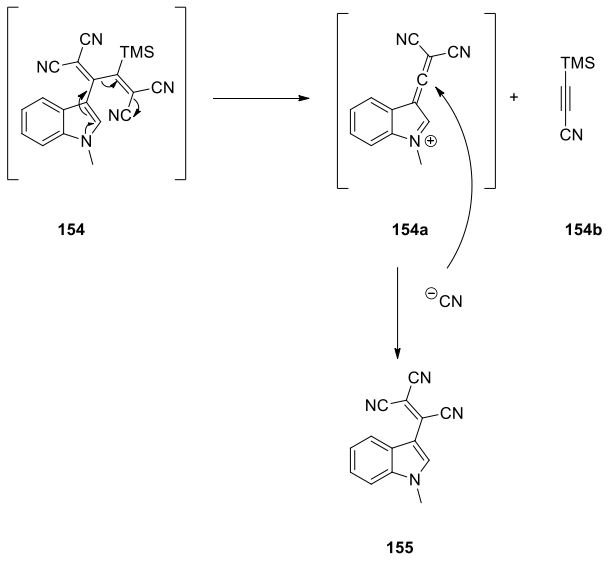

Scheme 34. The formation mechanism of compound number **155.**

Due to the instability problem of the indole-substituted alkynes **150** and **151** and the unsuccessful attempts towards the synthesis of desired push-pull type chromophores, we turned our attention on how indole-substituted alkynes can be stabilized by modifying the structures with relatively bulky electron deficient/rich groups.

3.1.2 Synthesis of Triazene-Substituted Metyl-Indole Alkynes

Due to encountered stability issues, we have changed our research perspective to increase the stability and activity of alkynes with possible structural changes. Hence, the first coupling reaction was carried out with the triazene-substituted alkyne. A new alkyne **156** was synthesized via coupling of aryl iodide **149** with diethyl triazene substrate **143a** in the presence of copper and palladium catalyst at room temperature (Scheme 34).

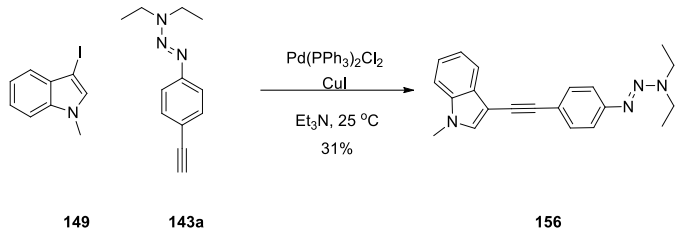

Scheme 35. Synthesis of compound **156**.

As expected, **156** was stable and can be stored at room conditions for months. We presume that increase in molecular weight and possible alkyne protection by side groups increase the stability of the compounds. After these encouraging results, we planned to synthesize several heterocyclic donor-substituted alkynes.

3.1.3 Synthesis of Alkyne Derivatives

After the successful triazene coupling, we focused on synthesizing several heterocyclic donor-substituted alkynes. For this purpose, we studied the synthesis of new alkyne derivatives to couple with methyl-indole. Synthesis of selected diethyl-aniline, Polycyclic aromatic hydrocarbon (PAH)-substituted alkynes was started. Commercially available phenylacetylene was also selected. TMS-protected alkynes **158**[98], **161** [99], **164**[99], and **167**[99] were successfully synthesized starting with the aryl halides **157**, [98] **160**, [99] **163**[99] and **166**[99] via the Sonogashira cross-coupling in the presence of copper and palladium. Then, aryl-substituted alkynes **159**[98], **162**, [99] **165**[99] and **168**[99] were accessed by deprotection using K_2CO_3 in a MeOH/THF mixture in 81%, 95%, 73%, and 86% yields, respectively (Scheme 35).

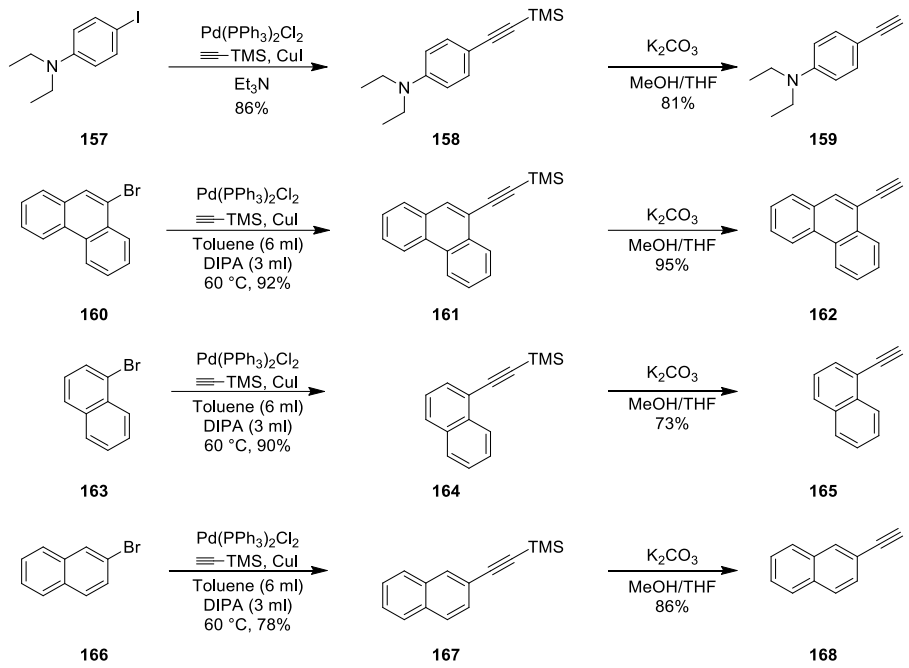

Scheme 36. Synthesis of alkyne derivatives.

3.1.4 Synthesis of Methyl-Indole-Substituted Alkynes

After synthesizing alkyne derivatives, final coupling reaction of alkynes with iodo methyl indole was carried out. All these synthesized coupling products **156**, **169-173** by using Sonagashira cross coupling reaction were quite stable at room conditions compared to methyl-indole alkyne **151** (Scheme 36).

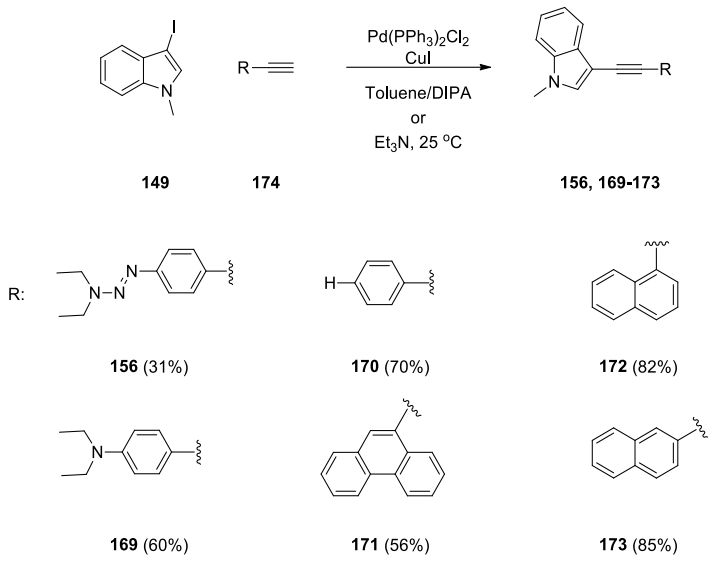

Scheme 37. Synthesis of disubstituted alkynes.

3.1.5 CA-RE of Methyl Indole-Substituted Alkynes with TCNE and TCNQ

After solving the stability issue of the alkynes, we directed our efforts to test the donor properties of methyl indole. For this purpose, we first investigated compound **169** as a substrate in CA-RE with TCNE even if the diethyl aniline group is well-known electron-donating group in the literature.[82] The CA-RE of the synthesized compound **169** and TCNE **103** was performed in 1,2-dichloroethane and the chromophore structure **175** was successfully synthesized in 94% yield (Scheme 37).

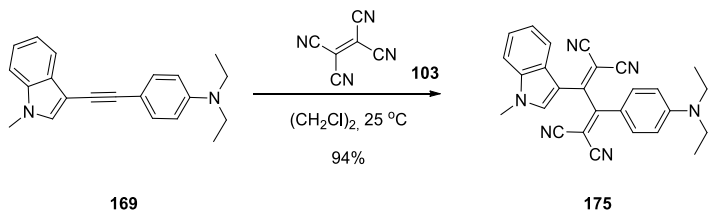

Scheme 38. Synthesis of **175**.

Following this initial result, we also treated compound **169** with another important electron-deficient alkene TCNQ **106** to yield target chromophore **176** in 99% yield (Scheme 38).

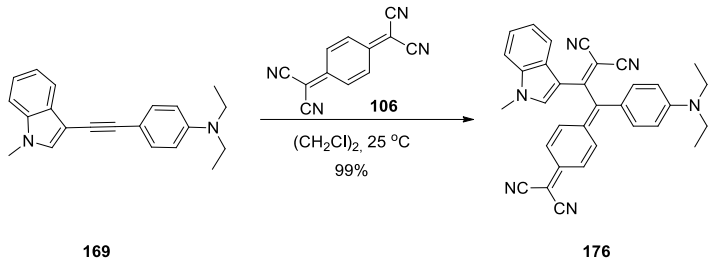

Scheme 39. Synthesis of chromophore **176**.

Initial reactions of **169** with TCNE and TCNQ clearly indicated that the alkynes are stable and successfully forms the target push-pull chromophores. However, it is still not clear which donor group diethyl aniline or methyl indole activates the alkyne for the subsequent CA-RE transformation. Since diethylaniline group is well-known donor group in CA-RE transformations, it is very important to confirm that methyl indole itself can also activate alkyne without the help of diethylaniline donor. Accordingly, we tested substrate **170** in CA-RE to support the alkyne activation capabilities of methyl indole. The phenyl group in **170** behaves as electron withdrawing group. If **170** undergoes a CA-RE with TCNE and/or TCNQ, we can claim that alkyne group can be activated with donor methyl-indole. Therefore, alkyne **170** was treated with TCNE and TCNQ and, as expected, this alkyne reacted with these acceptors smoothly. As a result of the reaction, targeted colorful chromophore structures **177** and **178** were successfully synthesized (Scheme 39).

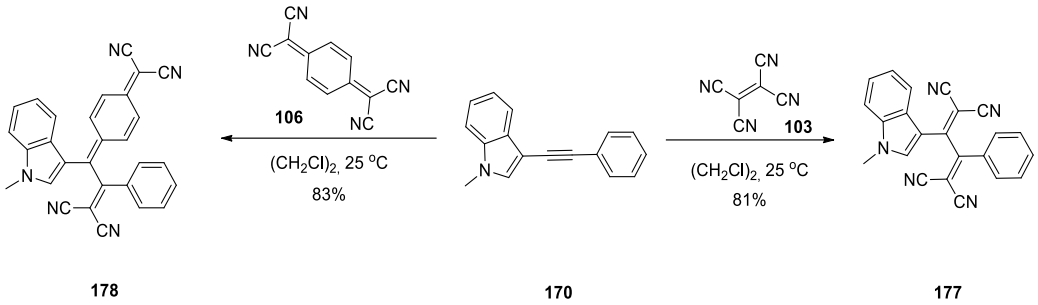

Scheme 40. CA-RE reactions of **170** with TCNE and TCNQ.

After confirming the donor behavior of methyl-protected indole, the [2+2] CA-RE reaction was tried with other alkyne substrates. The CA-RE transformations of substrates with TCNE occur under room temperature and yield is changing from 76% to 95% (Table 2). On the other hand, some of the TCNQ reactions, proceed under relatively higher temperatures and obtained yields were changing between 80% and 99% (Table 3). The requirement of high temperature is probably due to steric hindrance in the case of 1-napthaline, 2-napthaline and phenanthrene-substituted substrates.

In theory, there are two expected regioisomers **178** and **178b** that can be obtained during the reaction of TCNQ and alkyne **170** (Scheme 40). However, the reaction was fully regioselective and only provided regioisomer **178**. The reason behind this well-studied regioselectivity can be explained by resonance structures of **178a** and **178c**. Intramolecular charge transfer breaks the aromaticity of the indole ring (I) while forming a better one (II), as in the case of **178a**. Same resonance stabilization is not possible for resonance structure **178c**.[54]

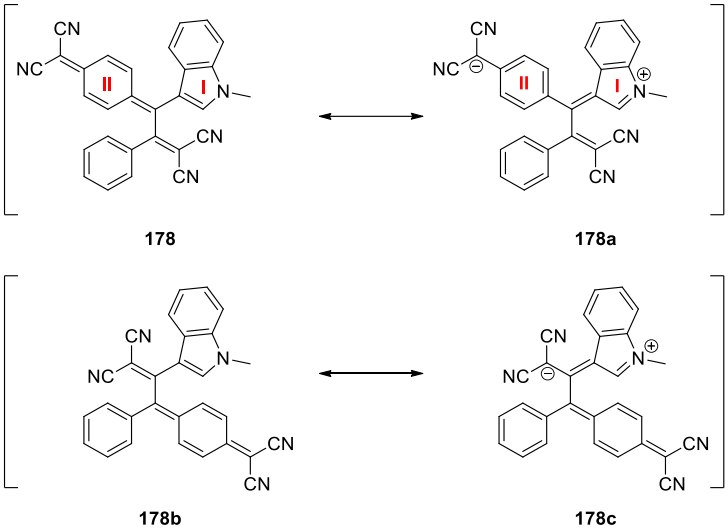

Scheme 41. Regioselective CA-RE reaction between TCNQ and alkyne **170**.

For the reactions of substrates **156** and **169** with TCNQ, situation was more complicated. Since both substrates possess two different donor substituents, aromatic stabilization is valid for both theoretical regioisomers **176**/**176'** and **180**/**180'** (Scheme 41).

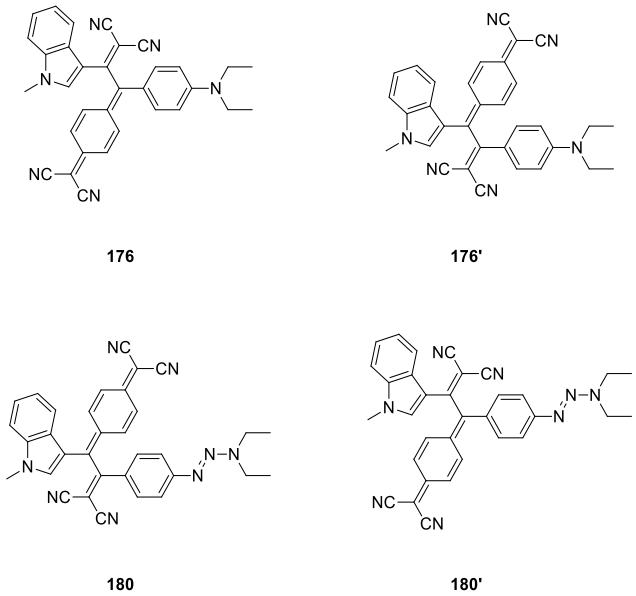

Scheme 42. Theoretical regioisomers in CA-RE reactions between TCNQ and alkynes **169** and **156**.

Interestingly, ^{1}H and ^{13}C NMR studies confirmed the formation of only one regioisomer in both cases. The question was "which one?". Our initial attempt was 2D NMR studies for structural elucidation. Unfortunately, complexity of 2D NMR results (COSY, HSQC and HMBC) prevented us to provide conclusive evidence. Several crystallization attempts to get X-ray proof was also failed. Luckily, chemical shifts of indole hydrogen at the 2-position provided clear evidence for the identification of the regioisomers.

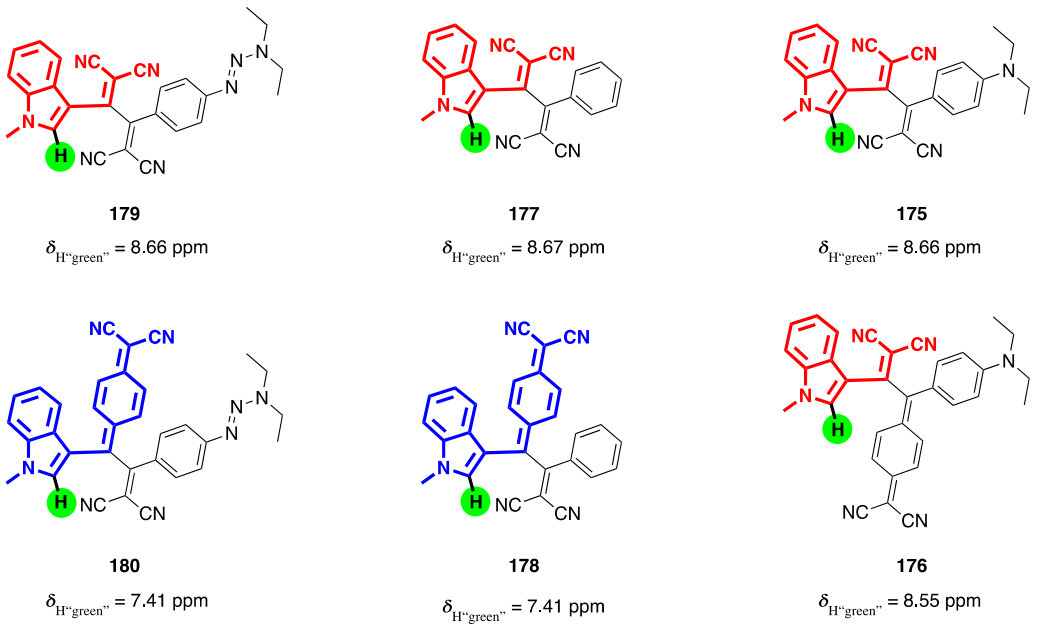

Scheme 43. Regioisomer structure confirmation by ^{1}H NMR analysis.

As can be seen in scheme 42, protons at the 2-position (highlighted in green) of indole ring in TCNE series **175**, **177** and **179** resonate at 8.66-8.67 ppm as singlets. When the deviation from the planarity in these molecules considered, these chemical shifts should be the outcome of (dicyanovinyl)indole (highlighted in red) substructures. Since the rest of structures is not in close proximity to the corresponding hydrogens, chemical shifts have not been affected much with different substituents such as, triazene, phenyl, and diethylaniline. In the series of TCNQ

products, protons at the 2-positions resonate at 7.41 for **178**/**180** and 8.55 ppm for **176**. This substantial difference in chemical shifts can be explained by the formation of different regioisomers. It is known in literature that dialkylaniline substituents are the best donor groups that can be utilized in the CA-RE reactions.[54] Similar structures and chemical shifts (8.66/8.67 ppm vs 8.55 ppm) for the protons at the 2 positions in compounds **175**, **177**, **179** and **176** confirmed that the dialkynaniline groups are stronger donor than indole. Accordingly, regioisomer **176** has been formed as only regioisomer. Slight difference in chemical shift should be originated from the quinoidal ring. On the other hand, chemical shift of 7.41 ppm was observed for compounds **178** and **180**. This substantial difference in chemical shifts can only be explained by the formation different regioisomers **178** and **180**. Since there is only one donor group (indole) in compound **178**, there is no doubt at the position of quinoidal ring (highlighted blue). With a simple comparison, it can be seen that the chemical shift of proton at the two position of indole is same in both **178** and **180**. This concludes that quinoidal ring should also be on the side of indole ring in **180**. In conclusion, the trend in donor strength follows the order diethylaniline > indole > diethyltriazene in corresponding series.

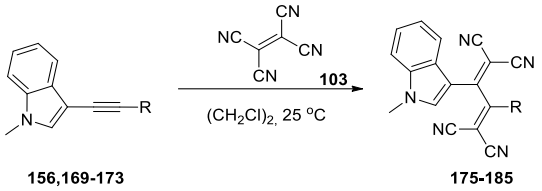

Table 2. [2+2] CA-RE of indole-substituted alkynes with TCNE.

Substrate	***R***	***Yield [%]***
175	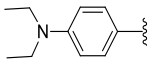	94%
177	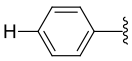	81%
179	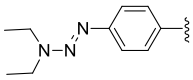	76%
181	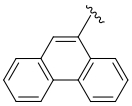	95%
183		95%
185	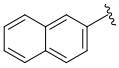	92%

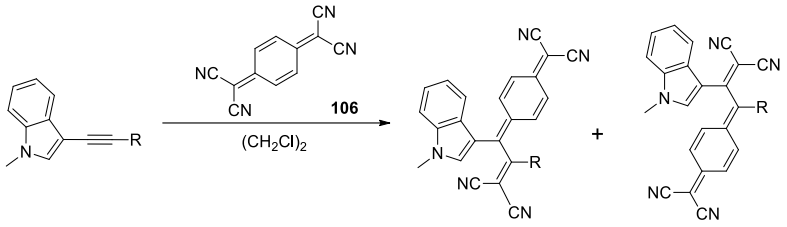

156, 169-173 178-186 176

Table 3. [2+2] CA-RE of indol-substituted alkynes with TCNQ.

Substrate	***R***	***Temperature***	***Yield [%]***
176	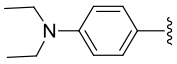	25 ºC	99%
178	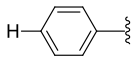	25 ºC	83%
180	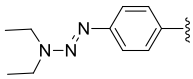	25 ºC	91%
182	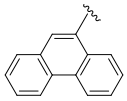	60 ºC	94%
184	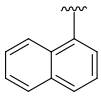	60 ºC	80%
186	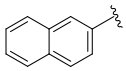	60 ºC	95%

In summary, we successfully came up with a solution to the stability problem of methyl-substituted alkynes and also synthesized new heterocyclic alkyne donor groups that have not been used in [2+2] CA-RE reactions in the literature.

3.2 UV-Vis Spectroscopy

The efficiency of the intramolecular charge transfer (ICT) interactions in the push-pull chromophores were measured by UV/Vis spectroscopy. Compounds **175-185** display intramolecular CT bands of various intensity with λ_{max}-values between 359 and 442 nm; 3.46–4.48 eV and ε-values between 9500 and 42000 M^{-1} cm^{-1} in CH_2Cl_2 (Figure 14). Especially, **175** and **179** display stronger CT band compared to other TCNE products (ε = 41963 M^{-1} cm^{-1} **175**, ε = 37185 M^{-1} cm^{-1} **179**) Also, some of the chromophores **183**, **185** show two different moderate-intensity CT band at different wavelengths. (367, 432, ε = 11786, 10370 M^{-1} cm^{-1} **183**; 359, 395 ε = 18033, 16928 M^{-1} cm^{-1} **185**). The phenyl-substituted chromophore **177** is lowest bathochromically shifted at 332 nm. (3.74 eV, ε =18268 M^{-1} cm^{-1}). These ICT bands are formed as a result of conjugation between the donor and acceptor parts of the chromophores. In products obtained by TCNE, there is correlation between electron-donor strength and λ_{max}-values. We observe that the ICT bands of **175** is bathochromically shifted and more intense with increasing electron-donor strength compared to others (λ_{max} ≈ 475 nm, ε = 41963 M^{-1} cm^{-1}).[72] The CT bands in the TCNE product series appear in the following sequence: λ_{max} = 332 nm (3.74 eV, **177**), 359, 395 nm (3.46 eV, 3.14 eV, **185**), 367, 432 nm (3.38 eV, 2.87 eV, **183**), 434 nm (2.86 eV, **181**), 442 nm (2.81 eV, **179**), 475 nm (2.61 eV, **175**).

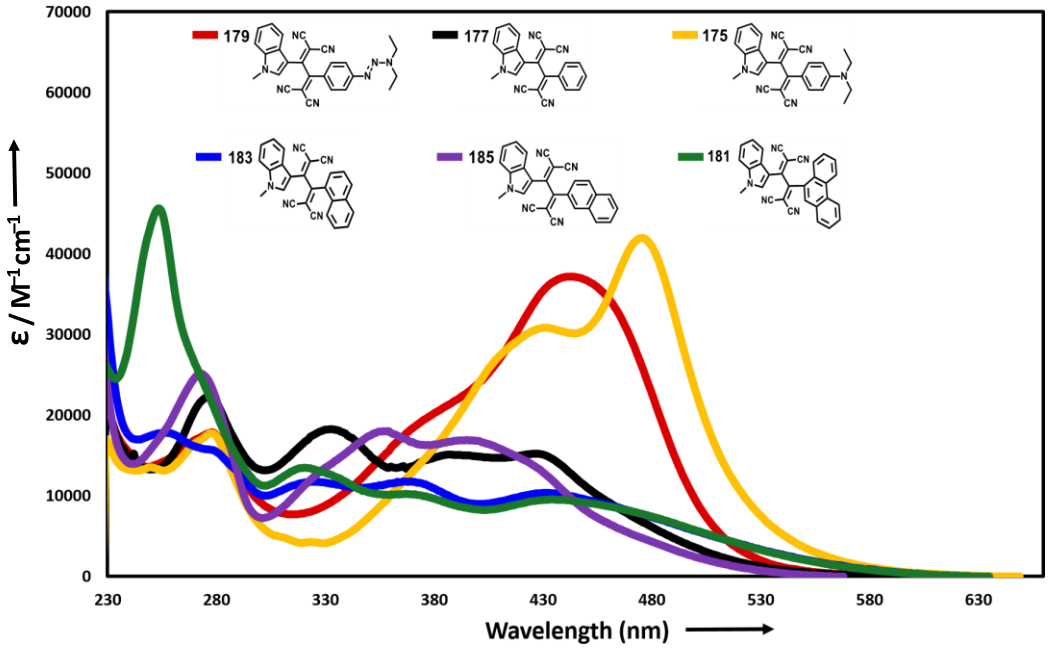

Figure 14. UV/Vis spectra of compounds **175** (yellow line), **177** (black line), **179** (red line), **181** (green line), **183** (dark-blue line) and **185** (purple line) in CH_2Cl_2 at 298 K.

Among all TCNE products, we selected compound **185** for solvatochromism studies (Figure 15). Less polar solutions of **185** exhibit light-yellow color, and polar solutions orange; with corresponding bathochromic shifts of approximately 11 nm (0.11 eV) from pure *n*-hexane (λ_{max} = 347 nm, 3.58 eV) to pure CH_2Cl_2 (λ_{max} = 358 nm, 3.47 eV).

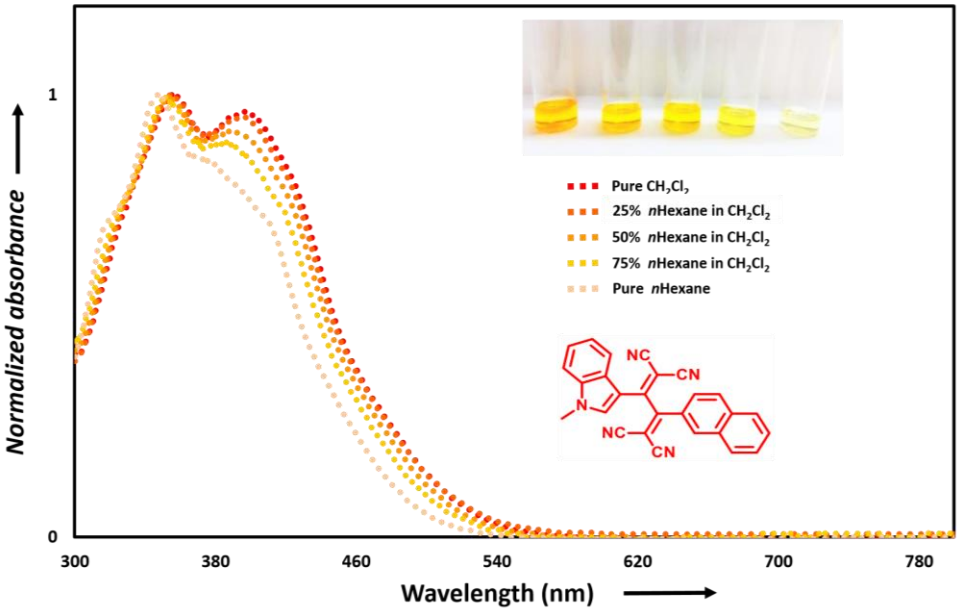

Figure 15. UV/Vis absorption spectra of chromophore **185** in CH_2Cl_2/*n*-hexane mixtures.

The absorption maxima of the π-conjugated chromophores, obtained by TCNQ reactions, exhibit intense CT bands (ε values between 13000 and 52000 M^{-1} cm^{-1} and λ_{max} values in the range of 402–682 nm (3.09–1.82 eV)) in CH_2Cl_2 with end-absorptions reaching to the NIR region (Figure 16). Similar to TCNE-based chromophores, there is a samilar correlation between donor strength and λ_{max}-values. The UV/Vis absorption spectrum of phenyl-substituted derivative **178** show the low-energy intramolecular CT band at 615 nm (2.02 eV; ε = 18842 M^{-1} cm^{-1}). However, other TCNQ-based structures feature CT transition at low energy and they are bathochromically shifted compared to the **175-185**. Diethylaniline-subtituted chromophore **176** is the most bathochromically shifted and shows strong intramolecular CT band at 682 nm (1.82 eV ε = 51101 M^{-1} cm^{-1}). Triazene-substituted chromophore is also bathochromically shifted and feature two close CT transitions of moderate intensity (**180**: $\lambda_{1,max}$ = 613 nm, 2.02 eV, ε = 28416 M^{-1} cm^{-1} and $\lambda_{2,max}$ = 402 nm, 3.09 eV, ε = 29167 M^{-1} cm^{-1}). The spectra of the napthaline-

substituted **190** and **192** display CT bands at λ_{max} = 654 (1.90 eV, ε = 18770 M^{-1} cm^{-1} **184**) and 618 nm (2.00 eV, ε = 19526 M^{-1} cm^{-1} **186**) (Figure 16). Lastly, the phenantrene derivative **182** show the lowest-energy intramolecular CT band at 660 nm (1.88 eV; e = 13968 M^{-1} cm^{-1}) compared to the other TCNQ products.

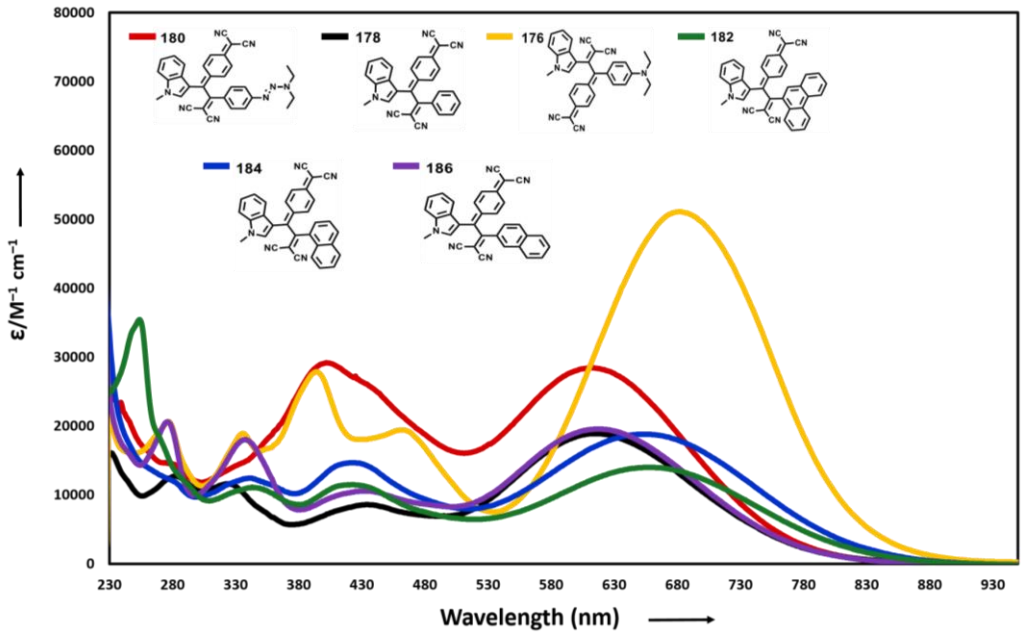

Figure 16. UV/Vis spectra of compounds **176** (yellow line), **178** (black line), **180** (red line), **182** (green line), **184** (dark-blue line) and **186** (purple line) in CH_2Cl_2 at 298 K.

All TCNQ products show bathochromic shift (positive solvatochromism) that further supports intramolecular CT interactions (Figure 17). Selected example **186** displays light purple in less polar solvent (*n*-hexane), and dark turquoise in more polar solvent (DCM); corresponding bathochromic shifts of approximately 70 nm (0.26 eV) are observed from pure *n*-hexane (λ_{max} = 546 nm, 2.27 eV) to pure CH_2Cl_2 (λ_{max} = 616 nm, 2.01 eV).

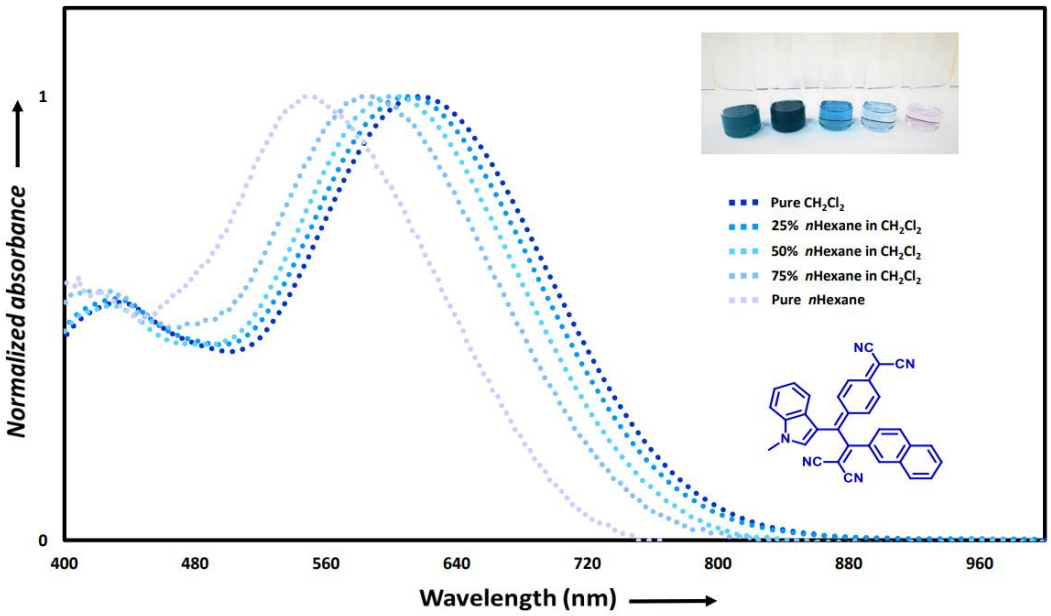

Figure 17. UV/Vis absorption spectra of chromophore **186** in CH_2Cl_2/*n*-hexane mixtures.

3.3 Computational Studies

After completing experimental studies and analyzing charge-transfer bands of reported compounds using UV/Vis spectroscopy, computational studies were utilized to examine optoelectronic properties of these molecules (Figure 18). All calculations (DFT and TD-DFT) were performed using Gaussian 09 program package.[100] For the computational studies, two chromophores **177** and **178** were selected. Firstly, the highest occupied molecular orbital (HOMO) and lowest unoccupied molecular orbital (LUMO) analyses has been done. Accordingly, we tried to explain ICT behavior in push-pull systems **177** and **178**. As can be seen in Figure 18, there is a substantial separation with distinct ovelap in frontier orbitals supporting ICT behaviour. The HOMO is mainly localized on methyl-indole part of the molecules and the LUMO covers cyano (CN)-rich side in selected chromophores.

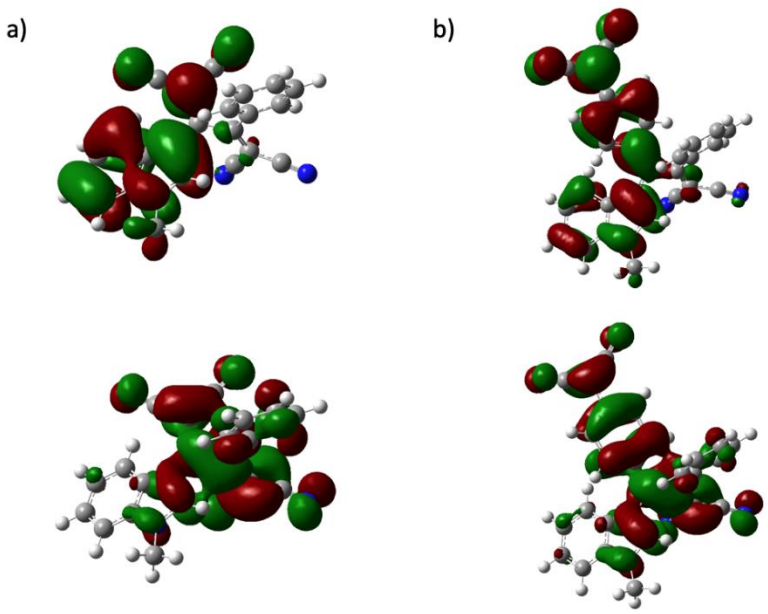

Figure 18. HOMO-LUMO orbital depiction of a) **177** and b) **178**. The upper plots represent the HOMOs, and the lower plots represent the LUMOs.

The selected molecules **177** and **178** were optimized at the CAM-B3LYP/6-31G(d)[93] level of theory with the CPCM solvation model in CH_2Cl_2. The vertical optical transitions were calculated by time-dependent density functional theory (TD-DFT) at the CAM-B3LYP/6-31G(d) level of theory, again with the CPCM solvation model in CH_2Cl_2 using the software package Gaussian 09.[94] In TCNE product **177**, the experimental UV/Vis spectra and corresponding theoretical spectra are in good agreement in terms of λ_{max} values (Figure 19a). Scaling of extinction coefficients was also required (scaled by 1.5) since these values are slightly overestimated by TD-DFT calculations. In figure 19b exhibit both theoretical and experimental UV/Vis spectra for TCNQ molecule **178**. The coherence between computed transition energies and experimental values of compound **178** are relatively better compared to TCNE product **177**. Extinction coefficients was scaled by 2.9 since overestimation was also seen in this case. TD-DFT results confirms charge-transfer bands originated from HOMO to LUMO transitions in chromophores **177** and **178**.

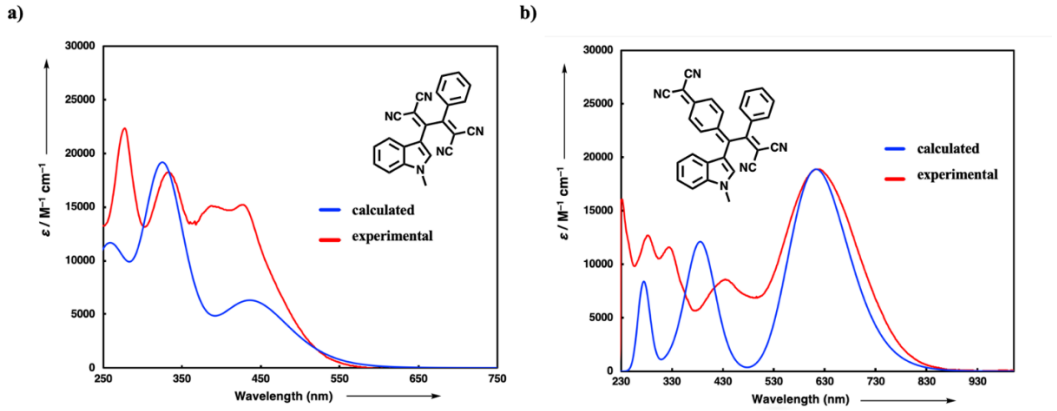

Figure 19. **a)** Calculated (scaled by 1.5, blue line) TD-DFT:CAM-B3LYP/6–31G(d) level of theory in CH_2Cl_2 and experimental UV/Vis spectrum of **177** in CH_2Cl_2 (red line). **b)** Calculated (scaled by 2.9, blue line) TD-DFT:CAM-B3LYP/6–31G(d) level of theory in CH_2Cl_2 and experimental UV/Vis spectrum of **178** in CH_2Cl_2 (red line).

CHAPTER 4

CONCLUSION

In the first part of thesis, six different triazene-substituted alkyne donors were synthesized and characterized to be used for the first time in thermal [2+2] cycloaddition reactions. Also, these activated alkynes' reactivity was tested toward [2+2] cycloadditions by using DDQ as an acceptor. The reactions between alkynes and DDQ occur in good yields under mild conditions without any catalysts. Due to these salient properties of the method used, target new class of push-pull chromophores were synthesized easily. Optoelectronic properties of DDQ adducts were investigated in detail by UV/Vis Spectroscopy. All these homoconjugated push-pull structures exhibit close intramolecular charge transfer bands in the visible region. And also, they show positive solvatochromism. In addition to UV/Vis studies, electronic/optical properties of homoconjugated dyes were investigated by using computational methods. As a result of these theoretical calculations, it was concluded that the target triazene-substituted alkynes are a highly effective donor group.

In the second part of thesis, different methyl-indole-substituted alkyne derivatives were synthesized via Sonagashira cross-coupling reactions as new donor substrates for [2+2] CA-RE reactions. Structural properties of the alkynes were characterized by using different spectroscopic techniques such as ^{1}H and ^{13}C NMR analysis, IR, and HRMS. Their donor properties were illustrated towards [2+2] CA-RE reactions. With these donor-substituted alkynes and acceptors (TCNE and TCNQ), click-type CA-RE reactions provided very colorful push-pull chromophores in high efficiency. Optoelectronic features of new TCNE and TCNQ product series were investigated by comprehensive study, involving X-ray analysis, UV/Vis spectroscopy, and computational analysis. Solvatochromism studies displayed red shift providing further proof of the intramolecular CT interaction for synthesized

chromophores. UV-Vis spectroscopy studies revealed high-energy CT bands in TCNQ product series. Compared to TCNQ product series, TCNE products exhibit hypsochromically shifted charge-transfer bands.

CHAPTER 5

EXPERIMENTAL

5.1 Materials and Methods

Reagents were purchased as reagent grade and used without further purification. Commercially available chemicals were purchased by Merck, Fluka, Across, Abcr and Sigma Aldrich.

Solvents for extraction or Flash column chromatography were distilled.

Reactions on exclusion of air and moisture were performed in oven-dried glassware and under N_2 atmosphere.

Analytical thin layer chromatography (TLC) was performed on aluminum sheets coated with 0.2 mm silica gel 60 F254 (Merck) and visualized with a UV lamp (254 or 366 nm).

Evaporation in vacuo was performed at 25–60 °C and 900–10 mbar. Reported yields refer to spectroscopically and chromatographically pure compounds that were dried under high vacuum (0.1–0.05 mbar) before analytical characterization.

Nuclear magnetic resonance (NMR) spectra were recorded on Bruker Avance III Ultrashield 400 Hz NMR spectrometer in $CDCl_3$. Chemical shifts δ are reported in ppm downfield from tetramethylsilane (TMS) using the residual solvent signals as an internal reference ($CDCl_3$: δ_H = 7.26 ppm, δ_C = 77.16 ppm. For ^{1}H NMR, coupling constants *J* are reported in Hz and the resonance multiplicity is defined as s (singlet), d (doublet), t (triplet), q (quartet), quint (quintet), sext (sextet), sept (septet), m (multiplet), and br. (broad). All spectra were recorded at 298 K. NMR spectra were processed by using MestReNova program.

Infrared (IR) Spectra were recorded on Thermo Scientific Nicolet iS10 ATR-IR spectrometer. Signal locations are reported as wavenumbers (cm^{-1}). The IR band intensities described as s (strong), m (medium), w (weak), br. (broad).

High-resolution mass spectrometry (HR-MS) was performed by the MS-service of the National Nanotechnology Research Center (UNAM) at Bilkent University and mass spectra recorded by LC-MS TOF electrospray ionization. Also, some HRMS result were obtained by MS-service of METU Center Laboratory. Spectra were processed in electro spray ionization with positive mode using Time of Flight mass analyzer. Masses are reported in m/z units as the molecule ion as $[M + H]^+$.

5.2 Synthetic Procedure

5.2.1 General Procedure of Triazene-Substituted Compounds 141a-f[91]

4-Iodoaniline **(140)** (1 g, 4.57 mmol, 1 equiv.) was dissolved in 38 mL of acetonitrile, 16 mL of water and 1.6 mL of concentrated hydrochloric acid was added subsequently, and the mixture was cooled to 0 °C. A solution of 1.1 equiv. of $NaNO_2$ (346.5 mg, 5.02 mmol) in 2 mL water was added slowly *via* syringe and the mixture was stirred for 45 min at 0 °C. Then, the mixture was transferred to a flask containing 3.4 equiv. K_2CO_3 (2.15 g, 15.52 mmol), dialkylamine (2 equiv.) in 25 mL of H_2O at 0 °C. The reaction was allowed to reach room temperature and stirred at this temperature for 2 hours before being extracted with EtOAc (3x100 mL). After extraction, the organic phase was dried over $MgSO_4$ and solvent was evaporated. A column chromatography (CC) (SiO_2; hexane/ethyl acetate) provided **141a-f** in 78–97% yields.

Compound 141a:

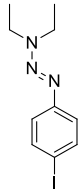

Yield: 1.16 g; a dark-orange liquid; 84%; CC: (SiO_2; 9:1 hexanes/ethyl acetate); R_f = 0.57 (SiO_2; 9:1 hexanes/ethyl acetate; ^{1}H NMR (400 MHz, $CDCl_3$, 298 K): δ = 1.20–1.33 (m, 6 H), 3.75 (q, J = 7.2 Hz, 4 H), 7.16 (quasi d, AA'part of AA'XX'-system, J = 8.7 Hz, 2 H), 7.61 ppm (quasi d, XX'part of AA'XX'-system, J = 8.7 Hz, 2 H); ^{13}C NMR (100 MHz, $CDCl_3$, 298 K): δ = 150.8, 137.6, 122.5, 89.0, 48.7, 41.1, 14.1, 11.5 ppm; HRMS: m/z calcd for $C_{10}H_{15}IN_3$: 304.03141; found: 304.03052 $[M + H]^+$.

Compound 141b:

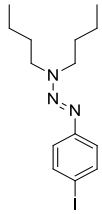

Yield: 1.42 g; an orange liquid; 87%; CC: (SiO_2; hexane); R_f = 0.82 (SiO_2; 9:1 hexane/ethyl acetate); ^{1}H NMR (400 MHz, $CDCl_3$, 298 K): δ = 0.95 (t, J = 7.3 Hz, 6 H), 1.35 (h, J = 7.3 Hz, 4 H), 1.58–1.72 (m, 4 H), 3.68 (t, J = 7.4 Hz, 4 H), 7.16 (quasi d, AA'part of AA'XX'-system, J = 8.6 Hz, 2 H), 7.61 ppm (quasi d, XX'part of AA'XX'-system, J = 8.6 Hz, 2 H); ^{13}C NMR (100 MHz, $CDCl_3$, 298 K): δ = 151.1, 137.8, 122.6, 89.0, 54.3, 46.5, 31.1, 28.2, 20.3, 14.0 ppm; HRMS: m/z calcd for $C_{14}H_{23}IN_3$: 360.09402; found: 360.09312 $[M + H]^+$.

Compound 141c:

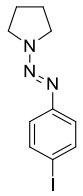

Yield: 1.07 g; a yellow solid; 78%; CC: (SiO_2; 9:1 hexanes/ethyl acetate); R_f = 0.32 (SiO_2; 9:1 hexanes/ethyl acetate); m.p.= 112–114 °C; ^{1}H NMR (400 MHz, $CDCl_3$, 298 K): δ = 1.98–2.06 (m, 4 H), 3.45–4.00 (m, 4 H), 7.17 (quasi d, AA'part of AA'XX'-system, J = 8.7 Hz, 2 H), 7.61 ppm (quasi d, XX'part of AA'XX'-system, J = 8.7 Hz, 2 H); ^{13}C NMR (100 MHz, $CDCl_3$, 298 K): δ = 151.2, 137.9, 122.5, 89.2, 51.4, 46.5, 23.9 ppm; HRMS: m/z calcd for $C_{10}H_{13}IN_3$: 302.01599; found: 302.01487 $[M+ H]^+$.

Compound 141d:

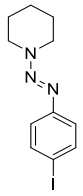

Yield: 1.21 g; a yellow solid; 84%; CC: (SiO_2; 9:1 hexane/ethyl acetate); R_f = 0.62 (SiO_2; 9:1 hexane/ethyl acetate); m.p.= 67–69 °C; ^{1}H NMR (400 MHz, $CDCl_3$, 298 K): δ = 1.66–1.76 (m, 6 H), 3.73–3.83 (m, 4 H), 7.18 (quasi d, AA'part of AA'XX'-system, J = 8.7 Hz, 2 H), 7.63 ppm (quasi d, XX'part of AA'XX'-system, J = 8.7 Hz, 2 H); ppm; ^{13}C NMR (100 MHz, $CDCl_3$, 298 K): δ = 150.4, 137.7, 122.5, 89.7, 47.8, 25.2, 24.3 ppm; HRMS: m/z calcd for $C_{11}H_{15}IN_3$: 316.03178; found: 316.03052 $[M + H]^+$.

Compound 141e:

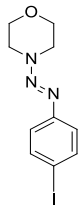

Yield: 1.17 g; a yellow solid; 81%; CC: (SiO_2; 7:3 hexanes/ethyl acetate); R_f = 0.33 (SiO_2; 9:1 hexanes/ethyl acetate); m.p.= 136–138 °C; ^{1}H NMR (400 MHz, $CDCl_3$, 298 K): δ = 3.79 (dd, J = 6.0 and 4.2 Hz, 4 H), 3.85 (dd, J = 6.0 and 4.2 Hz, 4 H), 7.19 (quasi d, AA'part of AA'XX'-system, J = 8.6 Hz, 2 H), 7.66 ppm (quasi d, XX'part of AA'XX'-system, J = 8.6 Hz, 2 H); ^{13}C NMR (100 MHz, $CDCl_3$, 298 K): δ = 149.7, 137.9, 122.8, 90.9, 66.4, 48.0 ppm; HRMS: m/z calcd for $C_{10}H_{13}IN_3O$: 318.00969; found: 318.00978 $[M + H]^+$.

Compound 141f:

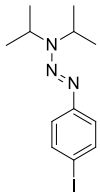

Yield: 1.47 g; a yellowish liquid; 97%; CC: (SiO_2; 9:1 hexane/ethyl acetate); R_f = 0.80 (SiO_2; 9:1 hexane/ethyl acetate); ^{1}H NMR (400 MHz, $CDCl_3$, 298 K): δ = 1.15–1.45 (m, 12 H), 3.85–4.15 (m, 1 H), 5.10–5.45 (m, 1 H), 7.16 (quasi d, AA'part of AA'XX'-system, J = 8.7 Hz, 2 H), 7.61 ppm (quasi d, XX'part of AA'XX'-system, J = 8.7 Hz, 2 H); ppm; ^{13}C NMR (100 MHz, $CDCl_3$, 298 K): δ = 151.5, 137.7, 122.4, 88.6, 48.9, 46.1, 23.9, 19.5 ppm; HRMS: m/z calcd for $C_{12}H_{19}IN_3$: 332.06197; found: 332.06182 $[M + H]^+$.

5.2.2 General Procedure of TMS-protecting Alkyne Derivatives[91]

In a 100 mL two-neck round bottom flask compound **141a-f** (2.50 mmol, 1 equiv.), bis (triphenylphosphine) palladium (II) chloride (0.075 mmol, 0.03 equiv.) and copper iodide (0.075 mmol, 0.03 equiv.) were added. The flask was flushed with nitrogen and triethylamine (20 mL) was added *via* syringe into flask, followed by addition of trimethylsilyacetylene (2.75 mmol, 1.10 equiv.). After stirring overnight at 25 °C, the reaction mixture was quenched with water, extracted with dichloromethane (3 x 100 mL), dried over $MgSO_4$ and filtered. The solvent was removed under reduced pressure and **142a-f** was isolated in 71–91% yields by performing column chromotograhy (CC) (SiO_2; hexane/ethyl acetate).

Compound 142a:

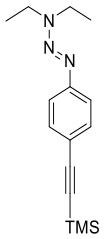

Yield: 615 mg; a brown solid; 90%; CC: (SiO_2; 9:1 hexane/ethyl acetate); R_f = 0.57 (SiO_2; 9:1 hexane/ethyl acetate); m.p.= 40–42 °C; ^{1}H NMR (400 MHz, $CDCl_3$, 298 K): δ = 0.25 (s, 9 H), 1.21–1.32 (m, 6 H), 3.76 (q, J = 7.2 Hz, 4 H), 7.34 (quasi d, AA'part of AA'XX'-system, J = 8.7 Hz, 2 H), 7.43 ppm (quasi d, XX'part of AA'XX'-system, J = 8.7 Hz, 2 H); ^{13}C NMR (100 MHz, $CDCl_3$, 298 K): δ = 151.2, 132.7, 120.3, 119.3, 105.9, 93.5, 48.4, 41.2, 13.8, 12.1, 0.2 ppm; HRMS: m/z calcd for $C_{15}H_{24}N_3Si$: 274.17389; found: 274.17340 $[M + H]^+$.

Compound 142b:

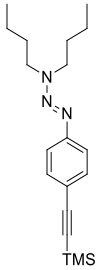

Yield: 610 mg; an orange liquid; 74%; CC: (SiO_2; 9:1 hexane/ethyl acetate); R_f = 0.15 (SiO_2; hexane); ^{1}H NMR (400 MHz, $CDCl_3$, 298 K): δ = 0.24 (s, 9 H), 0.95 (t, J = 7.3 Hz, 6 H), 1.36 (h, J = 7.3 Hz, 4 H), 1.57–1.75 (m, 4 H), 3.69 (t, J = 7.3 Hz, 4 H), 7.33 (quasi d, AA'part of AA'XX'-system, J = 8.5 Hz, 2 H), 7.42 ppm (quasi d, XX'part of AA'XX'-system, J = 8.5 Hz, 2 H); ^{13}C NMR (100 MHz, $CDCl_3$, 298 K): δ = 151.3, 132.8, 120.3, 119.3, 106.0, 93.6, 53.0, 46.7, 31.2, 28.3, 20.4, 14.0. 0.2 ppm; HRMS: m/z calcd for $C_{19}H_{32}N_3Si$: 330.23694; found: 330.23600 $[M + H]^+$.

Compound 142c:

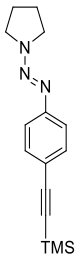

Yield: 611 mg; a yellow solid; 90%; CC: (SiO_2; 9:1 hexanes/ethyl acetate); R_f = 0.56 (SiO_2; 9:1 hexanes/ethyl acetate); m.p.= 111–113 °C; ^{1}H NMR (400 MHz, $CDCl_3$, 298 K): δ = 0.24 (s, 9 H), 1.96–2.08 (m, 4 H), 3.60–4.00 (m, 4 H), 7.34 (quasi d, AA'part of AA'XX'-system, J = 8.6 Hz, 2 H), 7.43 ppm (quasi d, XX'part of AA'XX'-system, J = 8.6 Hz, 2 H); ^{13}C NMR (100 MHz, $CDCl_3$, 298 K): δ = 151.5, 132.9, 120.3, 119.5, 105.9, 93.7, 23.9, 0.2 ppm (8 out of 9 signals expected); HRMS: m/z calcd for $C_{15}H_{22}N_3Si$: 272.15884; found: 272.15775 $[M + H]^+$.

Compound 142d:

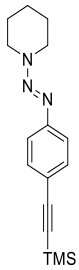

Yield: 507 mg; dark brown solid; 71%; CC: (SiO_2; 9:1 hexane/ethyl acetate); R_f = 0.78 (SiO_2; 9:1 hexane/ethyl acetate); m.p.= 72–73 °C; ^{1}H NMR (400 MHz, $CDCl_3$, 298 K): δ = 0.25 (s, 9 H), 1.65–1.77 (m, 6 H), 3.77–3.86 (m, 4 H), 7.36 (quasi d, AA'part of AA'XX'-system, J = 8.7 Hz, 2 H), 7.44 ppm (quasi d, XX'part of AA'XX'-system, J = 8.7 Hz, 2 H); ^{13}C NMR (100 MHz, $CDCl_3$, 298 K): δ = 150.8, 132.7, 120.4, 119.8, 105.8, 93.7, 48.0, 25.3, 24.4, 0.2 ppm; HRMS: m/z calcd for $C_{16}H_{24}N_3Si$: 286.17390; found: 286.17340 $[M + H]^+$.

Compound 142e:

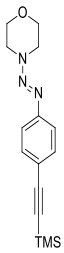

Yield: 654 mg; a brown solid; 91%; CC: (SiO_2; 9:1 hexanes/ethyl acetate); R_f = 0.36 (SiO_2; 9:1 hexanes/ethyl acetate); m.p.= 86–88 °C; ^{1}H NMR (400 MHz, $CDCl_3$, 298 K): δ = 0,26 (s, 9 H), 3.74–3.80 (m, 4 H), 3.81–3.86 (m, 4 H), 7.39 (quasi d, AA'part of AA'XX'-system, J = 8.6 Hz, 2 H), 7.46 ppm (quasi d, XX'part of AA'XX'-system, J = 8.6 Hz, 2 H); ^{13}C NMR (100 MHz, $CDCl_3$, 298 K): δ = 150.0, 132.8, 120.8, 120.7, 105.5, 94.4, 66.4, 48.1, 0.1 ppm; HRMS: m/z calcd for $C_{15}H_{22}N_3OSi$: 288.15306; found: 288.15267 $[M + H]^+$.

Compound 142f:

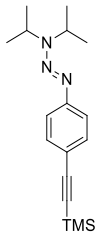

Yield: 543 mg; a yellow solid; 72%; CC: (SiO_2; 9:1 hexane/ethyl acetate); R_f = 0.84 (SiO_2; 9:1 hexane/ethyl acetate); m.p.= 82–84 °C; ^{1}H NMR (400 MHz, $CDCl_3$, 298 K): δ = 0.25 (s, 9 H), 1.17–1.45 (m, 12 H), 3.86–4.13 (m, 1 H), 5.16–5.43 (m, 1 H), 7.34 (quasi d, AA'part of AA'XX'-system, *J* = 8.6 Hz, 2 H), 7.42 ppm (quasi d, XX'part of AA'XX'-system, *J* = 8.6 Hz, 2 H); ^{13}C NMR (100 MHz, $CDCl_3$, 298 K): *δ* = 151.8, 132.8, 120.2, 119.0, 106.1, 93.4, 49.1, 46.3, 23.9, 19.6, 0.2 ppm; HRMS: m/z calcd for $C_{17}H_{28}N_3Si$: 302.20591; found: 302.20470 $[M + H]^+$.

5.2.3 General procedure of Triazene-Substituted Alkyne[91]

Compounds **142a-f** (1.55 mmol, 1 equiv.) was dissolved in methanol (25 mL) and potassium carbonate (5.12 mmol, 3.3 equiv.) was added to this solution. After filtration, evaporation and column chromatography (CC) (SiO_2; hexanes/ethyl acetate) alkynes **143a-f** were obtained in 30–77% yields.

Compound 143a:

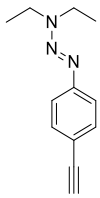

Yield: 240 mg; a dark-orange liquid; 77%; CC: (SiO_2; 9:1 hexanes/ethyl acetate); R_f = 0.52 (SiO_2; 9:1 hexanes/ethyl acetate); ^{1}H NMR (400 MHz, $CDCl_3$, 298 K): *δ* = 1.20–1.35 (m, 6 H), 3.07 (s, 1H), 3.77 (q, *J* = 7.1 Hz, 4 H), 7.36 (quasi d, AA'part of AA'XX'-system, *J* = 8.7 Hz, 2 H), 7.45 ppm (quasi d, XX'part of AA'XX'-system,

J = 8.7 Hz, 2 H); ^{13}C NMR (100 MHz, $CDCl_3$, 298 K): δ = 151.5, 132.8, 120.4, 118.2, 84.3, 76.8, 48.8, 41.3, 14.2, 11.9 ppm; HRMS: m/z calcd for $C_{12}H_{16}N_3$: 202.13434; found: 202.13387 $[M + H]^+$.

Compound 143b:

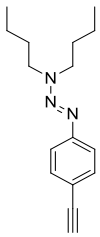

Yield: 267 mg; an orange liquid; 67%; CC: (SiO_2; hexane); R_f = 0.14 (SiO_2; 9:1 hexane/ethyl acetate); ^{1}H NMR (400 MHz, $CDCl_3$, 298 K): δ = 0.95 (t, J = 7.3 Hz, 6 H), 1.36 (h, J = 7.3 Hz, 4 H), 1.55–1.73 (m, 4 H), 3.07 (s, 1 H), 3.70 (t, J = 7.4 Hz, 4 H), 7.35 (quasi d, AA'part of AA'XX'-system, J = 8.4 Hz, 2 H), 7.45 ppm (quasi d, XX'part of AA'XX'-system, J = 8.4 Hz, 2 H); ^{13}C NMR (100 MHz, $CDCl_3$, 298 K): δ = 151.5, 132.8, 120.4, 118.2, 84.4, 76.7, 54.5, 46.7, 31.1, 28.1, 20.3, 13.9 ppm; HRMS: m/z calcd for $C_{16}H_{24}N_3$: 258.19751; found: 258.19647 $[M + H]^+$.

Compound 143c:

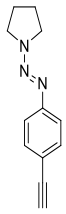

Yield: 207 mg; a yellow solid; 67%; CC: (SiO_2; 9:1 hexane/ethyl acetate); R_f = 0.41 (SiO_2; 9:1 hexane/ethyl acetate); m.p.= 96–98 °C; ^{1}H NMR (400 MHz, $CDCl_3$, 298 K): δ = 1.96–2.08 (m, 4 H), 3.07 (s, 1 H), 3.45–4.15 (m, 4 H), 7.36 (quasi d, AA'part of AA'XX'-system, J = 8.6 Hz, 2 H), 7.45 ppm (quasi d, XX'part of AA'XX'-system, J = 8.6 Hz, 2 H); ^{13}C NMR (100 MHz, $CDCl_3$, 298 K): δ = 151.7, 132.9, 120.3, 118.2, 84.2, 76.8, 51.1, 46.4, 23.7 ppm; HRMS: m/z calcd for $C_{12}H_{14}N_3$: 200.11893; found: 200.11822 $[M + H]^+$.

Compound 143d:

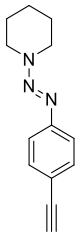

Yield: 205 mg; a light brown solid; 62%; CC: (SiO_2; 9:1 hexane/ethyl acetate); R_f = 0.69 (SiO_2; 9:1 hexane/ethyl acetate); m.p.= 53–54 °C; ^{1}H NMR (400 MHz, $CDCl_3$, 298 K): δ = 1.67–1.76 (m, 6 H), 3.08 (s, 1 H), 3.76–3.85 (m, 4 H), 7.38 (quasi d, AA'part of AA'XX'-system, J = 8.7 Hz, 2 H), 7.46 ppm (quasi d, XX'part of AA'XX'-system, J = 8.7 Hz, 2 H); ^{13}C NMR (100 MHz, $CDCl_3$, 298 K): δ = 151.0, 132.8, 120.4, 118.7, 84.1, 77.05, 48.1, 25.3, 24.2 ppm; HRMS: m/z calcd for $C_{13}H_{16}N_3$: 214.13487; found: 214.13387 $[M + H]^+$.

Compound 143e:

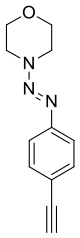

Yield: 100 mg; a pale yellow solid; 30%; CC: (SiO_2; 9:1 hexanes/ethyl acetate); R_f = 0.45 (SiO_2; 9:1 hexanes/ethyl acetate); m.p.= 154–156 °C; ^{1}H NMR (400 MHz, $CDCl_3$, 298 K): δ = 3.10 (s, 1 H), 3.76–3.82 (m, 4 H), 3.83–3.89 (m, 4 H), 7.40 (quasi d, AA'part of AA'XX'-system, J = 8.6 Hz, 2 H), 7.48 ppm (quasi d, XX'part of AA'XX'-system, J = 8.6 Hz, 2 H); ^{13}C NMR (100 MHz, $CDCl_3$, 298 K): δ = 150.3, 133.0, 120.9, 119.8, 84.0, 77.4, 66.5, 48.0 ppm; HRMS: m/z calcd for $C_{12}H_{14}N_3O$: 216.11378; found: 216.11314 $[M + H]^+$.

Compound 143f:

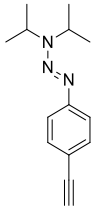

Yield: 227 mg; a brown solid; 64%; CC: (SiO_2; 9:1 hexane/ethyl acetate); R_f = 0.72 (SiO_2; 9:1 hexane/ethyl acetate); m.p.= 43–45 °C; ^{1}H NMR (400 MHz, $CDCl_3$, 298 K): δ = 1.15–1.45 (m, 12 H), 3.06 (s, 1 H), 3.85–4.20 (m, 1 H), 5.15–5.45 (m, 1 H), 7.36 (quasi d, AA'part of AA'XX'-system, *J* = 8.4 Hz, 2 H), 7.45 ppm (quasi d, XX'part of AA'XX'-system, *J* = 8.4 Hz, 2 H); ^{13}C NMR (100 MHz, $CDCl_3$, 298 K): *δ* = 152.0, 132.8, 120.2, 117.9, 84.4, 76.7, 49.0, 46.2, 23.9, 19.4 ppm; HRMS: m/z calcd for $C_{14}H_{20}N_3$: 230.16565; found: 230.16517 $[M + H]^+$.

5.2.4 General Procedure of Homoconjugated Push-Pull Chromophores[91]

A solution of **143a-f** (1.50 mmol, 1 equiv.) and DDQ **94** (1.80 mmol, 1.2 equiv.) in dichloromethane (20 mL) was stirred at 25 °C until complete consumption of starting material based on TLC analysis. Evaporation and CC (SiO_2; CH_2Cl_2) gave (±)-**145a-f** in 19–73 % yields.

Compound (±)-**144a:**

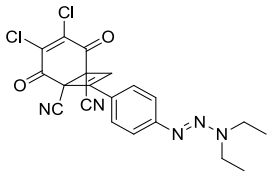

Yield: 385 mg; a dark-orange solid; 60%; CC: (SiO_2; CH_2Cl_2); R_f = 0.11 (SiO_2; CH_2Cl_2); m.p.= 167–168 °C decomposition; ^{1}H NMR (400 MHz, $CDCl_3$, 298 K): *δ* = 1.15–1.40 (m, 6 H), 3.81 (q, *J* = 7.1 Hz, 4 H), 6.52 (s, 1 H), 7.45–7.53 (m, 4 H);

^{13}C NMR (100 MHz, $CDCl_3$, 298 K): δ = 177.3, 176.8, 154.7, 150.6, 143.2, 142.9, 127.5, 124.1, 123.2, 121.4, 112.1, 111.9, 54.8, 51.6, 49.5, 41.6, 14.5, 11.3 ppm; UV/vis (CH_2Cl_2): λ_{max} (ε) = 238 (11500), 286 (13700), 352 (27600), 440 nm (3700 M^{-1} cm^{-1}); HRMS: m/z calcd for $C_{20}H_{16}Cl_2N_5O_2$: 428.06788; found: 428.06756 $[M + H]^+$.

Compound (±)**-144b:**

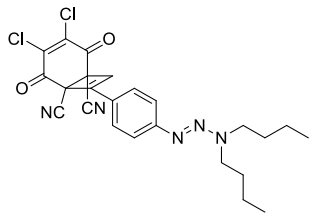

Yield: 392 mg; a red solid; 54%; CC: (SiO_2; 9:1 hexane/ethyl acetate); R_f = 0.25 (SiO_2; DCM); m.p.= 173–174 °C decomposition; ^{1}H NMR (400 MHz, $CDCl_3$, 298 K): δ = 0.90–1.02 (m, 6 H), 1.27–1.44 (m, 4 H), 1.54–1.76 (m, 4 H), 3.68–3.79 (m, 4 H), 6.52 (s, 1 H), 7.42–7.53 (m, 4 H); ^{13}C NMR (100 MHz, $CDCl_3$, 298 K): δ = 177.2, 176.8, 154.7, 150.4, 143.1, 142.9, 127.5, 124.0, 123.1, 121.3, 112.2, 111.9, 54.9, 54.8, 51.6, 47.1, 31.1, 28.1, 20.7, 20.0, 13.94, 13.86 ppm; UV/vis (CH_2Cl_2): λ_{max} (ε) = 240 (11400), 286 (13100), 356 (28100), 442 nm (3700 M^{-1} cm^{-1}); HRMS: m/z calcd for $C_{24}H_{24}Cl_2N_5O_2$: 484.13064; found: 484.13016 $[M + H]^+$.

Compound (±)**-144c:**

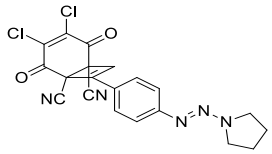

Yield: 121 mg; an orange solid; 19%; CC: (SiO_2; CH_2Cl_2); R_f = 0.33 (SiO_2; CH_2Cl_2); m.p.= 122–124 °C decomposition; ^{1}H NMR (400 MHz, $CDCl_3$, 298 K): δ = 1.94–2.14 (m, 4 H), 3.60–3.82 (m, 2 H), 3.90–4.10 (m, 2 H) 6.52 (s, 1 H), 7.43–7.54 (m, 4 H); ^{13}C NMR (100 MHz, $CDCl_3$, 298 K): δ = 177.3, 176.7, 154.8, 150.5, 143.2, 143.0, 127.5, 124.1, 123.3, 121,3, 112.1, 111.9, 54.8, 51.6, 47.0, 24.0, 23.7 ppm; UV/vis (CH_2Cl_2): λ_{max} (ε) = 234 (10100), 288 (11200), 354 (23700), 438 nm (3100

M^{-1} cm^{-1}); HRMS: m/z calcd for $C_{20}H_{14}Cl_2N_5O_2$: 426.05180; found: 426.05191 $[M + H]^+$.

Compound (±)**-144d:**

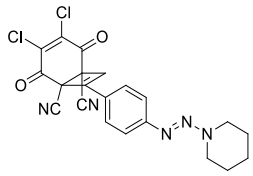

Yield: 350 mg; a brick red solid; 53%; CC: (SiO_2; DCM); R_f = 0.16 (SiO_2; DCM); m.p.= 174–175 °C; ^{1}H NMR (400 MHz, $CDCl_3$, 298 K): δ = 1.65–1.85 (m, 6 H), 3.80–3.95 (m, 4 H), 6.54 (s, 1 H), 7.45–7.60 (m, 4 H); ^{13}C NMR (100 MHz, $CDCl_3$, 298 K): δ = 177.3, 176.7, 154.2, 150.5, 143.2, 142.9, 127.5, 124.4, 123.7, 121.4, 112.1, 111.9, 54.9, 51.7, 41.5, 24.3, 22.7 ppm; UV/vis (CH_2Cl_2): λ_{max} (ε) = 236 (11100), 288 (13100), 352 (26200), 428 nm (3600 M^{-1} cm^{-1}); HRMS: m/z calcd for $C_{21}H_{16}Cl_2N_5O_2$: 440.06833; found: 440.06756 $[M + H]^+$.

Compound (±)**-144e:**

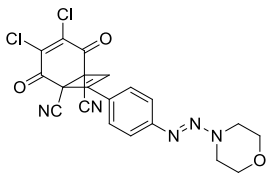

Yield: 318 mg; an orange solid; 48%; CC: (SiO_2; 19:1 hexane/ethyl acetate); R_f = 0.72 (SiO_2; 19:1 hexanes/ethyl acetate); m.p.= 172–174 °C; ^{1}H NMR (400 MHz, $CDCl_3$, 298 K): δ = 3.82–3.92 (m, 8 H), 6.58 (s, 1 H), 7.48–7.57 (m, 4 H); ^{13}C NMR (100 MHz, $CDCl_3$, 298 K): δ = 177.2, 176.6, 153.5, 150.4, 143.3, 143.1, 127.5, 125.1, 124.4, 121.8, 112.0, 111.8, 66.5, 54.8, 51.6 ppm (15 out of 16 signals); UV/vis (CH_2Cl_2): λ_{max} (ε) = 234 (12100), 290 (15600), 346 (26300), 430 nm (3800 M^{-1} cm^{-1}); HRMS: m/z calcd for $C_{20}H_{14}Cl_2N_5O_3$: 442.04676; found: 442.04682 $[M + H]^+$.

Compound (±)**-144f:**

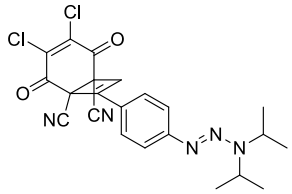

Yield: 500 mg; an orange-red solid; 73%; CC: (SiO_2; CH_2Cl_2); R_f = 0.44 (SiO_2; CH_2Cl_2); m.p.= 160–162 °C decomposition; ^{1}H NMR (400 MHz, $CDCl_3$, 298 K): δ = 1.25 (d, J = 6.7 Hz, 6 H), 1.40 (d, J = 6.7 Hz, 6 H), 4.05 (hept, J = 6.7 Hz, 1 H), 5.35 (hept, J = 6.7 Hz, 1 H), 6.51 (s, 1 H), 7.44–7.52 ppm (m, 4 H); ^{13}C NMR (100 MHz, $CDCl_3$, 298 K): δ = 177.3, 176.8, 155.2, 150.6, 143.2, 143.0, 127.5, 123.7, 122.9, 121.2, 112.1, 111.8, 54.8, 51.6, 49.7, 46.9, 24.0, 19.4 ppm; UV/vis (CH_2Cl_2): λ_{max} (ε) = 240 (11100), 286 (12600), 360 (27100), 448 nm (3500 M^{-1} cm^{-1}); HRMS: m/z calcd for $C_{22}H_{20}Cl_2N_5O_2$: 456.09802; found: 456.09886 $[M + H]^+$.

5.2.5 Synthetic Procedures for CA-RE products

Compound 148

To a solution of indole (1.0 g, 8.54 mmol, 1 equiv.) and potassium hydroxide (2.39 g, 42.68 mmol, 5 equiv.) in DMF (10 ml) was added iodomethane (2.42 g, 17 mmol). The reaction mixture was stirred at room temperature for 20 min. After 20 min., solution was filtered by using silica column. Then H_2O was added to the mixture. The water layer was extracted with DCM (2x50 ml). The organic layer was combined and dried over $MgSO_4$. *N*-methyl-1*H*-indole **148** was obtained as a yellow liquid. Yield: 692 mg; a; 62%. R_f = 0.73 (SiO_2; 1:1 hexanes/DCM).

Compound 149

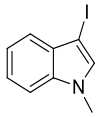

Potassium hydroxide (3.05 mmol, 2 equiv.) was added in a solution of methyl indole (1.52 mmol, 1 equiv.) in 5 mL DMF. Then, iodine was added into solution. The reaction mixture was stirred at room temperature for 10 min and checked by TLC. The reaction mixture is then poured into ice and water containing 10% $Na_2S_2O_3$. The white precipitate is filtered, wash with cold water, dried and weighed.[96,101] This compound could not be characterized because of the stability problem.

Compound 157

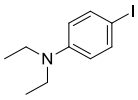

Target synthesis was carried out by following the literature. The data obtained are fully compatible with the literature. 4-iodoaniline **140** (6.00 g, 27.4 mmol), iodoethane (9.0 mL, 113 mmol) and sodium carbonate (5.10 g, 48.1 mmol) mixed in DMF (75 mL) at 70 °C for 14 h. Then, the solution was diluted with water (200 mL) and extracted with EtOAc (200 mL). After the organic phase was washed with brine (150 mL), it was dried over $MgSO_4$ and evaporated under vacuum. The target product was obtained after **157** column chromatography (SiO_2; hexane) as a dark-yellow liquid. (630 mg, 50%; R_f = 0.4 (SiO_2; hexane)). ^{1}H NMR (400 MHz, $CDCl_3$, 298 K): δ = 1.14 (t, J = 7.1 Hz, 6 H), 3.32 (q, J = 7.1 Hz, 4 H), 6.45 (d, J = 9.0 Hz, 2 H), 7.43 ppm (d, J = 9.0 Hz, 2 H); ^{13}C NMR (100 MHz, $CDCl_3$, 298 K): δ = 147.7, 138.2, 114.6, 76.1, 44.8, 12.8 ppm. Spectral data was consistent with literature.[98]

Compound 158

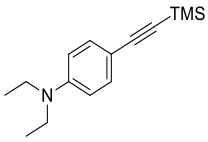

In a 100 mL round bottom flask compound **157** (1.00 mmol, 1 equiv.), bis (triphenylphosphine) palladium (II) dichloride (0.09 mmol, 0.03 equiv.) and copper iodide (0.09 mmol, 0.03 equiv.) were added. The flask was flushed with nitrogen for 30 minutes, triethylamine (15 mL) added *via* syringe into flask and flushed with nitrogen for an additional 30 minutes, followed by addition of trimethylsilyacetylene (3.40 mmol, 1,1 equiv.). After stirring overnight at 25 °C, the solvents were removed under reduced pressure, target TMS-protected alkynes **158** were isolated in 86% yields by performing column chromotograhy (CC) (SiO_2; Hexane/EtOAc 9:1). (520 mg, 86%; R_f = 0.4 (SiO_2; hexane)). ^{1}H NMR (400 MHz, $CDCl_3$, 298 K): δ = 0.23 (s, 9H), 1.16 (t, J = 7.1 Hz, 6H), 3.35 (q, J = 7.1 Hz, 4H), 6.55 (d, J = 9.0 Hz, 2H), 7.31 (d, J = 9.0 Hz, 2H). Spectral data was consistent with literature.[98]

Compound 159

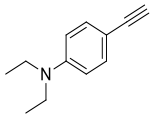

TMS-protected alkynes (1.00 mmol, 1 equiv.) were dissolved in methanol (15 mL). Then, potassium carbonate (9.50 mmol, 3.30 equiv.) was added to this solution. After filtration, evaporation, and column chromatography (CC) (SiO_2; Hexane/EtOAc 9:1) terminal alkynes **159** were obtained in 81% yields. ^{1}H NMR (400 MHz, $CDCl_3$, 298 K): δ = 1.17 (t, J = 7.0 Hz, 6H), 2.97 (s, 1H), 3.35 (q, J = 7.1 Hz, 4H), 6.58 (d, J = 9.0 Hz, 2H), 7.34 (d, J = 9.0 Hz, 2H). Spectral data was consistent with literature.[98]

General procedure of Synthesis of TMS-protected alkynes 161, 164, and 167

In a 25 mL round bottom flask aryl bromide (1.00 mmol, 1 equiv.), bis (triphenylphosphine) palladium (II) dichloride (0.09 mmol, 0.09 equiv.) and copper iodide (0.09 mmol, 0.09 equiv.) were added. The flask was flushed with nitrogen for 30 minutes, toluene (6 mL) and diisopropylamine (3 mL) were added *via* syringe into flask and flushed with nitrogen for an additional 15 minutes, followed by addition of trimethylsilyacetylene (3.00 mmol, 3 equiv.). After stirring overnight at 60 °C, the solvents were removed under reduced pressure, target TMS-protected alkynes **161**, **164**, and **167** were isolated in 78–92% yields by performing column chromotograhy (CC) (SiO_2; *c*-hexane).

Compound 161:

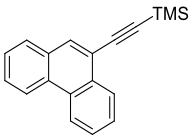

pale yellow oil; 92%; CC: (SiO_2; *c*-hexane); R_f = 0.37 (SiO_2; *c*-hexane); ^{1}H NMR (400 MHz, $CDCl_3$, 298 K): δ = 0.41 (s, 9 H), 7.56–7.63 (m, 1 H), 7.64–7.77 (m, 3 H), 7.85 (d, J = 7.9 Hz, 1 H), 8.06 (s, 1 H), 8.44–8.54 (m, 1 H), 8.60–8.74 ppm (m, 2 H); ^{13}C NMR (100 MHz, $CDCl_3$, 298 K): δ = 132.6, 131.24, 131.22, 130.5, 130.1, 128.7, 127.7, 127.21, 127.17, 127.08, 127.05, 122.9, 122.7, 119.6, 103.4, 99.3, 0.28 ppm. Spectral data was consistent with literature.[99]

Compound 164:

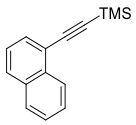

colorless oil; 90%; CC: (SiO_2; *c*-hexane); R_f = 0.40 (SiO_2; *c*-hexane); ^{1}H NMR (400 MHz, $CDCl_3$, 298 K): δ = 0.33 (s, 9 H), 7.41 (t, J = 7.7 Hz, 1 H), 7.52 (t, J = 7.5 Hz,

1 H), 7.58 (t, J = 7.6 Hz, 1 H), 7.70 (d, J = 7.1 Hz, 1 H), 7.83 (t, J = 7.5 Hz, 2 H), 8.33 ppm (d, J = 8.2 Hz, 1 H); ^{13}C NMR (100 MHz, $CDCl_3$, 298 K): δ = 133.5, 133.2, 131.0, 129.1, 128.4, 127.0, 126.5, 126.3, 125.3, 120.9, 103.2, 99.6, 0.26 ppm. Spectral data was consistent with literature.[99]

Compound 167:

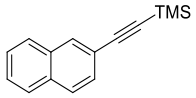

colorless oil; 78%; CC: (SiO_2; *c*-hexane); R_f = 0.33 (SiO_2; *c*-hexane); ^{1}H NMR (400 MHz, $CDCl_3$, 298 K): δ = 0.29 (s, 9 H), 7.44–7.54 (m, 3 H), 7.74–7.84 (m, 3 H), 8.00 ppm (s, 1 H); ^{13}C NMR (100 MHz, $CDCl_3$, 298 K): δ = 133.02, 132.99, 132.1, 128.7, 128.0, 127.92, 127.87, 126.8, 126.6, 120.5, 105.6, 94.7, 0.17 ppm. Spectral data was consistent with literature. [99]

Synthesis of terminal alkynes 162, 165, and 168 via TMS-deprotection

TMS-protected alkynes (1.00 mmol, 1 equiv.) were dissolved in methanol (10 mL) and THF (10 mL) mixture. Then, potassium carbonate (5.00 mmol, 5 equiv.) was added to this solution. After filtration, evaporation and column chromatography (CC) (SiO_2; *c*-hexanes) terminal alkynes **162**, **165**, and **168** were obtained in 73–95% yields.

Compound 162:

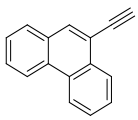

grey solid; 95%; CC: (SiO_2; *c*-hexane); R_f = 0.56 (SiO_2; DCM/*c*-hexane 1:4); ^{1}H NMR (400 MHz, $CDCl_3$, 298 K): δ = 3.48 (s, 1 H), 7.58–7.64 (m, 1 H), 7.65–7.74 (m, 3 H), 7.86 (d, J = 7.9 Hz, 1 H), 8.07 (s, 1 H), 8.42–8.52 (m, 1 H), 8.64–8.74 ppm

(m, 2 H); ^{13}C NMR (100 MHz, $CDCl_3$, 298 K): δ = 132.8, 131.0, 130.9, 130.4, 129.9, 128.5, 127.6, 127.0, 126.9, 126.7, 122.7, 122.5, 118.4, 81.8, 81.5 ppm (15 out of 16 signals expected). Spectral data was consistent with literature. [99]

Compound 165:

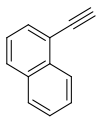

pale yellow solid; 73%; CC: (SiO_2; *c*-hexane); R_f = 0.55 (SiO_2; DCM/*c*-hexane 1:4); ^{1}H NMR (400 MHz, $CDCl_3$, 298 K): δ = 3.49 (s, 1 H), 7.44 (t, *J* = 7.7 Hz, 1 H), 7.54 (t, *J* = 6.9 Hz, 1 H), 7.60 (t, *J* = 6.9 Hz, 1 H), 7.75 (d, *J* = 7.1 Hz, 1 H), 7.87 (d, *J* = 8.3 Hz, 2 H), 8.37 ppm (d, *J* = 8.3 Hz, 1 H); ^{13}C NMR (100 MHz, $CDCl_3$, 298 K): δ = 133.6, 133.2, 131.4, 129.4, 128.4, 127.1, 126.6, 126.2, 125.2, 119.9, 82.1, 81.9 ppm. Spectral data was consistent with literature. [99]

Compound 168:

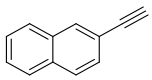

grey solid; 86%; CC: (SiO_2; *c*-hexane); R_f = 0.59 (SiO_2; DCM/*c*-hexane 1:4); ^{1}H NMR (400 MHz, $CDCl_3$, 298 K): δ = 3.16 (s, 1 H), 7.45–7.60 (m, 3 H), 7.75–7.90 (m, 3 H), 8.04 ppm (s, 1 H); ^{13}C NMR (100 MHz, $CDCl_3$, 298 K): δ = 133.1, 132.9, 132.4, 128.7, 128.2, 127.91, 127.90, 127.0, 126.8, 119.5, 84.1, 77.6 ppm. Spectral data was consistent with literature. [99]

Compound 156

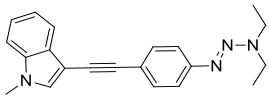

Iodo-indole compound **149** (391 mg, 1.52 mmol, 1 equiv.), bis (triphenylphosphine) palladium (II) chloride (32 mg, 0.046 mmol, 0.03 equiv.) and copper iodide (9 mg,

0.046 mmol, 0.03 equiv.) were added to two-necked round bottom flask and allowed to be stirred for 30 min under nitrogen atmosphere. Then, triethylamine (20 mL) was added into the flask *via* syringe and the solution was degassed for additional 15 min with nitrogen. Synthesized triazene alkyne (337 mg, 1.67 mmol, 1.1 equiv.) in triethylamine (8 mL) was added into the reaction medium. After stirring overnight at 25 °C, the reaction mixture was quenched with water, extracted with dichloromethane (3x50 mL), dried over $MgSO_4$ and filtered. The solvent was removed under reduced pressure and product **156** was isolated by performing column chromatography (CC) (SiO_2; 9:1 *c*-hexane/ethyl acetate).

Yield: 156,2 mg; yellow solid; 31%. CC: (SiO_2; 9:1 *c*-hexane/ethyl acetate); R_f = 0.37 (SiO_2; 9:1 *c*-hexane /ethyl acetate); m.p.= 79–81 °C. ^{1}H NMR (400 MHz, $CDCl_3$, 298 K): δ = 1.20–1.27 (m, 6H), 3.89–3.65 (m, 7H), 7.26 (m, 2H), 7.36–7.30 (m, 2H), 7.45–7.37 (m, 2H), 7.55–7.48 (m, 2H), 7.82 ppm (m, 1H); ^{13}C NMR (100 MHz, $CDCl_3$, 298 K): δ = 150.6, 136.4, 132.1, 129.4, 124.0, 122.8, 120.8, 120.5, 120.43, 120.41, 109.6, 97.6, 91.7, 82.8, 47.5, 43.0, 33.18, 13.20 ppm; IR (ATR): $\tilde{\nu}$ = 2200 (w), 1647 (w), 1595 (m), 1326 (s), 1233 (m), 740 (s) cm^{-1}; HRMS: m/z calcd for $C_{21}H_{23}N_4^+$: 331.1923; found: 331.1923 $[M + H]^+$.

Compound 169

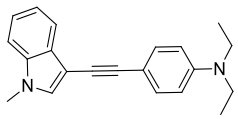

Iodo-indole compound **149** (400 mg, 1.56 mmol, 1 equiv.), bis (triphenylphosphine) palladium (II) chloride (33 mg, 0.047 mmol, 0.03 equiv.) and copper iodide (9 mg, 0.047 mmol, 0.03 equiv.) were added to two-necked round bottom flask and allowed to be stirred for 30 min under nitrogen atmosphere. Then, triethylamine (20 mL) was added into the flask *via* syringe and the solution was degassed for additional 15 min with nitrogen. Synthesized *N,N*-diethyl-4-ethynylaniline (297 mg, 1.71 mmol, 1.1 equiv.) in triethylamine (8 mL) was added into the reaction medium. After stirring

overnight at 25 °C, the reaction mixture was quenched with water, extracted with dichloromethane (3x50 mL), dried over $MgSO_4$ and filtered. The solvent was removed under reduced pressure and product **169** was isolated by performing column chromatography (CC) (SiO_2; 9:1 hexane/ethyl acetate).

Yield: 283 mg; yellow solid; 60%. CC: (SiO_2; 9:1 hexane/ethyl acetate); R_f = 0.7 (SiO_2; 9:1 hexane/ethyl acetate); m.p.= 79–83 °C decomposition. ^{1}H NMR (400 MHz, $CDCl_3$, 298K): δ = 1.18 (t, J = 7.1 Hz, 6H), 3.38 (q, J = 7.1 Hz, 4H), 3.79 (s, 3H), 6.64 (quasi d, AA'part of AA'XX'-system, J = 8.8 Hz, 2H), 7.20 (t, J = 7.3 Hz, 1H), 7.25–7.35 (m, 3H), 7.42 (quasi d, XX'part of AA'XX'-system, J = 8.8 Hz, 2H), 7.82 ppm (d, J = 7.8 Hz, 1H); ^{13}C NMR (100 MHz, $CDCl_3$, 298K); δ = 146.9, 136.1, 132.5, 131.3, 129.1, 122.3, 120.1, 119.8, 111.1, 109.9, 109.2, 97.7, 91.6, 79.8, 44.2, 32.8, 12.4 ppm. IR (ATR): $\tilde{\nu}$ = 3050 (w), 1353 (s), 1237 (m), 817(w) cm^{-1} (s); HRMS: m/z calcd for $C_{21}H_{23}N_2^+$: 303.1861; found: 303.1861 $[M + H]^+$.

Compound 170

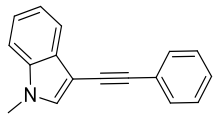

Iodo-indole compound **149** (223 mg, 0.87 mmol, 1 equiv.), bis (triphenylphosphine) palladium (II) chloride (18 mg, 0.026 mmol, 0.03 equiv.) and copper iodide (5 mg, 0.026 mmol, 0.03 equiv.) were added to two-necked round bottom flask and allowed to be stirred for 30 min under nitrogen atmosphere. Then, triethylamine (20 mL) was added into the flask *via* syringe and the solution was degassed for additional 15 min with nitrogen. Commercially available phenylacetylene (98 mg, 0.95 mmol, 1.1 equiv.) in triethylamine (8 mL) was added into the reaction medium. After stirring overnight at 25 °C, the reaction mixture was quenched with water, extracted with dichloromethane (3x50 mL), dried over $MgSO_4$ and filtered. The solvent was removed under reduced pressure and product **170** was isolated by performing column chromatography (CC) (SiO_2; 9:1 hexane/ethyl acetate)

Yield: 140 mg; yellow oil; 70%. CC: (SiO_2; 9:1 hexane/ethyl acetate); R_f = 0.33 (SiO_2; 9:1 hexane/ethyl acetate); ^{1}H NMR (400 MHz, $CDCl_3$, 298 K): δ = 3.79 (s, 3H), 7.23–7.41 (m, 7H), 7.61 (dd, *J* = 8.1, 1.3 Hz, 2H), 7.87 ppm (d, *J* = 7.7 Hz, 1H). Spectral data was consistent with literature.[102]

Compound 171

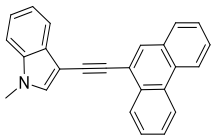

Iodo-indole compound **149** (167 mg, 0.65 mmol, 1 equiv.), bis (triphenylphosphine) palladium (II) chloride (41 mg, 0.06 mmol, 0.09 equiv.) and copper iodide (11 mg, 0.06 mmol, 0.09 equiv.) were added to two-necked round bottom flask and allowed to be stirred for 30 min under nitrogen atmosphere. Then, toluene (6 mL) and diisopropylamine (3 mL) was added into the flask *via* syringe and the solution was degassed for additional 15 min with nitrogen. Synthesized 9-ethynylphenanthrene (230 mg, 1.14 mmol, 1.75 equiv.) in toluene (6 mL) and diisopropylamine (3 mL) was added into the reaction medium. After stirring overnight at 25 °C, the reaction mixture was quenched with water, extracted with dichloromethane (3x50 mL), dried over $MgSO_4$ and filtered. The solvent was removed under reduced pressure and product **171** was isolated by performing column chromatography (CC) (SiO_2; 9:1 hexanes/ethyl acetate).

Yield: 120 mg; yellow solid; 56%; CC: (SiO_2; 9:1 hexanes/ethyl acetate); R_f = 0.29 (SiO_2; 9:1 hexanes/ethyl acetate). m.p = 146–150 °C; ^{1}H NMR (400 MHz, $CDCl_3$, 298K) δ = 3.87 (s, 3H), 7.28–7.36 (m, 2H), 7.40 (d, *J* = 7.7 Hz, 1H), 7.48 (s, 1H), 7.59–7.68 (m, 2H), 7.69–7.80 (m, 2H), 7.89 (d, *J* = 7.8 Hz, 1H), 7.97 (d, *J* = 8.0 Hz, 1H), 8.09 (s, 1H), 8.63–8.75 ppm (m, 3H); ^{13}C NMR (100 MHz, $CDCl_3$, 298K) δ = 136.5, 132.6, 131.7, 131.4, 130.9, 130.3, 130.1, 129.4, 128.5, 127.3, 127.14, 127.12, 127.08, 127.0, 122.93, 122.89, 122.7, 120.9, 120.7, 120.4, 109.8, 97.3, 89.5, 88.1,

33.3 ppm. IR (ATR): ν˜ = 3050 (w), 2195 (w), 1539 (w), 1326 (s), 875 (w) cm^{-1}; HRMS: m/z calcd for $C_{25}H_{18}N^+$: 331.1361; found: 331.1361 $[M + H]^+$.

Compound 172

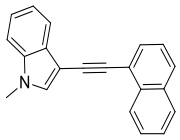

Iodo-indole compound **149** (100 mg, 3.90 mmol, 1 equiv.), bis (triphenylphosphine) palladium (II) chloride (25 mg, 0.035 mmol, 0.09 equiv.), and copper iodide (7 mg, 0.035 mmol, 0.09 equiv.) were added to two-necked round bottom flask and allowed to be stirred for 30 min under nitrogen atmosphere. Then, toluene (6 mL) and diisopropylamnie (3 ml) was added into the flask *via* syringe and the solution was degassed for additional 15 min with nitrogen. Synthesized 1-napthaline (163 mg, 1.07 mmol, 2.75 equiv.) in toluene (6 ml) and diisopropylamine (3ml) was added into the reaction medium. After stirring overnight at 25 °C, the reaction mixture was quenched with water, extracted with dichloromethane (3x50 mL), dried over $MgSO_4$, and filtered. The solvent was removed under reduced pressure and product **172** was isolated by performing column chromatography (CC) (SiO_2; 9:1 hexanes/ethyl acetate).

Yield: 90 mg; yellow solid; 82%. CC: (SiO_2; 9:1 hexane/ethyl acetate); R_f = 0.26 (SiO_2; 9:1 hexanes/ethyl acetate); m.p.= 128–132 °C. ^{1}H NMR (400 MHz, $CDCl_3$, 298K) δ = 3.86 (s, 3H), 7.27–7.35 (m, 2H), 7.39 (d, *J* = 7.7 Hz, 1H), 7.45 (s, 1H), 7.48 (d, *J* = 7.9 Hz, 1H), 7.54 (t, *J* = 7.7 Hz, 1H), 7.62 (t, *J* = 7.6 Hz, 1H), 7.78 (d, *J* = 7.1 Hz, 1H), 7.81 (d, *J* = 8.2 Hz, 1H), 7.87 (d, *J* = 8.2 Hz, 1H), 7.93 (d, *J* = 7.8 Hz, 1H), 8.56 ppm (d, *J* = 8.3 Hz, 1H); ^{13}C NMR (100 MHz, $CDCl_3$, 298K) δ = 136.5, 133.4, 133.2, 132.5, 129.7, 129.3, 128.4, 128.0, 126.7, 126.6, 126.4, 125.5, 122.9, 122.2, 120.6, 120.4, 109.8, 97.3, 89.3, 88.4, 33.2 ppm; IR (ATR): ν˜ = 2964 (w), 2197 (w), 1510 (w), 1271 (s), 742 (w) cm^{-1}; HRMS: m/z calcd for $C_{21}H_{16}N^+$: 281.1204; found: 281.1212 $[M + H]^+$.

Compound 173

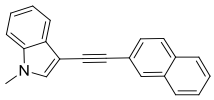

Iodo-indole compound **149** (257 mg, 1 mmol, 1 equiv.), bis (triphenylphosphine) palladium (II) chloride (63 mg, 0.09 mmol, 0.09 equiv.) and copper iodide (17 mg, 0.09 mmol, 0.09 equiv.) were added to two-necked round bottom flask and allowed to be stirred for 30 min under nitrogen atmosphere. Then, toluene (6 mL) and diisopropylamine (3 mL) was added into the flask *via* syringe and the solution was degassed for additional 15 min with nitrogen. Synthesized 2-napthaline (266 mg, 1.75 mmol, 1.75 equiv.) in toluene (6 mL) and diisopropylamine (3 mL) was added into the reaction medium. After stirring overnight at 25 °C, the reaction mixture was quenched with water, extracted with dichloromethane (3x50 mL), dried over $MgSO_4$ and filtered. The solvent was removed under reduced pressure and product **173** was isolated by performing column chromatography (CC) (SiO_2; 9:1 hexanes/ethyl acetate).

Yield: 240 mg; dark-yellow solid; 85%; CC: (SiO_2; 9:1 hexanes/ethyl acetate); R_f = 0.33 (SiO_2; 9:1 hexanes/ethyl acetate). m.p = 118–122 °C. ^{1}H NMR (400 MHz, $CDCl_3$, 298K) δ = 3.84 (s, 3H), 7.23–7.28 (m, 1H), 7.29–7.34 (m, 1H), 7.35–7.39 (m, 2H), 7.46–7.52 (m, 2H), 7.62 (dd, *J* = 8.5, 1.4 Hz, 1H), 7.80–7.84 (m, 3H), 7.88 (d, *J* = 7.8 Hz, 1H), 8.06 ppm (s, 1H); ^{13}C NMR (100 MHz, $CDCl_3$, 298K) δ = 136.3, 133.3, 132.50, 132.46, 130.6, 129.2, 128.6, 128.0, 127.8, 127.7, 126.5, 126.3, 122.8, 121.8, 120.5, 120.3, 109.7, 97.1, 91.6, 83.9, 33.1 ppm; IR (ATR): ν˜ = 2965 (w), 22202 (w), 1510 (w), 1270 (s), 818 (w) cm^{-1}; HRMS: m/z calcd for $C_{21}H_{16}N^+$: 281.1204; found: 281.1204 $[M + H]^+$.

Synthesis of TCNE Products 175-185

A solution of indole-substituted-alkyne **156**, **169-173** (1 equiv.) and TCNE **103** (1 equiv.) in 1,2-dichloroethane (5 mL) was stirred at 25 °C until complete

consumption of starting material based on TLC analysis (approximately 24h). Evaporation and CC (SiO_2; CH_2Cl_2) gave target product **175-185** in 94%, 76%, 95% yield, respectively.

Compound 175

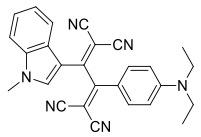

Yield: 47 mg; dark orange-red solid; 94%; CC: (SiO_2; DCM); R_f = 0.41 (SiO_2;DCM). m.p = 247–251 °C decompose. ^{1}H NMR (400 MHz, $CDCl_3$, 298K); δ = 1.24 (t, *J* = 7.1 Hz, 6H), 3.46 (q, *J* = 7.1 Hz, 4H), 3.97 (s, 3H), 6.67 (quasi d, AA'part of AA'XX'-system, *J* = 9.4 Hz, 2H), 7.21–7.24 (m, 1H), 7.34–7.39 (m, 2H), 7.43 (d, *J* = 8.7 Hz, 1H), 7.86 (quasi d, XX'part of AA'XX'-system, *J* = 9.1 Hz, 2H), 8.66 ppm (s, 1H); ^{13}C NMR (100 MHz, $CDCl_3$, 298K); δ = 164.2, 162.1, 152.8, 137.9, 137.1, 133.2, 125.5, 124.8, 124.4, 121.0, 117.8, 115.6, 115.1, 113.7, 113.2, 112.0, 111.3, 110.1, 73.8, 73.2, 45.2, 34.7, 12.7 ppm. IR (ATR): ν˜ = 2976 (w), 2217 (w), 1602 (m), 1277 (s), 1191 (m) cm^{-1}; HRMS: m/z calcd for $C_{27}H_{23}N_6$: 431.1984; found: 431.1984 $[M + H]^+$.

Compound 177

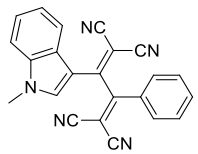

Yield: 52 mg; dark red-orange solid; 81%; CC: (SiO_2; DCM); R_f = 0.27 (SiO_2;DCM). m.p = 178–182 °C; ^{1}H NMR (400 MHz, $CDCl_3$, 298K); δ = 4.01 (s, 3H), 7.29 (t, *J* = 7.1 Hz, 1H), 7.38 (d, *J* = 8.1 Hz, 1H), 7.43 (t, *J* = 7.1 Hz, 1H), 7.49 (d, *J* = 8.2 Hz, 1H), 7.55 (t, *J* = 7.5 Hz, 2H), 7.66 (t, *J* = 7.6 Hz, 1H), 7.84 (d, *J* = 7.5 Hz, 2H), 8.67 ppm (s, 1H); ^{13}C NMR (100 MHz, $CDCl_3$, 298K); δ = 168.1, 159.6, 137.7, 137.1, 134.4, 131.1,

129.8, 129.7, 125.0, 124.9, 124.5, 120.1, 114.8, 112.5, 111.9, 111.4, 110.9, 109.2, 86.6, 73.6, 34.6 ppm. IR (ATR): ν˜ = 2219 (w), 1496 (w), 1316 (s), 744 (w) cm^{-1}; HRMS: m/z calcd for $C_{23}H_{14}N_5^+$: 359,1171; found: 359.1183 $[M + H]^+$.

Compound 179

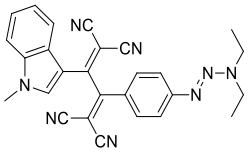

Yield: 63,2 mg; dark-red-orange solid; 76%; CC: (SiO_2; DCM); R_f =0.5 (SiO_2; DCM); m.p = 102–104 °C decomposition. ^{1}H NMR (400 MHz, $CDCl_3$, 298K); δ = 1.22 (t, *J* = 7.2 Hz, 3H), 1.35 (t, *J* = 7.2 Hz, 3H), 3.82 (q, *J* = 7.2 Hz, 4H), 3.99 (s, 3H), 7.24 (t, *J* = 8.1 Hz, 1H), 7.35 (d, *J* = 8.4 Hz, 1H), 7.38 (t, *J* = 7.1 Hz, 1H), 7.45 (d, *J* = 8.2 Hz, 1H), 7.52 (quasi d, AA'part of AA'XX'-system, *J* = 8.8 Hz, 2H), 7.88 (quasi d, XX'part of AA'XX'-system, *J* = 8.8 Hz, 2H), 8.66 ppm (s, 1H) ; ^{13}C NMR (100 MHz, $CDCl_3$, 298K); δ = 166.9, 160.9, 156.9, 138.0, 137.2, 131.7, 127.1, 125.4, 125.0, 124.6, 121.8, 120.7, 115.3, 113.3, 112.9, 112.2, 111.5, 109.9, 81.9, 74.0, 50.0, 42.3, 34.8, 14.5, 11.3 ppm ; IR (ATR): ν˜ = 2924 (m), 2219 (m), 1595 (m), 1497 (m), 1452 (m), 1161 cm^{-1} (m).; HRMS: m/z calcd for $C_{27}H_{23}N_8^+$: 459.2046; found: 459.2046 $[M + H]^+$.

Compound 181

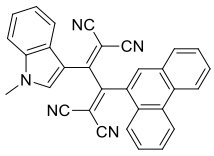

Yield: 80 mg; dark orange-red solid; 95%; CC: (SiO_2; DCM); R_f = 0.43 (SiO_2;DCM). m.p= 238–244 °C decompose. ^{1}H NMR (400 MHz, DMSO-d_6, 298K); δ = 3.93 (s, 3H), 7.30–7.50 (m, 2H), 7.65 (d, *J* = 6.2 Hz, 1H), 7.74–7.89 (m, 5H), 8.15 (d, *J* = 7.3

Hz, 1H), 8.37 (d, *J* = 6.6 Hz, 1H), 8.54 (s, 1H), 8.73 (s, 1H), 8.86–9.00 ppm (m, 2H).; ^{13}C NMR (100 MHz, DMSO-d_6, 298K) δ = 166.3, 159.2, 139.8, 138.1, 133.8, 131.6, 130.5, 130.4, 130.1, 129.7, 129.5, 128.2, 128.0, 127.8, 127.2, 125.9, 124.4, 124.1, 124.0, 123.2, 122.9, 121.8, 114.6, 113.8, 112.7, 112.2, 111.9, 110.6, 93.8, 77.5, 34.1 ppm. IR (ATR): ν˜ = 2202 (w), 1600 (m), 1507 (w), 1355 (s), 745 (w) cm^{-1}; HRMS: m/z calcd for $C_{31}H_{18}N_5^+$: 460.1562; found: 460.1562 [M + H]$^+$.

Compound 183

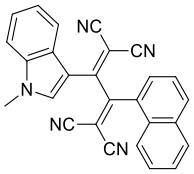

Yield: 56 mg; dark red-orange solid; 92%; CC: (SiO_2; DCM); R_f = 0.33 (SiO_2; DCM). m.p = 146–150 °C. ^{1}H NMR (400 MHz, $CDCl_3$, 298K); δ = 4.03 (s, 3H), 7.32 (t, *J* = 7.6 Hz, 1H), 7.46 (t, *J* = 7.6 Hz, 1H), 7.52–7.59 (m, 3H), 7.67 (m, 2H), 7.79 (d, *J* = 7.2 Hz, 1H), 7.99–8.03 (m, 1H), 8.08 (d, *J* = 8.0 Hz, 1H), 8.18 (d, *J* = 8.0 Hz, 1H), 8.51 ppm (s, 1H); ^{13}C NMR (100 MHz, $CDCl_3$, 298K); δ = 167.2, 160.6, 138.2, 137.3, 135.7, 134.1, 131.9, 130.4, 129.9, 129.8, 128.9, 127.8, 125.4, 125.2, 125.1, 125.0, 124.6, 120.4, 115.2, 112.8, 112.2, 111.9, 111.2, 110.5, 91.3, 75.8, 34.9 ppm; IR (ATR): ν˜ = 2216 (w), 1607 (m), 1502 (w), 1357 (s), 745 (w) cm^{-1}; HRMS: m/z calcd for $C_{27}H_{16}N_5^+$: 409.1327; found: 409.1328 [M + H]$^+$.

Compound 185

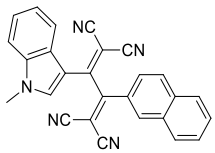

Yield: 69 mg; dark orange-red solid; 95%; CC: (SiO_2; DCM); R_f = 0.52 (SiO_2;DCM). m.p = 140–144 °C. ^{1}H NMR (400 MHz, $CDCl_3$, 298K); δ= 4.03 (s, 3H), 7.22–7.28

(m, 1H), 7.36–7.44 (m, 2H), 7.50 (d, *J* = 8.2 Hz, 1H), 7.60 (dd, *J* = 8.0, 7.1 Hz, 1H), 7.69 (t, *J* = 7.6 Hz, 1H), 7.88–7.92 (m, 3H), 7.98 (d, *J* = 8.8 Hz, 1H), 8.34 (s, 1H), 8.73 ppm (s, 1H); ^{13}C NMR (100 MHz, $CDCl_3$, 298K); δ = 168.1, 160.1, 138.0, 137.5, 135.8, 132.61, 132.56, 130.3, 130.1, 130.0, 128.6, 128.1, 128.0, 125.2, 125.1, 124.7, 124.5, 120.4, 115.2, 113.0, 112.6, 111.7, 111.5, 109.6, 86.1, 73.7, 34.8 ppm; IR (ATR): ν˜ = 2222 (w), 1506 (m), 1461 (w), 1320 (s), 747 (w) cm^{-1}; HRMS: m/*z* calcd for $C_{27}H_{16}N_5^+$: 410.1406; found: 410.1406 $[M + H]^+$.

Synthesis of TCNQ Products 176-180

A solution of indole-substituted-alkyne **156**, **169**, and **170** (1 equiv.) and TCNQ **106** (1.5 equiv.) in 1,2-dichloroethane (5 mL) was stirred at 25 ^{o}C until complete consumption of starting material based on TLC analysis (approximately 24 h). Evaporation and CC (SiO_2; DCM) gave target product in 99%, 83% and 91% yield respectively.

Compound 176

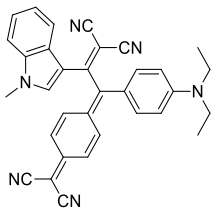

Yield: 86 mg; dark-green solid; 99%; CC: (SiO_2; DCM); R_f = 0.15 (SiO_2;DCM). m.p = 252–256 decompose; ^{1}H NMR (400 MHz, $CDCl_3$, 298K); δ = 1.24 (t, *J* = 7.1 Hz, 6H), 3.46 (q, *J* = 7.1 Hz, 4H), 3.96 (s, 3H), 6.69 (d, *J* = 9.1 Hz, 2H), 6.98–7.09 (m, 2H), 7.12 (t, *J* = 7.5 Hz, 1H), 7.26–7.34 (m, 3H), 7.40 (t, *J* = 8.2 Hz, 3H), 7.65 (dd, *J* = 9.5, 1.6 Hz, 1H), 8.55 ppm (s, 1H); ^{13}C NMR (100 MHz, $CDCl_3$, 298K); δ = 165.8, 154.6, 153.5, 151.4, 137.8, 135.9, 135.5, 134.7, 129.8, 125.9, 125.0, 124.6,

124.2, 123.9, 122.9, 121.2, 116.0, 115.5, 115.4, 113.9, 112.5, 112.4, 111.1, 75.8, 69.3, 45.1, 34.6, 12.8 ppm (28 out of 29 signals expected); IR (ATR): ν˜ = 2197 (w), 1611 (m) 1537 (w), 1324 (s), 744 (w) cm^{-1}; HRMS: m/z calcd for $C_{33}H_{27}N_6^+$: 507.2297; found: 507.2297 $[M + H]^+$.

Compound 178

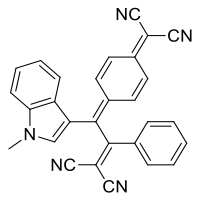

Yield: 76 mg; dark-blue solid; 83%; CC: (SiO_2; DCM); R_f = 0.12 (SiO_2;DCM). m.p = 183–187; ^{1}H NMR (400 MHz, $CDCl_3$, 298K); δ = 3.92 (s, 3H), 7.00 (dd, *J* = 9.6, 1.8 Hz, 1H), 7.15 (dd, *J* = 9.6, 1.8 Hz, 1H), 7.26–7.32 (m, 2H), 7.37–7.44 (m, 3H), 7.48 (t, *J* = 7.9 Hz, 2H), 7.52–7.59 (m, *J* = 7.6 Hz, 2H), 7.66 (dd, *J* = 9.6, 1.9 Hz, 1H), 7.74 ppm (d, *J* = 7.5 Hz, 2H); ^{13}C NMR (100 MHz, $CDCl_3$, 298K); δ = 171.4, 154.1, 145.4, 138.0, 136.3, 135.4, 134.3, 133.60, 133.55, 131.9, 129.6, 126.2, 125.2, 124.8, 124.6, 123.3, 120.0, 114.3, 114.2, 112.8, 111.9, 110.9, 86.8, 72.8, 33.9 ppm (25 out of 27 expected signals observed).; IR (ATR): ν˜ = 2205 (w), 1603 (m) 1510 (w), 1251 (s), 756 (w) cm^{-1}; HRMS: m/z calcd for $C_{29}H_{18}N_5^+$: 436.1562; found: 436.1563 $[M + H]^+$.

Compound 180

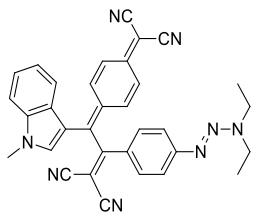

Yield: 47.2 mg; dark-green solid; 91%; CC: (SiO_2; DCM); R_f = 0.30 (SiO_2; DCM). m.p.= 149–152 °C (decomposition); ^{1}H NMR (400 MHz, $CDCl_3$, 298K) δ = 1.21 (t,

J = 7.1 Hz, 3H), 1.34 (t, *J* = 7.1 Hz, 3H), 3.80 (q, *J* = 7.1 Hz, 4H), 3.91 (s, 3H), 7.01 (dd, *J* = 9.5, 1.9 Hz, 1H), 7.14 (dd, *J* = 9.5, 2.0 Hz, 1H), 7.23–7.31 (m, 2H), 7.35–7.42 (m, 3H), 7.46 (quasi d, AA'part of AA'XX'-system, *J* = 8.8 Hz, 2H), 7.55 (d, *J* = 8.1 Hz, 1H), 7.68 (dd, *J* = 9.6, 1.9 Hz, 1H), 7.78 ppm (quasi d, XX'part of AA'XX'-system, *J* = 8.8 Hz, 2H); ^{13}C NMR (100 MHz, $CDCl_3$, 298K) δ = 170.3, 155.8, 154.4, 146.7, 138.1, 136.4, 135.4, 133.9, 131.5, 131.3, 129.9, 126.2, 124.9, 124.54, 124.45, 123.2, 121.2, 120.2, 114.58, 114.55, 114.4,113.7, 112.8, 110.7, 82.7, 71.9, 49.5, 41.8, 33.9, 14.1, 10.9 ppm. IR (ATR): ν˜ = 2200 (w), 1595 (m), 1457 (m), 1304 (s), 1506 (s) cm^{-1}; HRMS: m/z calcd for $C_{33}H_{27}N_8^+$: 535,2359; found: 535.2358 $[M + H]^+$.

Synthesis of TCNQ Products 182, 184, 186

A solution of indole-substituted-alkyne **171-173** (1 equiv.) and TCNQ **106** (1.5 equiv.) in 1,2-dichloroethane (5 mL) was stirred at 60 °C until complete consumption of starting material based on TLC analysis (approximately 24h). Evaporation and CC (SiO_2; DCM) gave target product **182-186**.

Compound 182

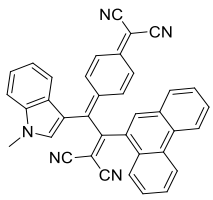

Yield: 99 mg; dark-green solid; 94%; CC: (SiO_2; DCM); R_f = 0.26 (SiO_2; DCM). m.p = 234–238 °C; ^{1}H NMR (400 MHz, $CDCl_3$, 298K); δ = 3.88 (s, 3H), 7.05 (d, *J* = 7.6, 1.3 Hz 1H), 7.22 (dd, *J* = 9.5, 1.6 Hz, 1H), 7.24–7.31 (m, 2H), 7.34–7.42 (m, 3H), 7.54 (dd, *J* = 9.5, 1.7 Hz, 1H), 7.61 (d, *J* = 8.0 Hz, 1H), 7.63–7.71 (m, 2H), 7.75 (t, *J* = 7.7 Hz, 1H), 7.80 (t, *J* = 7.7 Hz, 1H), 7.92 (d, *J* = 7.9 Hz, 1H), 8.02 (s, 1H),

8.13 (d, J = 8.2 Hz, 1H), 8.68 (d, J = 8.4 Hz, 1H), 8.76 ppm (d, J = 8.4 Hz, 1H); ^{13}C NMR (100 MHz, $CDCl_3$, 298K) δ = 170.9, 153.9, 146.4, 138.2, 136.8, 136.5, 134.8, 133.7, 133.23, 133.18, 132.2, 131.1, 130.4, 130.2, 129.9, 128.3, 128.0, 127.94, 127.85, 127.1, 125.8, 125.4, 125.1, 124.9, 124.2, 123.5, 123.0, 120.1, 115.6, 114.5, 114.4, 113.3, 112.3, 111.2, 91.7, 74.1, 34.2 ppm. IR (ATR): ν˜ = 2203 (w), 1598 (m), 1505 (w), 1345 (s), 738 (w) cm^{-1}; HRMS: m/z calcd for $C_{37}H_{22}N_5^+$: 536.1875; found: 536.1874 $[M + H]^+$.

Compound 184

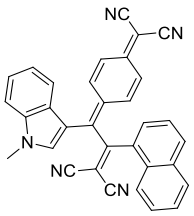

Yield: 69 mg; dark-green solid; 95%; CC: (SiO_2; DCM); R_f = 0.27 (SiO_2;DCM). m.p = 193–195 ºC. ^{1}H NMR (400 MHz, $CDCl_3$, 298K); δ = 3.90 (s, 3H), 7.04 (dd, J = 9.6, 1.6 Hz, 1H), 7.14 (dd, J = 9.6, 1.6 Hz, 1H), 7.20 (dd, J = 9.6, 1.8 Hz, 1H), 7.27–7.30 (m, 1H), 7.36–7.44 (m, 3H), 7.51–7.65 (m, 5H), 7.75 (d, J = 7.2 Hz, 1H), 7.92–7.97 (m, 1H), 8.05 ppm (dd, J = 8.1, 2.8 Hz, 2H); ^{13}C NMR (100 MHz, $CDCl_3$, 298K) δ = 171.0, 154.0, 146.6, 138.2, 137.0, 136.5, 134.4, 134.2, 134.1, 133.9, 133.7, 130.7, 129.9, 129.8, 128.7, 127.4, 127.0, 125.7, 125.2, 124.9, 124.0, 123.4, 120.2, 115.6, 114.6, 114.5, 113.3, 112.2, 111.2, 91.6, 73.7, 34.2 ppm. (32 out of 33 signals expected); IR (ATR): ν˜ = 2228 (w), 1600 (m), 1504 (w), 1332 (s), 754 (w) cm^{-1}; HRMS: m/z calcd for $C_{33}H_{20}N_5^+$: 485.1640; found: 485.1639 $[M + H]^+$.

Compound 186

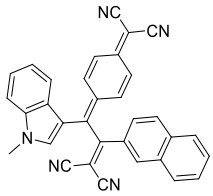

Yield: 69 mg; dark-turquoise solid; 80%; CC: (SiO_2; DCM); R_f = 0.38 (SiO_2;DCM). m.p = 175–179 °C. ^{1}H NMR (400 MHz, $CDCl_3$, 298K); δ = 3.91 (s, 3H), 7.05 (dd, *J* = 9.5, 1.7 Hz, 1H), 7.14 (dd, *J* = 9.5, 1.7 Hz, 1H), 7.25–7.32 (m, 2H), 7.35–7.43 (m, 2H), 7.45 (s, 1H), 7.54–7.62(m, 2H), 7.64 (t, *J* = 6.9 Hz, 1H), 7.71 (dd, *J* = 9.6, 1.7 Hz, 1H), 7.79 (dd, *J* = 8.7, 1.7 Hz, 1H), 7.86 (d, *J* = 8.7 Hz, 2H), 7.91 (d, *J* = 8.7 Hz, 1H), 8.26 ppm (s, 1H).; ^{13}C NMR (100 MHz, $CDCl_3$, 298K); δ = 171.6, 154.4, 146.0, 138.4, 136.7, 135.7, 135.4, 134.0, 132.7, 132.3, 132.03, 132.00, 130.0, 129.9, 129.8, 128.1, 127.9, 126.5, 125.5, 125.1, 124.9, 124.8, 123.6, 120.3, 114.7, 114.6, 113.5, 112.5, 111.2, 86.7, 72.9, 34.3 ppm (32 out of 33 signals expected); IR (ATR): ν˜ = 2202 (w), 1600 (m), 1430 (w), 1337 (s), 740 (w) cm^{-1}; HRMS: m/z calcd for $C_{33}H_{20}N_5^+$: 486.1719; found: 486.1719 $[M + H]^+$.

REFERENCES

1. Jacob, M. V. Organic Semiconductors: Past, Present and Future. *Electronics* **2014**, *3* (4), 594–597. DOI: 10.3390/electronics3040594
2. Forrest, S. R.; Thompson, M. E. Introduction: Organic electronics and optoelectronics. *Chem. Rev.* **2007**, *107* (4), 923–925. DOI: 10.1021/cr0501590
3. Reyes-Reyes, M.; Carroll, D. L.; Blau, W.; López-Sandoval, R. Materials and devices for organic electronics. *J. Nanotechnol.* **2011**, *2011* DOI:10.1155/2011/589241
4. Stowell, A.; Hardy, J.; Cass, N.; Stewart, H. Organic electronics: benefits, barriers and opportunities: A violet biotechnology understanding of organic electronics with a focus on display technology. *Lancaster University Management School*, **2020**, 24. DOI:10.5281/ZENODO.4058351.
5. Liu, Z.; Zhang, G.; Zhang, D. Modification of Side Chains of Conjugated Molecules and Polymers for Charge Mobility Enhancement and Sensing Functionality. *Acc. Chem. Res.* **2018**, *51* (6), 1422–1432. DOI:10.1021/acs.accounts.8b00069
6. Liao, C.; Zhang, M.; Yao, M. Y.; Li, T. H.; Yan, F. Flexible Organic Electronics in Biology: *Materials and Devices*. *Adv. Mater.* **2015**, *27* (46), 7493–7527. DOI: 10.1002/adma.201402625
7. Bolm, C. Cross-coupling reactions. *Org. Lett.* **2012**, *14* (12), 2925–2928. DOI: 10.1021/ol301436v
8. Osedach, T. P.; Andrew, T7. L.; Bulović, V. Effect of synthetic accessibility on the commercial viability of organic photovoltaics. *Energy Environ. Sci.* **2013**, *6* (3), 711–718. DOI: 10.1039/c3ee24138f
9. Anastas, P. T.; Beach, E. S. Green chemistry: the emergence of a transformative framework. *Green Chem. Lett. Rev.* **2007**, *1* (1), 9–24. DOI: 10.1080/17518250701882441
10. Moses, J. E.; Moorhouse, A. D. The growing applications of click chemistry. *Chem. Soc. Rev.* **2007**, *36* (8), 1249–1262. DOI: 10.1039/b613014n

11. Kolb, H. C.; Finn, M. G.; Sharpless, K. B. Click Chemistry: Diverse Chemical Function from a Few Good Reactions. *Angew. Chem*. **2001**, *40* (11), 2004–2021. DOI: 10.1002/1521-3773(20010601)40:11<2004::aid-anie2004>3.3.co;2-x
12. Xi, W.; Scott, T. F.; Kloxin, C. J.; Bowman, C. N. Click chemistry in materials science. *Adv. Funct. Mater.* **2014**, *24* (18), 2572–2590. DOI: 10.1002/adfm.201302847
13. Hein, C. D.; Liu, X.-M.; Wang, D. A Powerful Tool for Pharmaceutical Sciences. *Pharm. Res*. **2008**, *25* (10), 2216–2230. DOI: 10.1007/s11095-008-9616-1
14. Hosseinnejad, T.; Fattahi, B; Heravi, M. M. Computational studies on the regioselectivity of metal-catalyzed synthesis of 1,2,3 triazoles via click reaction: a review. *J. Mol. Model.* **2015**, *21* (10), 1–37. DOI: 10.1007/s00894-015-2810-2
15. Brittain, W. D. G.; Buckley, B. R.; Fossey, J. S. Asymmetric Copper Catalyzed Azide-Alkyne Cycloadditions. *ACS Catal.* **2016**, *6* (6), 3629–3636. DOI: 10.1021/acscatal.6b00996
16. Arseneault, M.; Wafer, C.; Morin, J. F. Recent advances in click chemistry applied to dendrimer synthesis. *Molecules* **2015**, *20* (5), 9263–9294. DOI: 10.3390/molecules20059263
17. Zhang, L.; Chen, X.; Xue, P.; Sun, H. H. Y.; Williams, I. D.; Sharpless, K. B.; Fokin, V. V.; Jia, G. Ruthenium-catalyzed cycloaddition of alkynes and organic azides. *J. Am. Chem. Soc.* **2005**, *127* (46), 15998–15999. DOI: 10.1021/ja054114s
18. Liang, L.; Astruc, D. The copper(I)-catalyzed alkyne-azide cycloaddition (cuaac) “click” reaction and its applications. *Coord. Chem. Rev.* **2011**, *255* (23-24), 2933–2945. DOI: 10.1016/j.ccr.2011.06.028
19. Rodionov, V. O.; Fokin, V. V.; Finn, M. G. Mechanism of the ligand-free cui-catalyzed azide-alkyne cycloaddition reaction. *Angew. Chem.* **2005**, *44* (15), 2210–2215. DOI: 10.1002/anie.200461496
20. Rodionov, V. O.; Presolski, S. I.; Díaz, D. D.; Fokin, V. V.; Finn, M. G. Ligand-

accelerated Cu-catalyzed azide-alkyne cycloaddition: a mechanistic report. *J. Am. Chem. Soc.* **2007**, *129* (42), 12705–12712. DOI: 10.1021/ja072679d

21. Hizal, G.; Tunca, U.; Sanyal, A. Discrete macromolecular constructs via the Diels–Alder "Click" reaction. *J. Polym. Sci. A Polym. Chem.* **2011**, *49* (19), 4103–4120. DOI: 10.1002/pola.24835
22. Tasdelen, M. A. Diels-Alder "click" reactions: Recent applications in polymer and material science. *Polym. Chem.* **2011**, *2* (10), 2133–2145. DOI: 10.1039/c1py00041a
23. Meghani, N. M.; Amin, H. H.; Lee, B.-J. Mechanistic applications of click chemistry for pharmaceutical drug discovery and drug delivery. *Drug Discov. Today* **2017**, *22*, 1604–1619. DOI: 10.1016/j.drudis.2017.07.007
24. Mushtaq, S.; Yun, S. J.; Jeon, J. Recent advances in bioorthogonal click chemistry for efficient synthesis of radiotracers and radiopharmaceuticals. *Molecules* **2019**, *24* (19), 3567. DOI: 10.3390/molecules24193567
25. Lowe, A. B. Thiol-ene "click" reactions and recent applications in polymer and materials synthesis. *Polym. Chem.* **2009**, *1* (1), 17–36. DOI: 10.1039/b9py00216b
26. Posner, T. Beiträge zur Kenntniss der ungesättigten Verbindungen. II. Ueber die Addition von Mercaptanen an ungesättigte Kohlenwasserstoffe. Berichte Der Deutschen Chemischen Gesellschaft. *Eur. J. Inorg.* **1905**, *38* (1), 646–657. DOI: 10.1002/cber.190503801106
27. Hoyle, C. E.; Bowman, C. N. Thiol-ene click chemistry. *Angew. Chem.* **2010**, *49* (9), 1540–153. DOI: 10.1002/anie.200903924
28. Gress, A.; Völkel, A.; Schlaad, H. 2007. Thio-click modification of poly[2-(3-butenyl)-2-oxazoline]. *Macromolecules* **2007**, *40* (22), 7928–7933. DOI: 10.1021/ma071357r
29. Cramer, N. B.; Bowman, C. N. CHAPTER 1:Thiol-ene and Thiol-yne Chemistry in Ideal Network Synthesis. *Thiol-X Chemistries in Polymer and Materials Science*. The Royal Society of Chemistry: 2013; pp 1–27. DOI: 10.1039/9781849736961-00001

30. Hoyle, C. E.; Lowe, A. B.; Bowman, C. N. 2010. Thiol-click chemistry: a multifaceted toolbox for small molecule and polymer synthesiswz. *Chem. Soc. Rev.* **2010**, *39* (4), 1355–1387. DOI: 10.1039/b901979k
31. Mather, B. D.; Viswanathan, K.; Miller, K. M.; Long, T. E. Michael addition reactions in macromolecular design for emerging technologies. *Prog. Polym. Sci*. **2006**, *31*(5), 487–531. DOI: 10.1016/j.progpolymsci.2006.03.001
32. Nair, D. P.; Podgórski, M. P.; Chatani, S.; Gong, T.; Xi, W.; Fenoli, C. R.; Bowman, C. N. The Thiol-Michael Addition Click Reaction: A Powerful and Widely Used Tool in Materials Chemistry. *Chem. Mater.* **2013**, *26* (1), 724–744. DOI: 10.1021/cm402180t
33. Opsteen, J. A.; Van Hest, J. C. M. Modular synthesis of block copolymers via cycloaddition of terminal azide and alkyne functionalized polymer. *Chem. Comm*. **2004**, *2005* (1), 57–59. DOI: 10.1039/b412930j
34. Liu, Z.; Zhang, G.; Zhang, D. Modification of Side Chains of Conjugated Molecules and Polymers for Charge Mobility Enhancement and Sensing Functionality. *Acc. Chem. Res.* **2018**, *51* (6), 1422–1432. DOI: 10.1021/acs.accounts.8b00069
35. Binder, W. H.; Sachsenhofer, R. "Click" chemistry in polymer and materials science. *Macromol. Rapid Commun.* **2007**, *28* (1), 15–54. DOI: 10.1002/marc.200600625.
36. Durmaz, H.; Sanyal, A.; Hizal, G.; Tunca, U. Double click reaction strategies for polymer conjugation and post-functionalization of polymers. *Polym. Chem.* **2012**, *3* (4), 825–835. DOI: 10.1039/c1py00471a
37. Johnson, J. A.; Finn, M. G.; Koberstein, J. T.; Turro, N. J. Construction of linear polymers, dendrimers, networks, and other polymeric architectures by copper-catalyzed azide-alkyne cycloaddition "click" chemistry. *Macromol. Rapid Commun.* **2008**, *29* (12-13), 1052–1072. DOI: 10.1002/marc.200800208
38. Díaz, D. D.; Punna, S.; Holzer, P.; Mcpherson, A. K.; Sharpless, K. B.; Fokin, V. V.; Finn, M. G. Click chemistry in materials synthesis. 1. Adhesive polymers from copper-catalyzed azide-alkyne cycloaddition. *J. Polym. Sci.* **2004**, *42* (17),

4392–4403.DOI: 10.1002/pola.20330

39. Tasdelen, M. A. Diels-Alder “click” reactions: Recent applications in polymer and material science. *Polym. Chem.* **2011**, *2* (10), 2133–2145. DOI: 10.1039/c1py00041a
40. Lallana, E.; Fernandez-Trillo, F.; Sousa-Herves, A.; Riguera, R.;Fernandez-Megia, E. Click Chemistry with Polymers, Dendrimers, and Hydrogels for Drug Delivery. *Pharm. Res.* **2012**, *29* (4), 902–921. DOI: 10.1007/s11095-012-0683y
41. Tomalia, D. A.; Baker, H.; Dewald, J. R.; Hall, M.; Kallos, G.; Martin, S.; Roeck, J.; Ryder, J.; Smith, P. A new class of polymers: starburst-dendritic macromolecules. *Polym. J.* **1985**, *17* (1), 117–132. DOI: 10.1295/polymj.17.117
42. Tomalia, D. A.; Baker, H.; Dewald, J. R.; Hall, M.; Kallos, G.; Martin, S.; Roeck, J.; Ryder, J.; Smith, P. Dendritic macromolecules: synthesis of starburst dendrimers. *Macromolecules* **1986**, *19* (9), 2466–2468. DOI:10.1021/ma00163a029
43. Newkome, G. R.; Yao, Z.-Q.; Baker, G. R.; Gupta, K.J. Micelles. Part 1. Cascade molecules: a new approach to micelles. A [27]-arborol. *J. Org. Chem.* **1985**, *50* (11), 2003–2004. DOI: 10.1021/jo00211a052
44. Bosman, A. W.; Janssen, H. M.; Meijer, E. W. About Dendrimers: Structure, Physical Properties, and Applications. *Chem. Rev.* **1999**, *99* (7), 1665–1688. DOI: 10.1021/cr970069y
45. Franc, G.; Kakkar, A. K. “Click” methodologies: Efficient, simple and greener routes to design dendrimers. *Chem. Soc. Rev.* **2010**, *39* (5), 1536–1544. DOI: 10.1039/b913281n
46. Wu, P.; Feldman, A. K.; Nugent, A. K.; Hawker, C. J.; Scheel, A.; Voit, B.; Pyun, J.; Fréchet, J. M. J.; Sharpless, K. B.; Fokin, V. V. Efficiency and fidelity in a click-chemistry route to triazole dendrimers by the copper(I)-catalyzed ligation of azides and alkynes. *Angew. Chem.* ***2004,*** *43* (30), 3928–3932. DOI: 10.1002/anie.200454078.
47. Camponovo, J.; Hadad, C.; Ruiz, J.; Cloutet, E.; Gatard, S.; Muzart, J.;

Bouquillon, S.; Astruc, D. “Click” Glycodendrimers Containing 27, 81, and 243 Modified Xylopyranoside Termini. *J. Org. Chem*. **2009**, *74* (14), 5071–5074. DOI: 10.1021/jo900554b

48. Killops, K. L.; Campos, L. M.; Hawker, C. J. 2008. Robust, Efficient, and Orthogonal Synthesis of Dendrimers via Thiol-ene “Click” Chemistry. *J. Am. Chem. Soc.* **2008**, *130* (15), 5062–5064. DOI: 10.1021/ja8006325
49. Morgenroth, F.; Reuther, E.; Müllen, K. Polyphenylene Dendrimers: From Three-Dimensional to Two-Dimensional Structures. *Angew. Chem.* **1997**, *36* (6), 631–634. DOI: 10.1002/anie.199706311
50. Kose, M. M.; Yesilbag, G.; Sanyal, A. Segment Block Dendrimers via Diels-Alder Cycloaddition. *Org. Lett.* **2007**, *9* (12), 37. DOI: 10.1021/ol800553t
51. Kelley, T. W.; Baude, P. F.; Gerlach, C.; Ender, D. E.; Muyres, D.; Haase, M. A.; Vogel, D. E.; Theiss, S. D. Recent progress in organic electronics: Materials, devices, and processes. *Chem. Mater*. **2004**, *16* (23), 4413–4422. DOI: 10.1021/cm049614j
52. Gómez, P.; Cerdá, J.; Más-Montoya, M.; Georgakopoulos, S.; Silva, I.; García, A.; Ortí, E.; Aragó, J.; Curiel, D. Effect of molecular geometry and extended conjugation on the performance of hydrogen-bonded semiconductors in organic thin-film field-effect transistors. *J. Mater. Chem. C.* **2021**. DOI: 10.1039/d1tc01328a
53. Uygun, M.; Tasdelen, M. A.; Yagci, Y. Influence of Type of Initiation on Thiol-Ene “Click” Chemistry. *Macromol. Chem. Phys.* **2010**, *211* (1), 103–110. DOI: 10.1002/macp.200900442
54. Michinobu, T.; Diederich, F. The [2+2] Cycloaddition-Retroelectrocyclization (CA-RE) Click Reaction: Facile Access to Molecular and Polymeric Push-Pull Chromophores. *Angew. Chem.* **2018**, *57* (14), 3552–3577. DOI: 10.1002/anie.201711605
55. Jordan, M.; Kivala, M.; Boudon, C.; Gisselbrecht, J.-P.; Schweizer, W. B.; Seiler, P.; Diederich, F. Switching the Regioselectivity in Cycloaddition-Retro-Electrocyclizations between Donor-Activated Alkynes and the Electron-

Accepting Olefins TCNE and TCNQ. *Chem.: Asian J.* **2011**, *6* (2), 396–401. DOI: 10.1002/asia.201000539

56. Ha, S.; Lee, Y.; Kwak, Y.; Mishra, A.; Yu, E.; Ryou, B.; Park, C. M. Alkyne–Alkene [2+2] cycloaddition based on visible light photocatalysis. *Nat. Commun.* **2020**, *11* (1), 2509. DOI: 10.1038/s41467-020-16283-9
57. Hoffmann R.; Woodward R. B. Selection Rules for Concerted Cycloaddition Reactions. *J. Am. Chem. Soc.* **1965**, *87* (9), 2046–2048. DOI: 10.1021/ja01087a034; Hoffmann R.; Womontoyaodward R. B. The Conservation of Orbital Symmetry. *Angew. Chem.* **1969**, *8* (11), 781–853. DOI: 10.1002/anie.196907811; Hoffmann R. And Woodward R. B. 1971. The Conservation of orbitalsymmetry, 1st ed.; Academic Press, 1971. DOI: 10.1016/B978-1-4832-3290-4.50006-4
58. Vollmer, J. J.; Servis, K. L. Woodward-Hoffmann Rules: Cycloaddition Reactions. *J. Chem. Educ.* **1970**, *47* (7), 491–500. DOI: 10.1021/ed047p491
59. Alcaide, B.; Almendros, P.; Aragoncillo, C. Exploiting [2+2] cycloaddition chemistry: achievements with allenes. *Chem. Soc. Rev.* **2010**, *39* (2), 783–816. DOI: 10.1039/b913749a
60. Sarkar, D.; Bera, N.; Ghosh, S. [2+2] Photochemical Cycloaddition in Organic Synthesis. *Eur. J. Org. Chem.* **2019**, *2020* (10), 1310–1326. DOI: 10.1002/ejoc.201901143
61. Alcaide, B.; Almendros, P.; Aragoncillo, C. Exploiting [2+2] cycloaddition chemistry: achievements with allenes. *Chem. Soc. Rev.* **2010**, *39* (2), 783–816. DOI: 10.1039/b913749a
62. Ischay, M. A.; Lu, Z.; Yoon, T. P. Cycloadditions by oxidative visible light photocatalysis. *J. Am. Chem. Soc.* **2010**, *132* (25), 8572–8574. DOI: 10.1021/ja103934y
63. Bach, T. Stereoselective intermolecular [2+2]-photocycloaddition reactions and their application in synthesis. *Synth.* **1998**, *1998* (5), 683–703. DOI: 10.1055/s-1998-2054.
64. Ciamician, G.; Silber, P. Chemische Lichtwirkungen. *Chem. Ber.* **1908**, *41* (1),

1071-1080. DOI: 10.1002/cber.190804101211

65. Crimmins, M. T. Synthetic Applications of Intramolecular Enone-Olefin Photocycloadditions. *Chem. Rev.* **1988**, *88* (8), 1453–1473. DOI: 10.1021/CR00090A002
66. Schuster, D. I.; Lem, G.; Kaprinidis, N. A. New Insights into an Old Mechanism: [2+2] Photocycloaddition of Enones to Alkenes. *Chem. Rev.* **1993**, *93* (1), 3–22. DOI: 10.1021/cr00017a001
67. Reinhoudt, D. N.; Kouwenhoven, C. G. Cycloaddition reactions involving carbon-carbon double bonds of heteroaromatic compounds. *Recl. Trav. Chim. Pays-Bas* **1974**, *93* (12), 321–324. DOI: 10.1002/recl.19740931207
68. Reinhoudt, D. N. (2+2)-Cycloaddition and (2+2)-Cycloreversion Reactions of Heterocyclic Compounds. *Adv Heterocycl Chem.* **1977**, *21* (C), 253–321. DOI: 10.1016/S0065-2725(08)60734-5
69. Trofimov, B. A.; Sobenina, L. N.; Stepanova, Z. V.; Ushakov, I. A.; Sinegovskaya, L. M.; Vakulskaya, T. I.; Mikhaleva, A. I. Facile [2+2] cycloaddition of DDQ to an alkyne: Synthesis of pyrrolyl- and indolylbicyclo[4.2.0]octadienes from C -ethynylpyrroles or C -ethynylindoles. *Synth.* **2010**, *2010* (3), 470–476. DOI: 10.1055/s-0029-1217133
70. Kato, S. I.; Beels, M. T. R.; La Porta, P.; Schweizer, W. B., Boudon, C.; Gisselbrecht, J. P.; Biaggio, I.; Diederich, F. Homoconjugated push-pull and spiro systems: Intramolecular charge-transfer interactions and third-order optical nonlinearities. *Angew. Chem.* **2010**, *49* (35), 6207–6211. DOI: 10.1002/anie.201002236
71. Shoji, T.; Maruyama, M.; Shimomura, E.; Maruyama, A.; Ito, S.; Yasunami, M.; Higashi, J.; Toyota, K.; Morita, N. Synthesis, Properties, And Crystal Structure of Ddq-Adducts of Ethynylated 2h-Cyclohepta[B]Furan-2-Ones. *Heterocycles* **2014**, *88* (1), 319–329. DOI: 10.3987/COM-13-S(S)24
72. Dengiz, C.; Dumele, O.; Kato, S.; Zalibera, M.; Cias, P.; Schweizer, W. B.; Boudon, C.; Gisselbrecht, J.-P.; Gescheidt, G.; Diederich, F. From Homoconjugated Push-Pull Chromophores to Donor-Acceptor-Substituted

Spiro Systems by Thermal Rearrangement. *Chem. Eur. J.* **2014**, *20* (5), 1279–1286. DOI: 10.1002/chem.201303533

73. Donckele, E. J.; Finke, A. D.; Ruhlmann, L.; Boudon, C.; Trapp, N.; Diederich, F. The [2+2] Cycloaddition-Retroelectrocyclization and [4+2] Hetero-Diels-Alder Reactions of 2-(Dicyanomethylene)indan-1,3-dione with Electron-Rich Alkynes: Influence of Lewis Acids on Reactivity. *Org. Lett.* **2015**, *17* (14), 3506–3509. DOI: 10.1021/acs.orglett.5b01598
74. Breitena, B.; Biaggiob, I.; Diederich, F. Nonplanar push-pull chromophores for opto-electronic applications. *Chimia* **2010**, *64* (6), 409–413. DOI: 10.2533/chimia.2010.409
75. Kato, S.; Diederich, F. Non-planar push-pull chromophores. *Chem. Comm.* **2010**, *46* (12), 1994–2006. DOI: 10.1039/b926601a
76. Michinobu, T.; Diederich, F. The [2+2] Cycloaddition-Retroelectrocyclization (CA-RE) Click Reaction: Facile Access to Molecular and Polymeric Push-Pull Chromophores. *Angew. Chem.* **2018**, *57* (14), 3552–3577. DOI: 10.1002/ange.201711605
77. Bruce, M. I.; Rodgers, J. R.; Snow, M. R.; Swincer, A. G. Cyclopentadienyl-ruthenium and -osmium chemistry. Cleavage of tetracyanoethylene under mild conditions: X-ray crystal structures of [Ru{η3-C(CN)2cphc[double bond, length as m-dash]C(CN)2}(pph3)(η-C5H5)] and [Ru{C[[double bond, length as m-dash]C(CN)2]cph[double bond, length as m-dash]C(CN)2}-(cnbut)(pph3)(η-C5H5)]. *J. Chem. Soc., Chem. Comm.* **1981**, 271–272.DOI: 10.1039/C39810000271
78. a) Bruce, M. I.; Hambley, T. W.; Snow, M. R.; Swincer. A. G. Reactions of tetracyanoethylene with transition-metal acetylides: synthesis and structure of Rh(C□cph) [η2-C2(CN)4] (ncme)(pph3)2. *J. Organomet. Chem.* **1982**, *235* (1) 105–112. DOI: 10.1016/S0022-328X(00)85726-5; b) Hussain, M.; Albert, D.; Wartchow, R.; Butenschön, H. The First Cyclopentadienylalkylphosphane Nickel Chelates: Synthesis, Structures, and Reactions. *Asian J. Chem.* **2007**, *2* (6), 782–793. DOI: 10.1002/asia.200700032

79. Onitsuka, K.; Takahashi, S. Synthesis and structure of s-cis-and s-trans-μ-butadiene-2,3-diyldiplatinum complexes by the reaction of μ-ethynediyldiplatinum complexes with tetracyanoethylene. *J. Chem. Soc., Chem. Commun*. **1995**, 2095–2096. DOI: 10.1039/C39950002095
80. a) Wu, X.; Wu, J.; Liu, Y.; Jen, A. K.-Y. Highly Efficient, Thermally and Chemically Stable Second Order Nonlinear Optical Chromophores Containing a 2-Phenyl-tetracyanobutadienyl Acceptor. *J. Am. Chem. Soc.* **1999**, *121* (2), 472–473. DOI: 10.1021/ja983537; b) Cai, C.; Liakatas, I.; Wong, M.S.; Bösch, M.; Bosshard C.; Günter, P.; Concilio S.; Tirelli, N.; Suter U. W. Donor−Acceptor-Substituted Phenylethenyl Bithiophenes: Highly Efficient and Stable Nonlinear Optical Chromophores. *Org. Lett*. **1999**, *1* (11), 1847–1849. DOI: 10.1021/ol991118r
81. Morioka, Y.; Yoshizawa, N.; Nishida, J.; Yamashita, Y. Novel donor-pi-acceptor compounds containing 1,3-dithiol-2-ylidene and tetracyanobutadiene units. *Chem. Lett.* **2004**, *33* (9), 1190–1191. DOI: 10.1246/cl.2004.1190
82. Michinobu, T.; May, J. C.; Lim, J. H.; Boudon, C.; Gisselbrecht, J.-P.; Seiler, P.; Gross, M.; Biaggio, I.; Diederich, F. A new class of organic donor-acceptor molecules with large third-order optical nonlinearities. *Chem.Comm.* **2005**, 737–739. DOI: 10.1039/b417393g
83. Michinobu, T.; Boudon, C.; Gisselbrecht, J. P.; Seiler, P.; Frank, B.; Moonen, N. N. P.; Gross, M.; Diederich, F.Donor-substituted 1,1,4,4-tetracyanobtadienes (tcbds):New chromophores with efficient intramolecular charge-transfer interactions by atom-economic synthesis. *Chem. Eur. J.* **2006**, *12* (7), 1889–1905. DOI: 10.1002/chem.200501113
84. Wu, Y. L.; Jarowski, P. D.; Schweizer, W. B.; Diederich, F. Mechanistic investigation of the dipolar [2+2] cycloaddition-cycloreversion reaction between 4-(N,N-dimethylamino)phenylacetylene and arylated 1,1-dicyanovinyl derivatives to form intramolecular charge-transfer chromophores. *Chem. Eur. J.* **2010**, *16* (1), 202–211. DOI: 10.1002/chem.200902645
85. a) Tang, X.; Liu, W.; Wu, J.; Lee, C.-S.; You, J.; Wang, P. Synthesis, Crystal

Structures, and Photophysical Properties of Triphenylamine-Based Multicyano Derivatives. *J. Org. Chem.* **2010**, *75* (21), 7273–7278. DOI: 10.1021/jo101456v; b) Niu, S.; Ulrich, G.; Retailleau, P.; Ziessel R. Regioselective Synthesis of 5-Monostyryl and 2-Tetracyanobutadiene BODIPY Dyes. *Org. Lett.* **2011**, *13* (19), 4996–4999. DOI: 10.1021/ol201600s; c) Betou, M.; Kerisit, N.; Meledje, E.; Leroux, Y. R.; Katan, C.; Halet, J.-F.; Guillemin, J.-C.; Trolez, Y. High-Yield Formation of Substituted Tetracyanobutadienes from Reaction of Ynamides with Tetracyanoethylene. *Chem. Eur. J.* **2014**, *20* (31), 9553–9557. DOI: 10.1002/chem.201402653; d) Okuno, T.; Iwahashi, H. 2-Methyl-3-(10H-pheno-thia-zin-10-yl)buta-1,3-diene-1,1,4,4-tetra-carbo-nitrile. *Acta Crystallogr. E* **2013**, 69 (5), o665. DOI: 10.1107/S1600536813008799; e) Mochida, T.; Yamazaki, S. Mono- and diferrocenyl complexes with electron-accepting moieties formed by the reaction of ferrocenylalkynes with tetracyanoethylene. *J. Chem. Soc., Dalton Trans.* **2002**, 3559–3564. DOI: 10.1039/B204168E; f) Shoji, T.; Ito, S.; Toyota, K.; Yasunami, M.; Morita, N. Synthesis, Properties, and Redox Behavior of Mono-, Bis-, and Tris[1,1,4,4,-tetracyano-2-(1-azulenyl)-3-butadienyl] Chromophores Binding with Benzene and Thiophene Cores. *Chem. Eur. J.* **2008**, *14* (27), 8398–8408. DOI: 10.1002/chem.200701981; g) Shoji, T.; Ito, S.; Okujima, T.; Morita, N. Synthesis and [2+2] Cycloaddition with Tetracyanoethylene of Ene–Diyne Scaffolds Bearing Ferrocenes at the Periphery. *Eur. J. Org. Chem.* **2011**, *2011* (26), 5134–5140. DOI: 10.1002/ejoc.201100650; h) Kato, S; Kivala, M.; Schweizer, W. B.; Boudon, C.; Gisselbrecht, J.-P.; Diederich, F. Origin of Intense Intramolecular Charge-Transfer Interactions in Nonplanar Push-Pull Chromophores. *Chem. Eur. J.* **2009**, *15* (35), 8687–8691. DOI: 10.1002/chem.200901630; i) Kato, S.-i.; Noguchi, H.; Jin, S.; Nakamura, Y. Synthesis and Electronic, Optical, and Electrochemical Properties of a Series of Tetracyanobutadiene-Substituted Carbazoles. *Asian J. Org. Chem.* **2016**, *5* (2), 246–256. DOI: 10.1002/ajoc.201500431

86. Finke, A. D.; Dumele, O.; Zalibera, M.; Confortin, D.; Cias, P.; Jayamurugan,

G.; Gisselbrecht, J.-P.; Boudon, C.; Schweizer, W. B.; Gescheidt, G.; Diederich, F. 6,6-Dicyanopentafulvenes:Electronic Structure and Regioselectivity in [2+2] Cycloaddition−Retroelectrocyclization Reactions. *J. Am. Chem. Soc.* **2012**, *134* (43), 18139−18146. DOI: 10.1021/ja309141r

87. a) Kivala, M.; Boudon, C.; Gisselbrecht, J.-P.; Seiler, P.; Gross, M.; Diederich, F. A novel reaction of 7,7,8,8-tetracyanoquinodimethane (TCNQ): charge-transfer chromophores by [2+2] cycloaddition with alkynes. *ChemComm*. **2007**, 4731–4733. DOI: 10.1039/B713683H; b) Kivala, M.; Boudon, C.; Gisselbrecht, J.-P.; Enko, B.; Seiler, P.; Müller, I. B.; Langer, N.; Jarowski, P. D.; Gescheidt, G.; Diederich, F. Organic Super-Acceptors with Efficient Intramolecular Charge-Transfer Interactions by [2+2] Cycloadditions of TCNE, TCNQ, and F4-TCNQ to Donor-Substituted Cyanoalkynes. *Chem. Eur. J.* **2009**, *15* (16), 4111–4123. DOI: 10.1002/chem.200802563

88. a) Silvestri, F.; Jordan, M.; Howes, K.; Kivala, M.; Rivera-Fuentes, P.; Boudon, C.; Gisselbrecht, J. P.; Schweizer, W. B.; Seiler, P.; Chiu, M.; Diederich, F. Regular Acyclic and Macrocyclic [AB] Oligomers by Formation of Push–Pull Chromophores in the Chain-Growth Step. *Chem. Eur. J.* **2011**, *17* (22), 6088–6097. DOI: 10.1002/chem.201003672; b) Donckele, E. J.; Finke, A. D.; Ruhlmann, L.; Boudon, C.; Trapp, N.; Diederich, F. The [2+2] Cycloaddition-Retroelectrocyclization and [4+2] Hetero-Diels-Alder Reactions of 2-(Dicyanomethylene)indan-1,3-dione with Electron-Rich Alkynes: Influence of Lewis Acids on Reactivity. *Org. Lett*. **2015**, *17* (14), 3506-3509. DOI: 10.1021/acs.orglett.5b01598; c) Chiu, M.; Jaun, B.; Beels, M. T.; Biaggio, I.; Gisselbrecht, J.-P.; Boudon, C.; Schweizer, W. B.; Kivala, M.; Diederich, F. N,N′-Dicyanoquinone Diimide-Derived Donor–Acceptor Chromophores: Conformational Analysis and Optoelectronic Properties. *Org. Lett.* **2012**, *14* (1), 54–57. DOI: 10.1021/ol202815q; d) Finke, A. D.; Dumele, O.; Zalibera, M.; Confortin, D.; Cias, P.; Jayamurugan, G.; Gisselbrecht, J.-P.; Boudon, C.; Schweizer, W. B.; Gescheidt, G.; Diederich, F. 6,6-Dicyanopentafulvenes: Electronic Structure and Regioselectivity in [2+2] Cycloaddition–

Retroelectrocyclization Reactions. *J. Am. Chem. Soc.* **2012**, *134* (43), 18139–18146. DOI: 10.1021/ja309141r; e) Jarowski, P. D.; Wu, Y.-L.; Boudon, C.; Gisselbrecht, J.-P.; Gross, M.; Schweizer, W. B.; Diederich, F. New donor–acceptor chromophores by formal [2+2] cycloaddition of donor-substituted alkynes to dicyanovinyl derivatives. *Org. Biomol. Chem.* **2009**, *7*, 1312–1322. DOI: 10.1039/B821230A

89. a) Moore, J. S.; Xu, Z. Synthesis of rigid dendritic macromolecules: enlarging the repeat unit size as a function of generation, permitting growth to continue. *Macromolecules* **1991**, *24* (21), 5893–5894. DOI: 10.1021/ma00021a030; b) Pesak, D. J.; Moore, J. S.; Wheat, T. E. Synthesis and Characterization of Water-Soluble Dendritic Macromolecules with a Stiff, Hydrocarbon Interior. *Macromolecules* **1997**, *30* (21), 6467–6482. DOI: 10.1021/ma970454p
90. a) Marchesi, F.; Turriziani, M.; Tortorelli, G.; Avvisati, G.; Torino, F.; Vecchis, L. Triazene compounds: mechanism of action and related DNA repair systems. *Pharmacol. Res.* **2007**, *56* (4), 275–287. DOI: 10.1016/j.phrs.2007.08.003 ; b) Newell, D.R.; Foster, B.J.; Carmichael, J.; Harris, A.L.; Jenns, K.; Gumbrell, L.A.; Calvert, A.H. 1990 ed.; Triazenes: Chemical, Biological And Clinical Aspects, Springer, 1990. DOI: 10.1007/978-1-4615-3832-5
91. Erden K.; Savas, I.; Dengiz, C. Synthesis of triazene-substituted homoconjugated push-pull chromophores by formal [2+2] cycloadditions. *Tetrahedron Lett.* **2019**, 60 (30), 1982–1985. DOI: 10.1016/j.tetlet.2019.06.046
92. Zarei, A.; Khazdooz, L.; Aghaei H.; Azizi, G.; Chermahini, A. N.; Hajipour A. R. Synthesis of triazenes by using aryl diazonium silica sulfates under mild conditions.*Dyes Pigm.* **2014**, *101*, 295–302. DOI: 10.1016/j.dyepig.2013.10.022
93. a) Lee, C.; Yang, W.; Parr, R. G. Development of the Colle-Salvetti correlation-energy formula into a functional of the electron density. *Phys. Rev. B.* **1988**, *37* (2-15), 785–789. DOI: 10.1103/PhysRevB.37.785; b) Becke, A. D. 1993. Density-functional thermochemistry. III. The role of exact exchange. *J. Chem. Phys.* **1993**, *98*, 5648–5652. DOI: 10.1063/1.464913
94. Frisch, et al. Gaussian 09, D.01 Ed. Gaussian, Inc., Wallingford, Ct 2009.

95. Sha, F.; Tao, Y.; Tang, C.-Y.; Zhang, F.; Wu, X.-Y. Construction of Benzo[c]carbazoles and Their Antitumor Derivatives through the Diels–Alder Reaction of 2-Alkenylindoles and Arynes. *J. Org. Chem.* **2015**, *80* (16), 8122–8133. DOI: 10.1021/acs.joc.5b01223
96. De Simone, F.; Saget, T.; Benfatti, F.; Almeida, S .;Waser, J. Formal Homo-Nazarov and Other Cyclization Reactions of Activated Cyclopropanes. *Chem. Eur. J.* **2011**, *17* (51), 14527–14538. DOI: 10.1002/chem.201102583
97. Thorley, K. J.; Hales, J. M.; Kim, H.; Ohira, S.; Brédas, J.-L.; Perry, J. W.; Anderson, H. L. Cyanine-Like Dyes with Large Bond-Length Alternation. *Chem. Eur. J.* **2013**, *19* (31), 10370–10377. DOI: 10.1002/chem.201300609
98. Tancini, F.; Wu, Y. L.; Schweizer, W. B.; Gisselbrecht, J. P.; Boudon, C.; Jarowski, P. D.; Beels, M. T.; Biaggio, I.; Diederich, F. 1,1-Dicyano-4-[4-(diethylamino)phenyl]buta-1,3-dienes: Structure-Property Relationships. *Eur. J. Org. Chem.* **2012**, *2012* (14), 2756–2765. DOI: 10.1002/ejoc.201200111
99. Wu, Z.; Li, A.; Fan, B.; Xue, F.; Adachi, C.; Ouyang, J. Phenanthrene-functionalized 3,6-dithiophen-2-yl-2,5-dihydropyrrolo[3,4–c]pyrrole-1,4-diones as donor molecules for solution-processed organic photovoltaic cells. *Sol. Energy Mater. Sol. Cells* **2011**, *95* (8), 2516–2523. DOI: 10.1016/j.solmat.2011.05.006
100. Frisch, M.J.; Trucks, G.W.; Schlegel, H.B.; Scuseria, G.E.; Robb, M.A.; Cheeseman, J.R. et al. Gaussian 09, revision D.01. Gaussian Inc, Wallingford 2013.
101. Bhavani, S.; Ashfaq, M. A.; Rambabu, D.; Basaveswara, R. M. V.; Pal, M. Ultrasound assisted Mizoroki–Heck reaction catalyzed by Pd/C: Synthesis of 3-vinyl indoles as potential cytotoxic agents. *Arab. J. Chem.* **2019**, *12* (8), 3836–3846. DOI: 10.1016/j.arabjc.2016.02.002
102. Chatzopoulou E.; Davies P. W. Highly regioselective synthesis of 2,4,5-(hetero)aryl substituted oxazoles by intermolecular [3+2]-cycloaddition of unsymmetrical internal alkynes. *ChemComm.* **2013**, *49* (77), 8617–8619. DOI: 10.1039/C3CC45410J

APPENDICES

A. ^{1}H and ^{13}C NMR Spectra

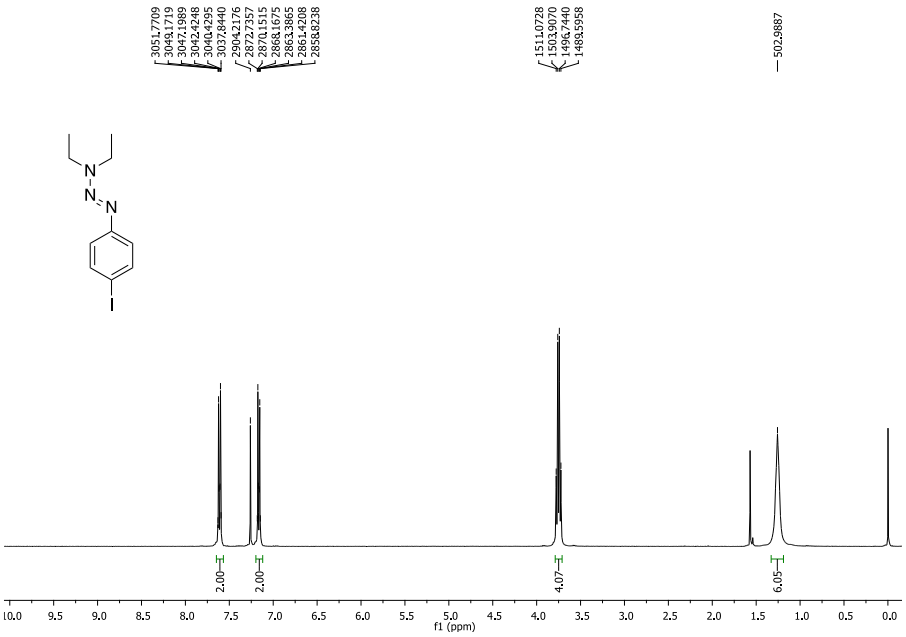

Figure 20. ^{1}H NMR spectrum of **141a** in $CDCl_3$ solution (400 MHz).

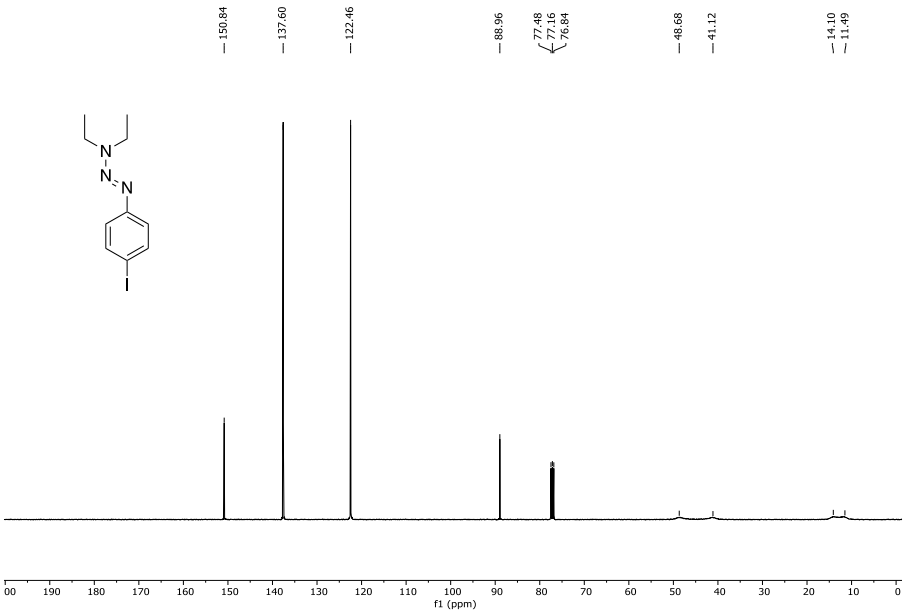

Figure 21. ^{13}C NMR spectrum of **141a** in $CDCl_3$ solution (100 MHz).

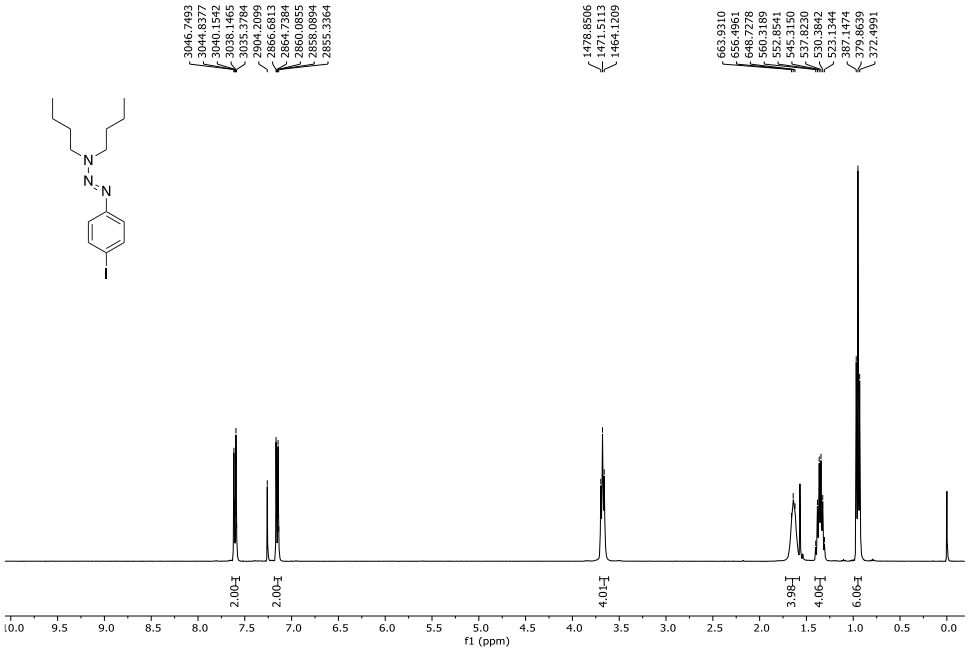

Figure 22. ^{1}H NMR spectrum of **141b** in $CDCl_3$ solution (400 MHz).

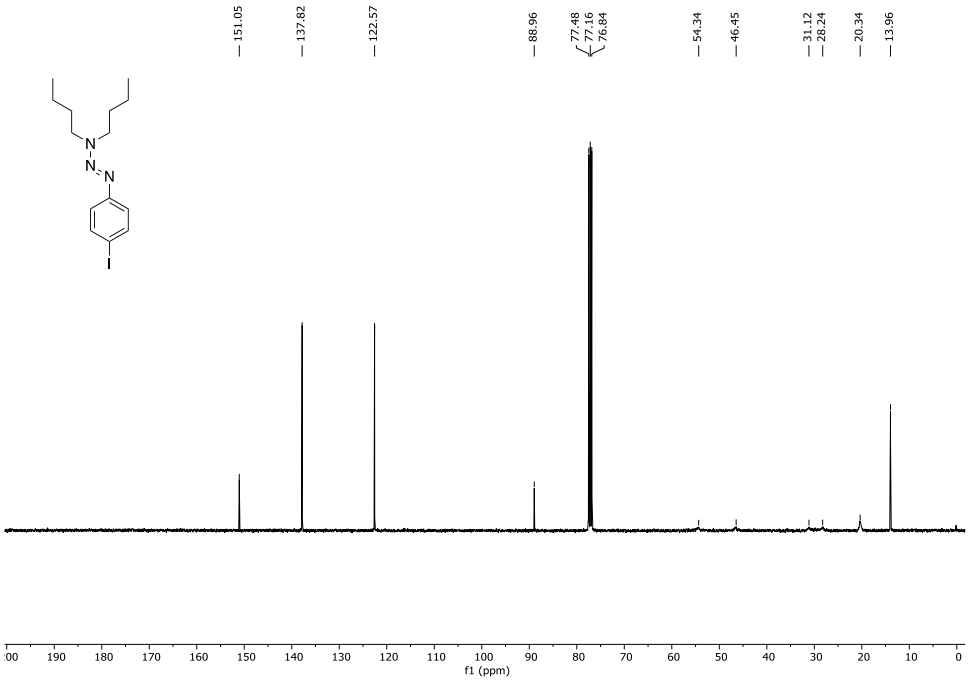

Figure 23. ^{13}C NMR spectrum of **141b** in $CDCl_3$ solution (100 MHz).

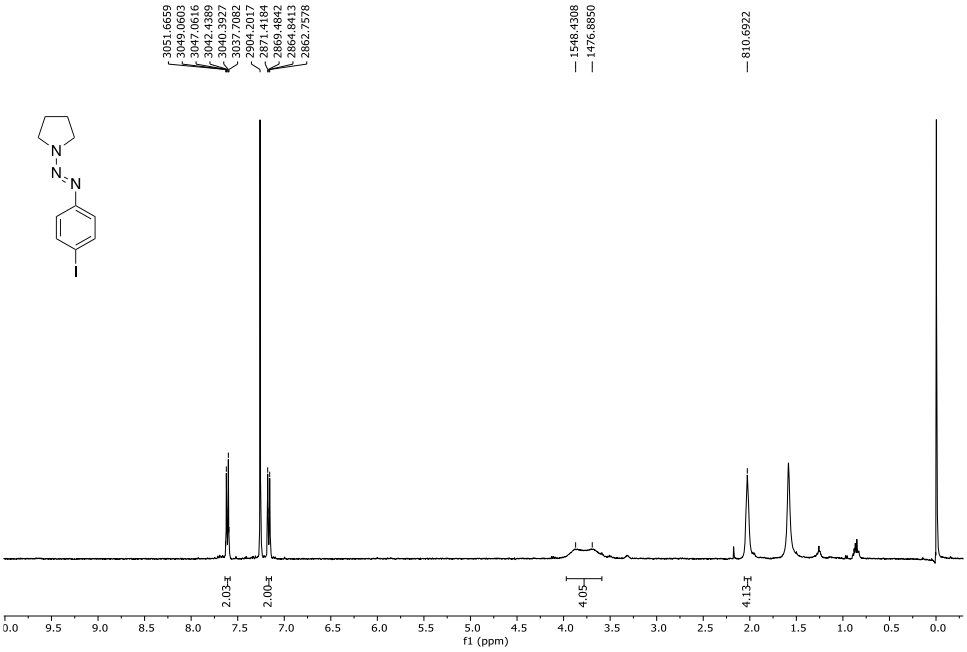

Figure 24. ^{1}H NMR spectrum of **141c** in $CDCl_3$ solution (400 MHz).

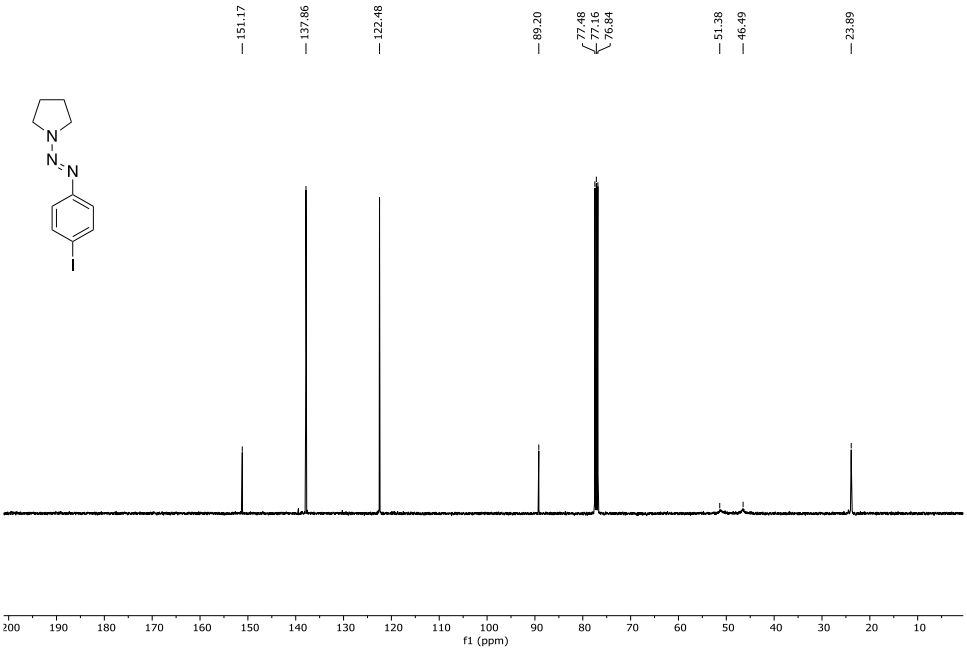

Figure 25. ^{13}C NMR spectrum of **141c** in $CDCl_3$ solution (100 MHz).

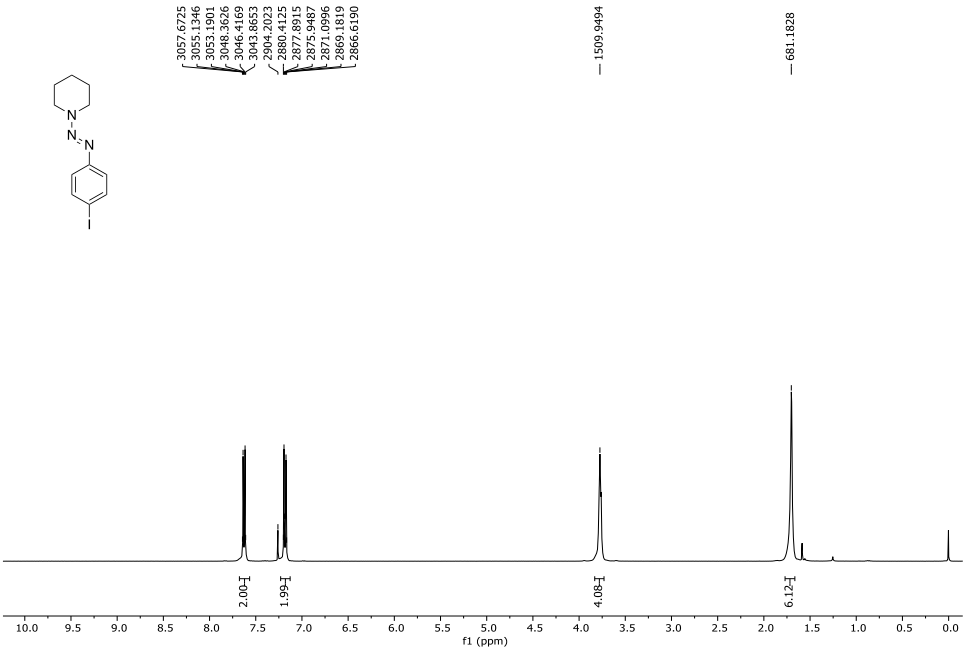

Figure 26. ^{1}H NMR spectrum of **141d** in $CDCl_3$ solution (400 MHz).

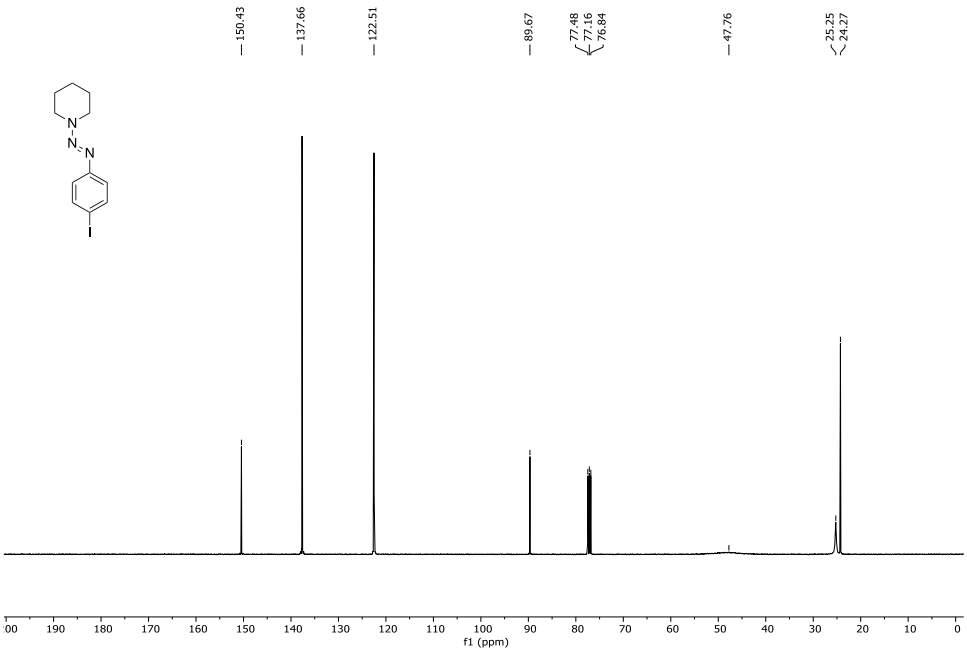

Figure 27. ^{13}C NMR spectrum of **141d** in $CDCl_3$ solution (100 MHz).

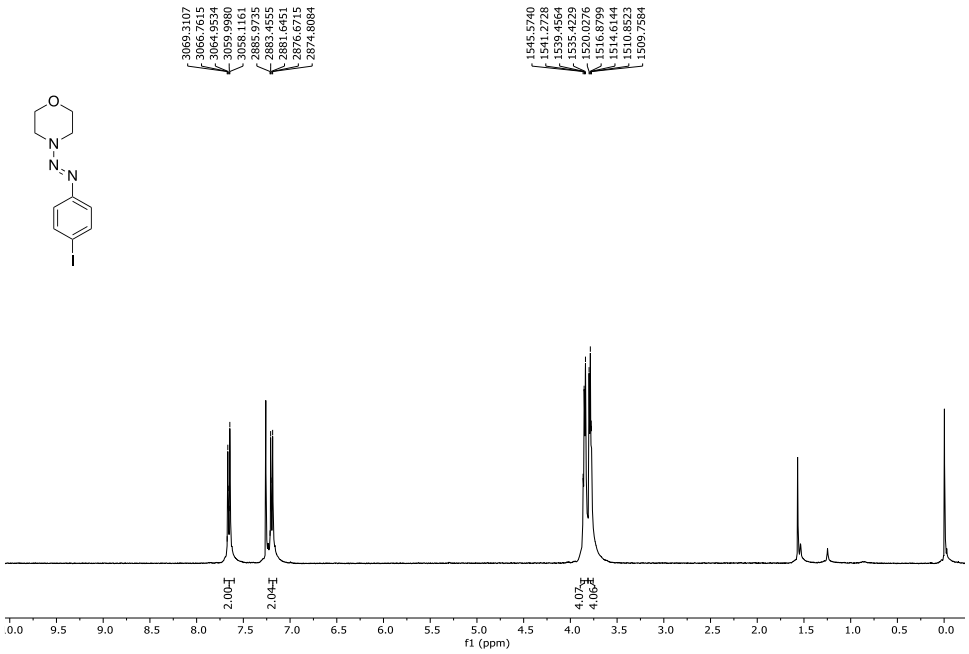

Figure 28. ^{1}H NMR spectrum of **141e** in $CDCl_3$ solution (400 MHz).

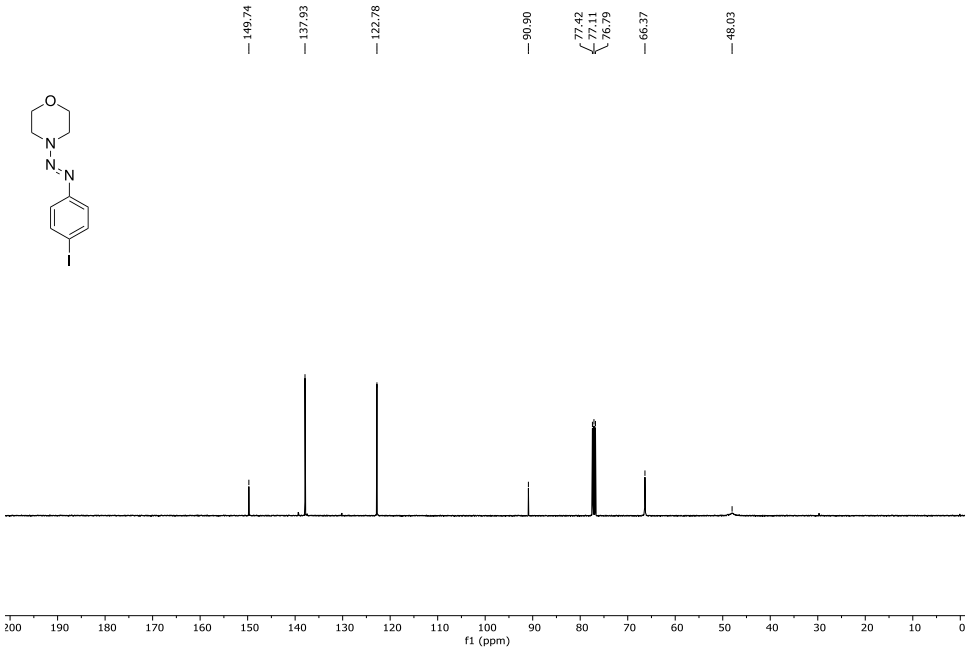

Figure 29. ^{13}C NMR spectrum of **141e** in $CDCl_3$ solution (100 MHz).

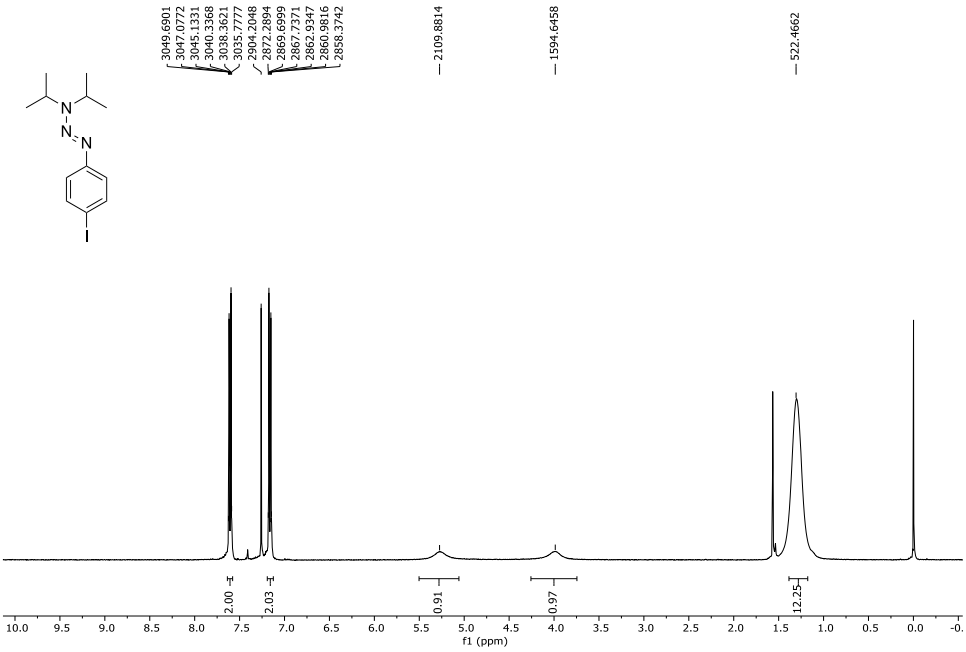

Figure 30. ^{1}H NMR spectrum of **141f** in $CDCl_3$ solution (400 MHz).

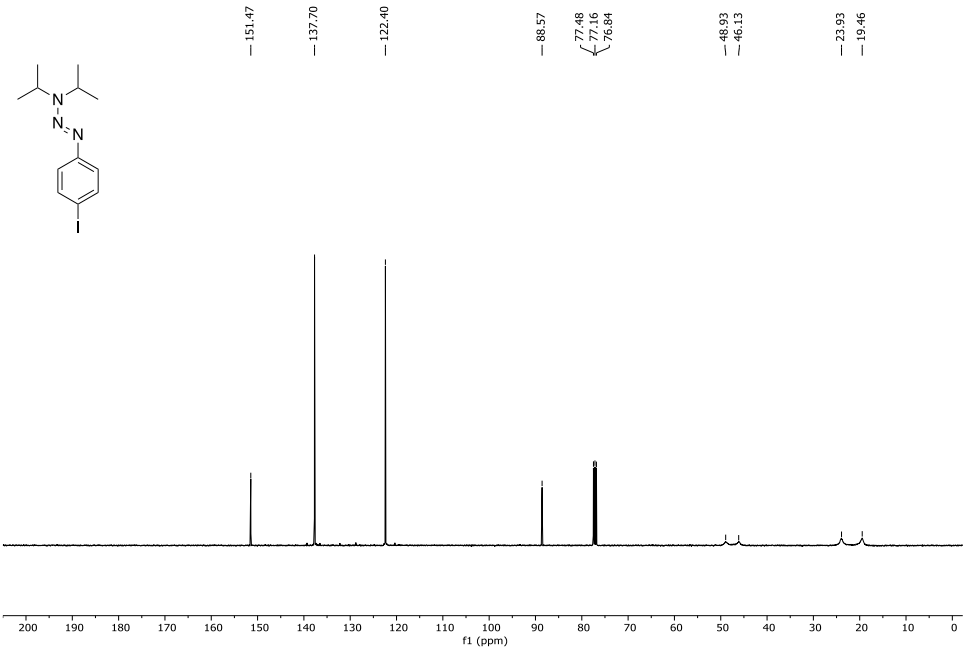

Figure 31. ^{13}C NMR spectrum of **141f** in $CDCl_3$ solution (100 MHz).

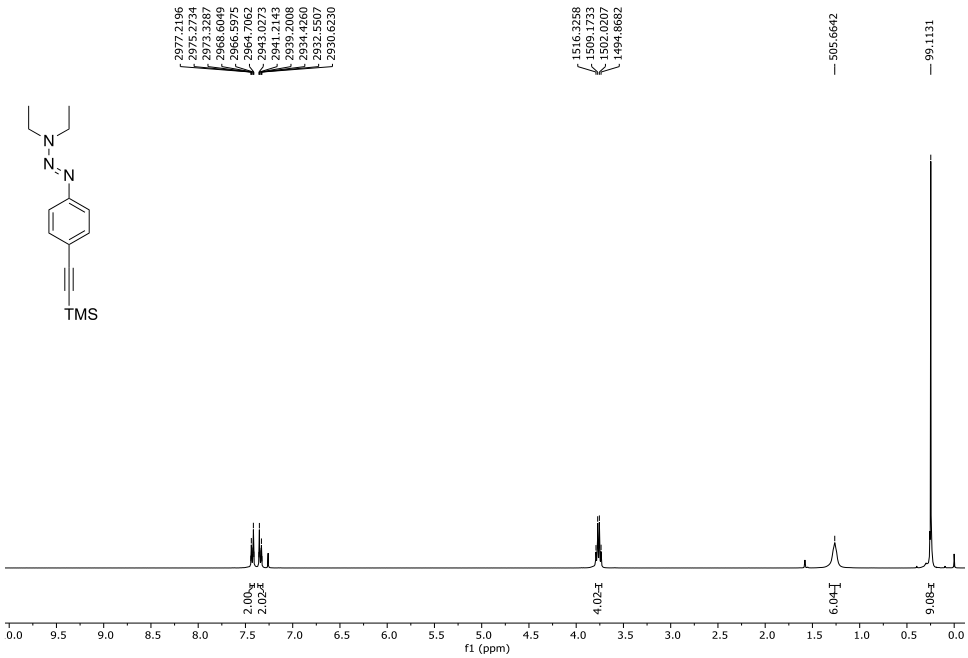

Figure 32. ^{1}H NMR spectrum of **142a** in $CDCl_3$ solution (400 MHz).

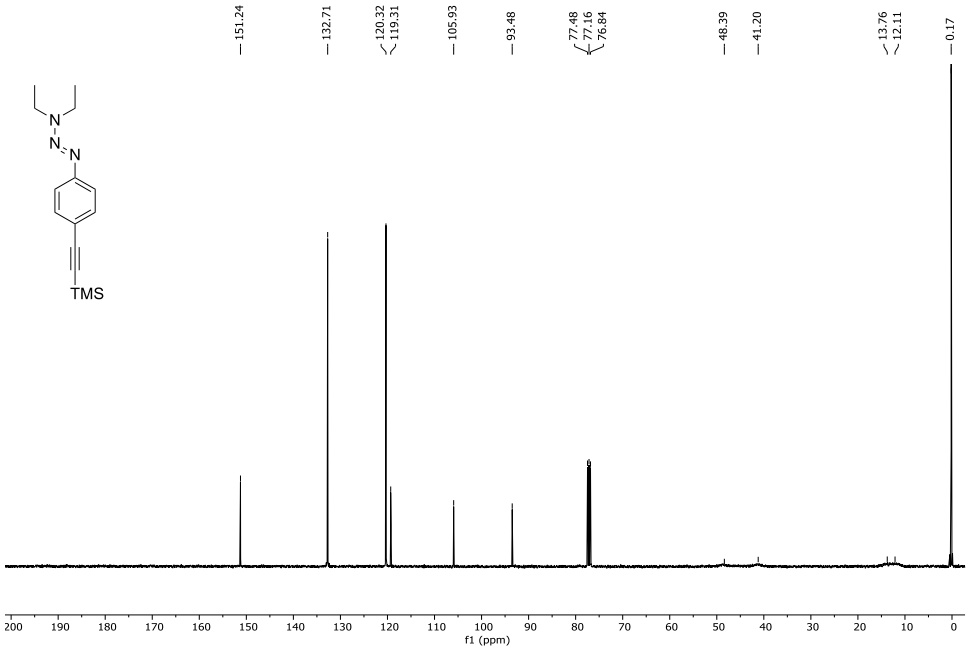

Figure 33. ^{13}C NMR spectrum of **142a** in $CDCl_3$ solution (400 MHz).

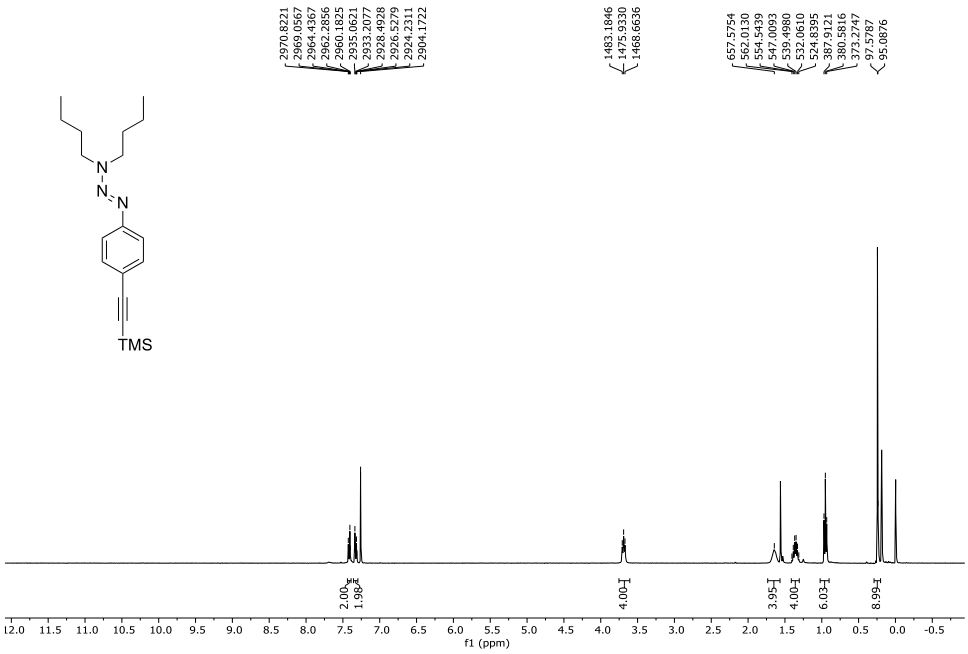

Figure 34. ^{1}H NMR spectrum of **142b** in $CDCl_3$ solution (400 MHz).

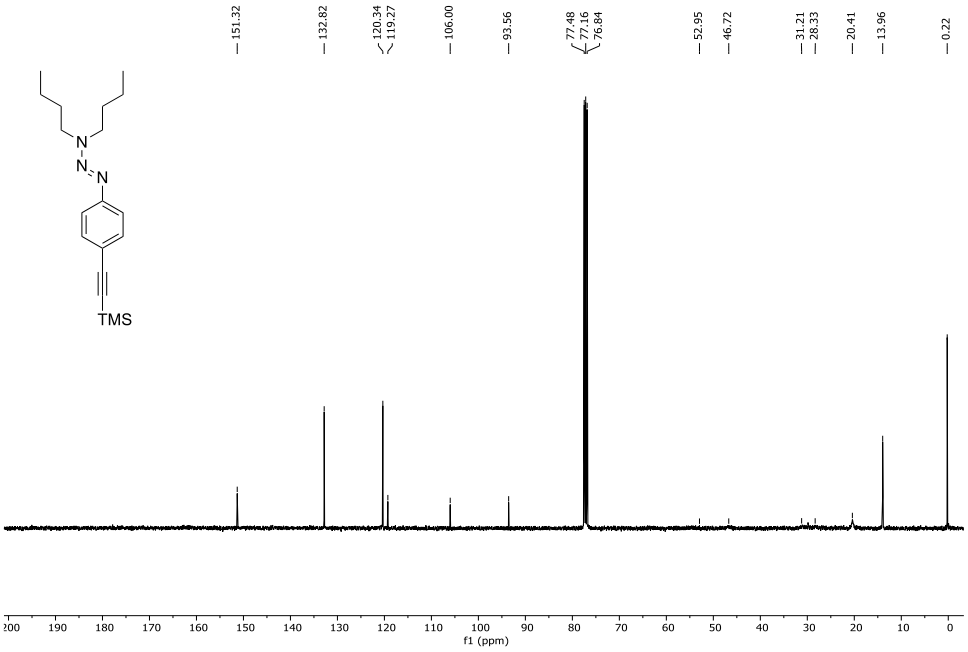

Figure 35. ^{13}C NMR spectrum of **142b** in $CDCl_3$ solution (100 MHz).

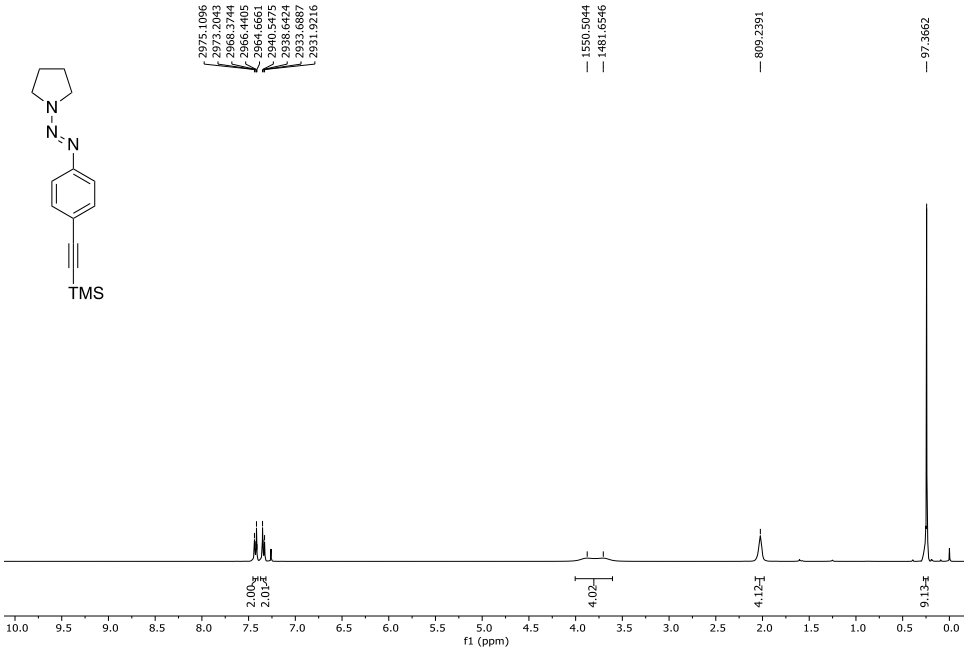

Figure 36. ^{1}H NMR spectrum of **142c** in $CDCl_3$ solution (400 MHz).

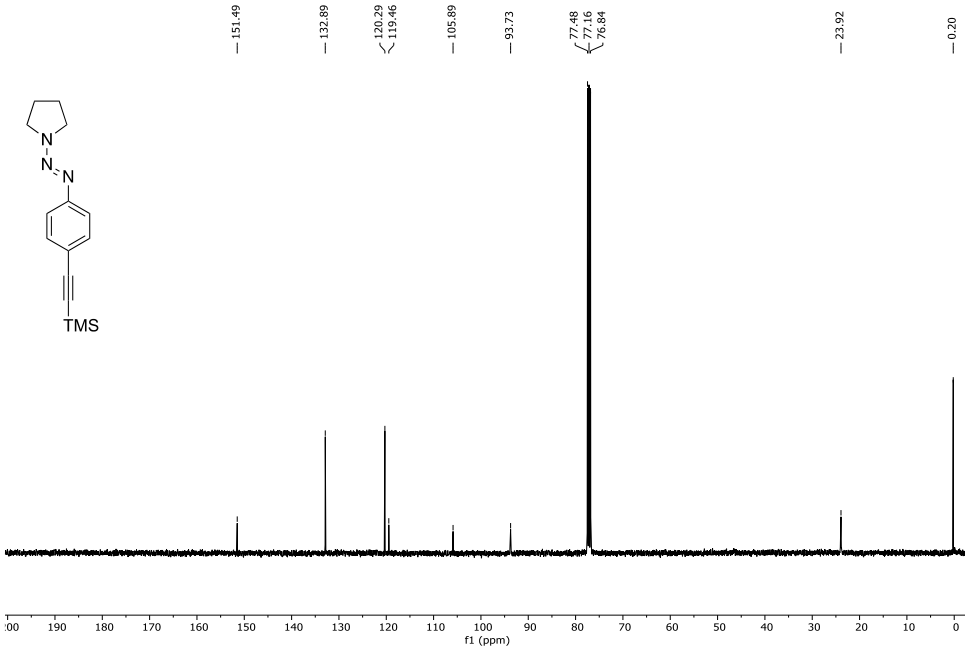

Figure 37. ^{13}C NMR spectrum of **142c** in $CDCl_3$ solution (100 MHz).

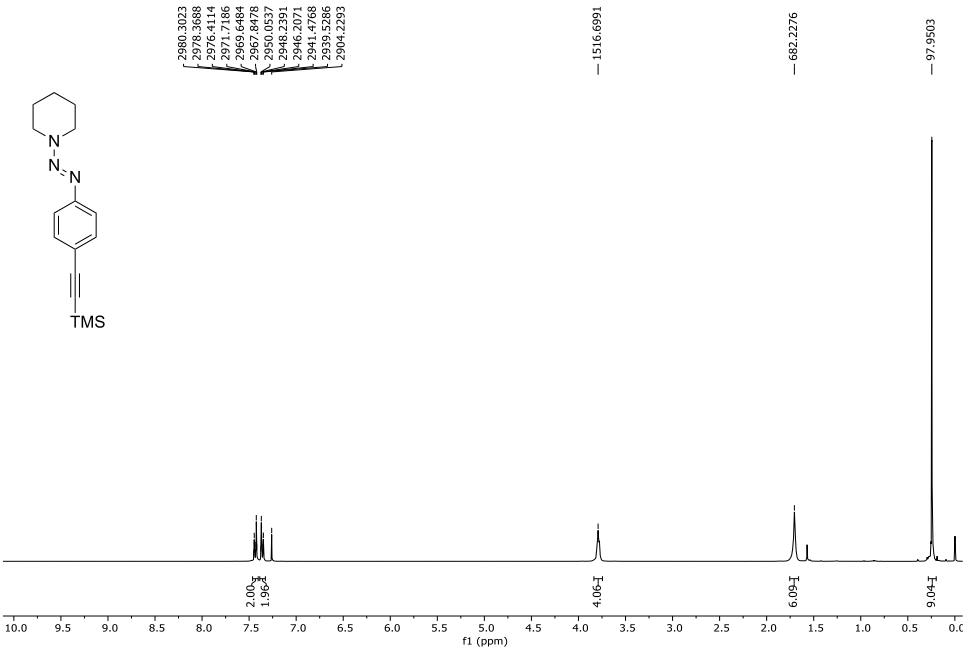

Figure 38. ^{1}H NMR spectrum of **142d** in $CDCl_3$ solution (400 MHz).

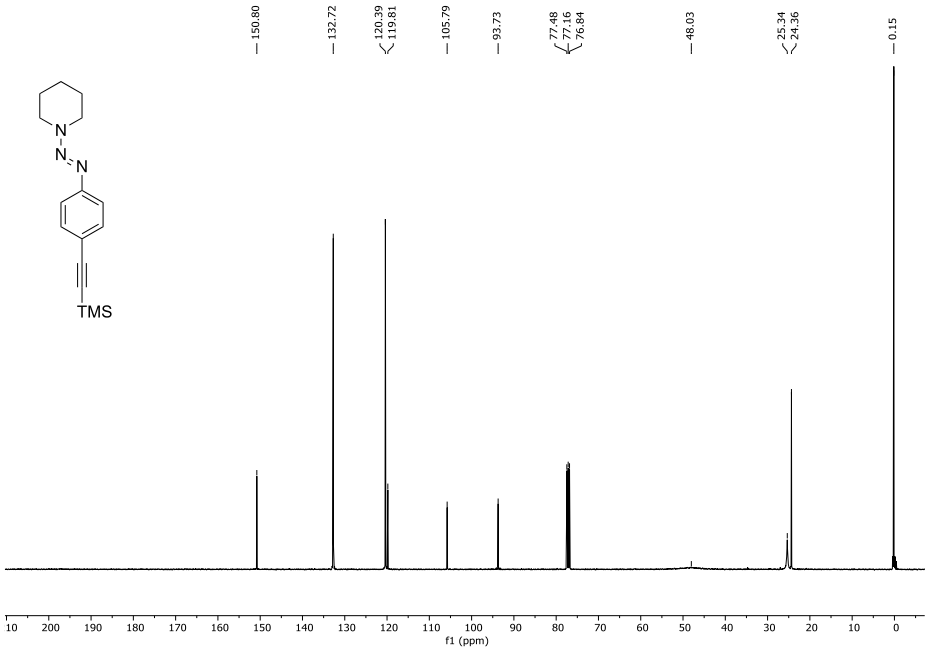

Figure 39. ^{13}C NMR spectrum of **142d** in $CDCl_3$ solution (100 MHz).

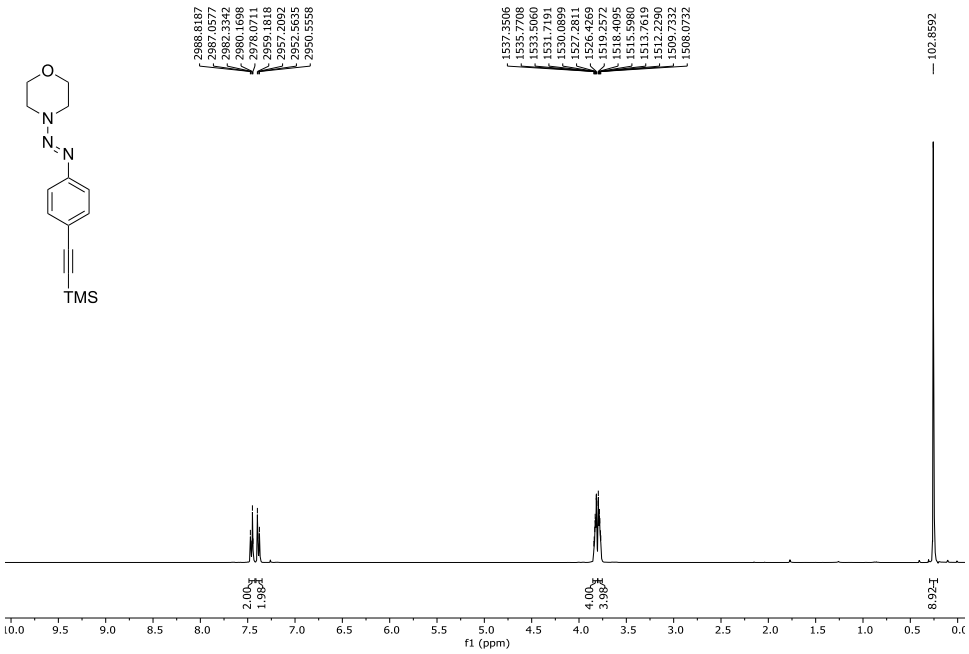

Figure 40. ^{1}H NMR spectrum of **142e** in $CDCl_3$ solution (400 MHz).

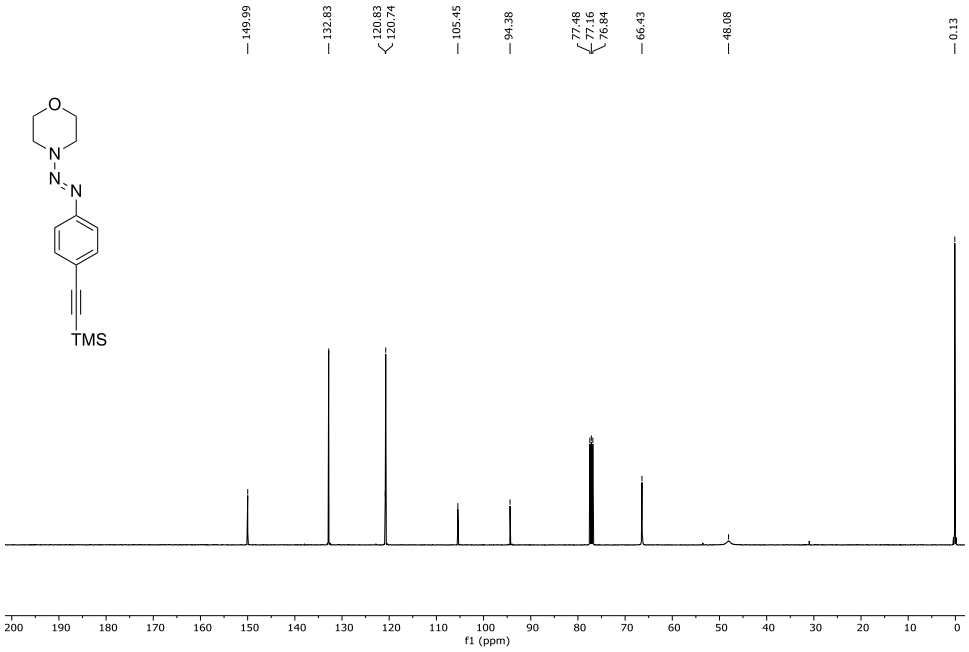

Figure 41. ^{13}C NMR spectrum of **142e** in $CDCl_3$ solution (100 MHz).

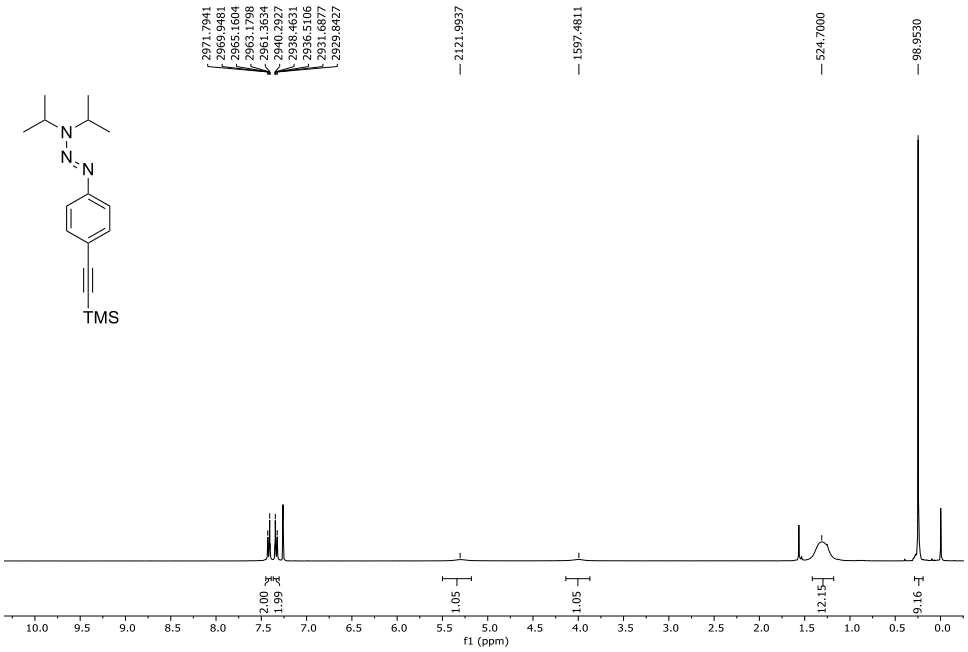

Figure 42. ^{1}H NMR spectrum of **142f** in $CDCl_3$ solution (400 MHz).

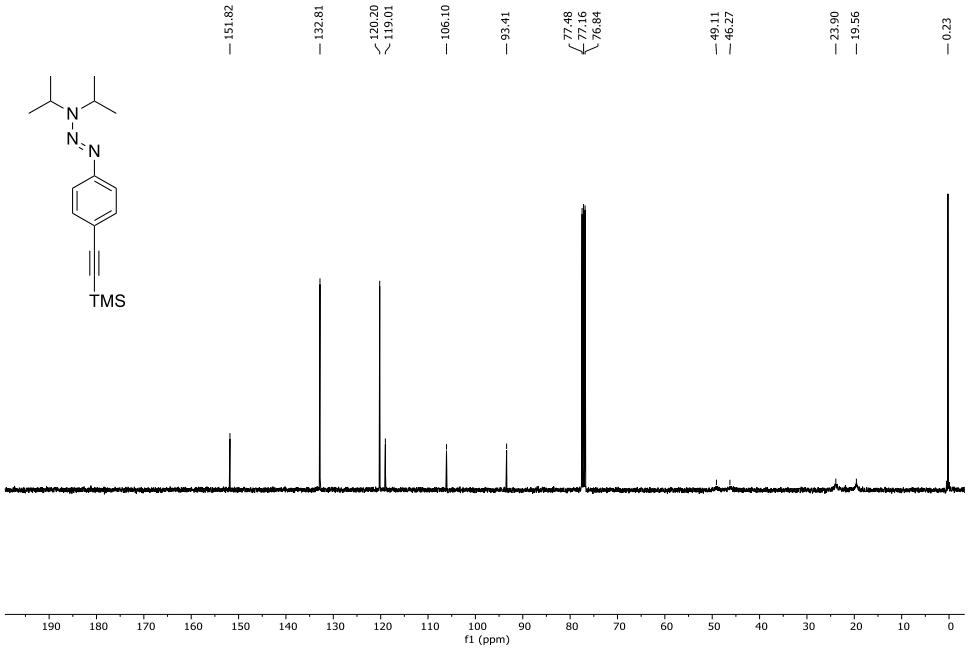

Figure 43. ^{13}C NMR spectrum of **142f** in $CDCl_3$ solution (100 MHz).

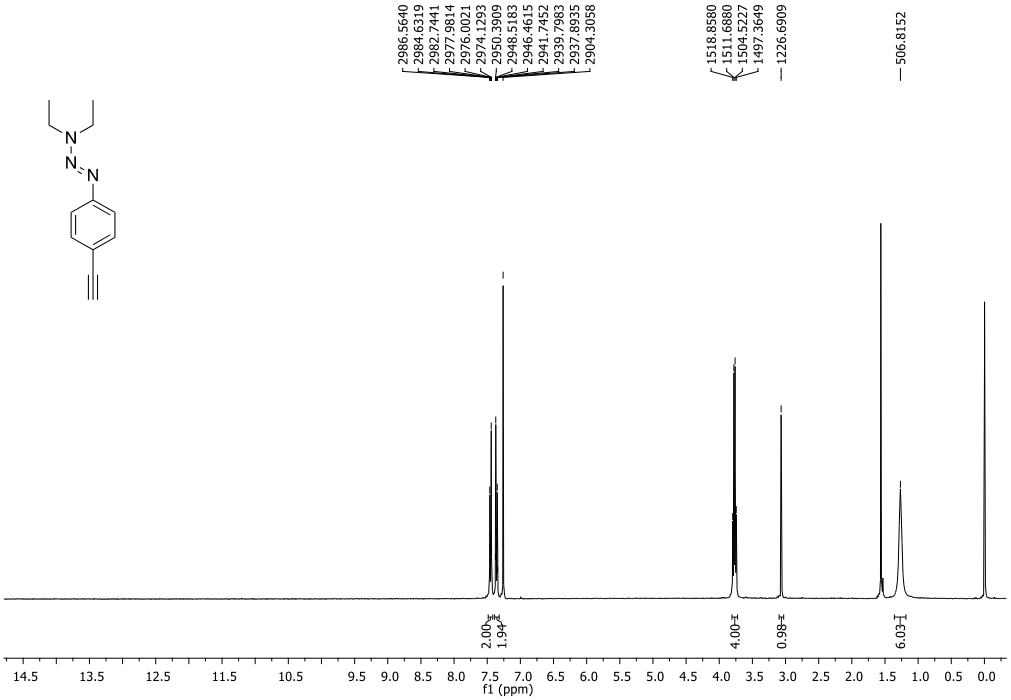

Figure 44. ^{1}H NMR spectrum of **143a** in $CDCl_3$ solution (400 MHz).

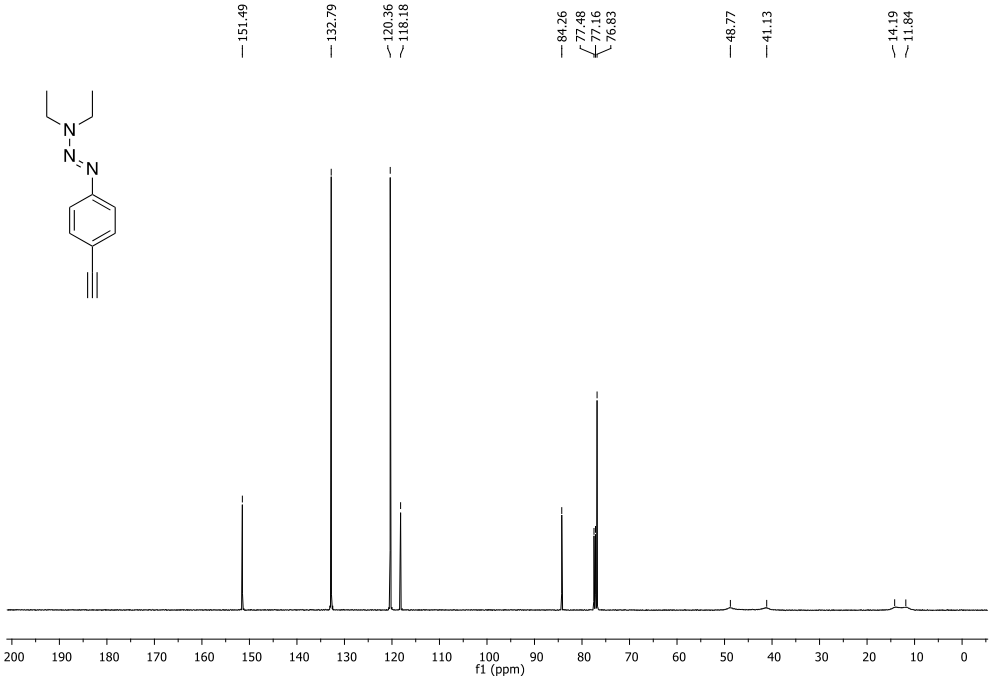

Figure 45. ^{13}C NMR spectrum of **143a** in $CDCl_3$ solution (100 MHz).

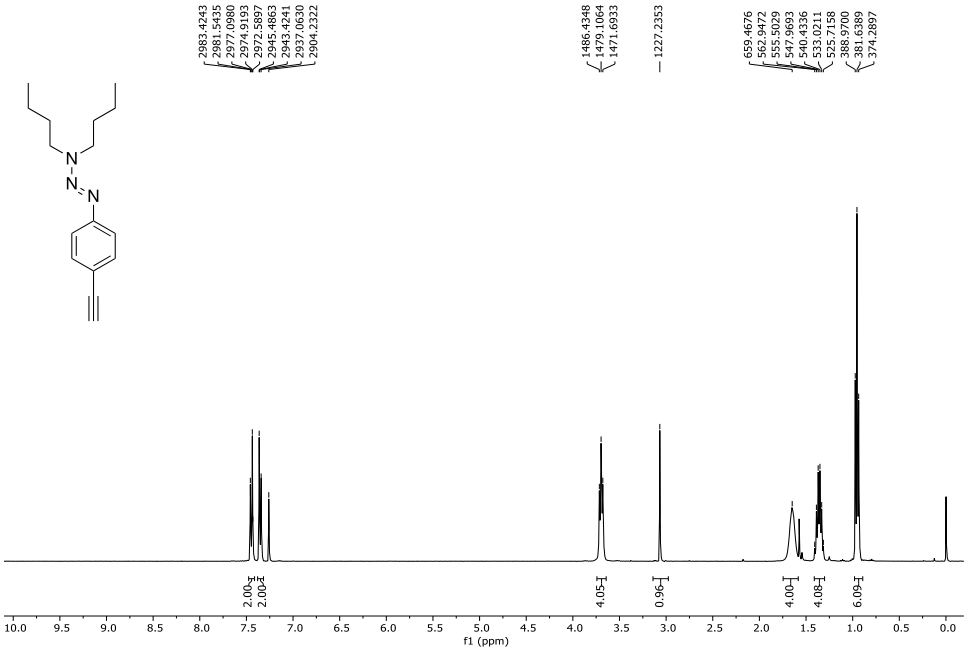

Figure 46. ^{1}H NMR spectrum of **143b** in $CDCl_3$ solution (400 MHz).

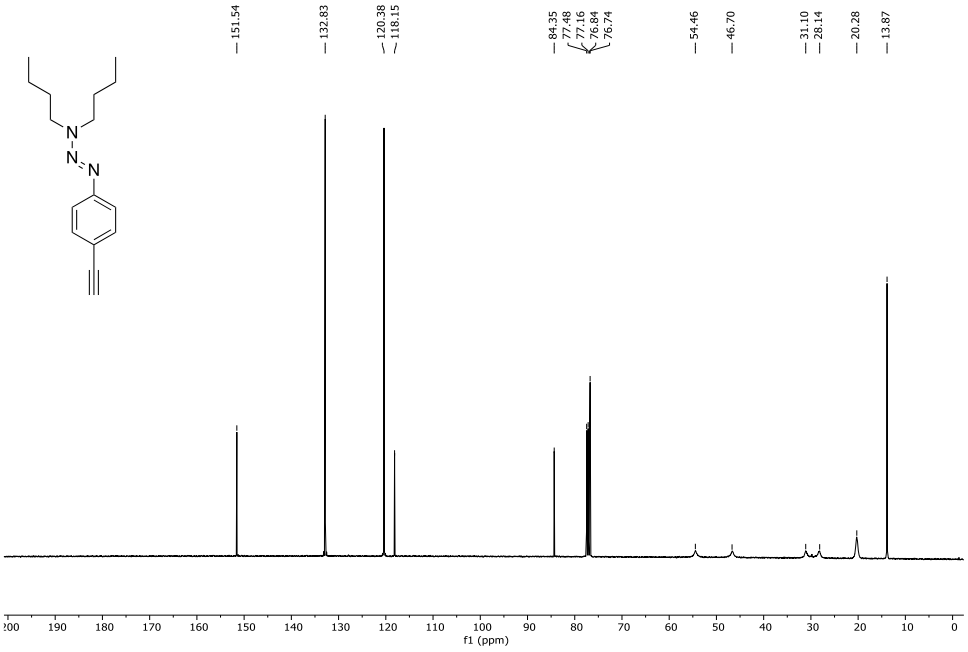

Figure 47. ^{13}C NMR spectrum of **143b** in $CDCl_3$ solution (100 MHz).

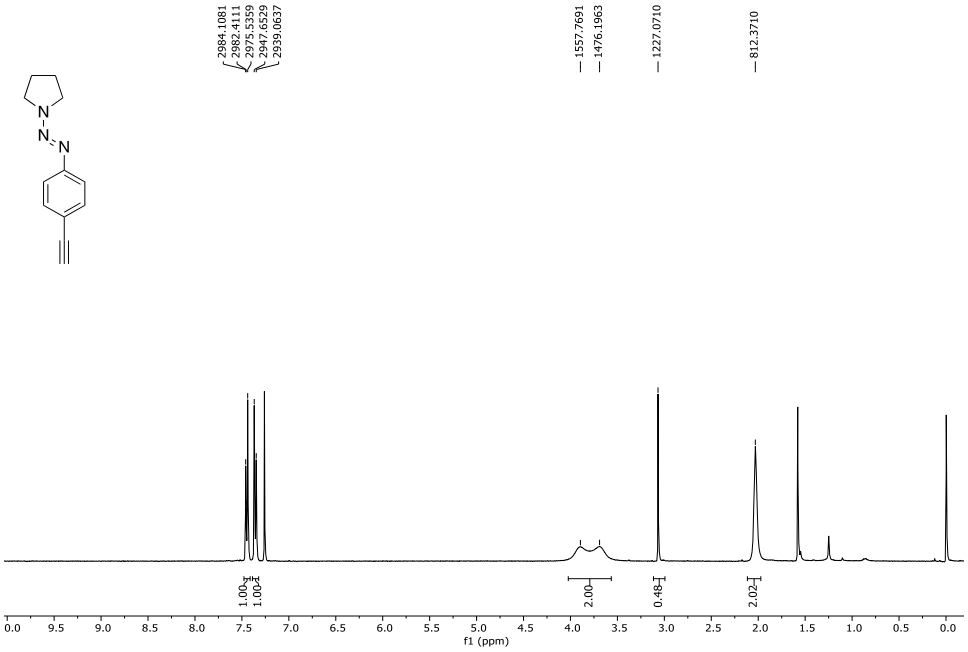

Figure 48. ^{1}H NMR spectrum of **143c** in $CDCl_3$ solution (400 MHz).

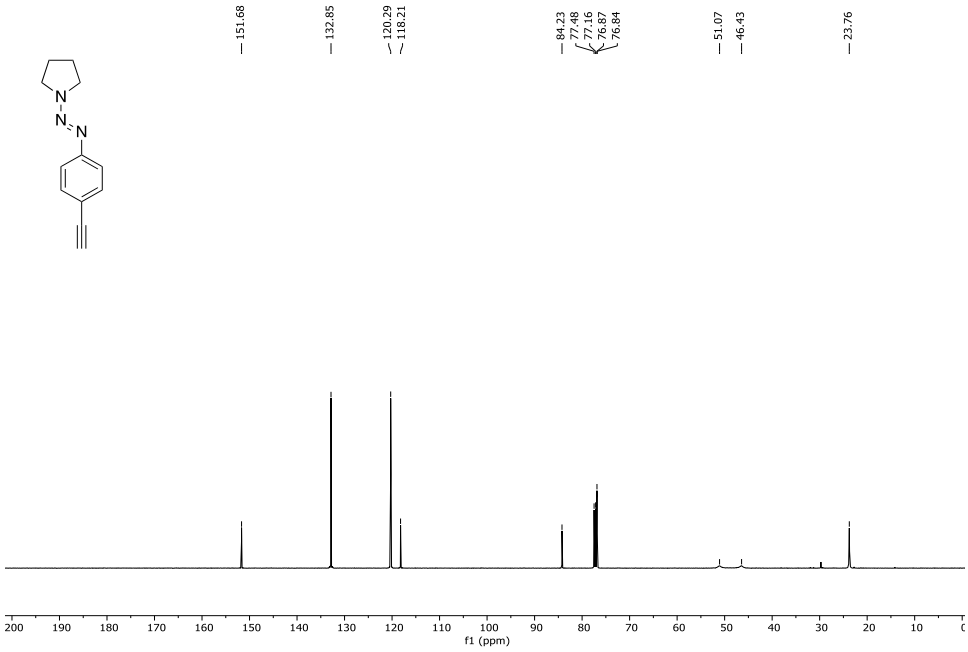

Figure 49. ^{13}C NMR spectrum of **143c** in $CDCl_3$ solution (100 MHz).

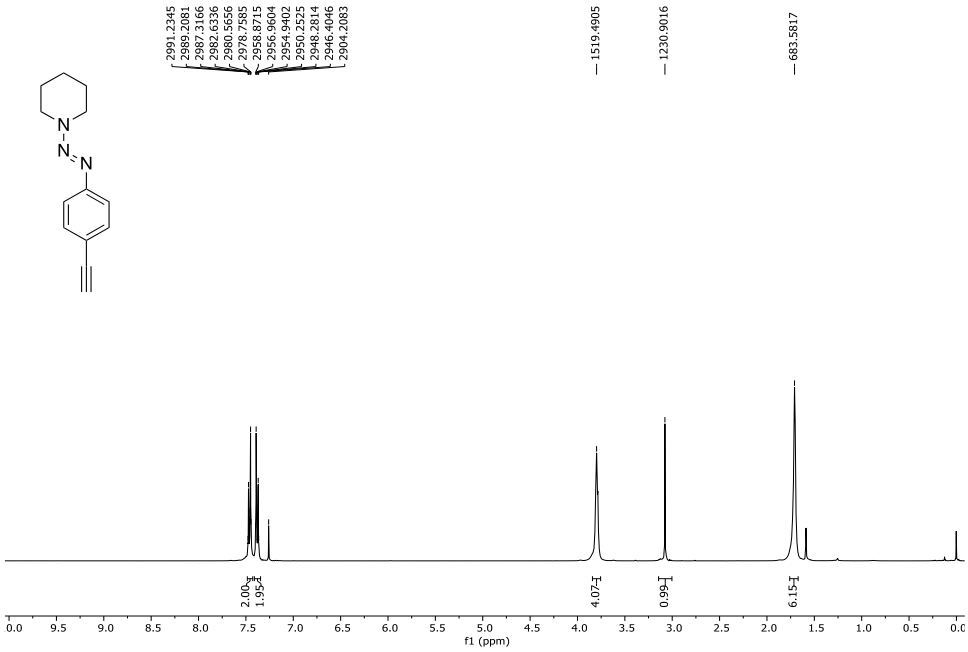

Figure 50. ^{1}H NMR spectrum of **143d** in $CDCl_3$ solution (400 MHz).

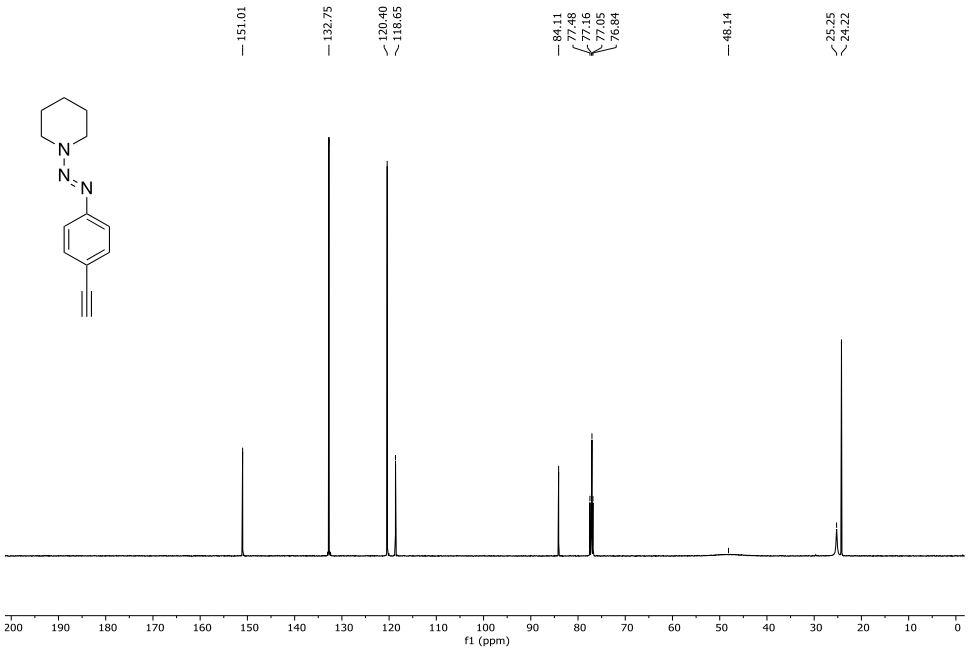

Figure 51. ^{13}C NMR spectrum of **143d** in $CDCl_3$ solution (100 MHz).

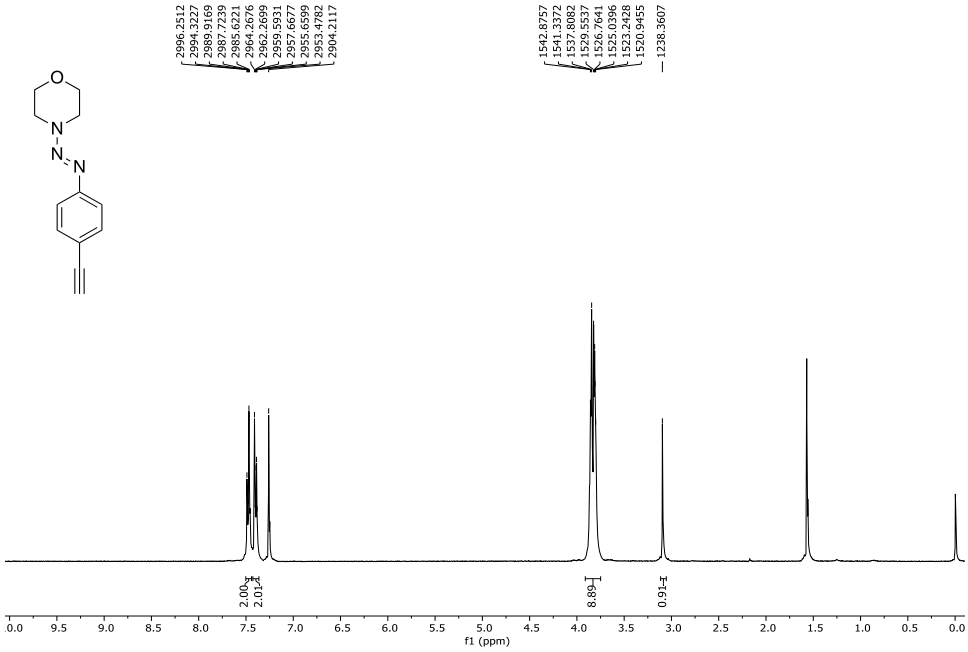

Figure 52. ^{1}H NMR spectrum of **143e** in $CDCl_3$ solution (400 MHz).

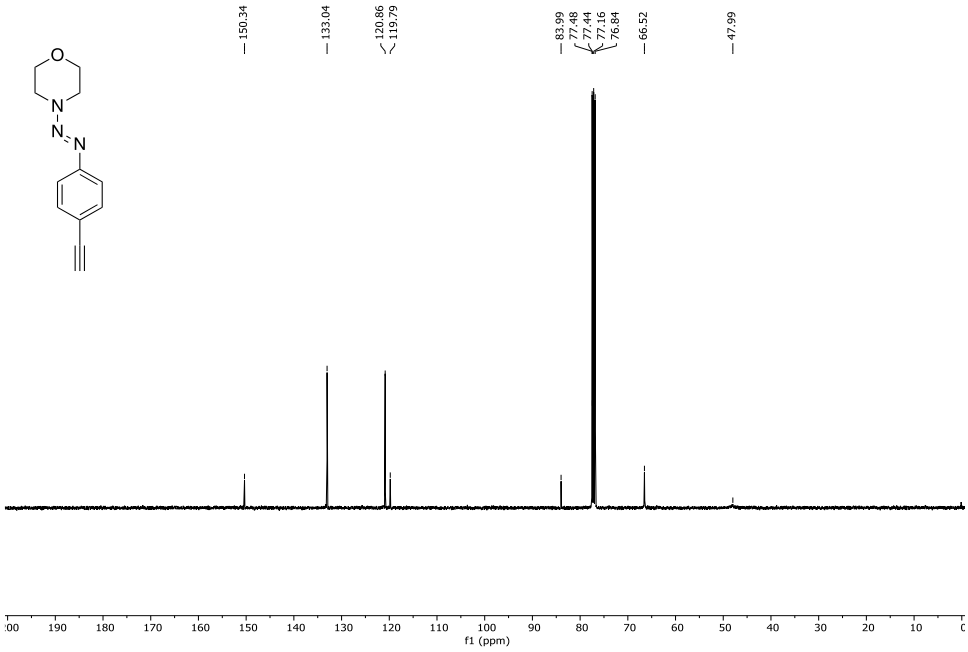

Figure 53. ^{13}C NMR spectrum of **143e** in $CDCl_3$ solution (100 MHz).

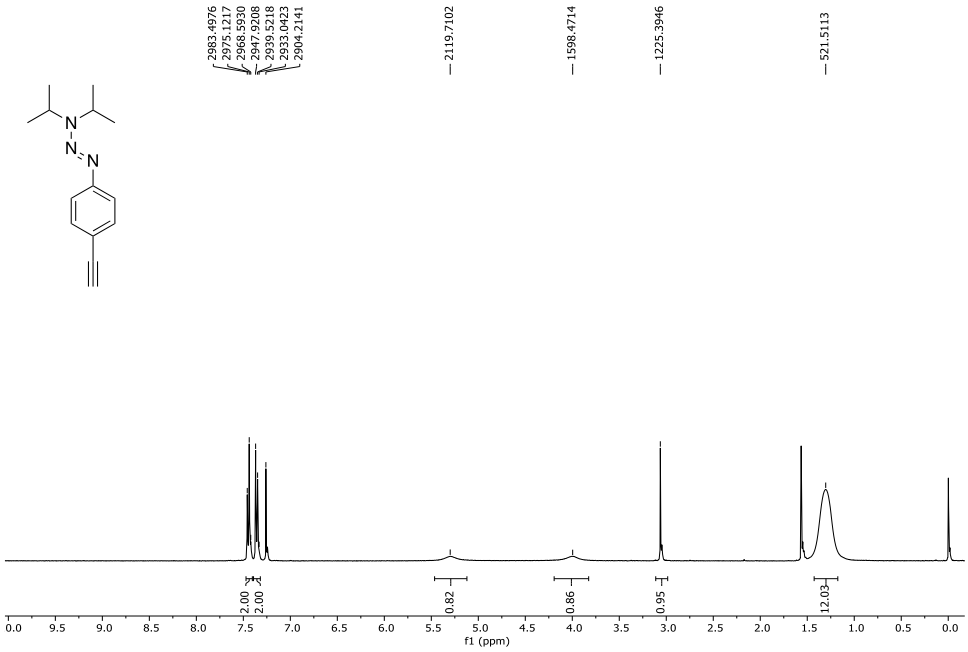

Figure 54. ^{1}H NMR spectrum of **143f** in $CDCl_3$ solution (400 MHz).

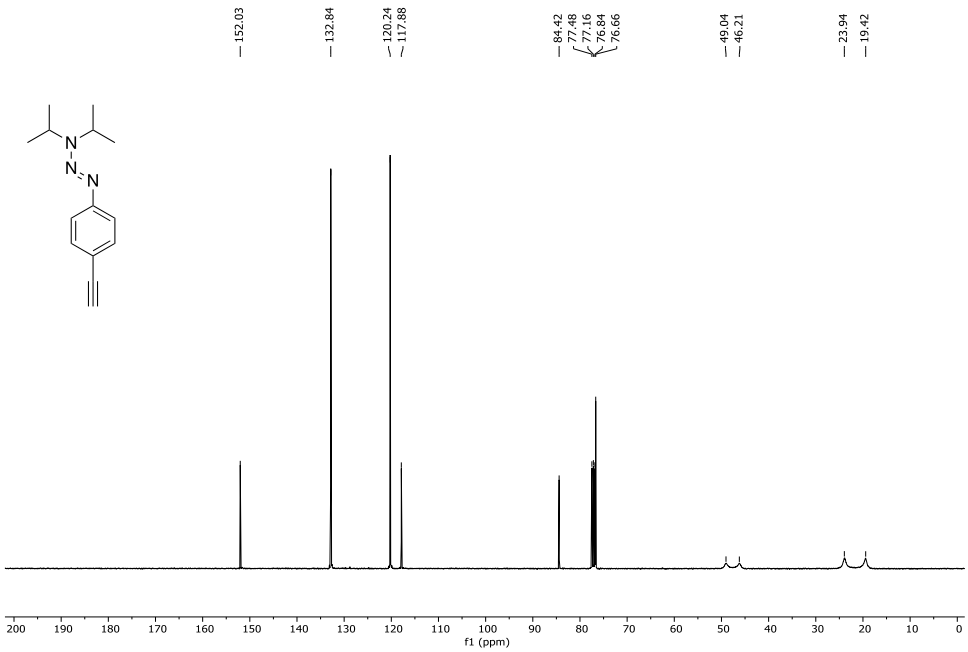

Figure 55. ^{13}C NMR spectrum of **143f** in $CDCl_3$ solution (100 MHz).

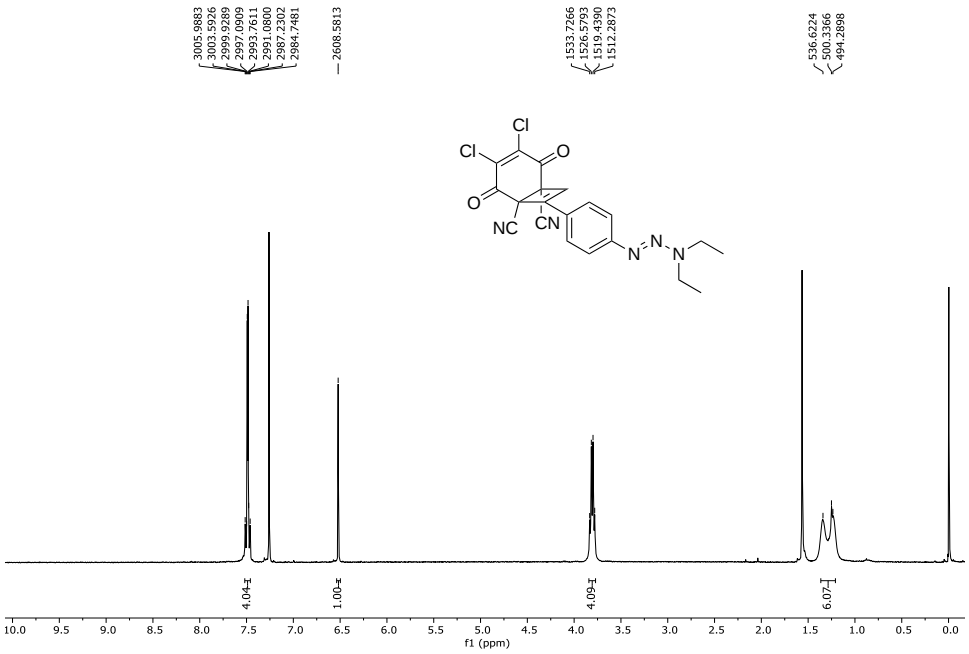

Figure 56. ^{1}H NMR spectrum of (±)-**144a** in $CDCl_3$ solution (400 MHz).

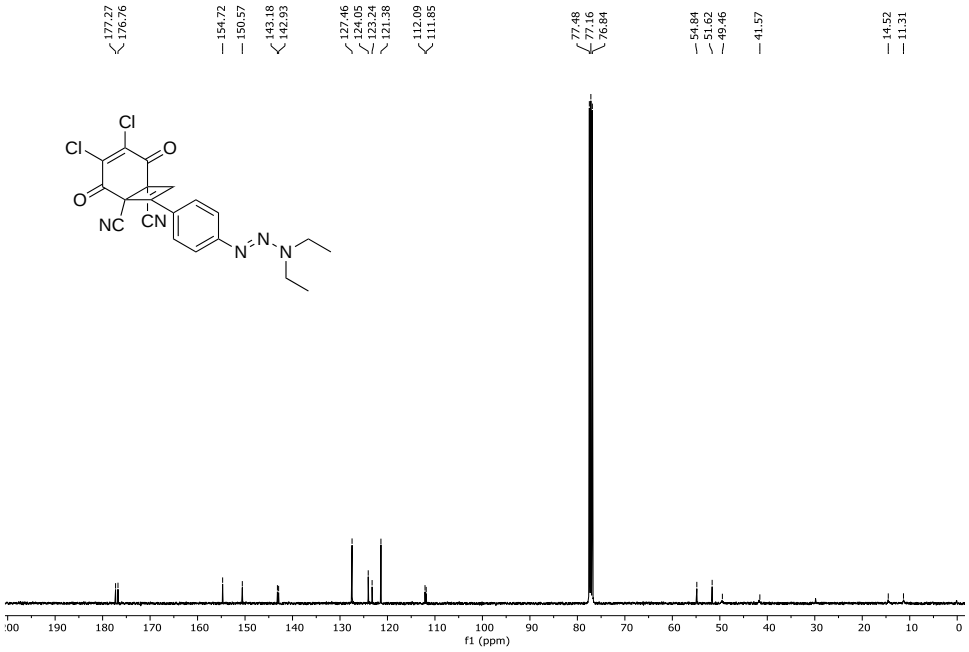

Figure 57. ^{13}C NMR spectrum of (±)-**144a** in $CDCl_3$ solution (100 MHz).

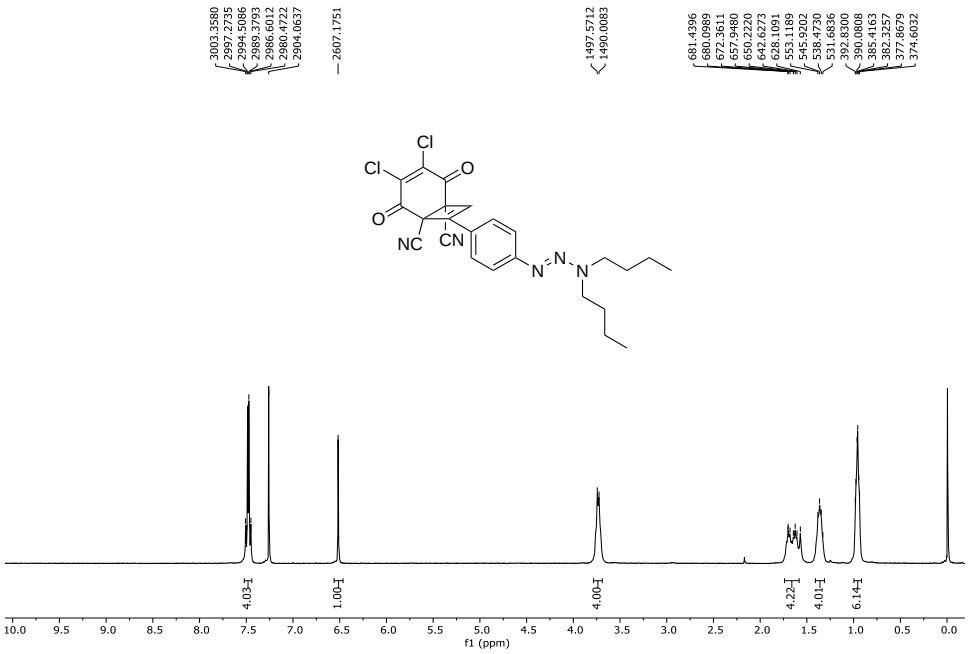

Figure 58. ^{1}H NMR spectrum of (±)-**144b** in $CDCl_3$ solution (400 MHz).

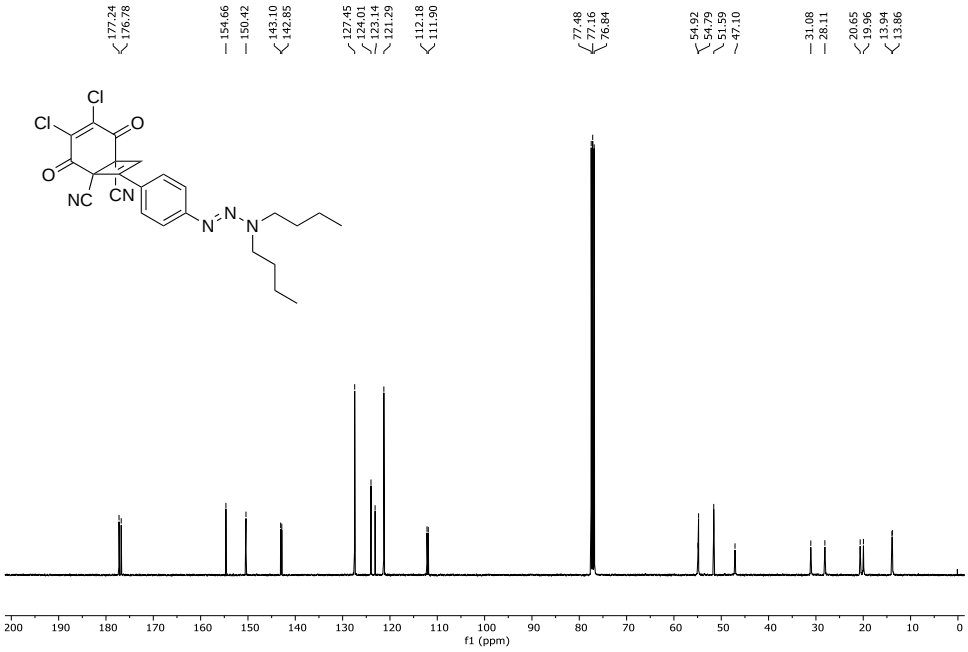

Figure 59. ^{13}C NMR spectrum of (±)-**144b** in $CDCl_3$ solution (100 MHz).

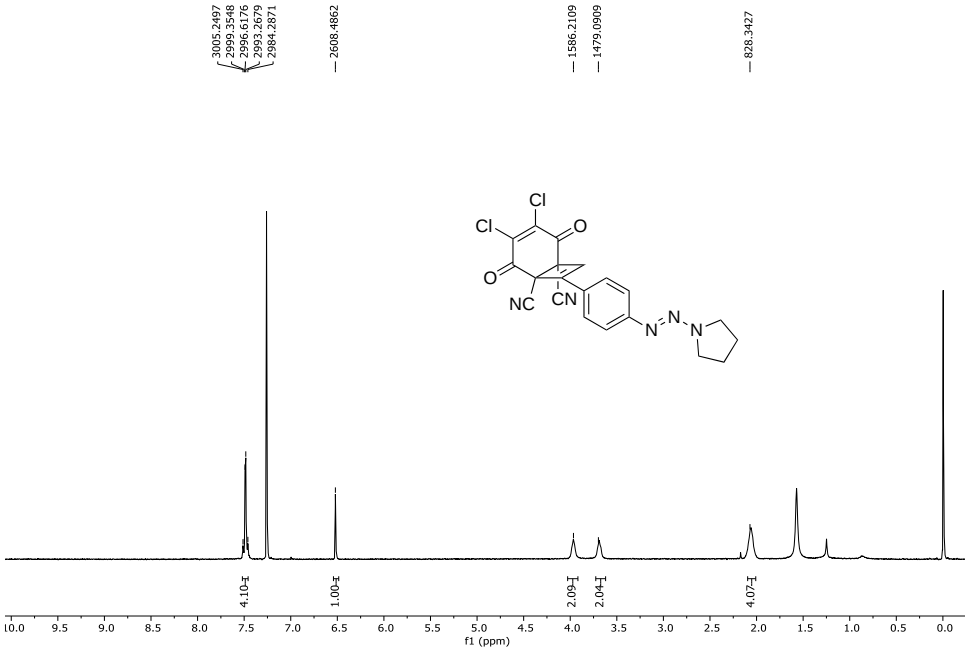

Figure 60. ^{1}H NMR spectrum of (±)-**144c** in $CDCl_3$ solution (400 MHz).

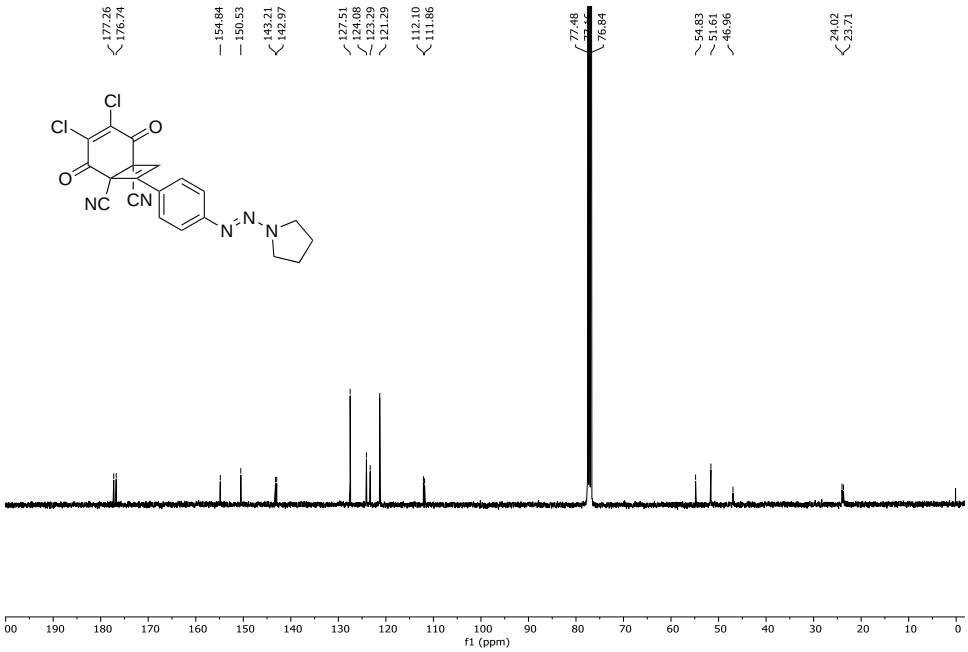

Figure 61. ^{13}C NMR spectrum of (±)-**144c** in $CDCl_3$ solution (100 MHz).

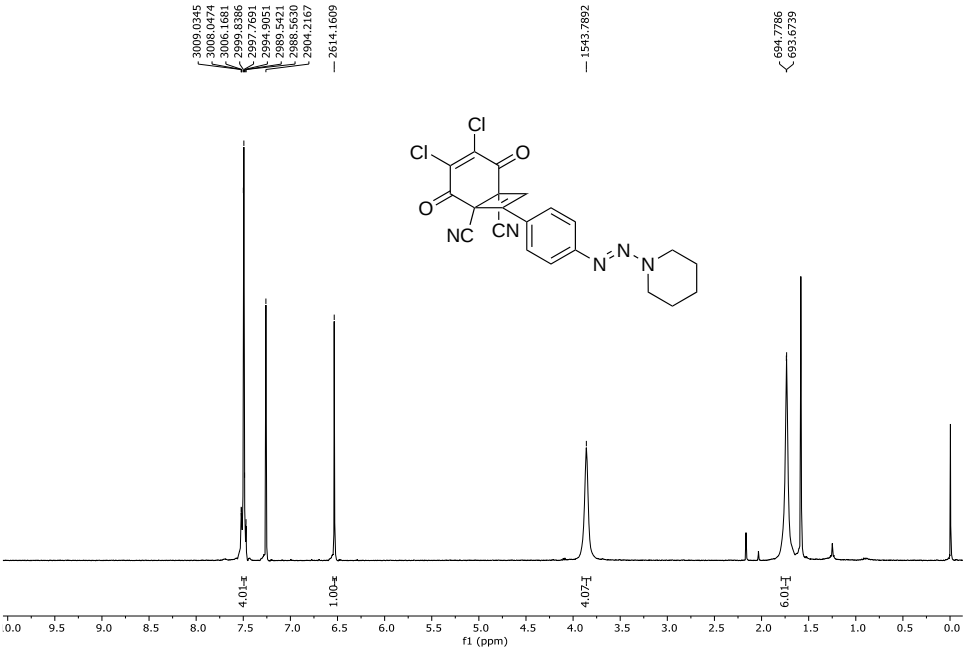

Figure 62. ^{1}H NMR spectrum of (±)-**144d** in $CDCl_3$ solution (400 MHz).

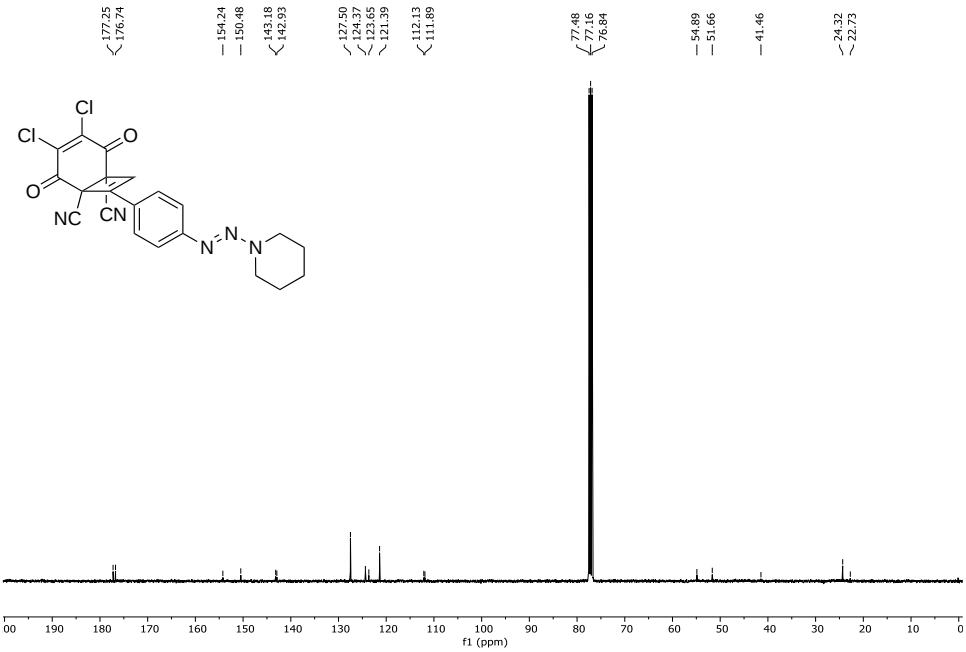

Figure 63. ^{13}C NMR spectrum of (±)-**144d** in $CDCl_3$ solution (100 MHz).

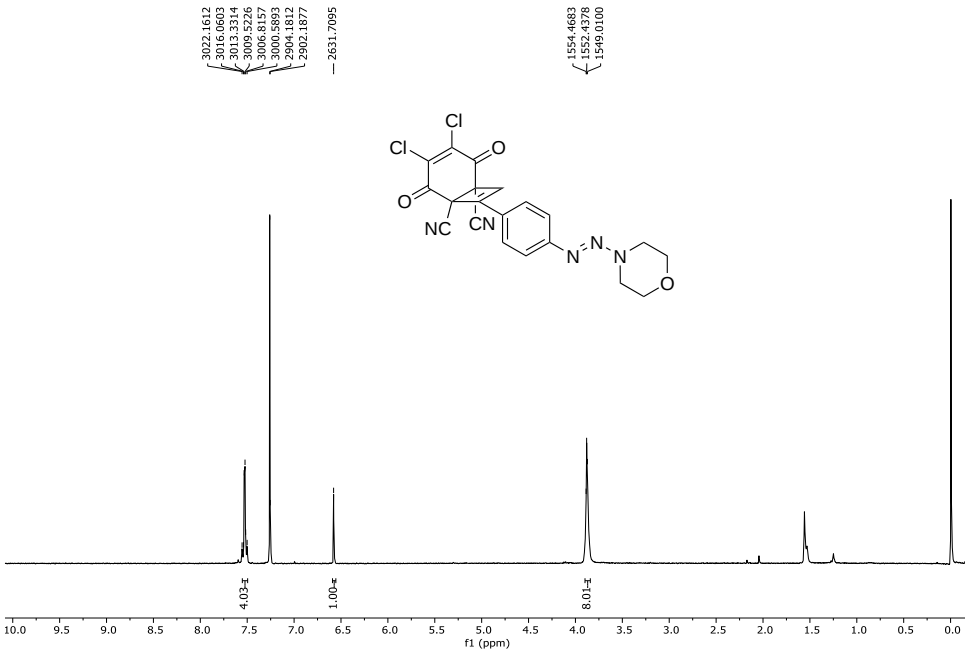

Figure 64. ^{1}H NMR spectrum of (±)-**144e** in $CDCl_3$ solution (400 MHz).

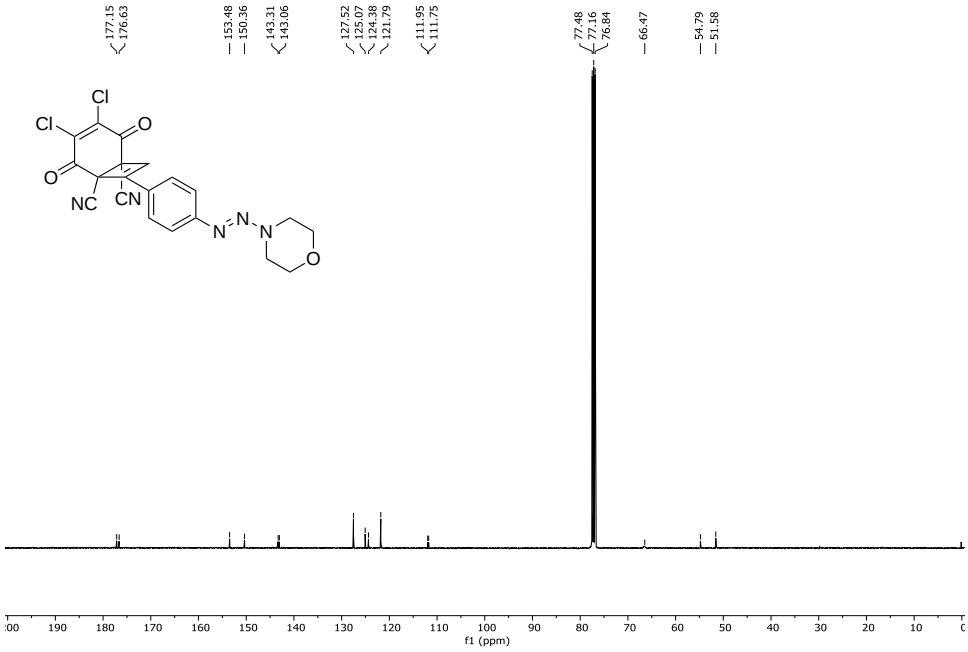

Figure 65. ^{13}C NMR spectrum of (±)-**144e** in $CDCl_3$ solution (100 MHz).

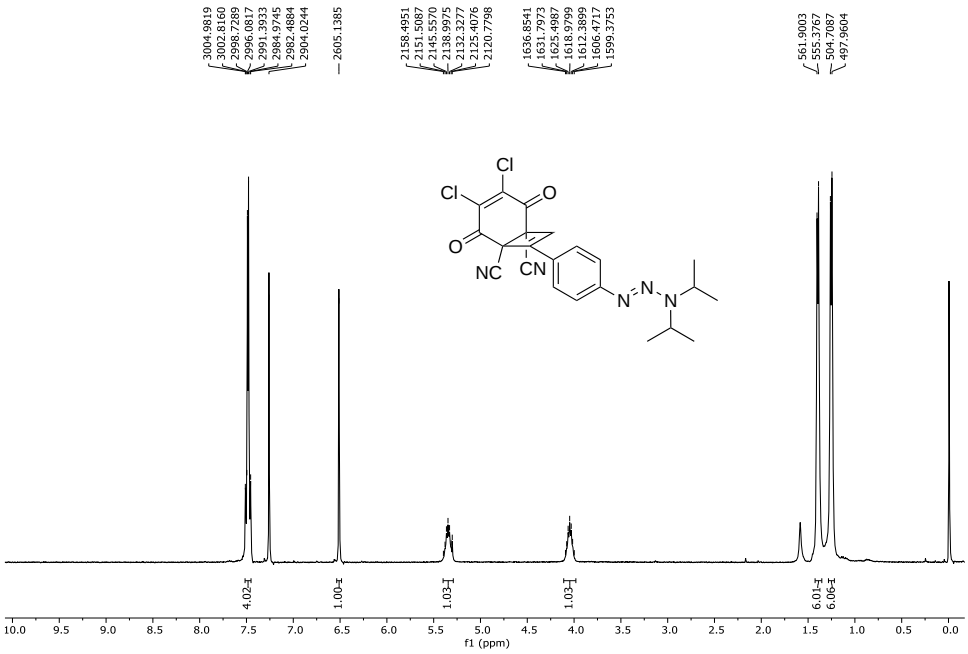

Figure 66. ^{1}H NMR spectrum of (±)-**144f** in $CDCl_3$ solution (400 MHz).

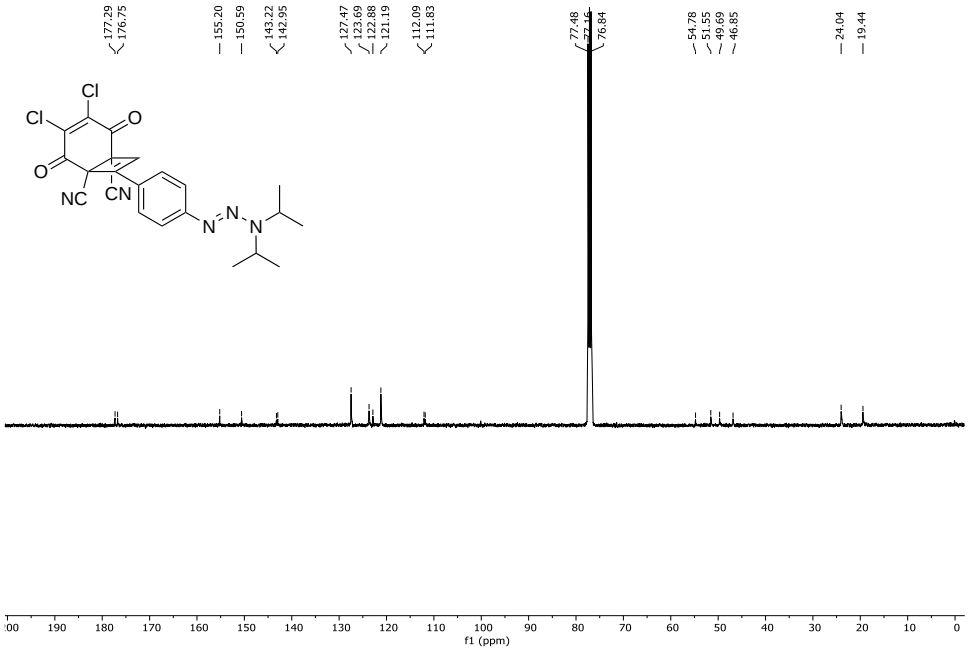

Figure 67. ^{13}C NMR spectrum of (±)-**144f** in $CDCl_3$ solution (100 MHz).

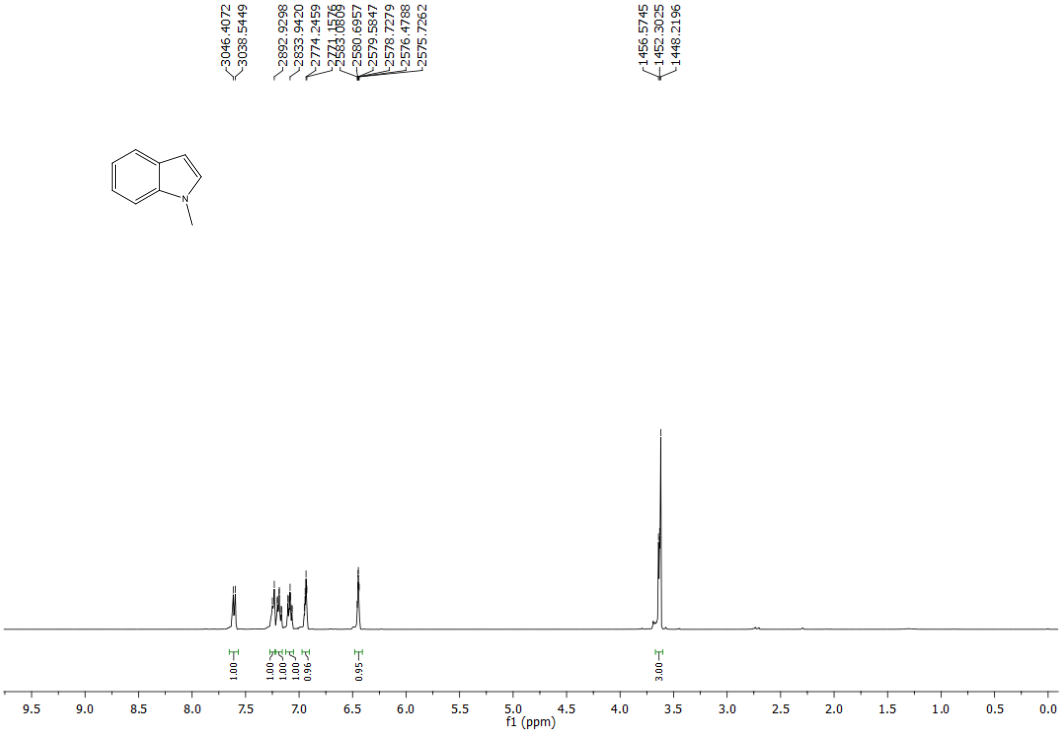

Figure 68. ^{1}H NMR spectrum of **148** in $CDCl_3$ solution (400 MHz).

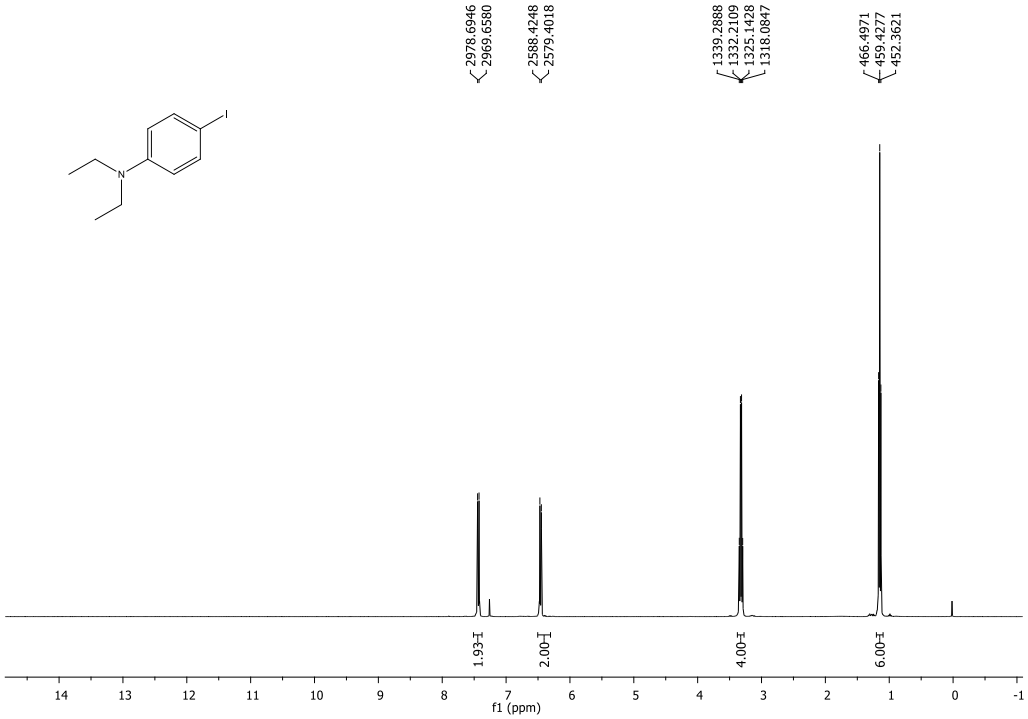

Figure 69. ^{1}H NMR spectrum of **157** in $CDCl_3$ solution (400 MHz).

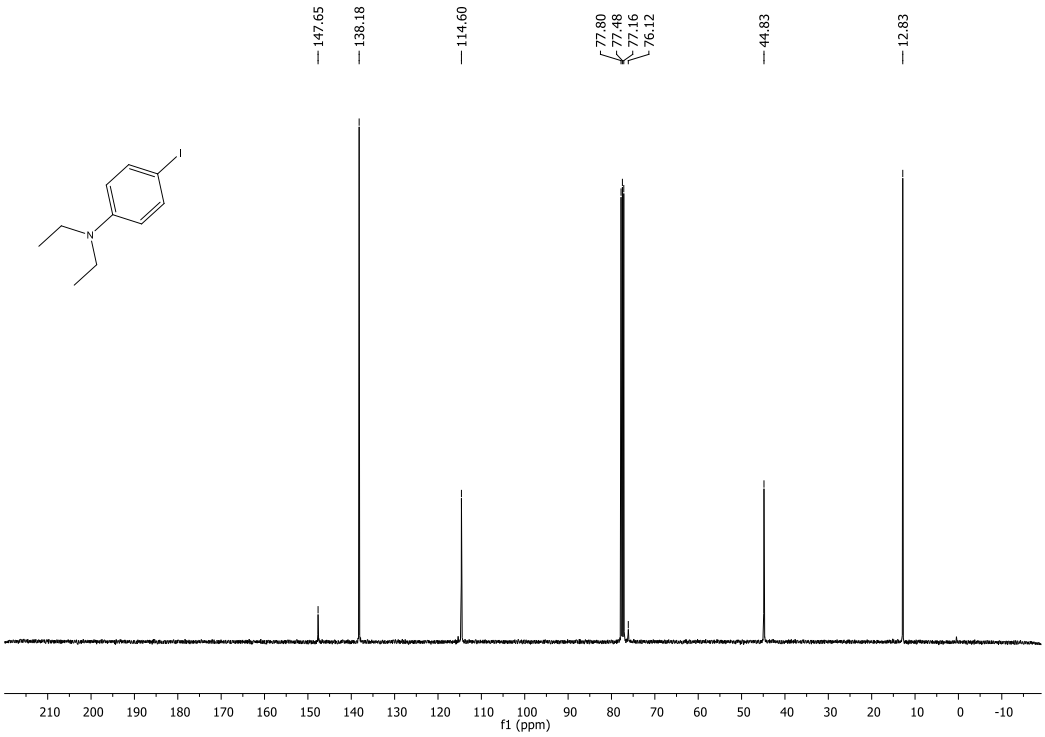

Figure 70. ^{13}C NMR spectrum of **157** in $CDCl_3$ solution (100 MHz).

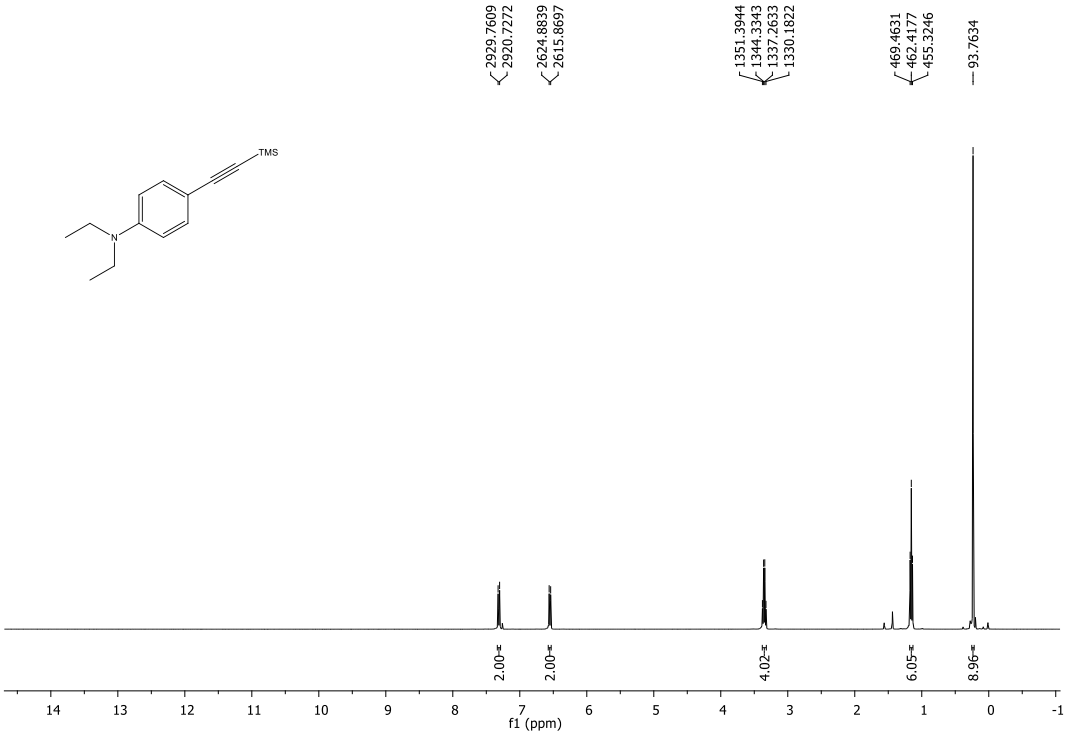

Figure 71. ^{1}H NMR spectrum of **158** in $CDCl_3$ solution (400 MHz).

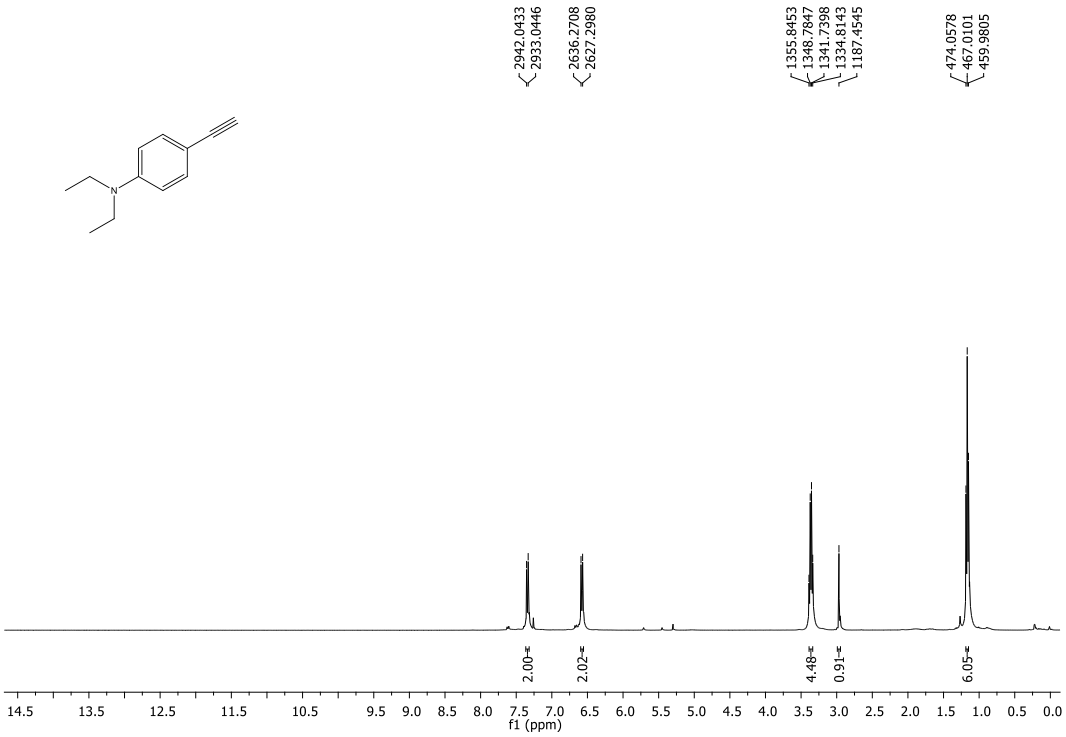

Figure 72. ^{1}H NMR spectrum of **159** in $CDCl_3$ solution (400 MHz).

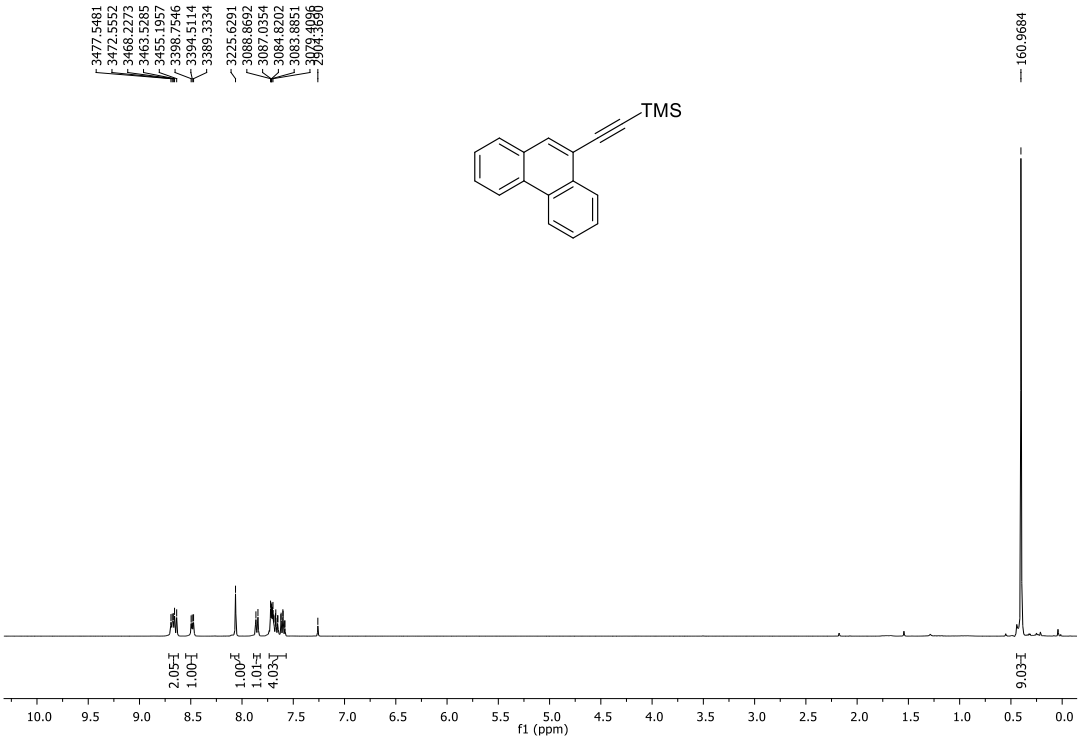

Figure 73. ^{1}H NMR spectrum of **161** in $CDCl_3$ solution (400 MHz).

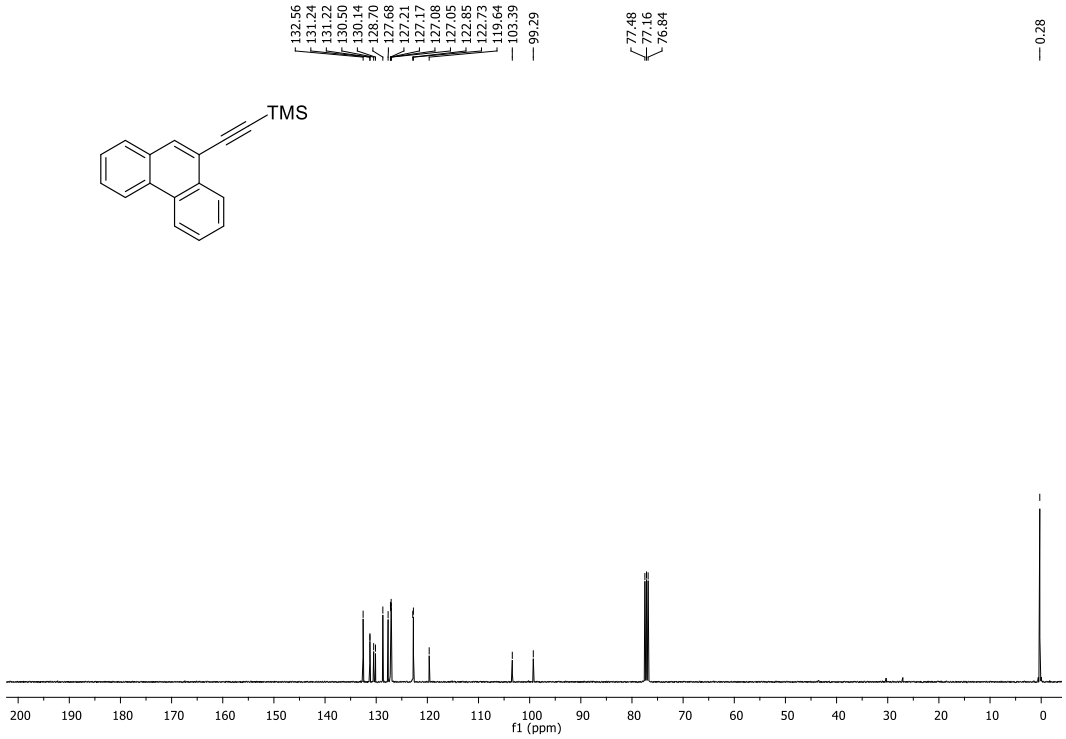

Figure 74. ^{13}C NMR spectrum of **161** in $CDCl_3$ solution (100 MHz).

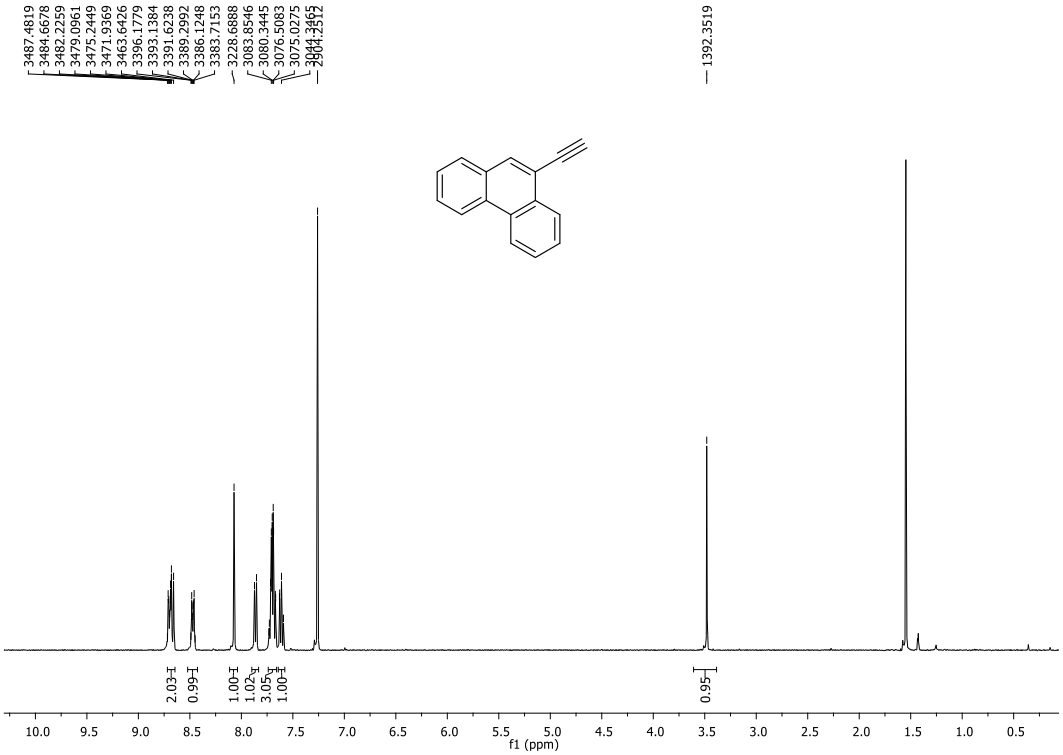

Figure 75. ^{1}H NMR spectrum of **162** in $CDCl_3$ solution (400 MHz).

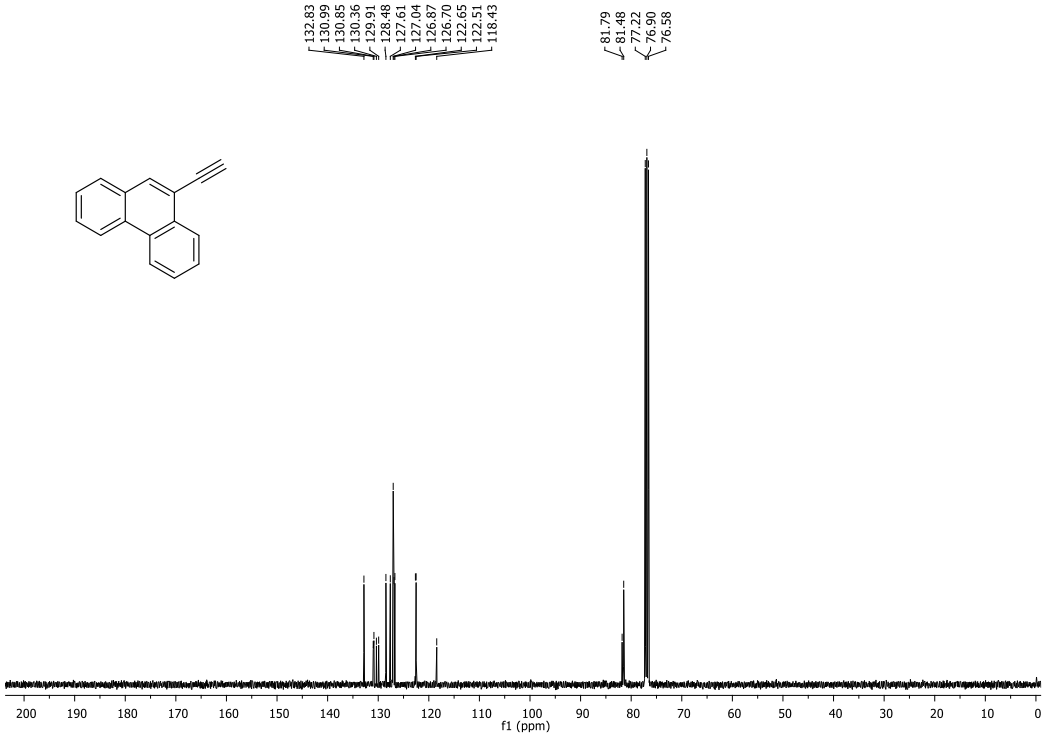

Figure 76. ^{13}C NMR spectrum of **162** in $CDCl_3$ solution (100 MHz).

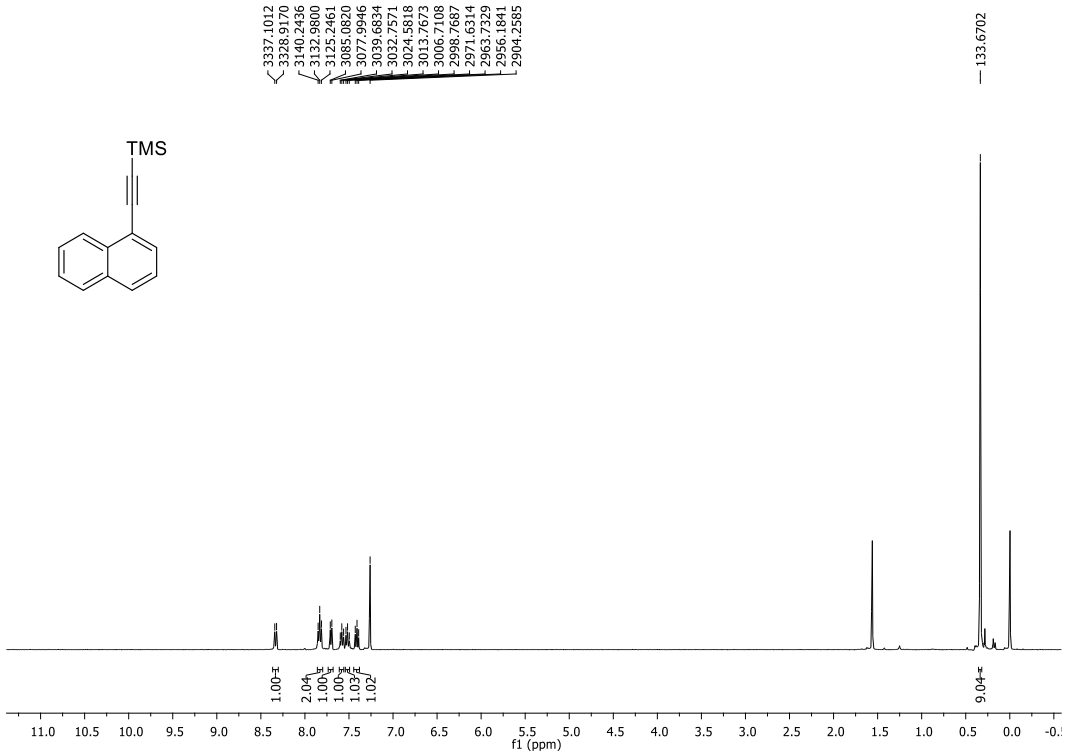

Figure 77. ^{1}H NMR spectrum of **164** in CDCl3 solution (400 MHz).

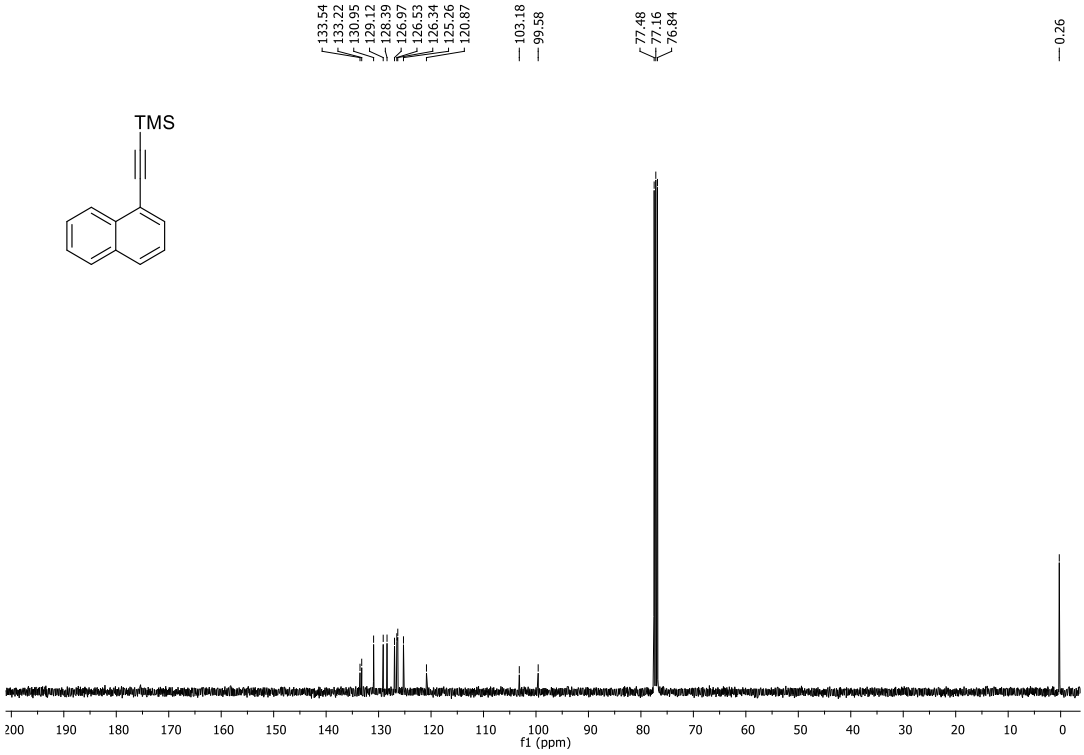

Figure 78. ^{13}C NMR spectrum of **164** in $CDCl_3$ solution (100 MHz).

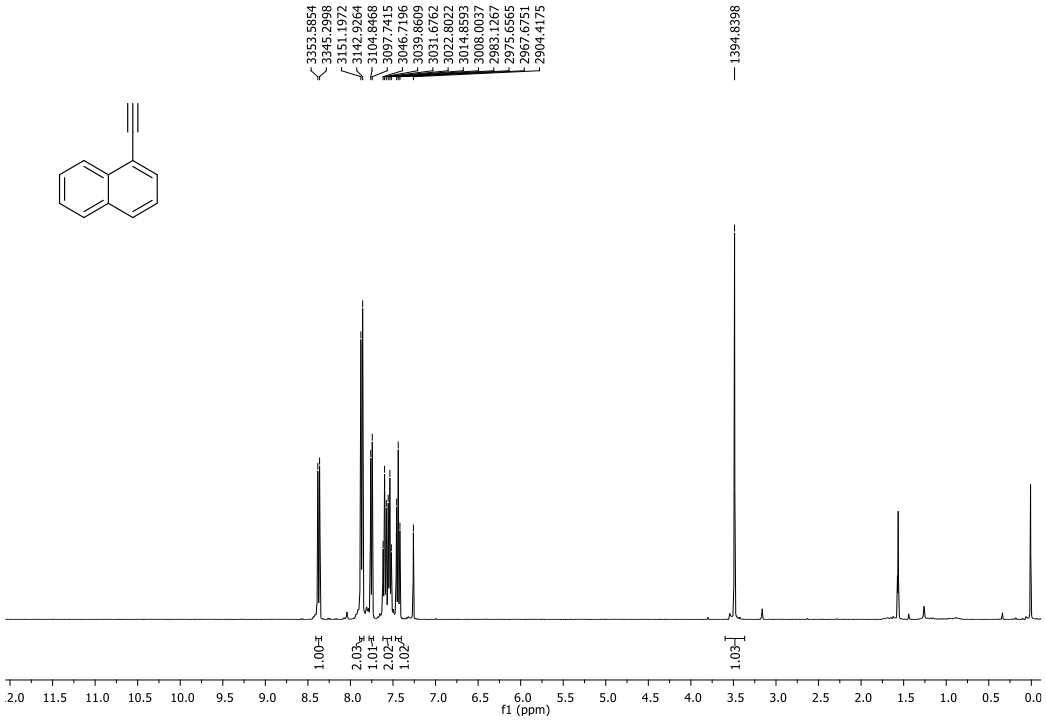

Figure 79. ^{1}H NMR spectrum of **165** in $CDCl_3$ solution (400 MHz).

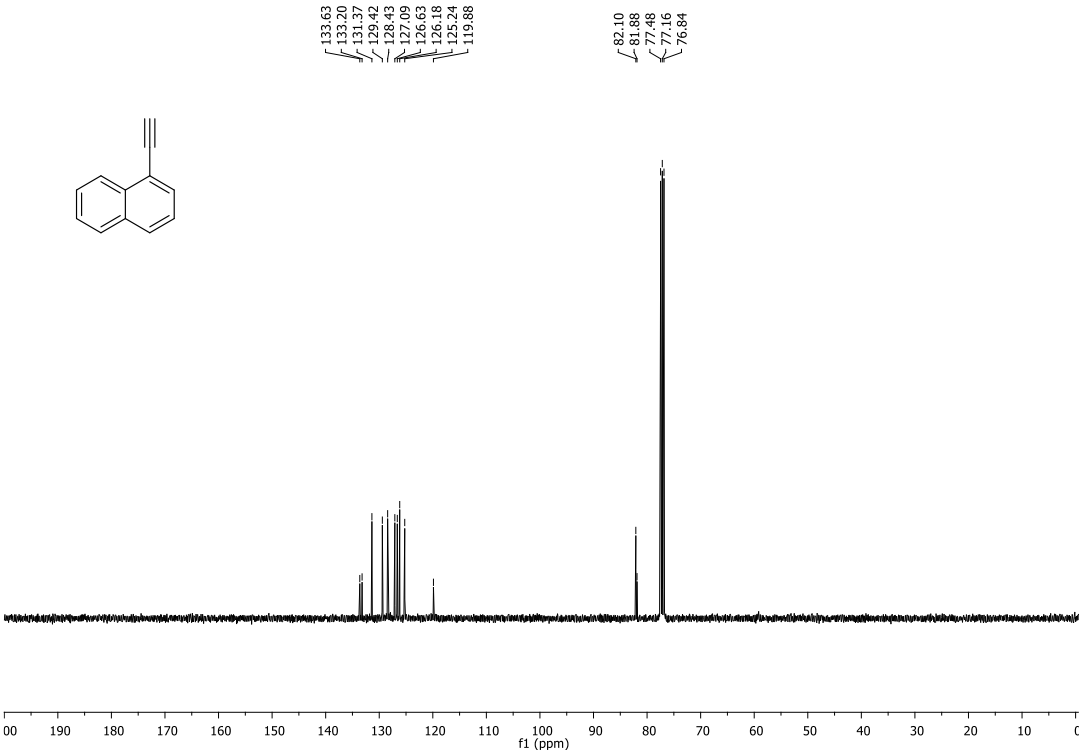

Figure 80. ^{13}C NMR spectrum of **165** in $CDCl_3$ solution (100 MHz).

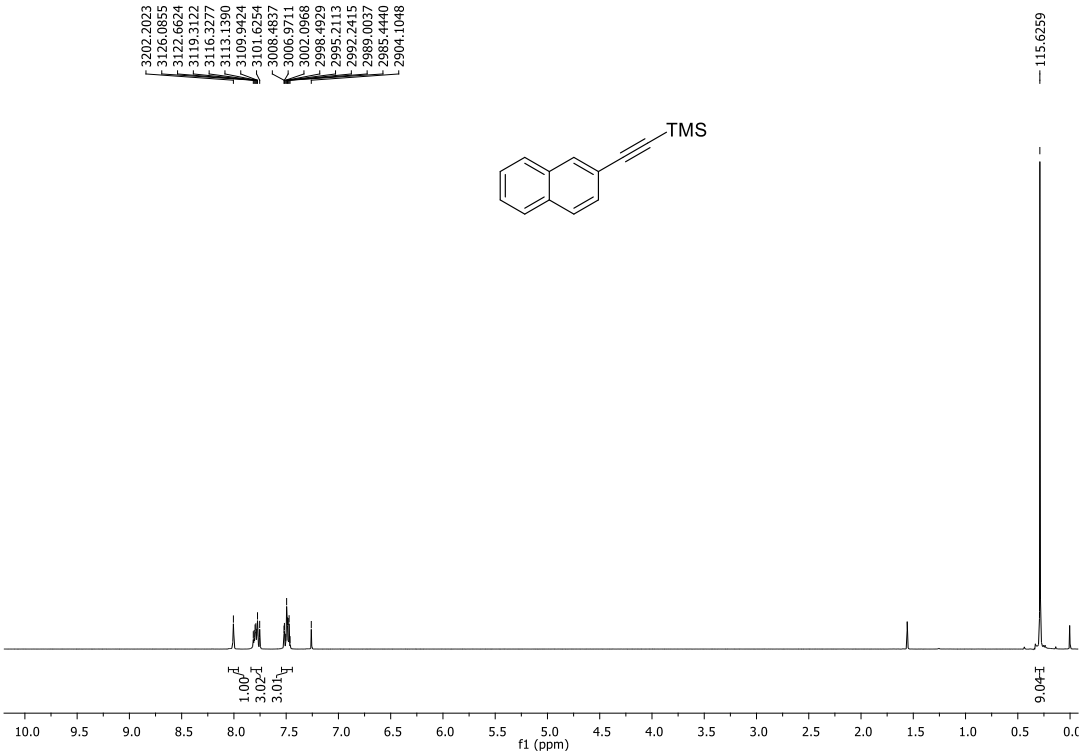

Figure 81. ^{1}H NMR spectrum of **167** in $CDCl_3$ solution (400 MHz).

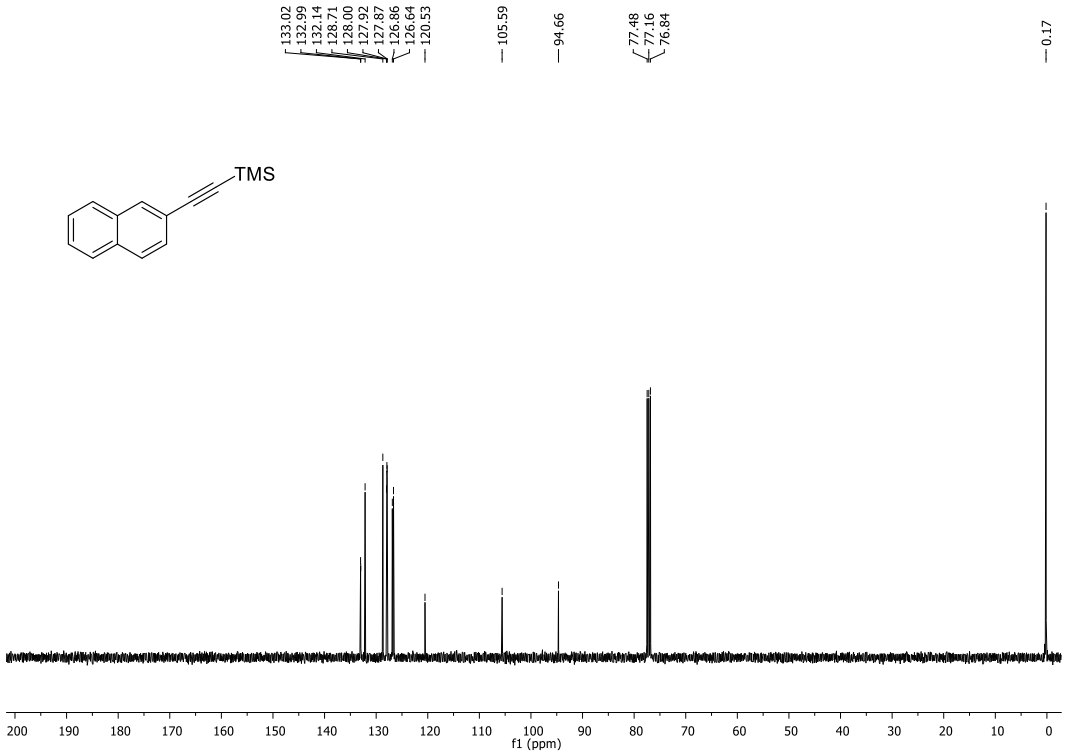

Figure 82. ^{13}C NMR spectrum of **167** in $CDCl_3$ solution (100 MHz).

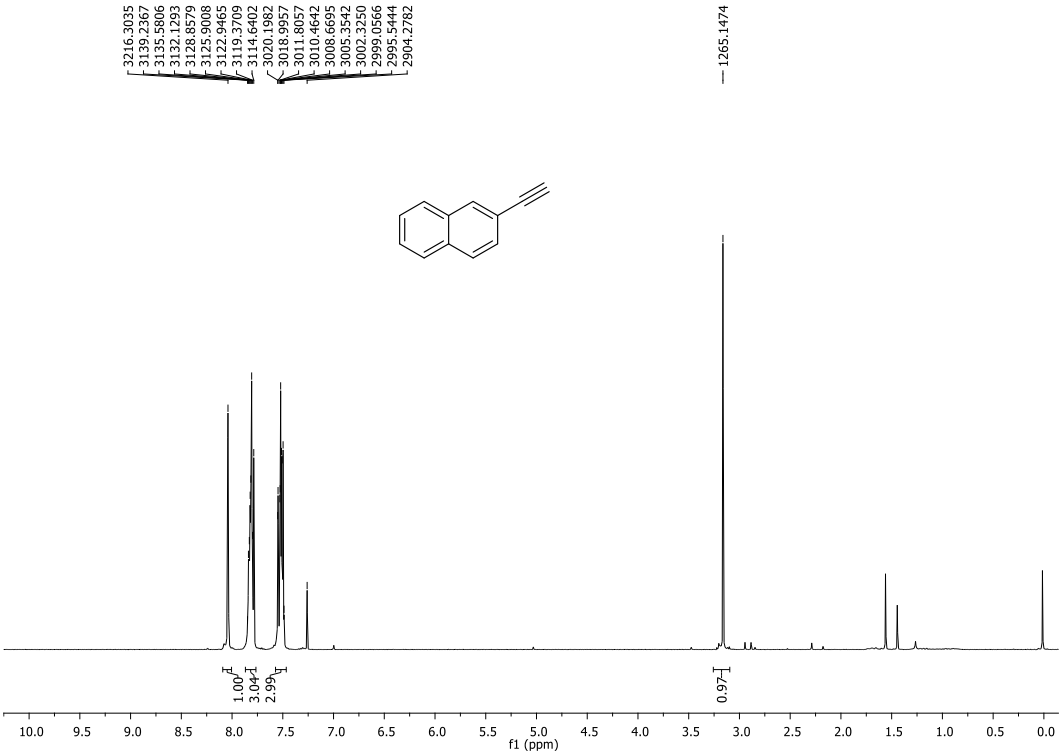

Figure 83. ^{1}H NMR spectrum of **168** in $CDCl_3$ solution (400 MHz).

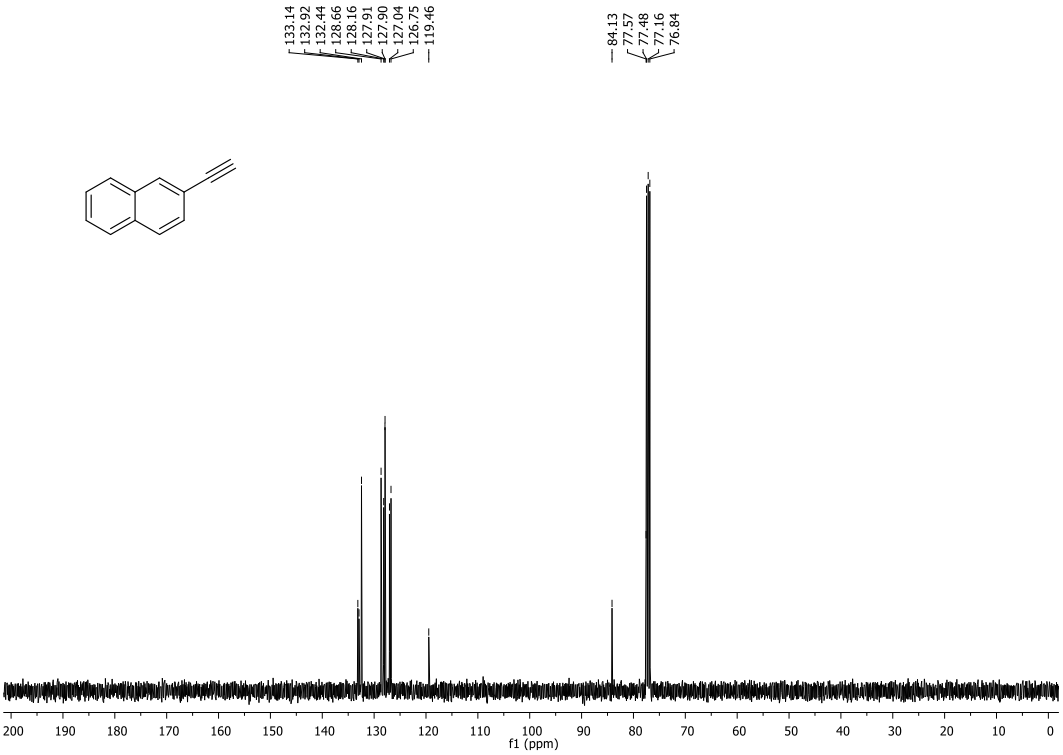

Figure 84. ^{13}C NMR spectrum of **168** in $CDCl_3$ solution (100 MHz).

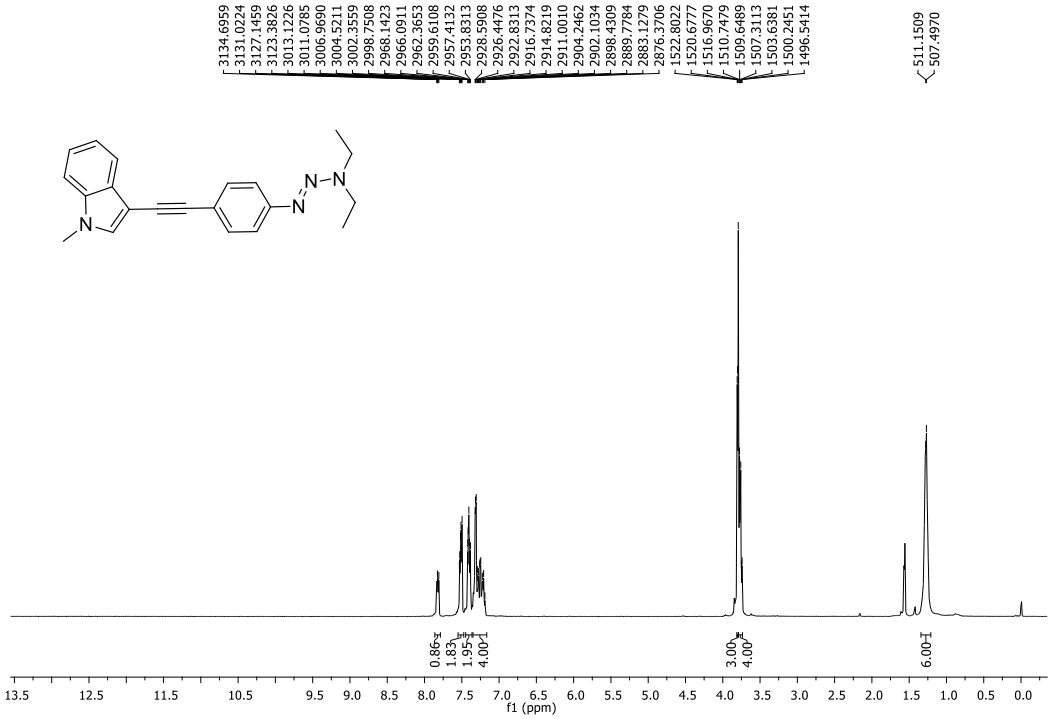

Figure 85. ^{1}H NMR spectrum of **156** in $CDCl_3$ solution (400 MHz).

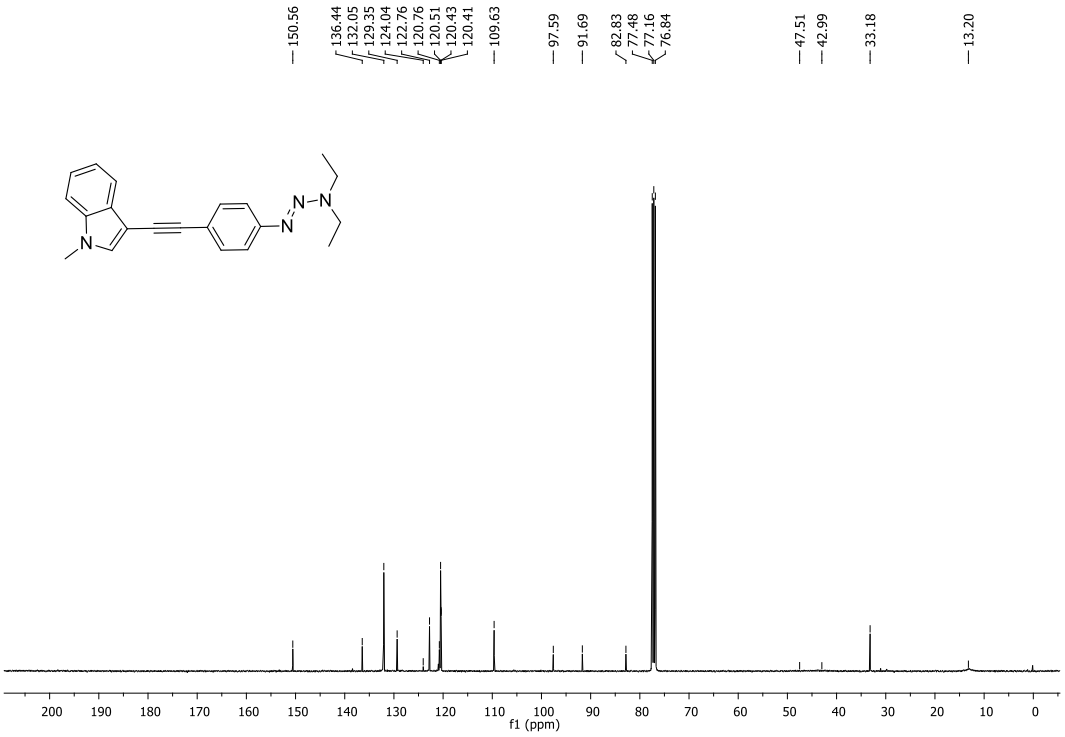

Figure 86. ^{13}C NMR spectrum of **156** in $CDCl_3$ solution (100 MHz).

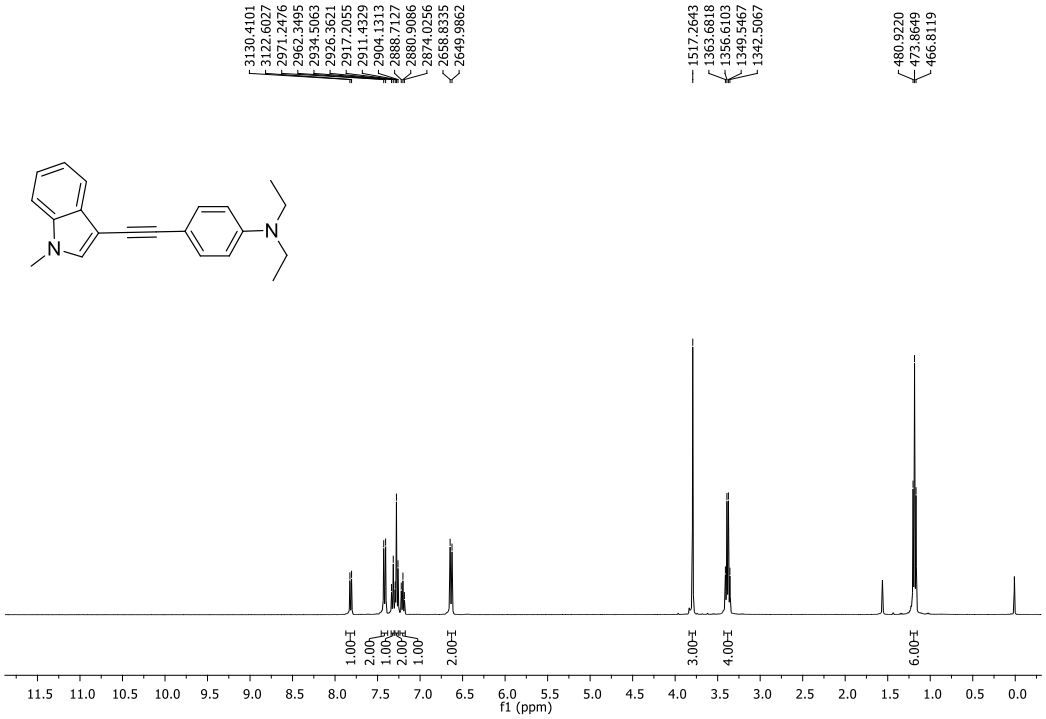

Figure 87. ^{1}H NMR spectrum of **169** in $CDCl_3$ solution (400 MHz).

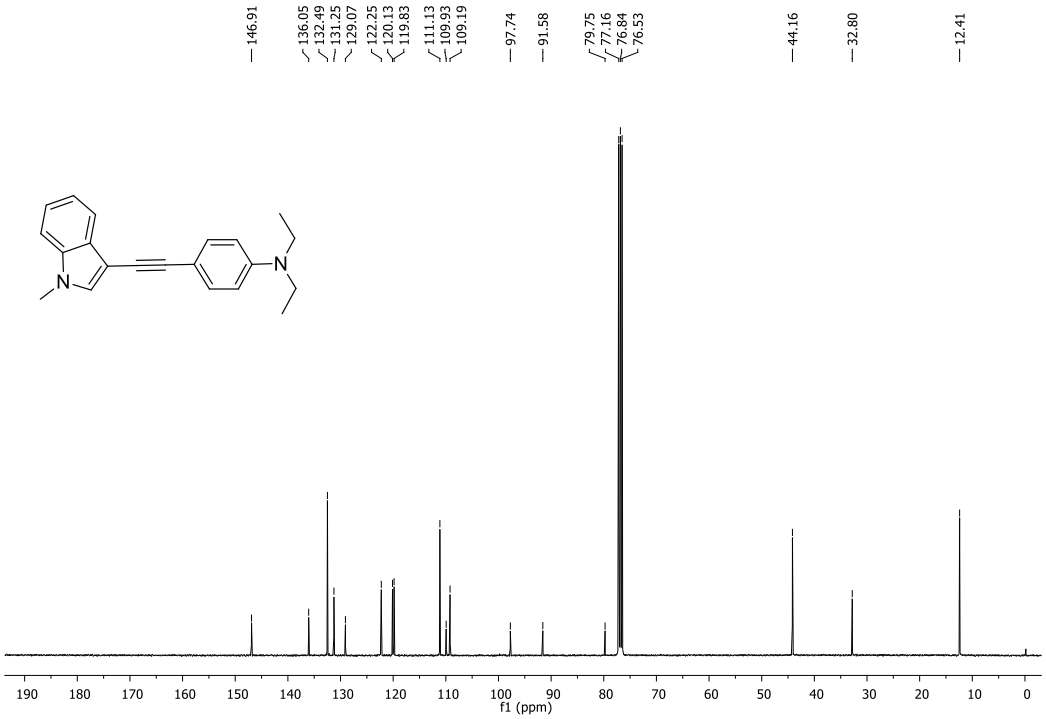

Figure 88. ^{13}C NMR spectrum of **169** in $CDCl_3$ solution (100 MHz).

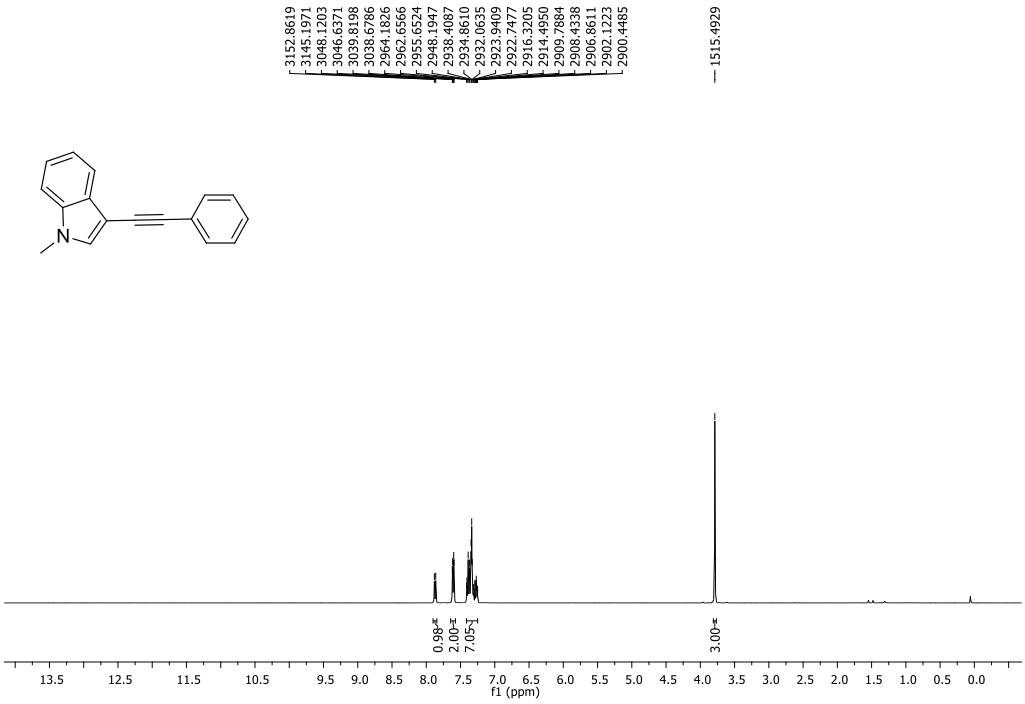

Figure 89. ^{1}H NMR spectrum of **170** in $CDCl_3$ solution (400 MHz).

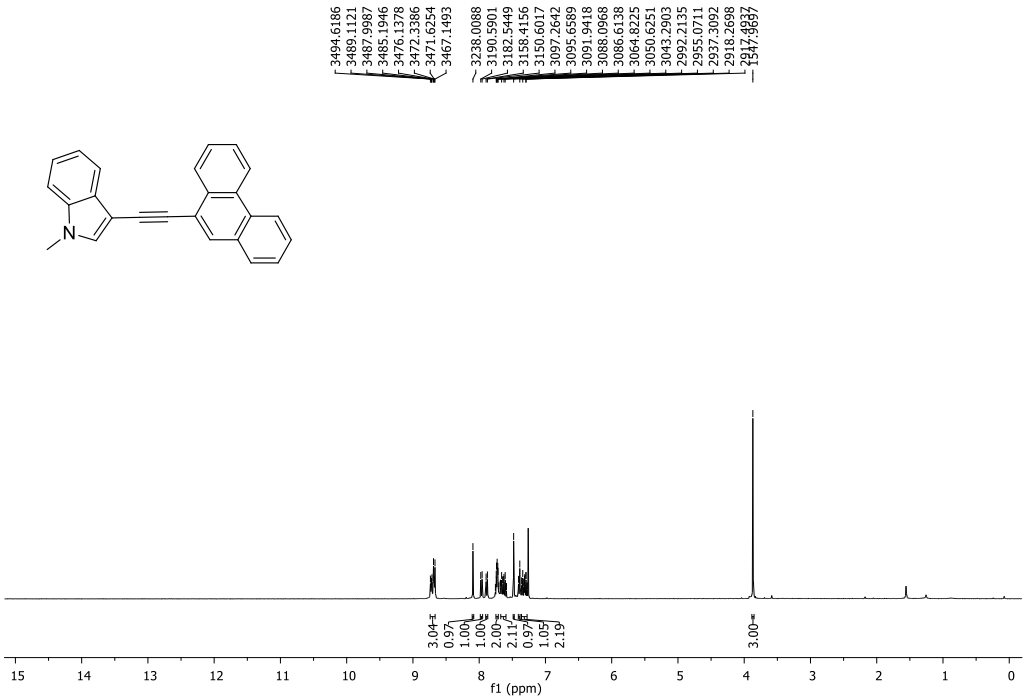

Figure 90. ^{1}H NMR spectrum of **171** in $CDCl_3$ solution (400 MHz).

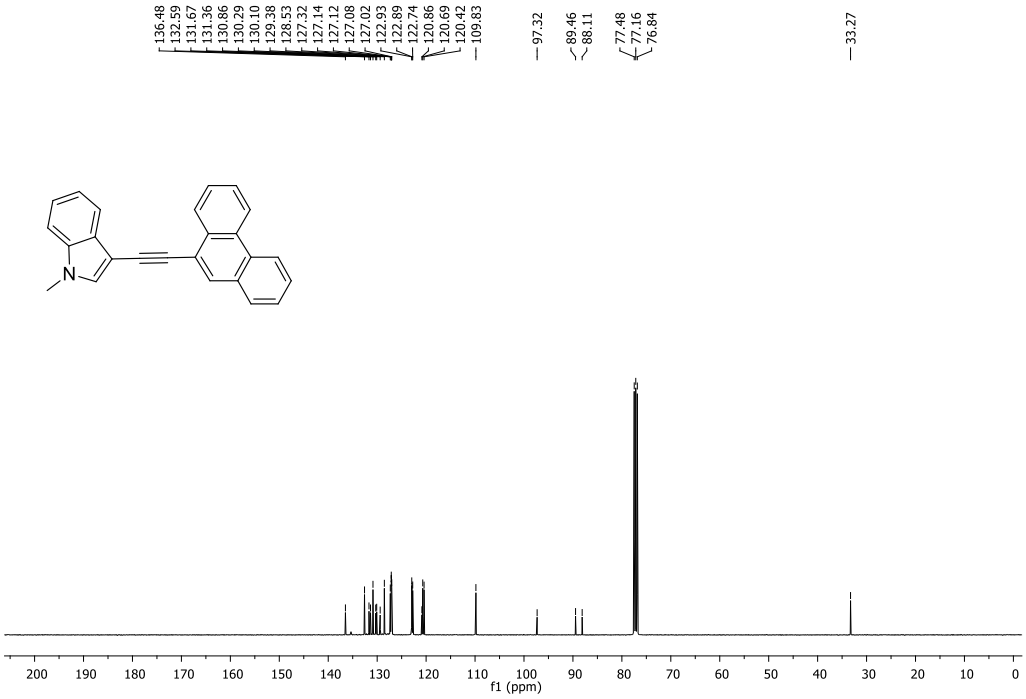

Figure 91. ^{13}C NMR spectrum of **171** in $CDCl_3$ solution (100 MHz).

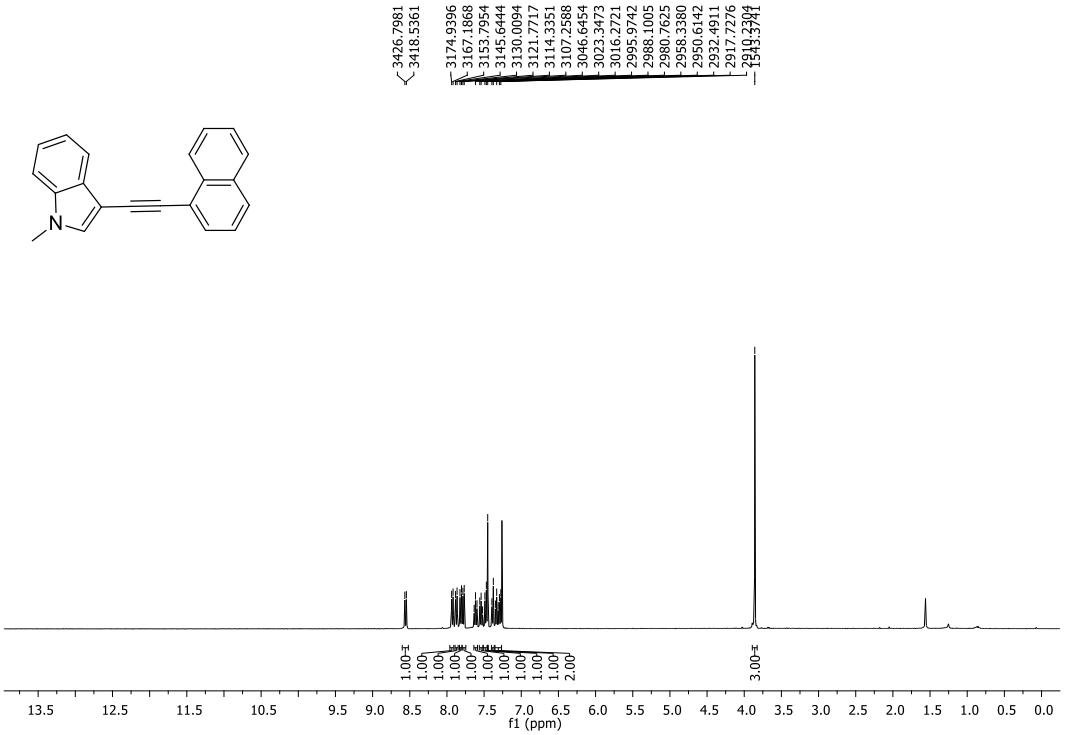

Figure 92. ^{1}H NMR spectrum of **172** in CDCl3 solution (400 MHz).

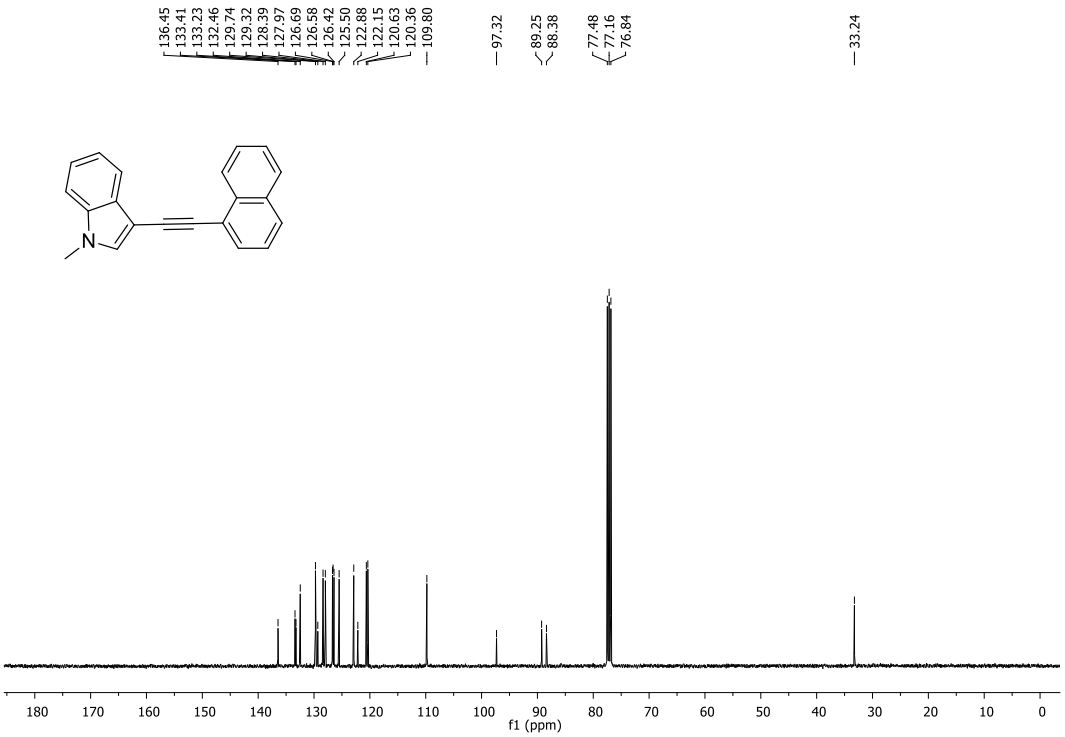

Figure 93. ^{13}C NMR spectrum of **172** in CDCl3 solution (100 MHz).

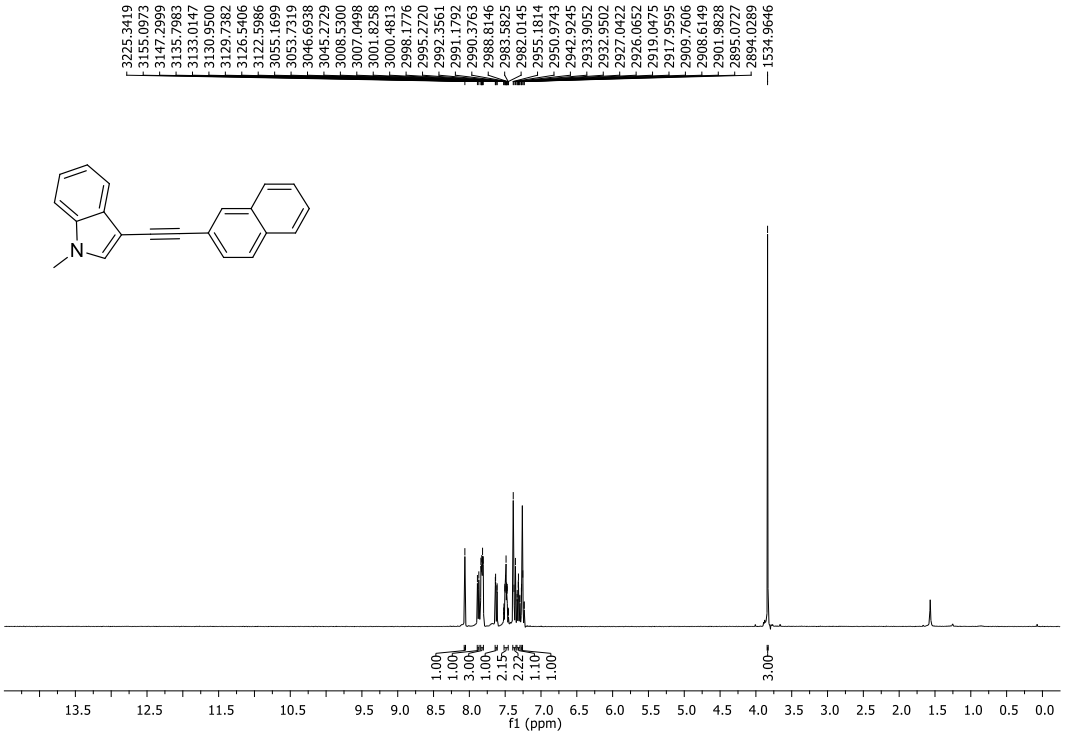

Figure 94. ^{1}H NMR spectrum of **173** in $CDCl_3$ solution (400 MHz).

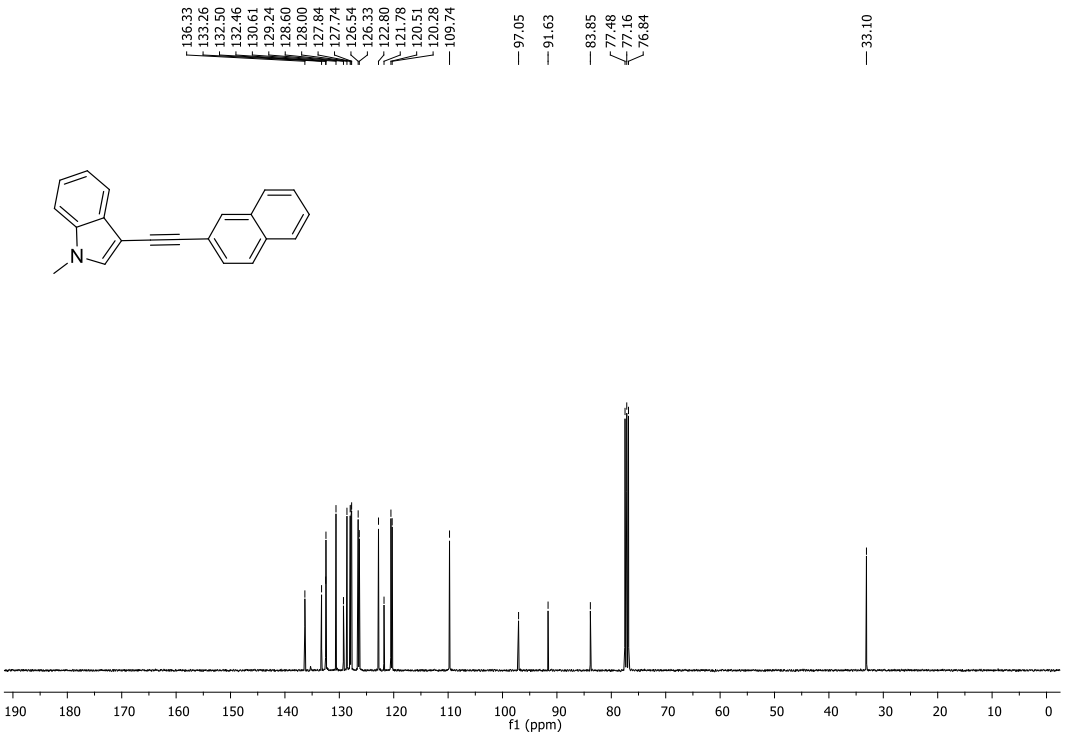

Figure 95. ^{13}C NMR spectrum of **173** in $CDCl_3$ solution (100 MHz).

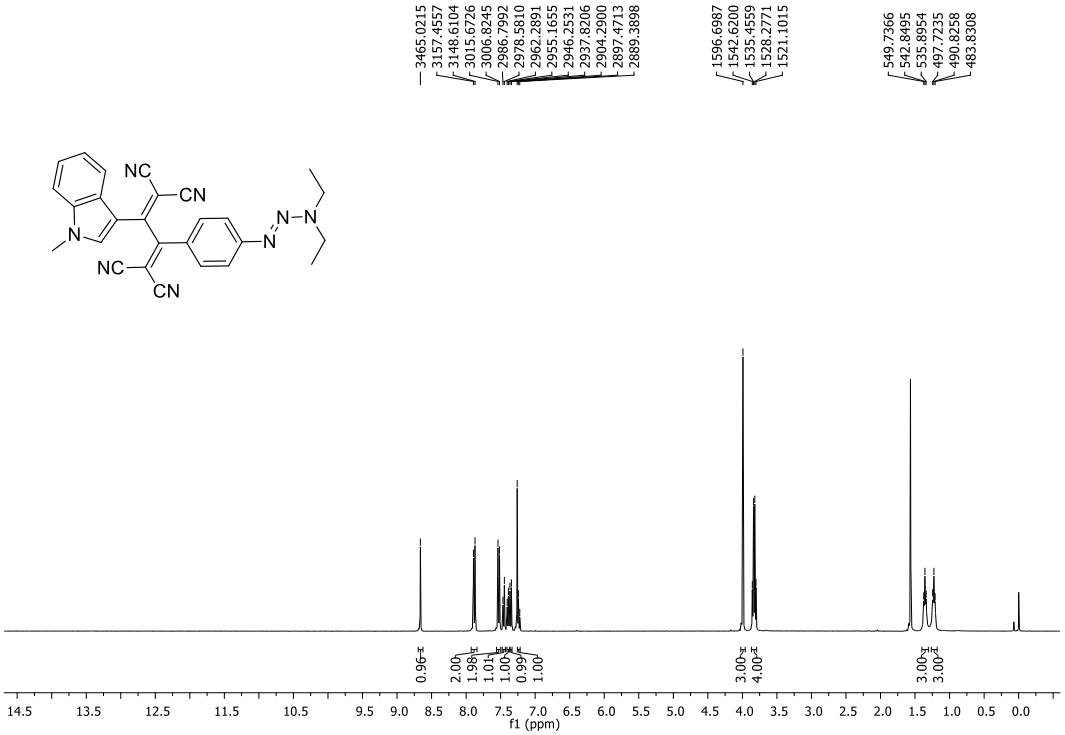

Figure 96. ^{1}H NMR spectrum of **179** in $CDCl_3$ solution (400 MHz).

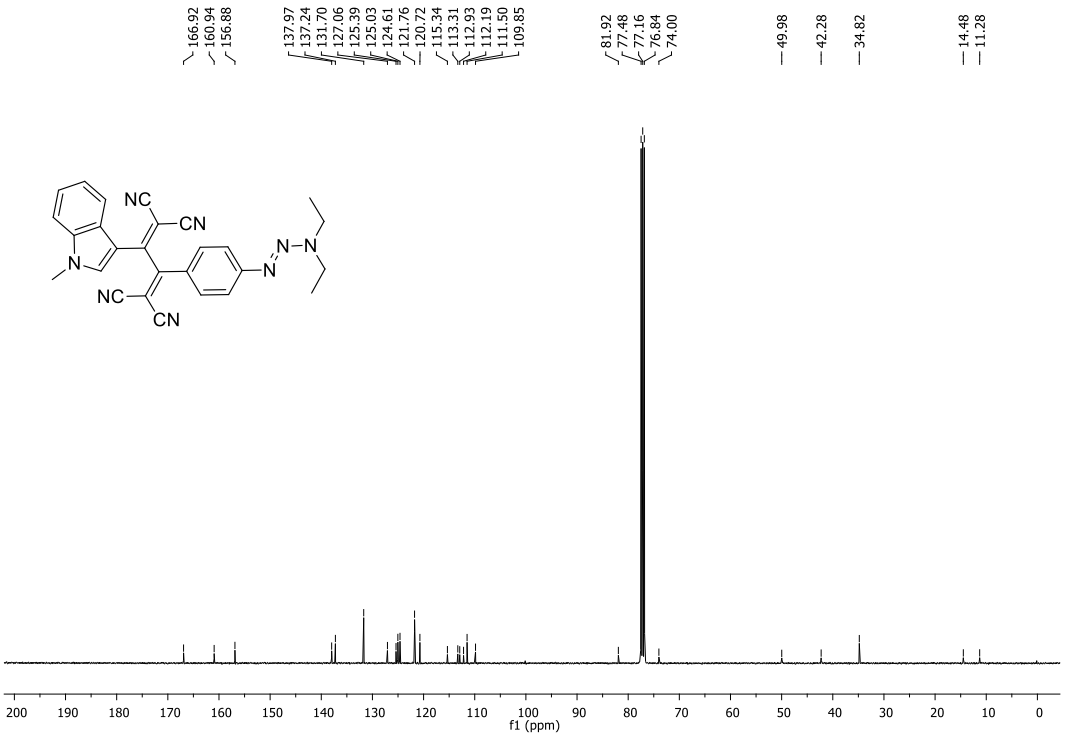

Figure 97. ^{13}C NMR spectrum of **179** in $CDCl_3$ solution (100 MHz).

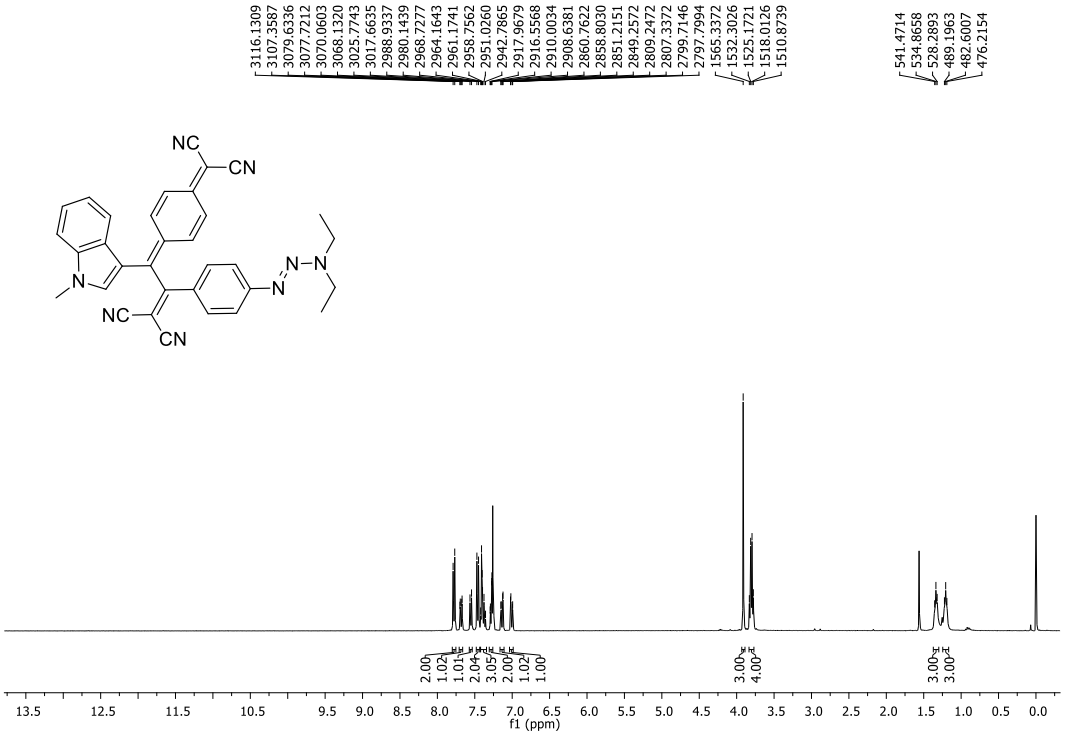

Figure 98. ^{1}H NMR spectrum of **180** in $CDCl_3$ solution (400 MHz).

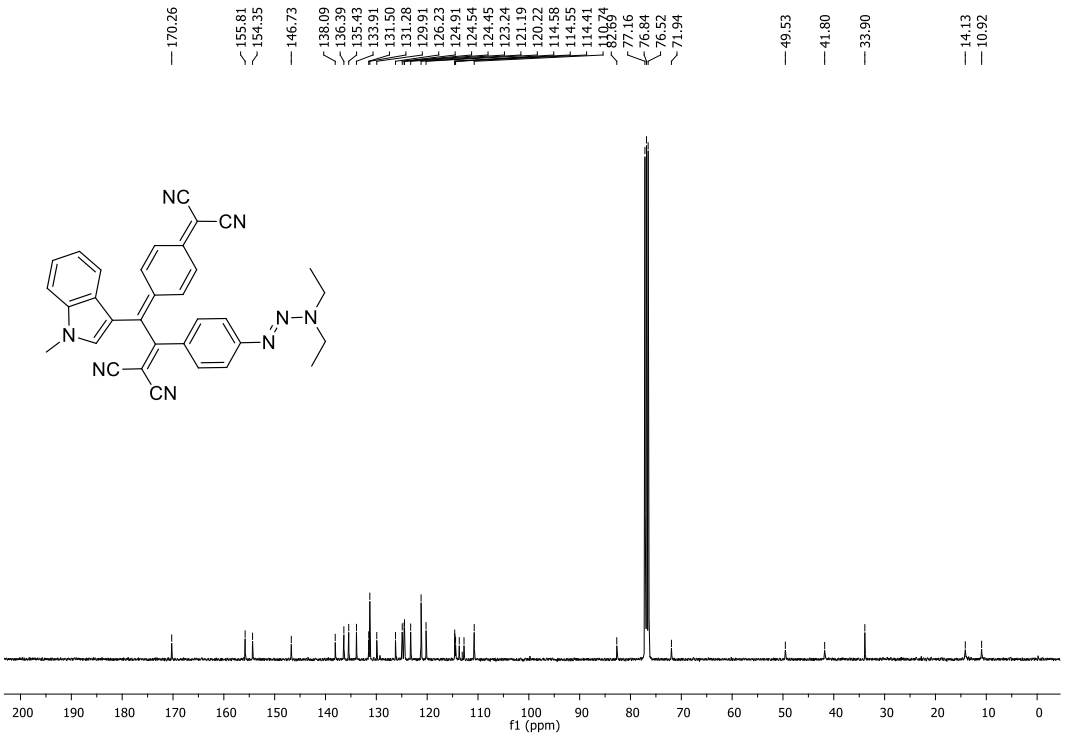

Figure 99. ^{13}C NMR spectrum of **180** in $CDCl_3$ solution (100 MHz).

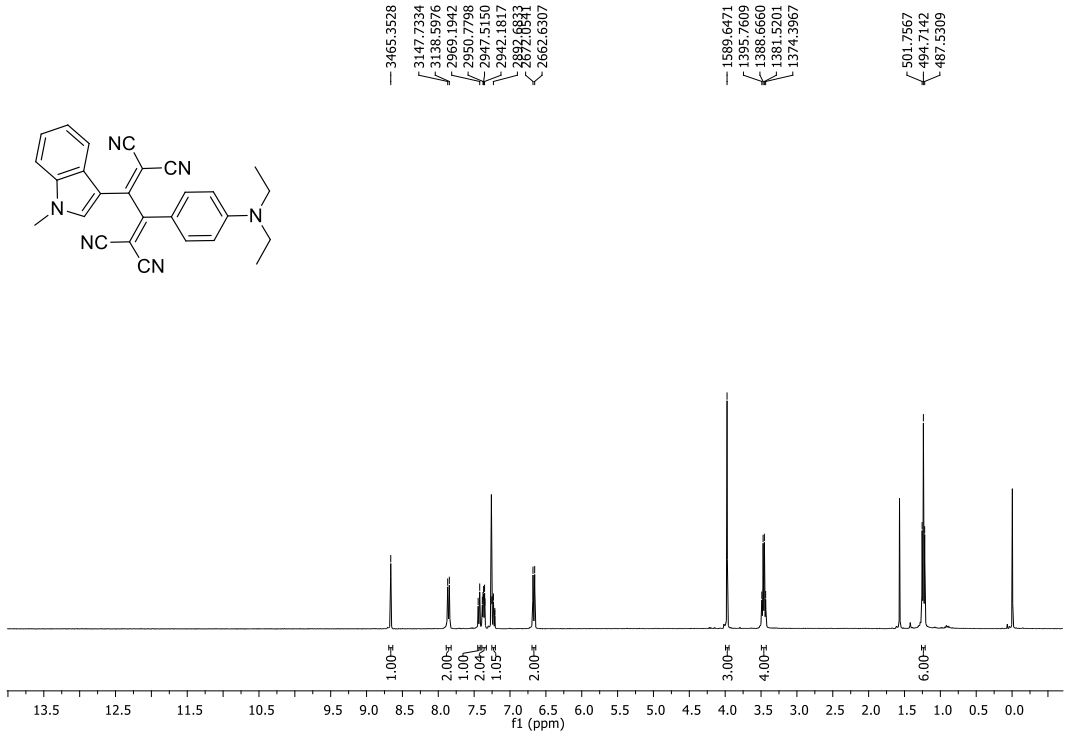

Figure 100. ^{1}H NMR spectrum of **175** in $CDCl_3$ solution (400 MHz).

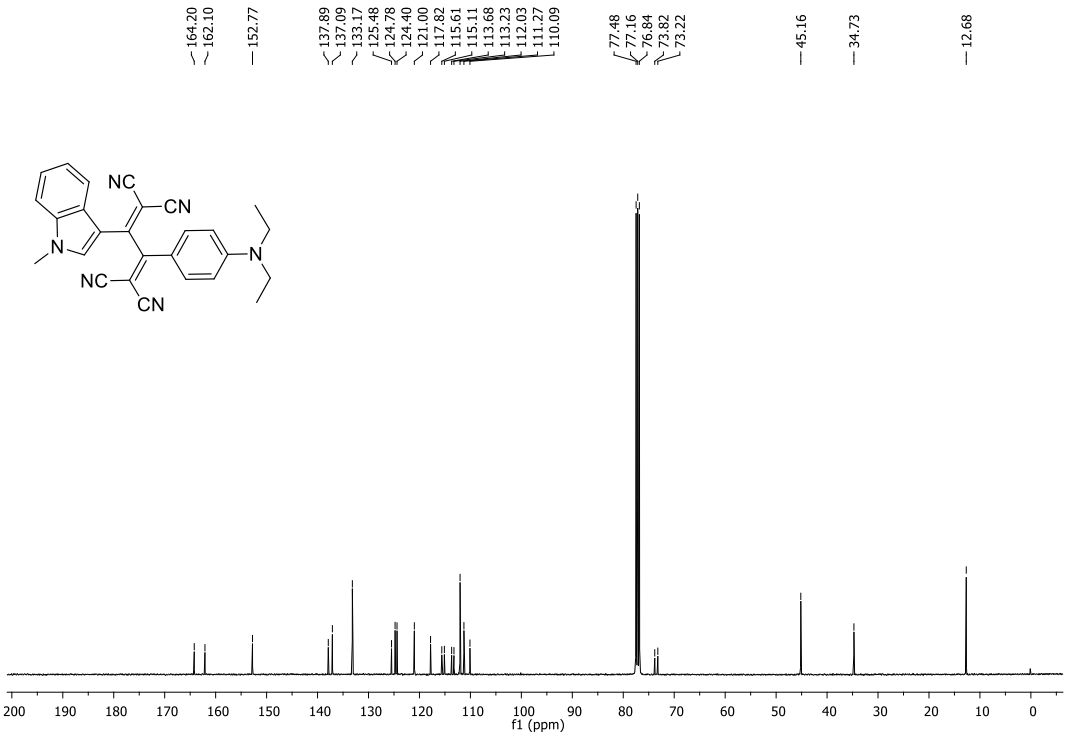

Figure 101. ^{13}C NMR spectrum of **175** in $CDCl_3$ solution (100 MHz).

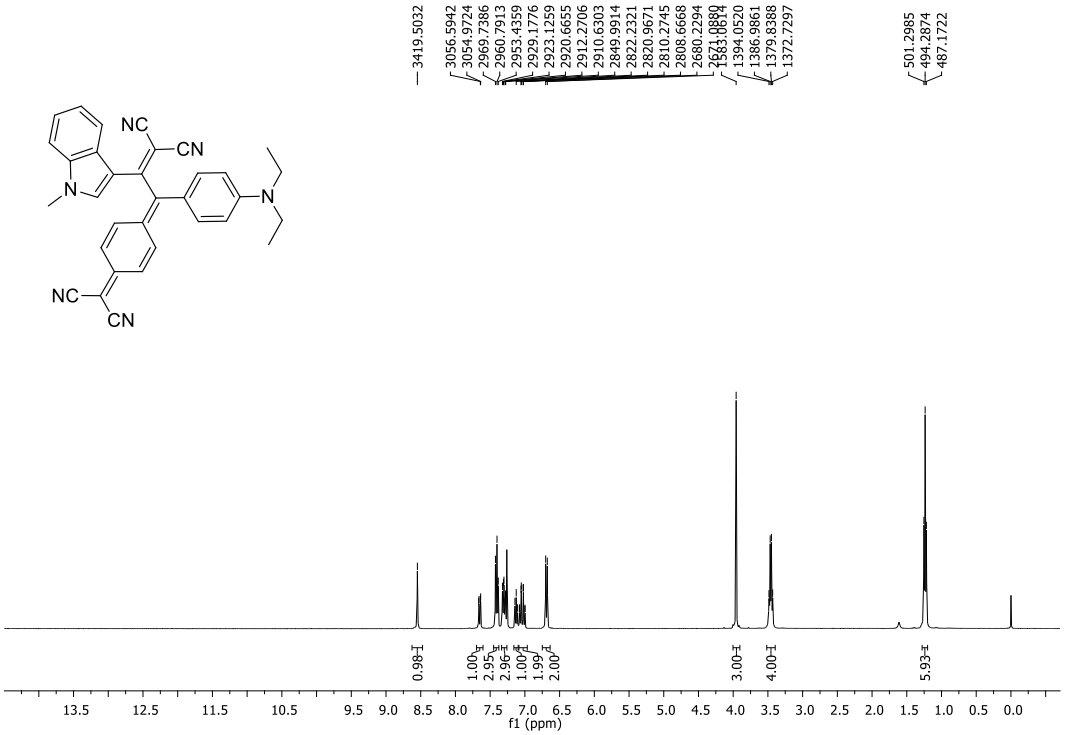

Figure 102. ^{1}H NMR spectrum of **176** in $CDCl_3$ solution (400 MHz).

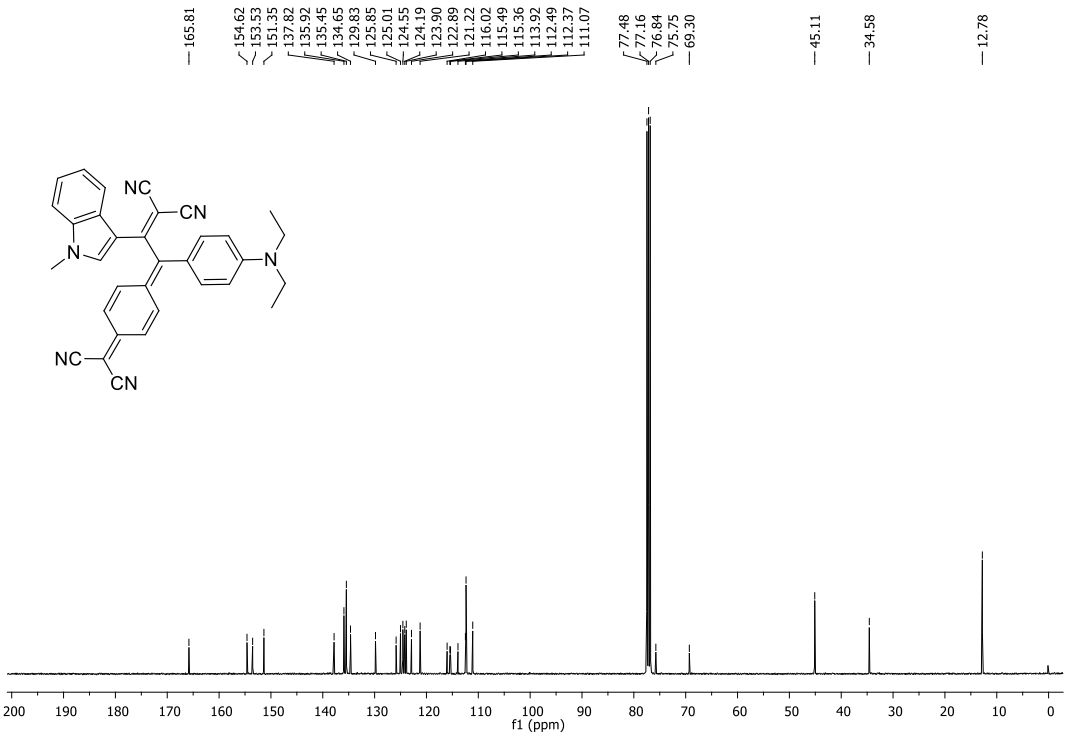

Figure 103. ^{13}C NMR spectrum of **176** in $CDCl_3$ solution (100 MHz).

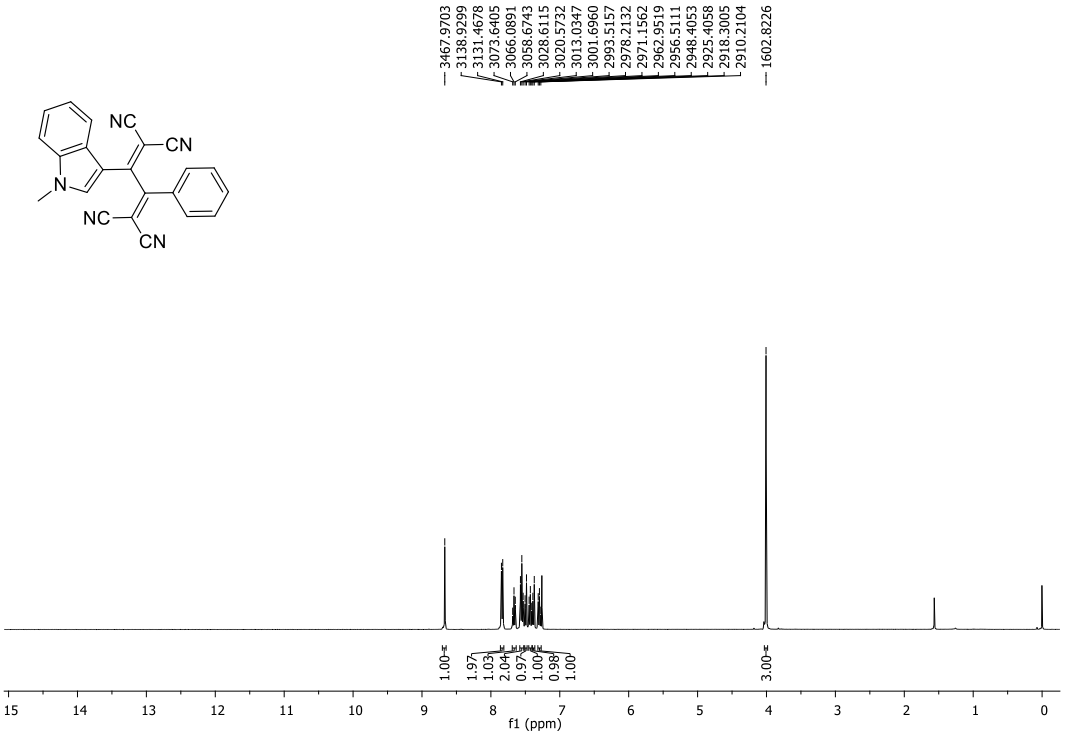

Figure 104. ^{1}H NMR spectrum of **177** in $CDCl_3$ solution (400 MHz).

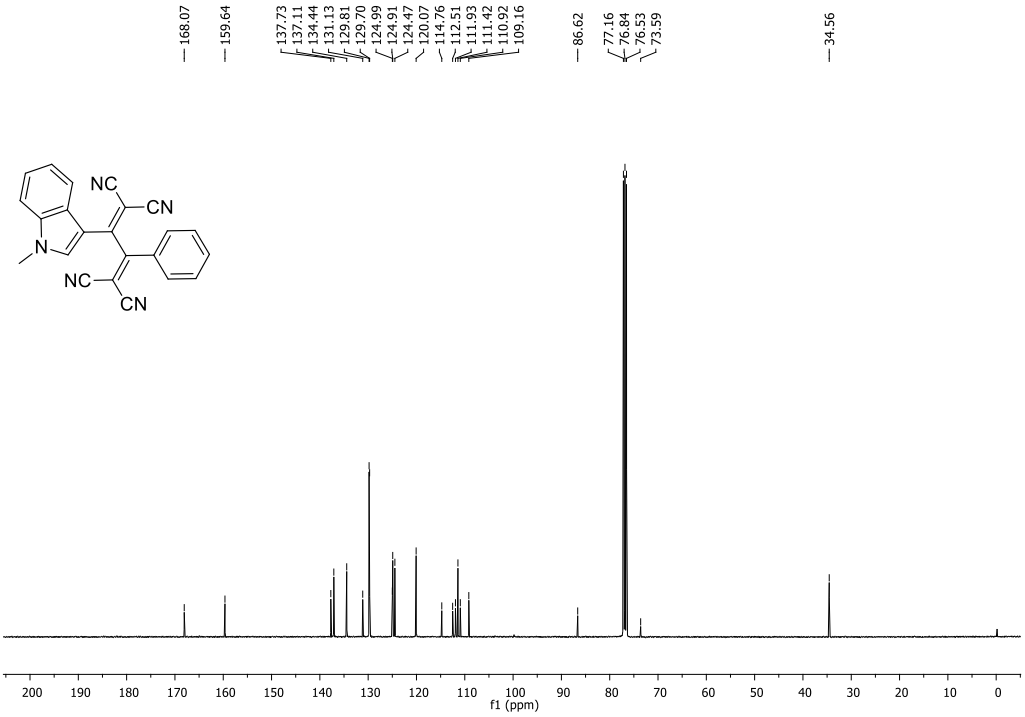

Figure 105. ^{13}C NMR spectrum of **177** in $CDCl_3$ solution (100 MHz).

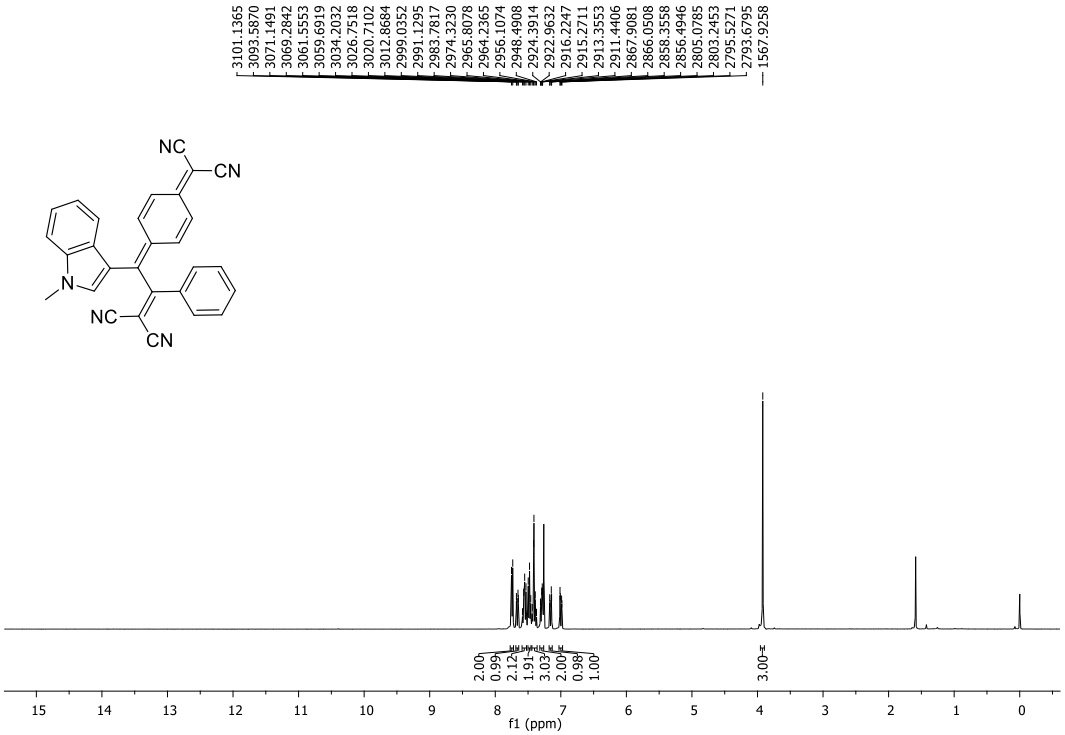

Figure 106. ^{1}H NMR spectrum of **178** in $CDCl_3$ solution (400 MHz).

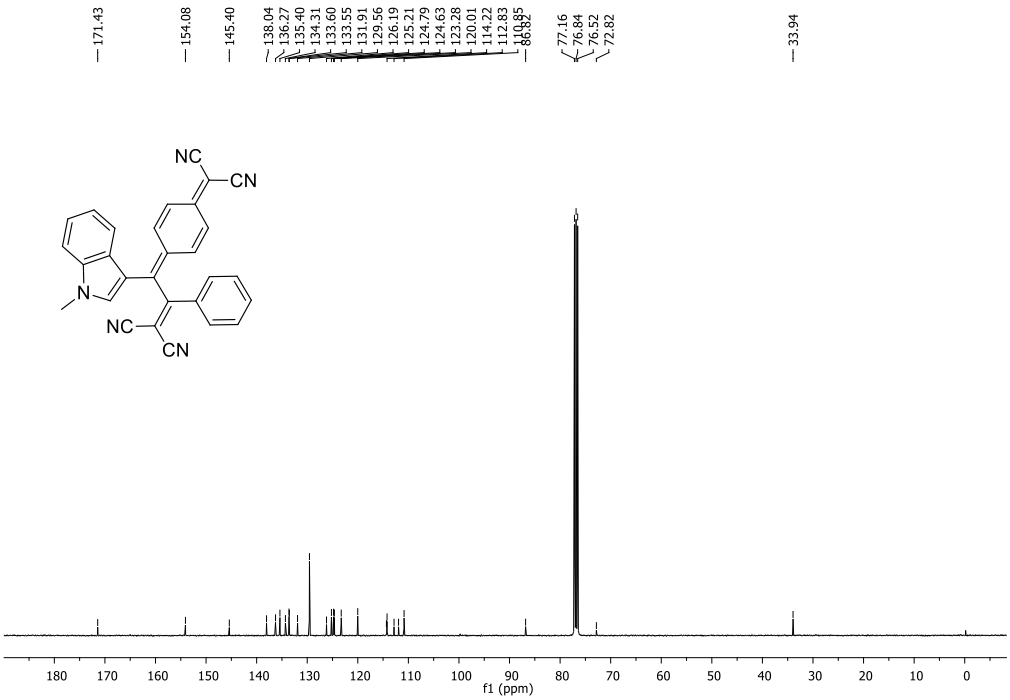

Figure 107. ^{13}C NMR spectrum of **178** in $CDCl_3$ solution (100 MHz).

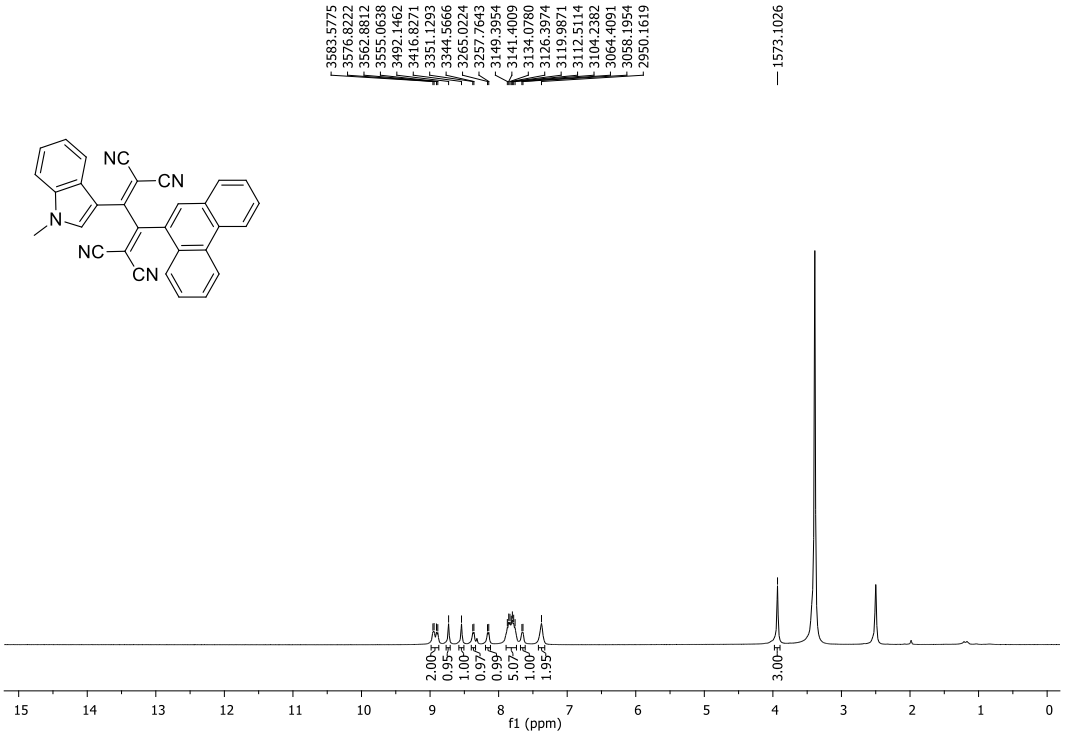

Figure 108. ^{1}H NMR spectrum of **181** in DMSO solution (400 MHz).

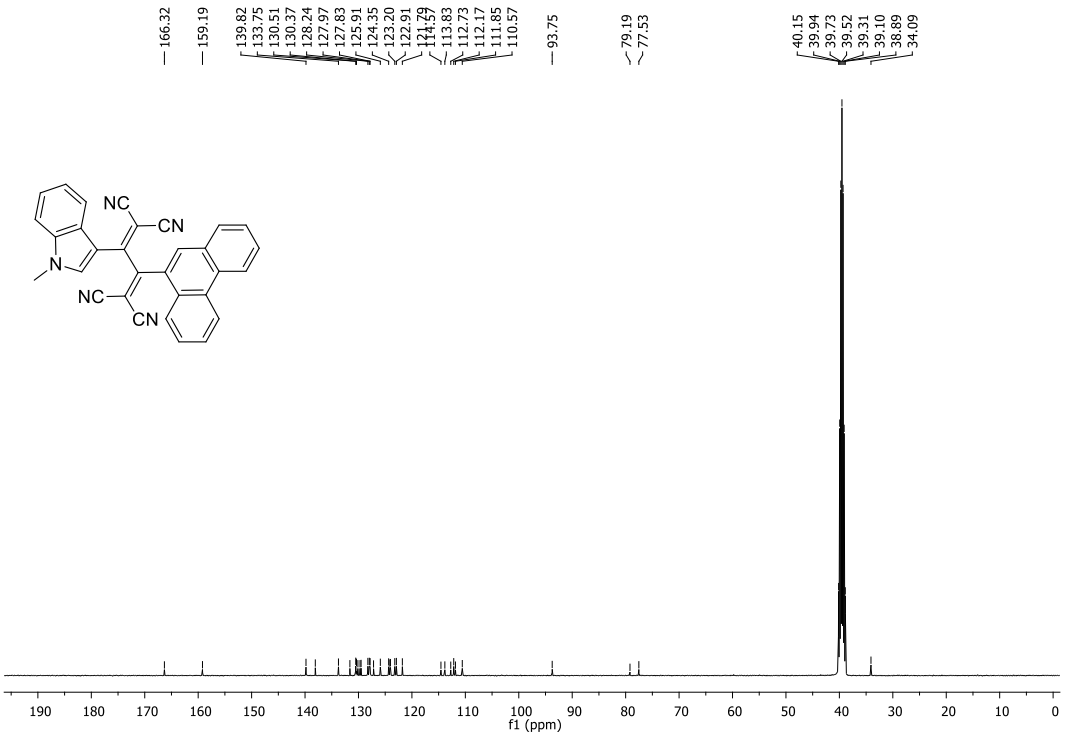

Figure 109. ^{13}C NMR spectrum of **181** in DMSO solution (100 MHz).

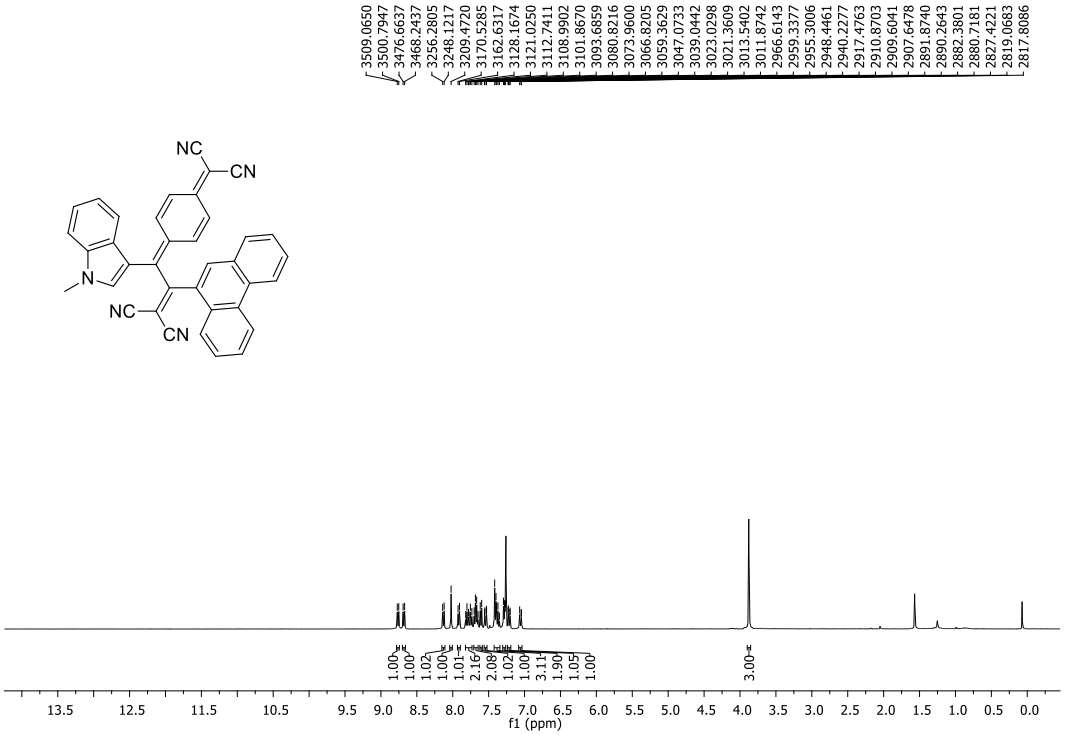

Figure 110. ^{1}H NMR spectrum of **182** in $CDCl_3$ solution (400 MHz).

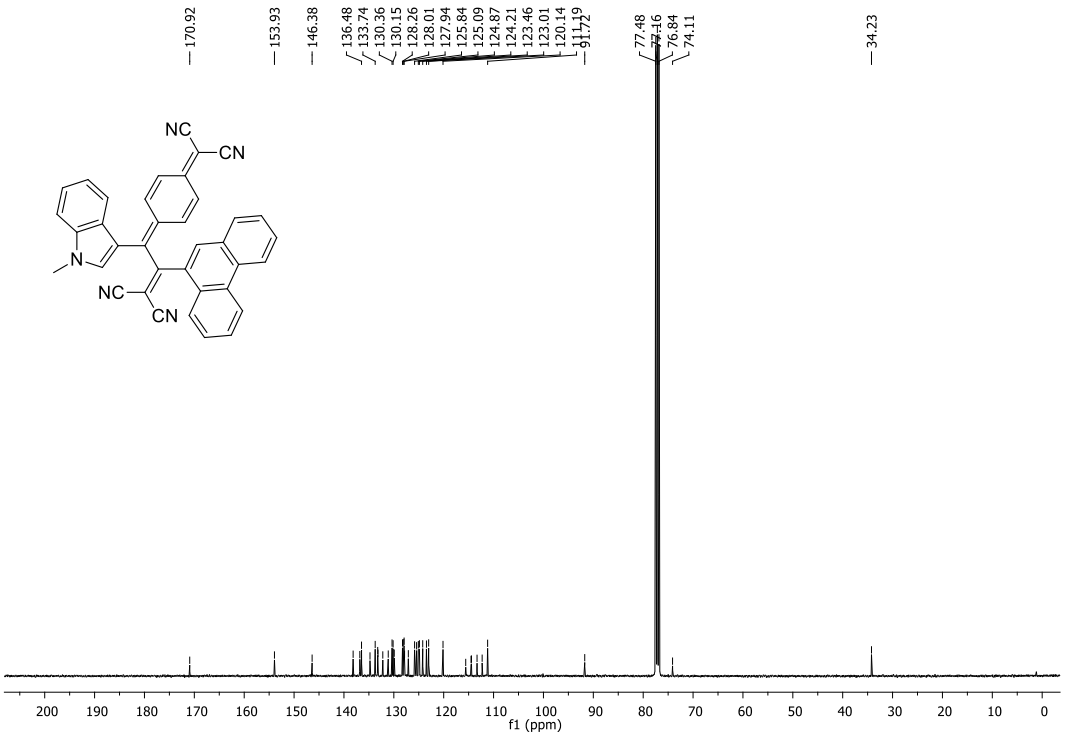

Figure 111. ^{13}C NMR spectrum of **182** in $CDCl_3$ solution (100 MHz).

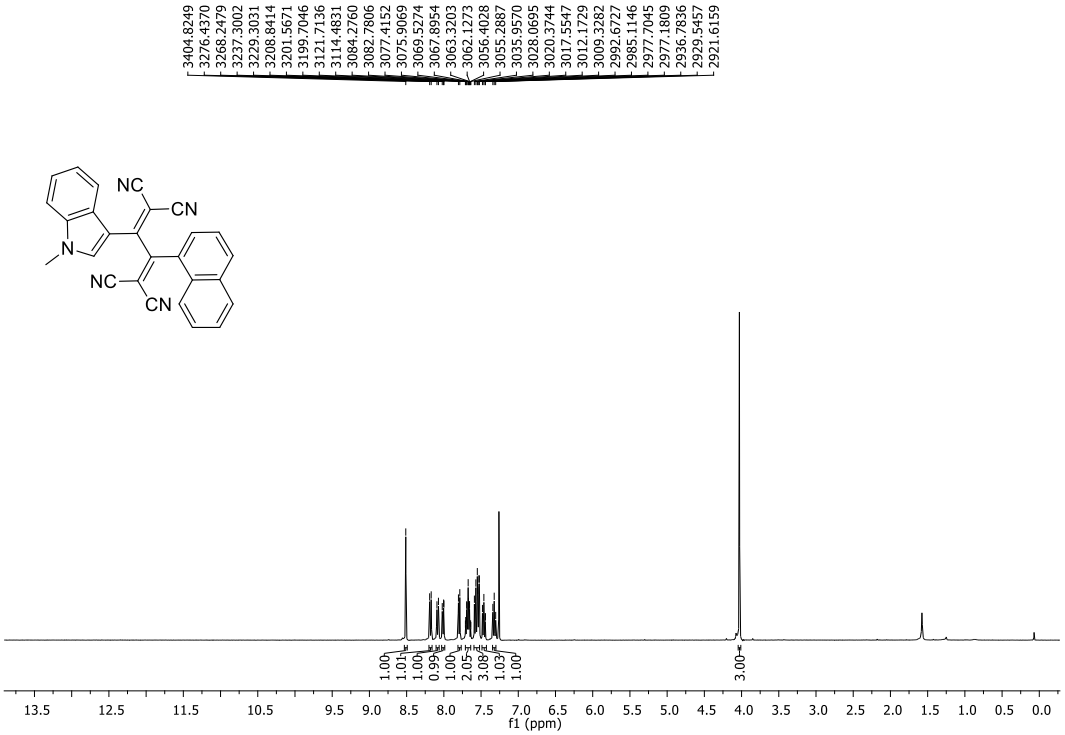

Figure 112. ^{1}H NMR spectrum of **183** in $CDCl_3$ solution (400 MHz).

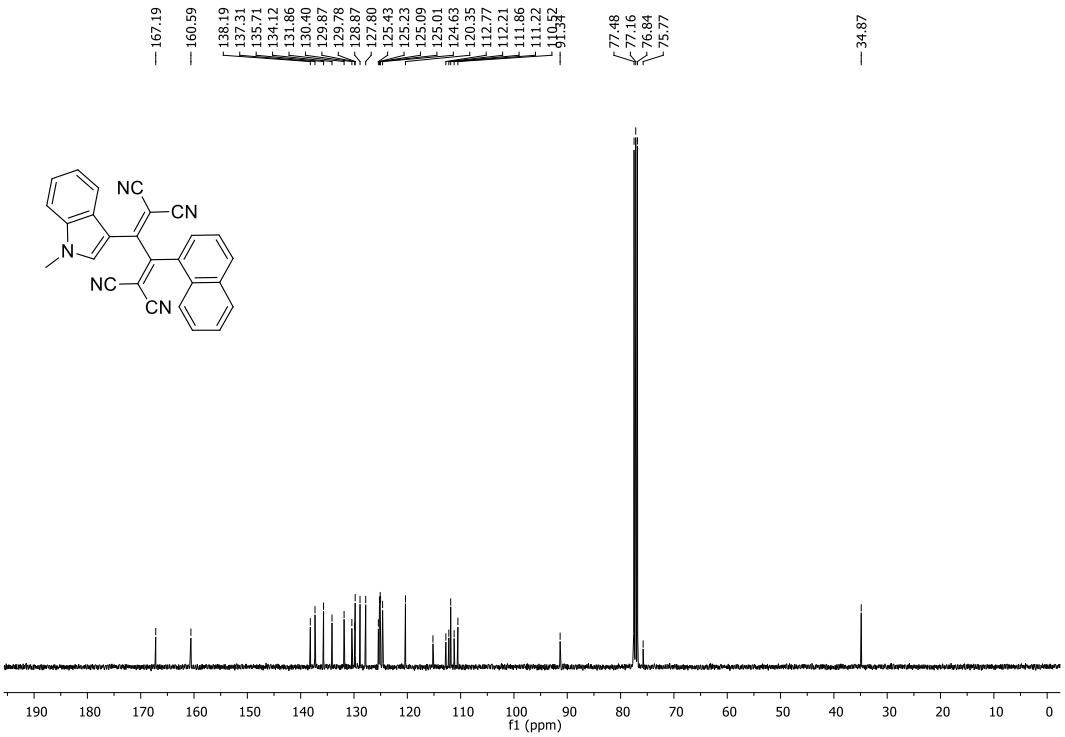

Figure 113. ^{13}C NMR spectrum of **183** in $CDCl_3$ solution (100 MHz).

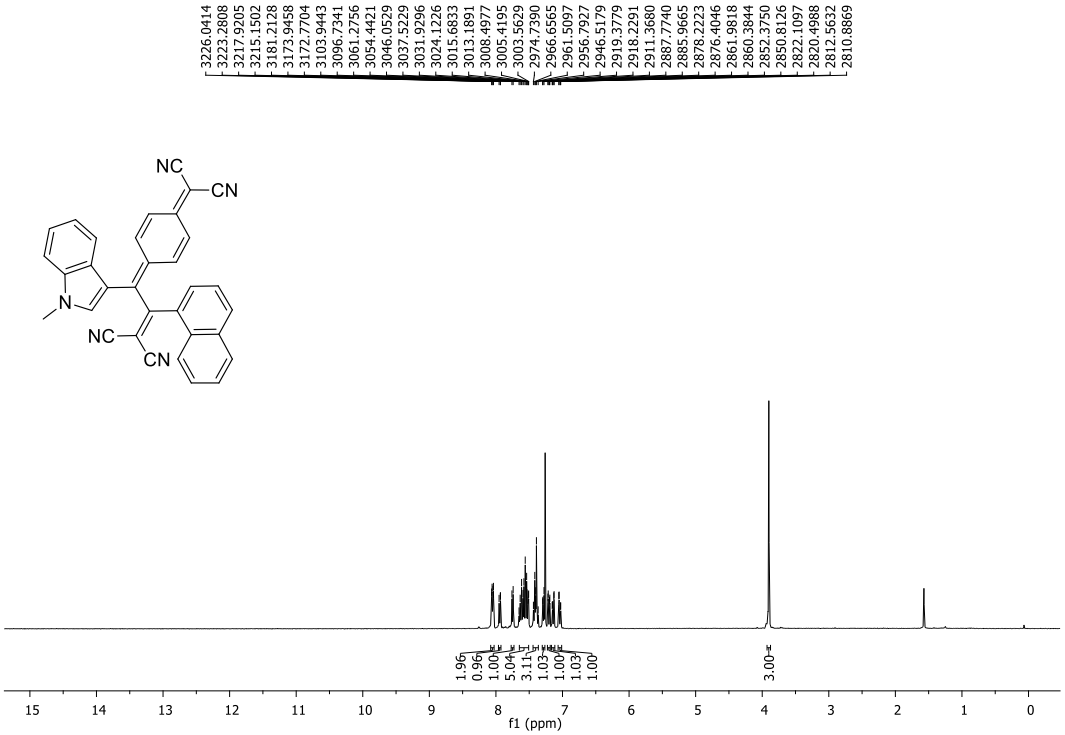

Figure 114. ^{1}H NMR spectrum of **184** in $CDCl_3$ solution (400 MHz).

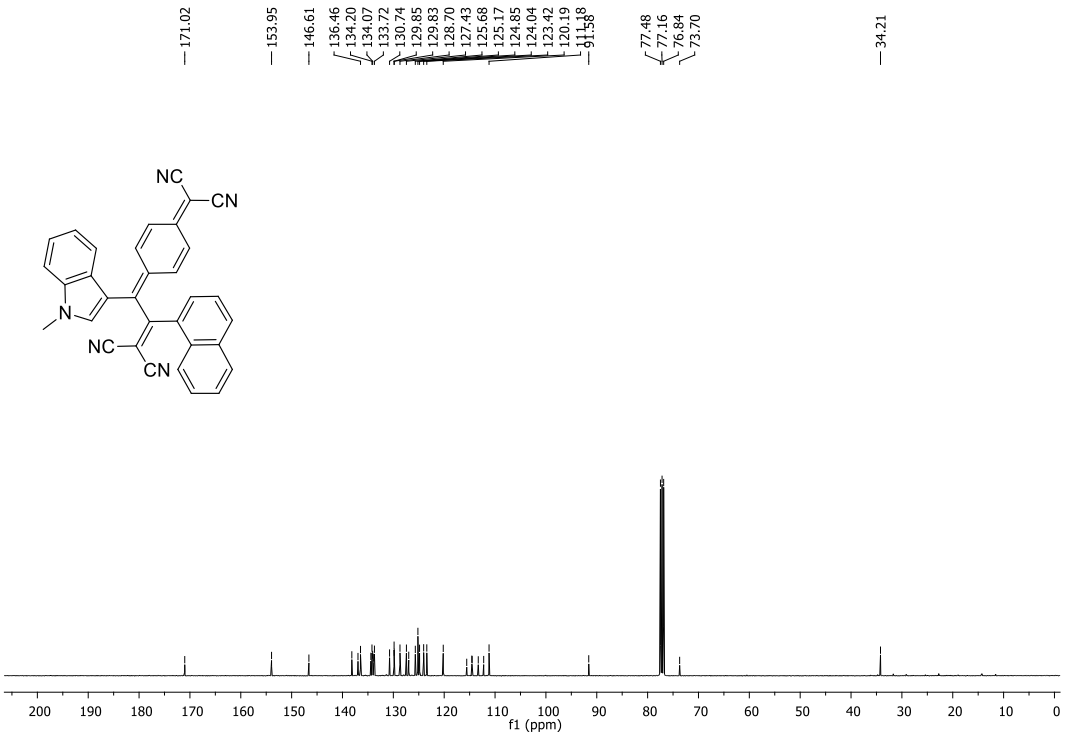

Figure 115. ^{13}C NMR spectrum of **184** in $CDCl_3$ solution (100 MHz).

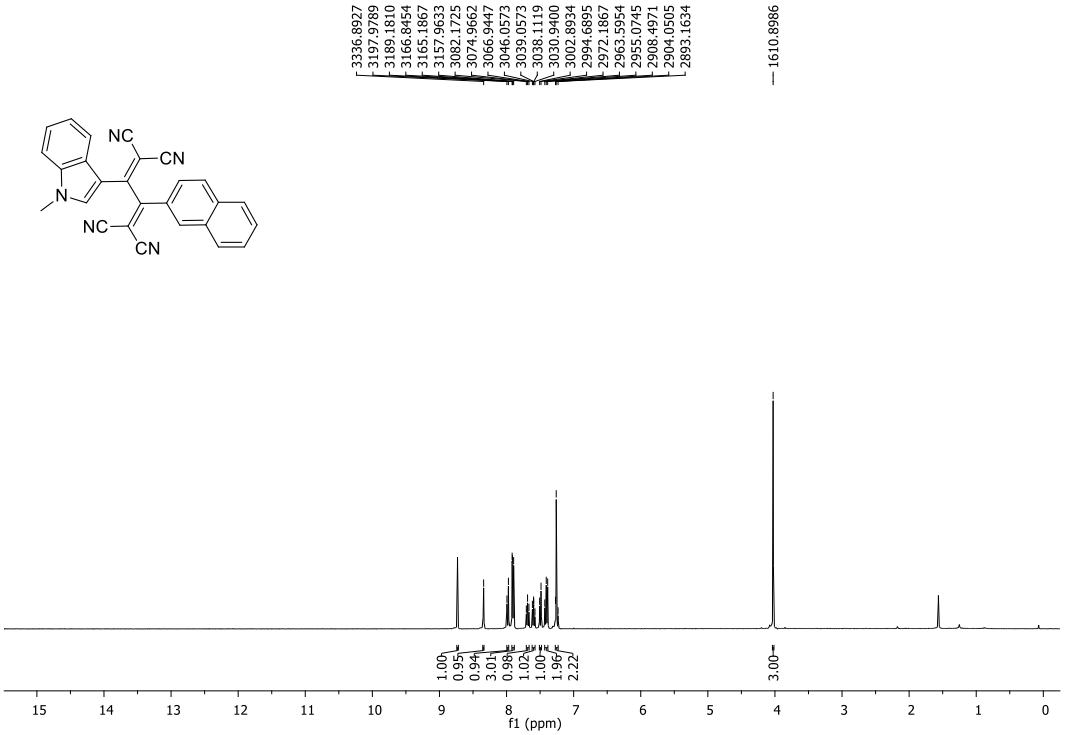

Figure 116. ^{1}H NMR spectrum of **185** in $CDCl_3$ solution (400 MHz).

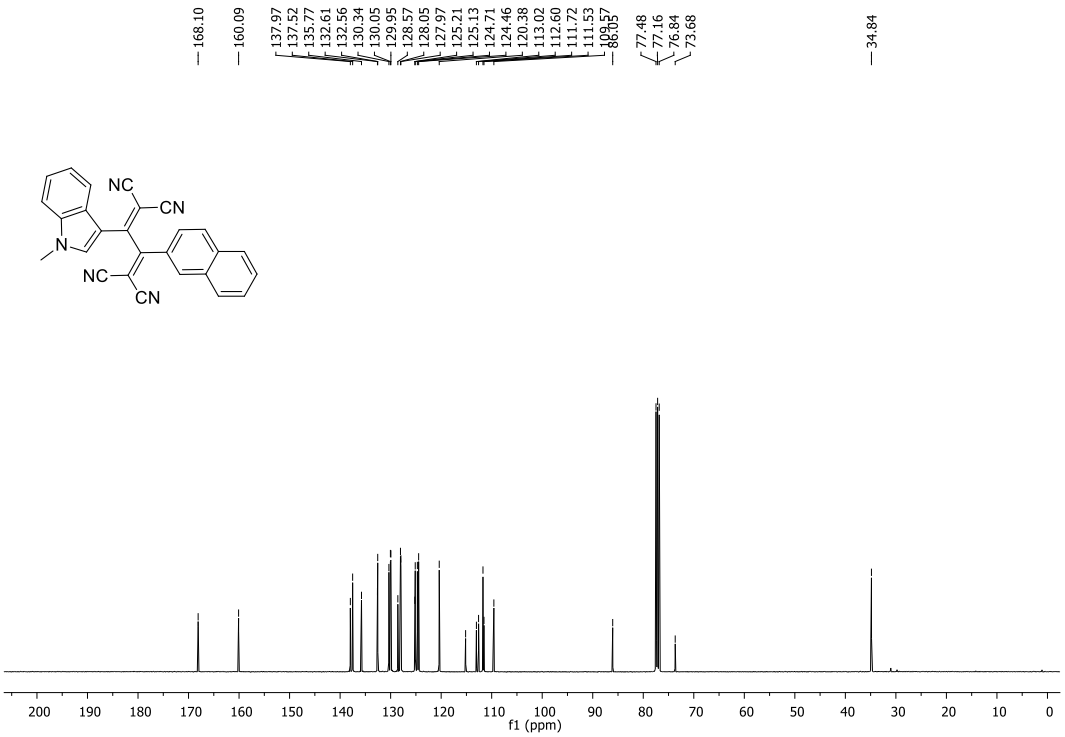

Figure 117. ^{13}C NMR spectrum of **185** in $CDCl_3$ solution (100 MHz).

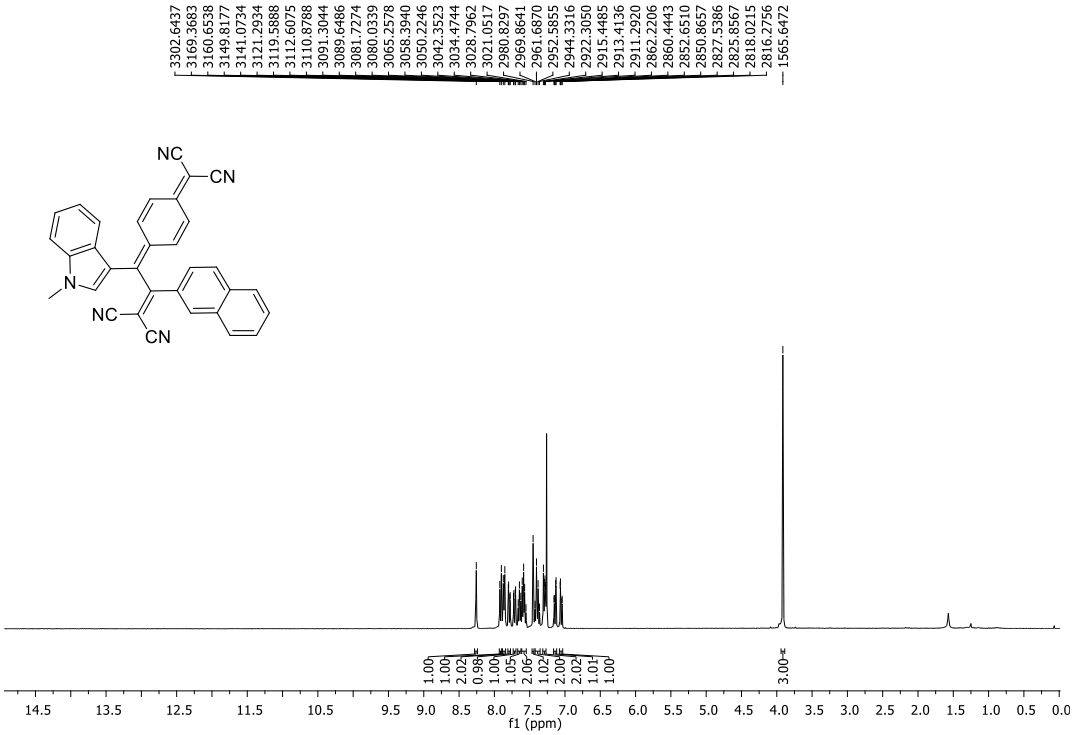

Figure 118. ^{1}H NMR spectrum of **186** in $CDCl_3$ solution (400 MHz).

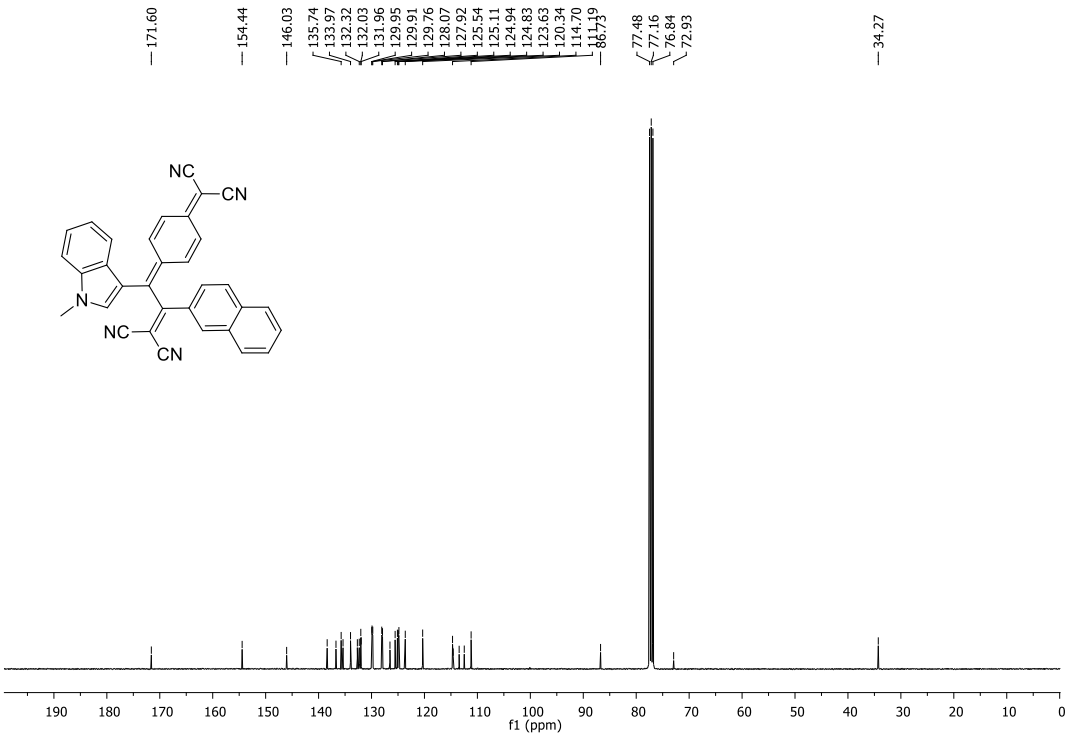

Figure 119. ^{13}C NMR spectrum of **186** in $CDCl_3$ solution (100 MHz)

B. IR Spectrum

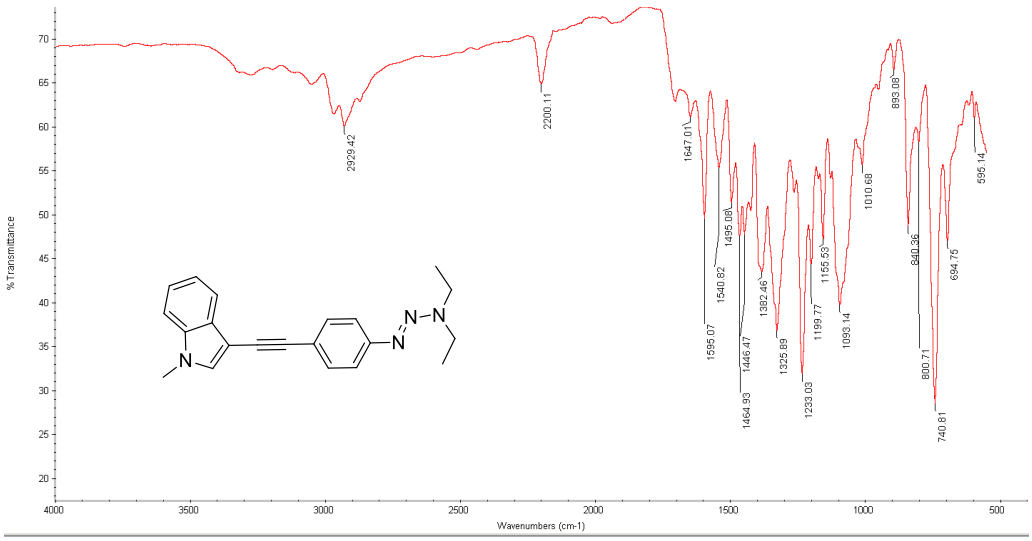

Figure 120. IR Spectrum of Compound **156**

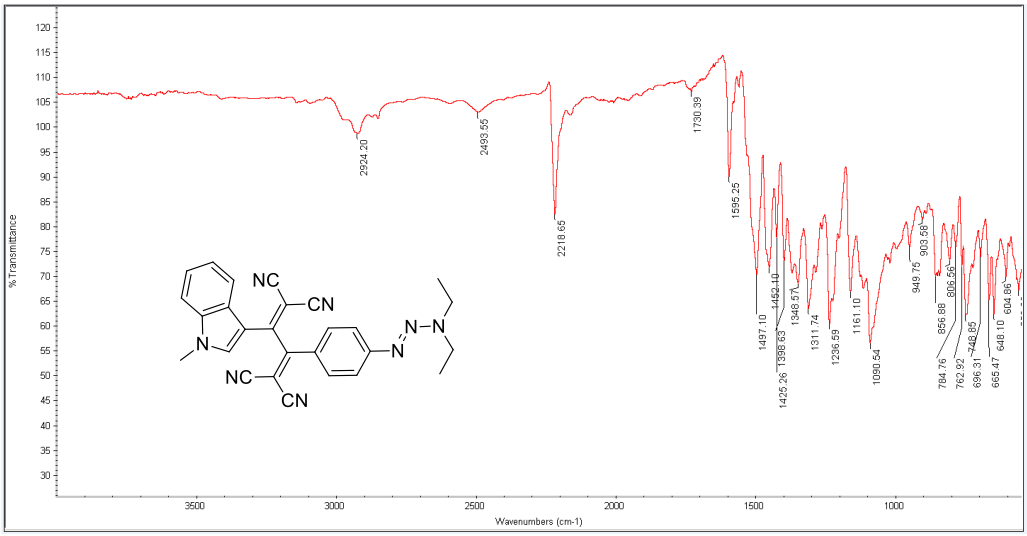

Figure 121. IR Spectrum of Compound **179**

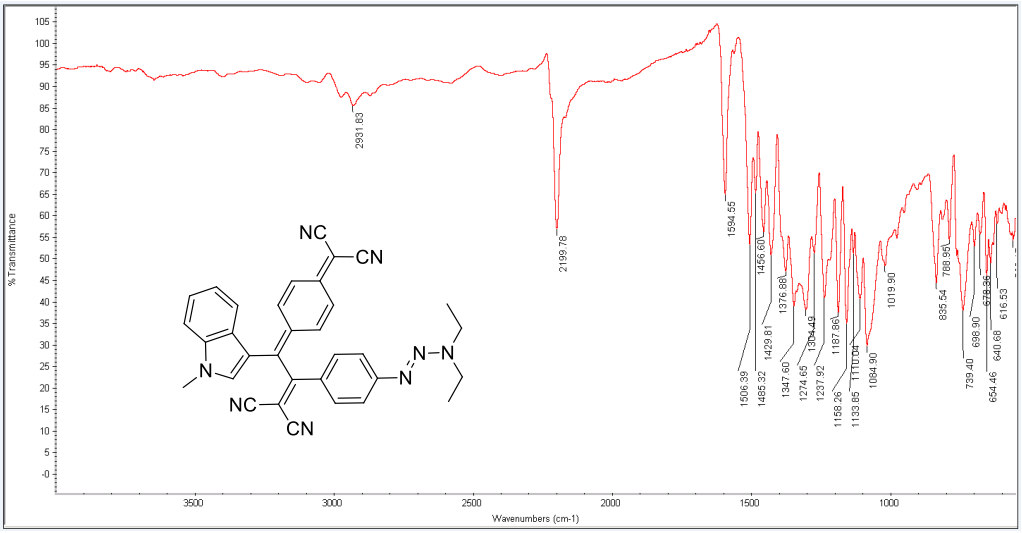

Figure 122. IR Spectrum of Compound **180**

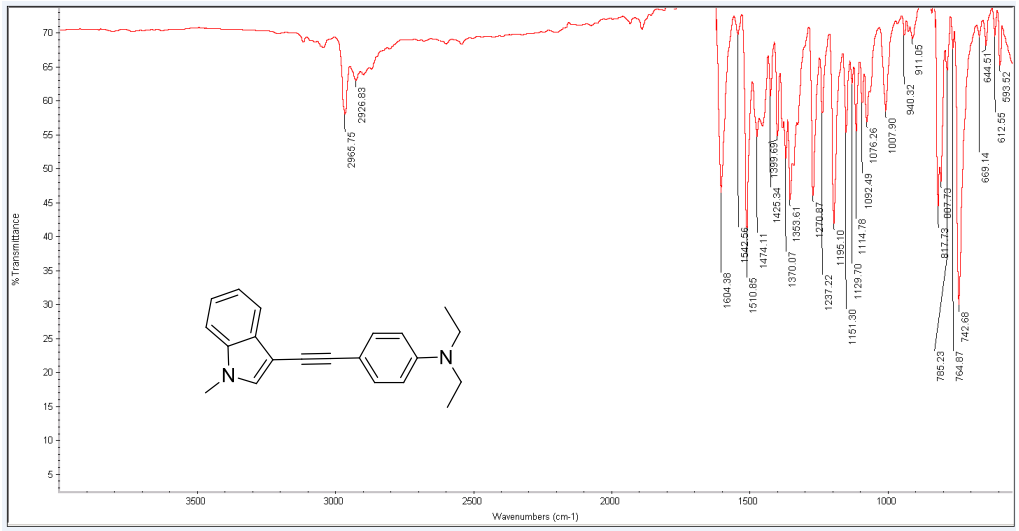

Figure 123. IR Spectrum of Compound **169**

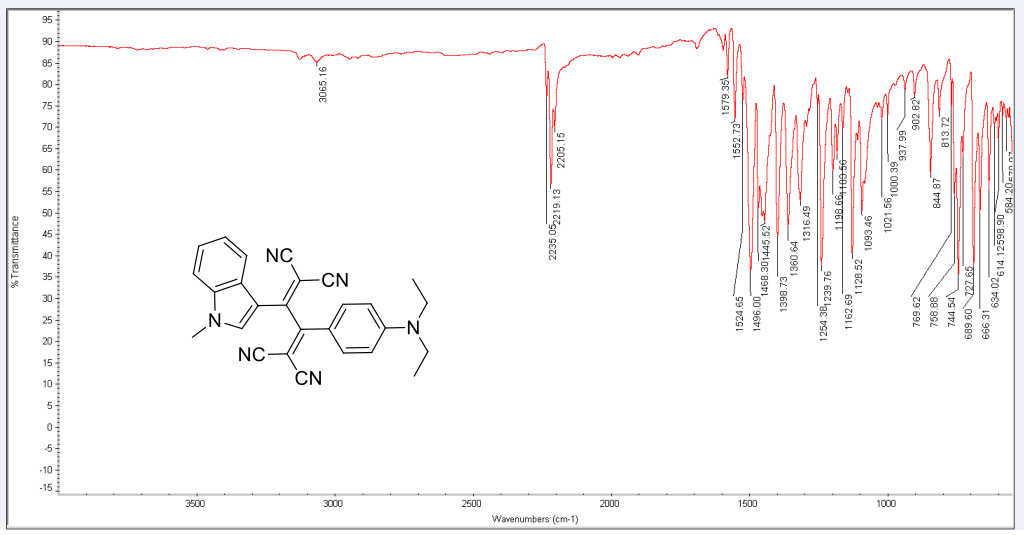

Figure 124. IR Spectrum of Compound **175**

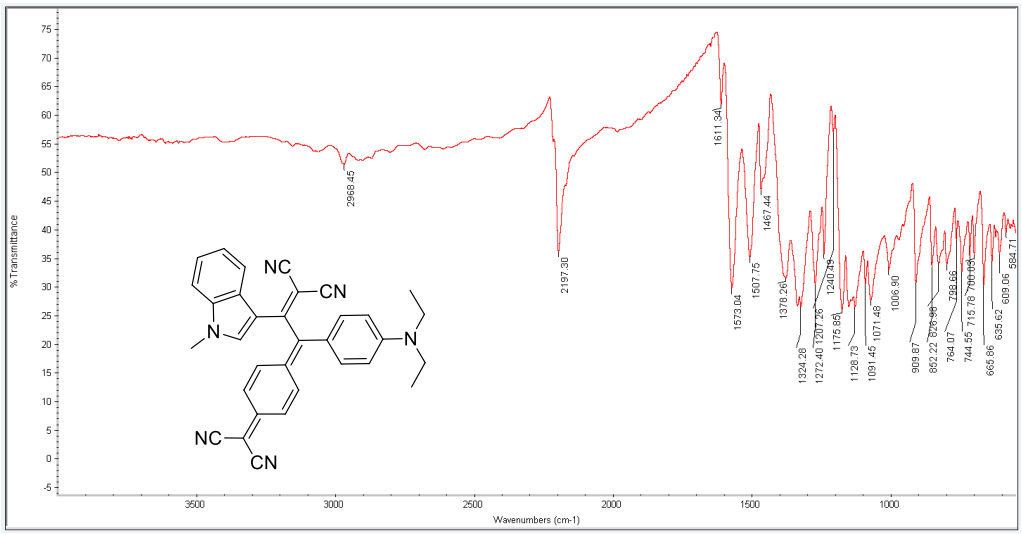

Figure 125. IR Spectrum of Compound **176**

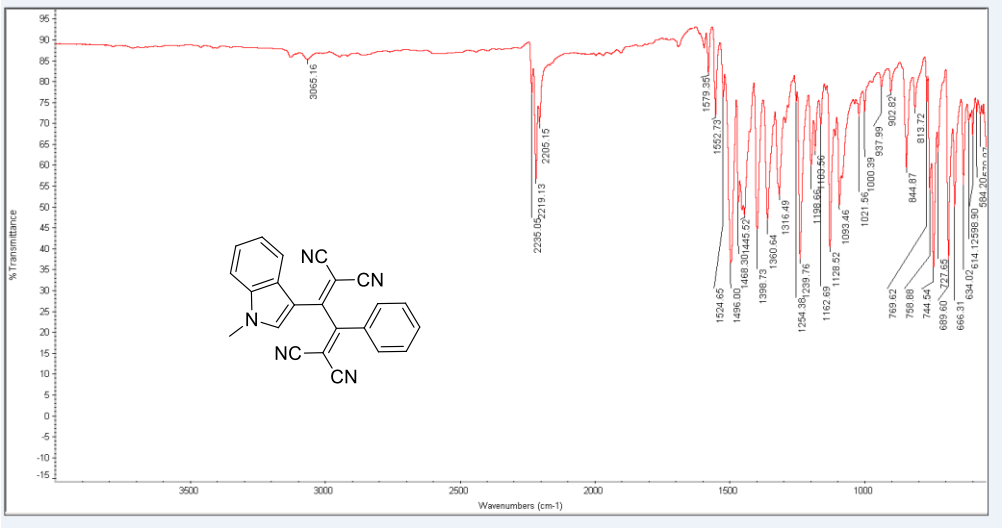

Figure 126. IR Spectrum of Compound **177**

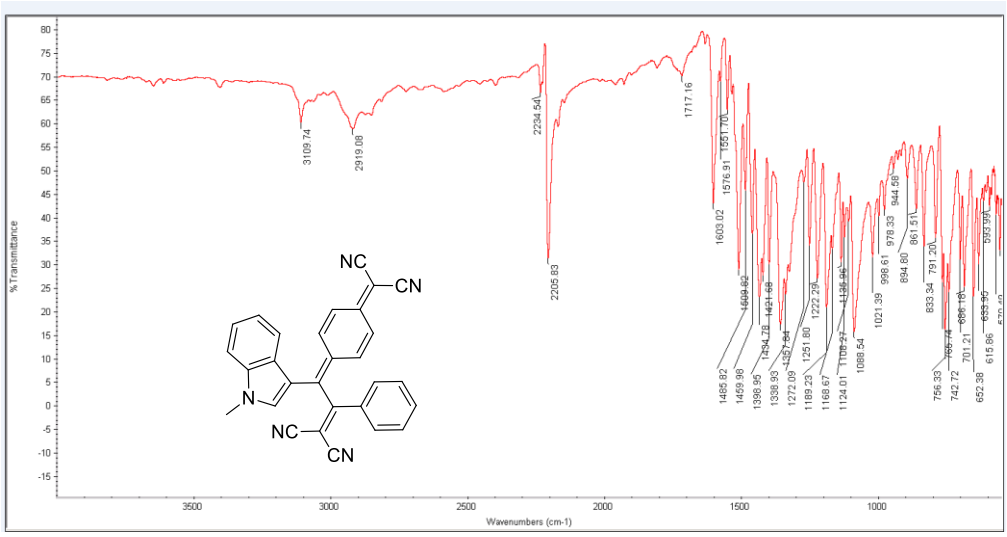

Figure 127. IR Spectrum of Compound **178**

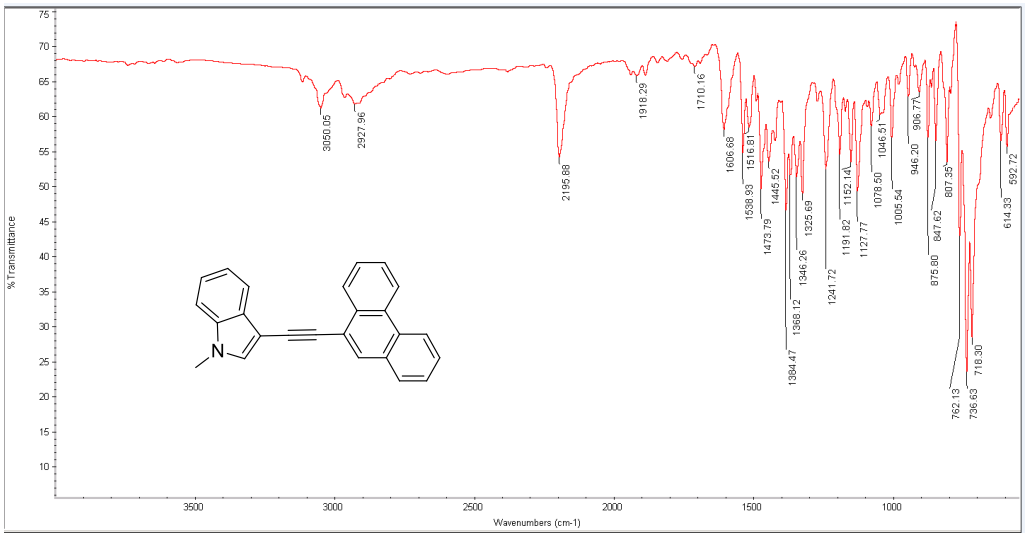

Figure 128. IR Spectrum of Compound **171**

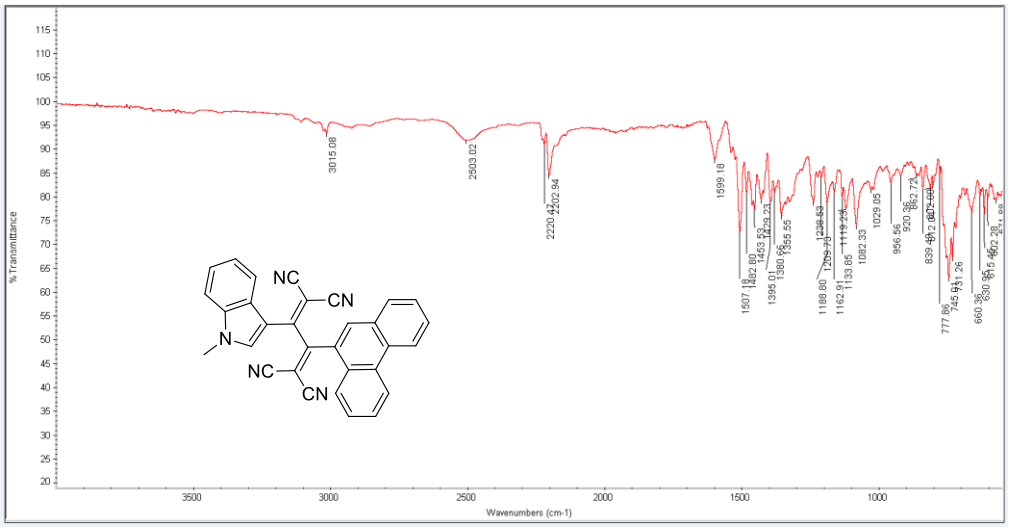

Figure 129. IR Spectrum of Compound **181**

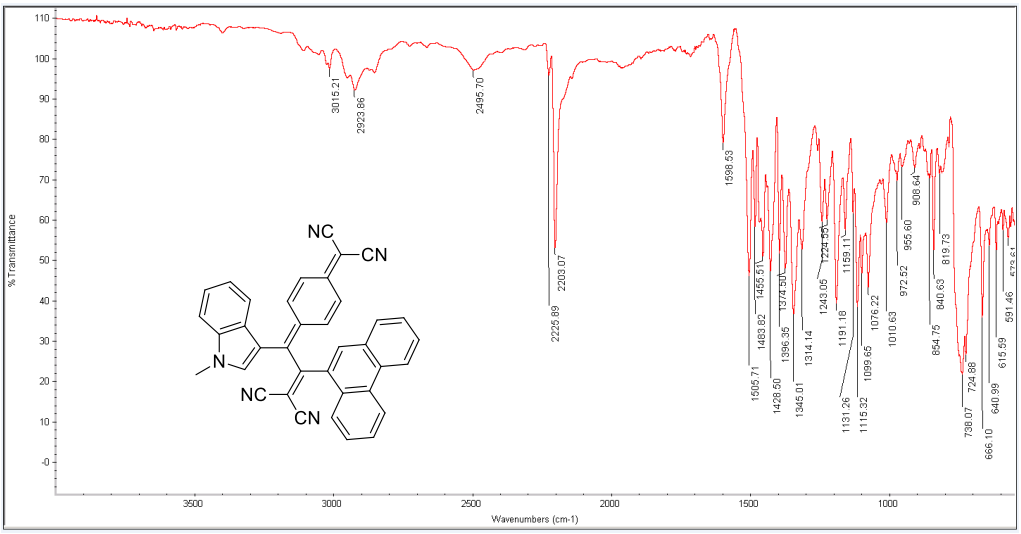

Figure 130. IR Spectrum of Compound **182**

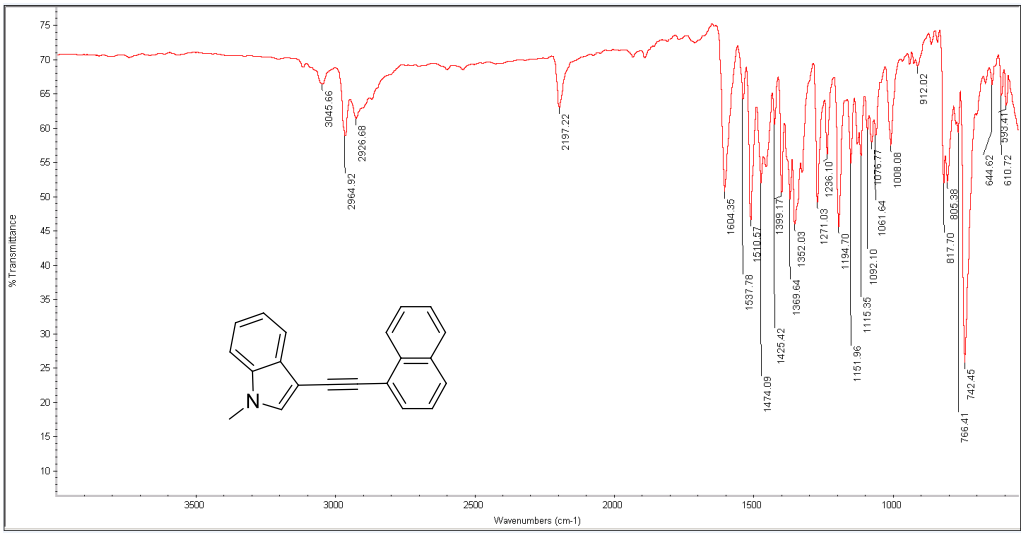

Figure 131. IR Spectrum of Compound **172**

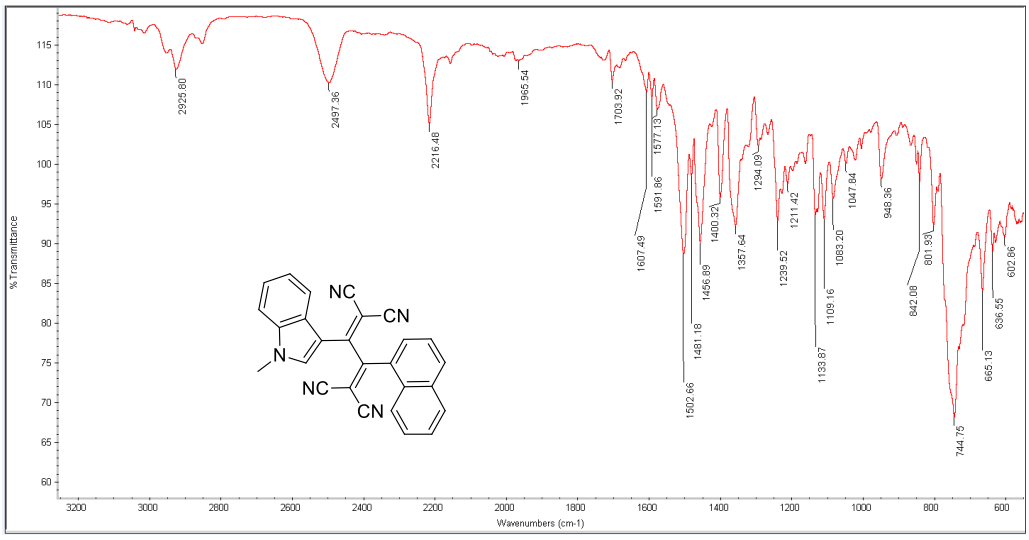

Figure 132. IR Spectrum of Compound **183**

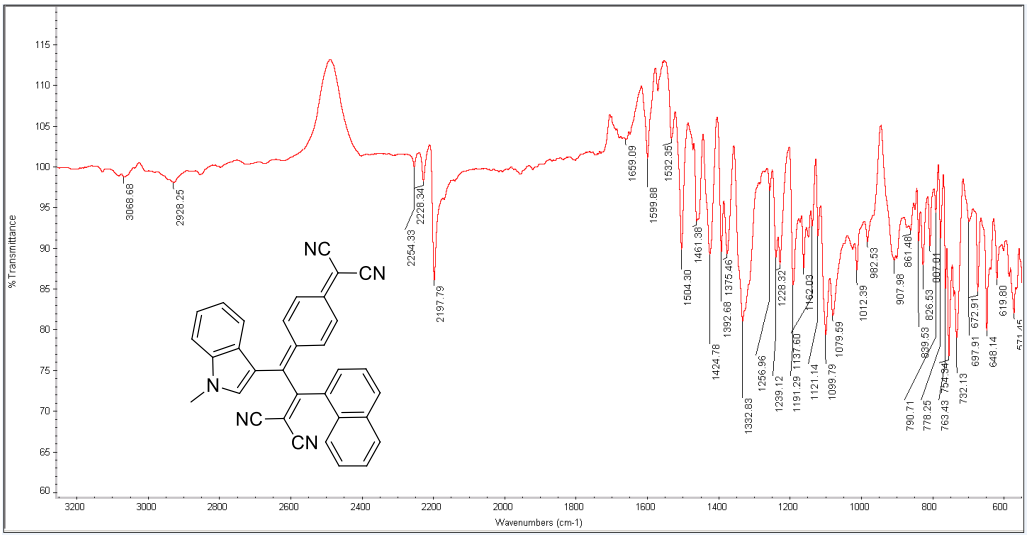

Figure 133. IR Spectrum of Compound **184**

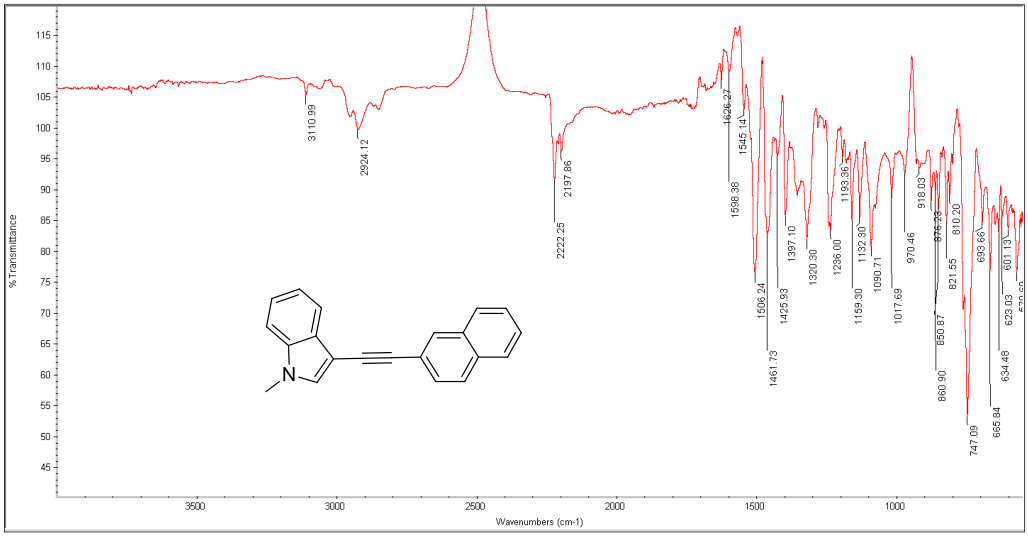

Figure 134. IR Spectrum of Compound **173**

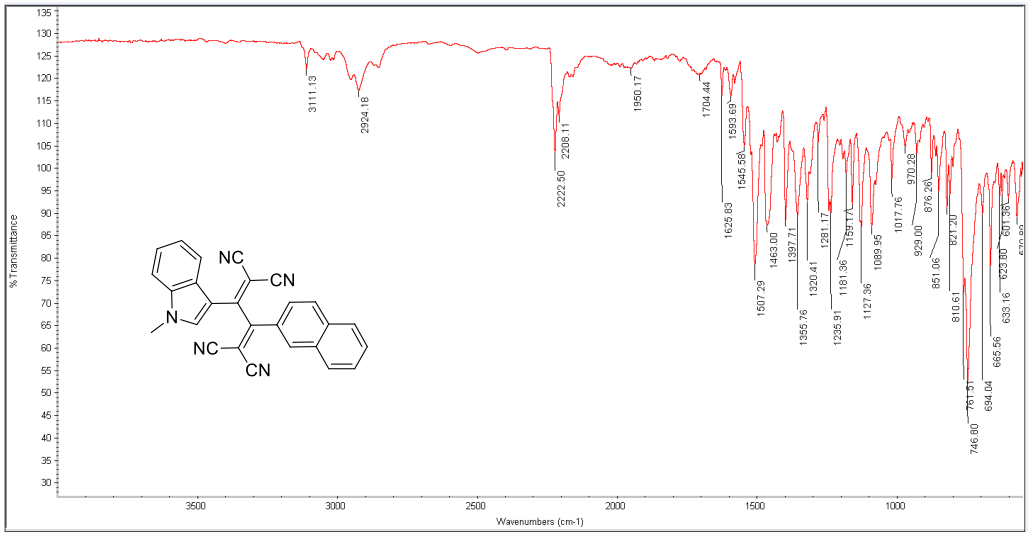

Figure 135. IR Spectrum of Compound **185**

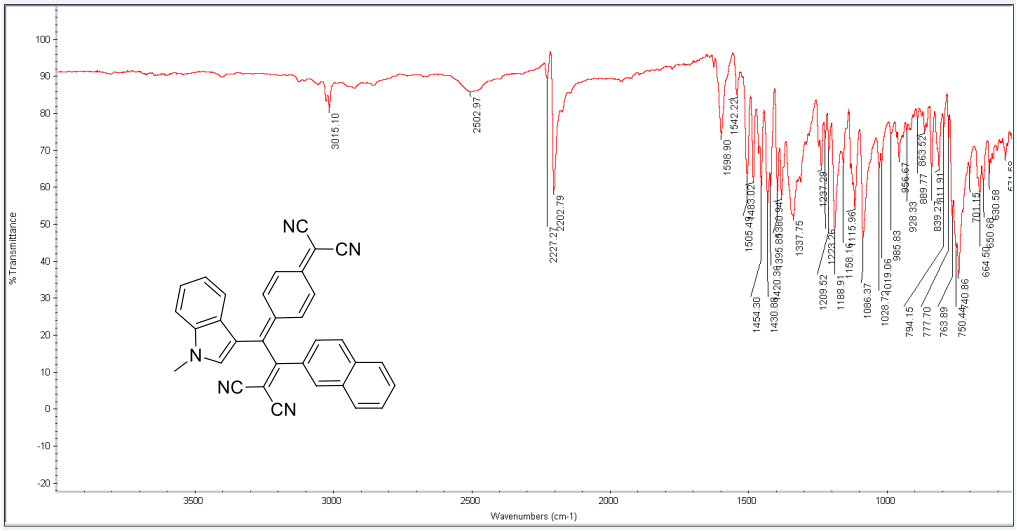

Figure 136. IR Spectrum of Compound **186**

C. HRMS

Elemental Composition Report **Page 1**

Single Mass Analysis
Tolerance = 1000.0 PPM / DBE: min = -5.5, max = 1000.0
Element prediction: Off
Number of isotope peaks used for i-FIT = 3

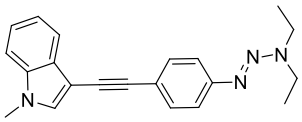

Monoisotopic Mass, Odd and Even Electron Ions
1 formula(e) evaluated with 1 results within limits (all results (up to 1000) for each mass)
Elements Used:
C: 21-21 H: 22-23 N: 4-4
Cagatay Dengiz
32149_20210326_01-03 2 (0.104) Cm (1:7)

1: TOF MS ES+
4.04e+004

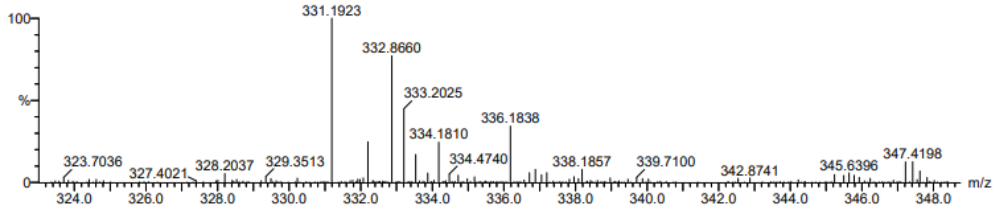

Minimum:				-5.5			
Maximum:		1000.0	1000.0	1000.0			
Mass	Calc. Mass	mDa	PPM	DBE	i-FIT	i-FIT (Norm)	Formula
331.1923	331.1923	0.0	0.0	12.5	334.6	0.0	C21 H23 N4

Elemental Composition Report **Page 1**

Single Mass Analysis
Tolerance = 1000.0 PPM / DBE: min = -5.5, max = 1000.0
Element prediction: Off
Number of isotope peaks used for i-FIT = 3

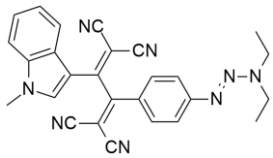

Monoisotopic Mass, Odd and Even Electron Ions
1 formula(e) evaluated with 1 results within limits (all results (up to 1000) for each mass)
Elements Used:
C: 27-27 H: 22-23 N: 8-8
Cagatay Dengiz
32149_20210326_02-06 21 (0.829) Cm (16:22)

1: TOF MS ES+
2.68e+005

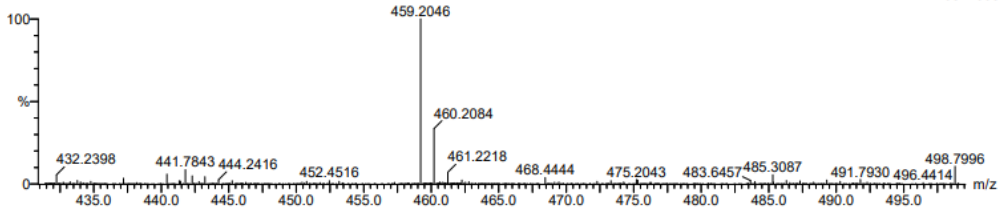

Minimum:				-5.5			
Maximum:		1000.0	1000.0	1000.0			
Mass	Calc. Mass	mDa	PPM	DBE	i-FIT	i-FIT (Norm)	Formula
459.2046	459.2046	0.0	0.0	20.5	515.5	0.0	C27 H23 N8

Elemental Composition Report **Page 1**

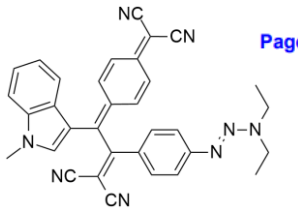

Single Mass Analysis
Tolerance = 1000.0 PPM / DBE: min = -5.5, max = 1000.0
Element prediction: Off
Number of isotope peaks used for i-FIT = 3

Monoisotopic Mass, Odd and Even Electron Ions
1 formula(e) evaluated with 1 results within limits (all results (up to 1000) for each mass)
Elements Used:
C: 33-33 H: 26-27 N: 8-8
Cagatay Dengiz
32149_20210326_03-04 25 (0.965) Cm (17:25)

1: TOF MS ES+
4.70e+004

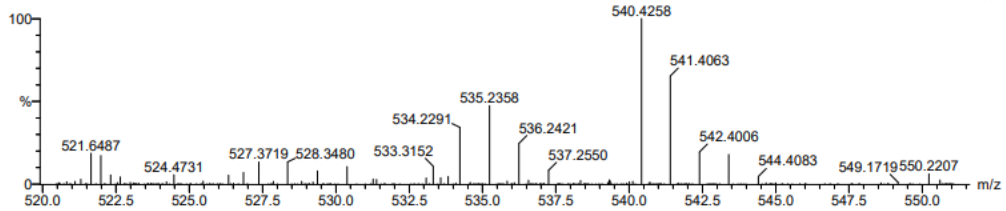

Minimum:				-5.5			
Maximum:		1000.0	1000.0	1000.0			
Mass	Calc. Mass	mDa	PPM	DBE	i-FIT	i-FIT (Norm)	Formula
535.2358	535.2359	-0.1	-0.2	24.5	243.2	0.0	C33 H27 N8

Elemental Composition Report **Page 1**

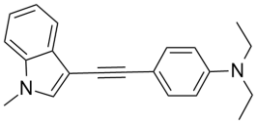

Single Mass Analysis
Tolerance = 1000.0 PPM / DBE: min = -5.5, max = 1000.0
Element prediction: Off
Number of isotope peaks used for i-FIT = 3

Monoisotopic Mass, Even Electron Ions
1 formula(e) evaluated with 1 results within limits (all results (up to 1000) for each mass)
Elements Used:
C: 21-21 H: 22-23 N: 2-2
Cagatay Dengiz
32149_20210326_06-01 12 (0.484) Cm (1:17)

1: TOF MS ES+
4.07e+006

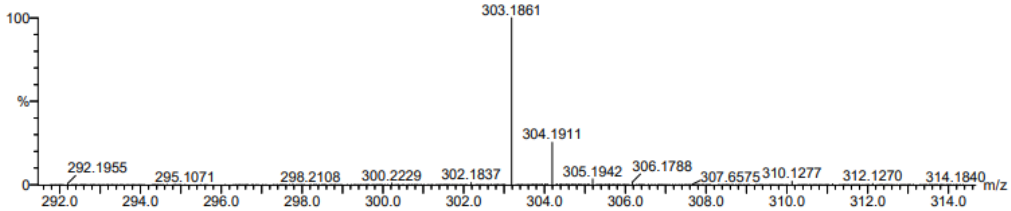

Minimum:				-5.5			
Maximum:		1000.0	1000.0	1000.0			
Mass	Calc. Mass	mDa	PPM	DBE	i-FIT	i-FIT (Norm)	Formula
303.1861	303.1861	0.0	0.0	11.5	898.5	0.0	C21 H23 N2

Elemental Composition Report **Page 1**

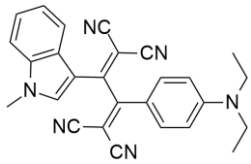

Single Mass Analysis
Tolerance = 1000.0 PPM / DBE: min = -5.5, max = 1000.0
Element prediction: Off
Number of isotope peaks used for i-FIT = 3

Monoisotopic Mass, Even Electron Ions
1 formula(e) evaluated with 1 results within limits (all results (up to 1000) for each mass)
Elements Used:
C: 27-27 H: 22-23 N: 6-6
Cagatay Dengiz
32149_20210326_07-03 6 (0.260) Cm (1:6)

1: TOF MS ES+
1.98e+005

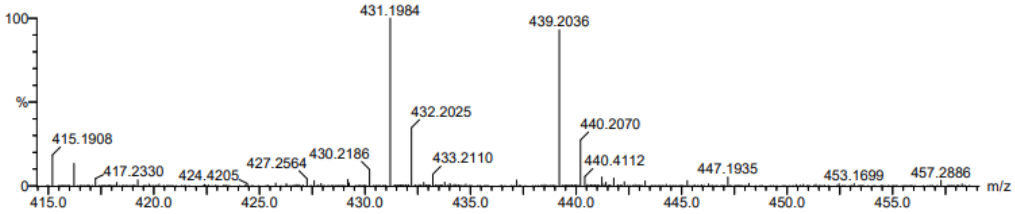

Minimum:				-5.5			
Maximum:		1000.0	1000.0	1000.0			
Mass	Calc. Mass	mDa	PPM	DBE	i-FIT	i-FIT (Norm)	Formula
431.1984	431.1984	0.0	0.0	19.5	439.7	0.0	C27 H23 N6

Elemental Composition Report **Page 1**

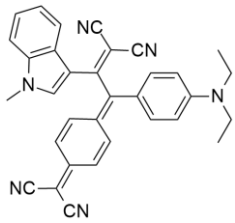

Single Mass Analysis
Tolerance = 1000.0 PPM / DBE: min = -5.5, max = 1000.0
Element prediction: Off
Number of isotope peaks used for i-FIT = 3

Monoisotopic Mass, Even Electron Ions
1 formula(e) evaluated with 1 results within limits (all results (up to 1000) for each mass)
Elements Used:
C: 33-33 H: 26-27 N: 6-6
Cagatay Dengiz
32149_20210326_08-01 8 (0.328) Cm (8:24)

1: TOF MS ES+
2.07e+006

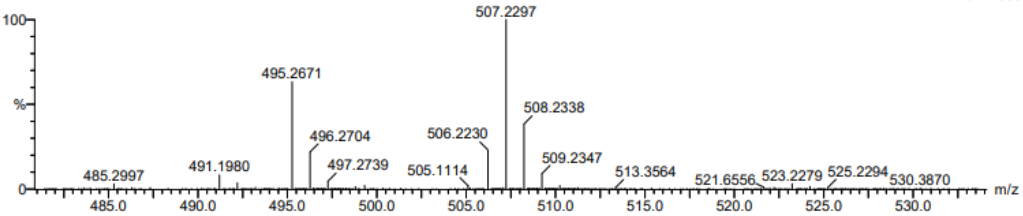

Minimum:				-5.5			
Maximum:		1000.0	1000.0	1000.0			
Mass	Calc. Mass	mDa	PPM	DBE	i-FIT	i-FIT (Norm)	Formula
507.2297	507.2297	0.0	0.0	23.5	610.1	0.0	C33 H27 N6

Elemental Composition Report

Page 1

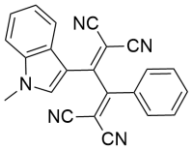

Single Mass Analysis

Tolerance = 1000.0 PPM / DBE: min = -5.5, max = 1000.0
Element prediction: Off
Number of isotope peaks used for i-FIT = 3

Monoisotopic Mass, Odd and Even Electron Ions
1 formula(e) evaluated with 1 results within limits (all results (up to 1000) for each mass)
Elements Used:
C: 23-23 H: 13-14 N: 5-5

Cagatay Dengiz
32149_20210326_04-02 3 (0.138) Cm (1:6)

1: TOF MS ES+
2.23e+004

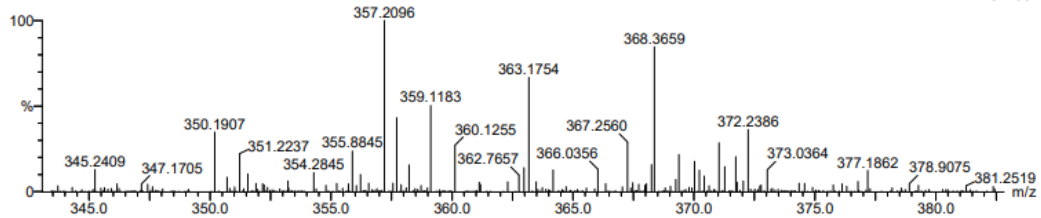

Minimum:				-5.5			
Maximum:		1000.0	1000.0	1000.0			
Mass	Calc. Mass	mDa	PPM	DBE	i-FIT	i-FIT (Norm)	Formula
359.1183	359.1171	1.2	3.3	20.0	155.4	0.0	C23 H13 N5

Elemental Composition Report

Page 1

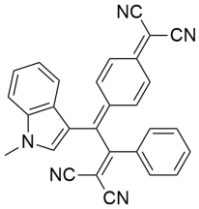

Single Mass Analysis

Tolerance = 1000.0 PPM / DBE: min = -5.5, max = 1000.0
Element prediction: Off
Number of isotope peaks used for i-FIT = 3

Monoisotopic Mass, Even Electron Ions
1 formula(e) evaluated with 1 results within limits (all results (up to 1000) for each mass)
Elements Used:
C: 29-29 H: 17-18 N: 5-5

Cagatay Dengiz
32149_20210326_05-02 16 (0.639) Cm (1:16)

1: TOF MS ES+
1.34e+004

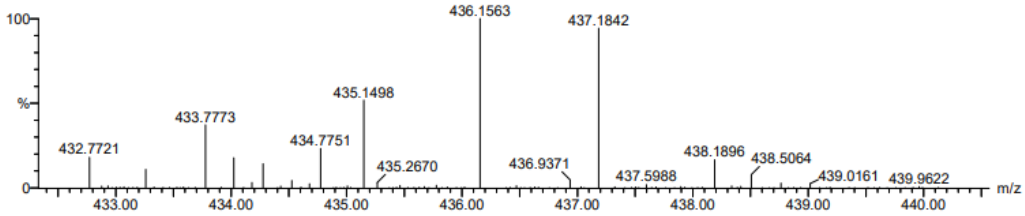

Minimum:				-5.5			
Maximum:		1000.0	1000.0	1000.0			
Mass	Calc. Mass	mDa	PPM	DBE	i-FIT	i-FIT (Norm)	Formula
436.1563	436.1562	0.1	0.2	23.5	244.6	0.0	C29 H18 N5

Elemental Composition Report

Page 1

Single Mass Analysis

Tolerance = 1000.0 PPM / DBE: min = -5.5, max = 1000.0
Element prediction: Off
Number of isotope peaks used for i-FIT = 3

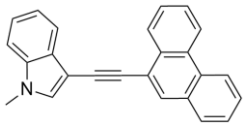

Monoisotopic Mass, Odd and Even Electron Ions
1 formula(e) evaluated with 1 results within limits (all results (up to 1000) for each mass)
Elements Used:
C: 25-25 H: 17-18 N: 1-1

Cagatay Dengiz
32149_20210326_15-02 7 (0.294) Cm (1:10)

1: TOF MS ES+
2.70e+005

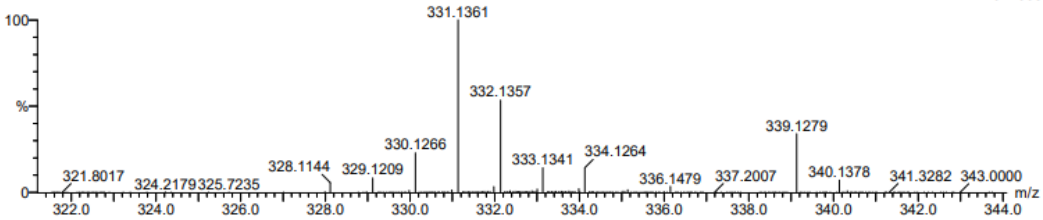

Minimum:				-5.5			
Maximum:		1000.0	1000.0	1000.0			
Mass	Calc. Mass	mDa	PPM	DBE	i-FIT	i-FIT (Norm)	Formula
331.1361	331.1361	0.0	0.0	18.0	649.0	0.0	C25 H17 N

Elemental Composition Report

Page 1

Single Mass Analysis

Tolerance = 1000.0 PPM / DBE: min = -5.5, max = 1000.0
Element prediction: Off
Number of isotope peaks used for i-FIT = 3

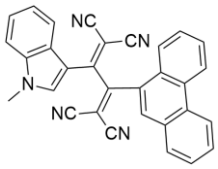

Monoisotopic Mass, Odd and Even Electron Ions
1 formula(e) evaluated with 1 results within limits (all results (up to 1000) for each mass)
Elements Used:
C: 31-31 H: 17-18 N: 5-5

Cagatay Dengiz
32149_20210326_16-03 25 (0.965) Cm (7:25)

1: TOF MS ES+
9.76e+004

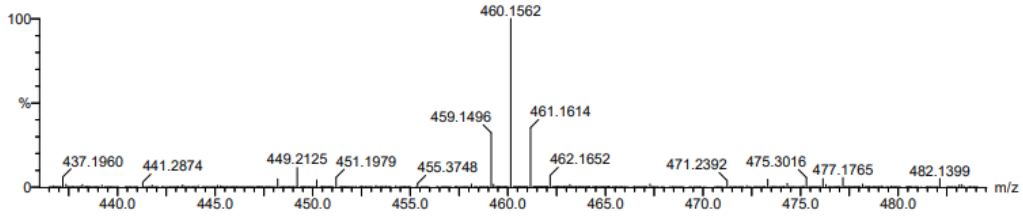

Minimum:				-5.5			
Maximum:		1000.0	1000.0	1000.0			
Mass	Calc. Mass	mDa	PPM	DBE	i-FIT	i-FIT (Norm)	Formula
460.1562	460.1562	0.0	0.0	25.5	479.0	0.0	C31 H18 N5

Elemental Composition Report

Page 1

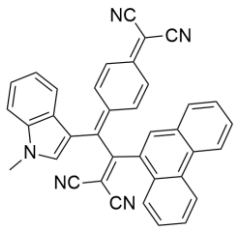

Single Mass Analysis

Tolerance = 1000.0 PPM / DBE: min = -5.5, max = 1000.0
Element prediction: Off
Number of isotope peaks used for i-FIT = 3

Monoisotopic Mass, Odd and Even Electron Ions
1 formula(e) evaluated with 1 results within limits (all results (up to 1000) for each mass)
Elements Used:
C: 37-37 H: 21-22 N: 5-5

Cagatay Dengiz
32149_20210326_17-01 21 (0.829) Cm (1:25)

1: TOF MS ES+
2.26e+005

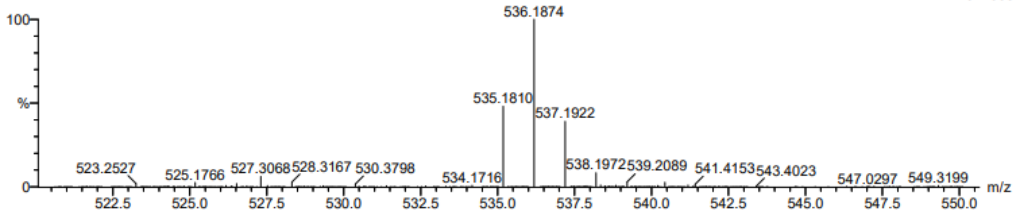

Minimum:				-5.5			
Maximum:		1000.0	1000.0	1000.0			
Mass	Calc. Mass	mDa	PPM	DBE	i-FIT	i-FIT (Norm)	Formula
536.1874	536.1875	-0.1	-0.2	29.5	457.7	0.0	C37 H22 N5

Elemental Composition Report

Page 1

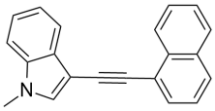

Single Mass Analysis

Tolerance = 1000.0 PPM / DBE: min = -5.5, max = 1000.0
Element prediction: Off
Number of isotope peaks used for i-FIT = 3

Monoisotopic Mass, Odd and Even Electron Ions
1 formula(e) evaluated with 1 results within limits (all results (up to 1000) for each mass)
Elements Used:
C: 21-21 H: 15-16 N: 1-1

Cagatay Dengiz
32149_20210326_09-03 5 (0.206) Cm (1:13)

1: TOF MS ES+
9.33e+005

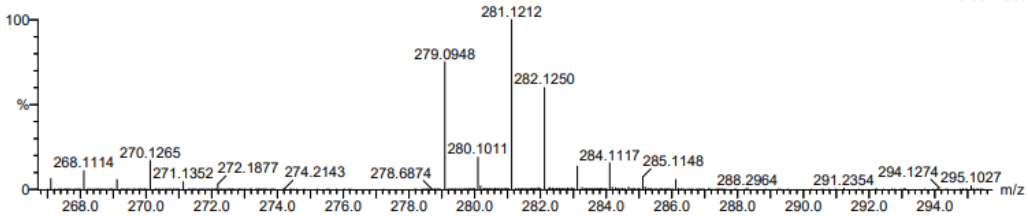

Minimum:				-5.5			
Maximum:		1000.0	1000.0	1000.0			
Mass	Calc. Mass	mDa	PPM	DBE	i-FIT	i-FIT (Norm)	Formula
281.1212	281.1204	0.8	2.8	15.0	788.4	0.0	C21 H15 N

Elemental Composition Report

Page 1

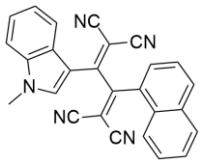

Single Mass Analysis

Tolerance = 1000.0 PPM / DBE: min = -5.5, max = 1000.0
Element prediction: Off
Number of isotope peaks used for i-FIT = 3

Monoisotopic Mass, Odd and Even Electron Ions
1 formula(e) evaluated with 1 results within limits (all results (up to 1000) for each mass)
Elements Used:
C: 27-27 H: 15-16 N: 5-5

Cagatay Dengiz
32149_20210326_10-03 8 (0.328) Cm (1:12)

1: TOF MS ES+
3.91e+004

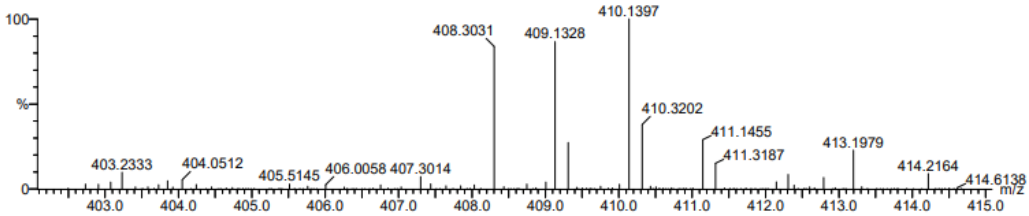

Minimum:				-5.5			
Maximum:		1000.0	1000.0	1000.0			
Mass	Calc. Mass	mDa	PPM	DBE	i-FIT	i-FIT (Norm)	Formula
409.1328	409.1327	0.1	0.2	23.0	344.7	0.0	C27 H15 N5

Elemental Composition Report

Page 1

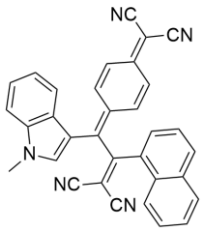

Single Mass Analysis

Tolerance = 1000.0 PPM / DBE: min = -5.5, max = 1000.0
Element prediction: Off
Number of isotope peaks used for i-FIT = 3

Monoisotopic Mass, Odd and Even Electron Ions
1 formula(e) evaluated with 1 results within limits (all results (up to 1000) for each mass)
Elements Used:
C: 33-33 H: 19-20 N: 5-5

Cagatay Dengiz
32149_20210326_11-02 4 (0.172) Cm (1:12)

1: TOF MS ES+
1.60e+005

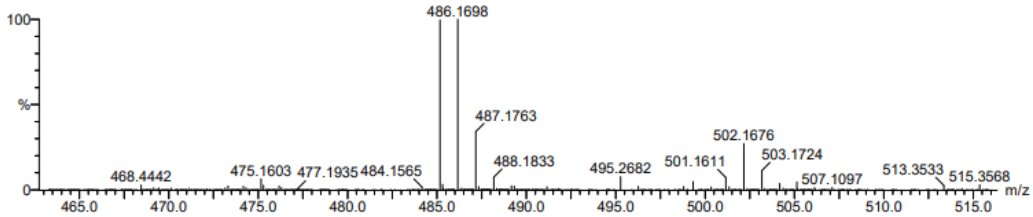

Minimum:				-5.5			
Maximum:		1000.0	1000.0	1000.0			
Mass	Calc. Mass	mDa	PPM	DBE	i-FIT	i-FIT (Norm)	Formula
485.1639	485.1640	-0.1	-0.2	27.0	460.1	0.0	C33 H19 N5

Elemental Composition Report **Page 1**

Single Mass Analysis
Tolerance = 1000.0 PPM / DBE: min = -5.5, max = 1000.0
Element prediction: Off
Number of isotope peaks used for i-FIT = 3

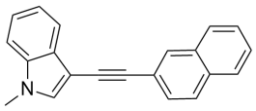

Monoisotopic Mass, Odd and Even Electron Ions
1 formula(e) evaluated with 1 results within limits (all results (up to 1000) for each mass)
Elements Used:
C: 21-21 H: 15-16 N: 1-1
Cagatay Dengiz
32149_20210326_12-03 7 (0.294) Cm (5:20)

1: TOF MS ES+
6.10e+005

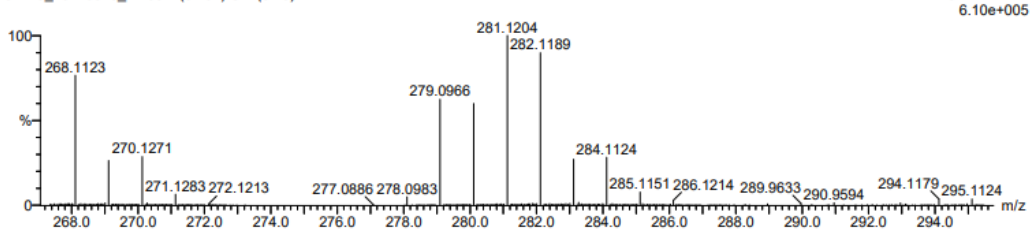

Minimum:				-5.5			
Maximum:		1000.0	1000.0	1000.0			
Mass	Calc. Mass	mDa	PPM	DBE	i-FIT	i-FIT (Norm)	Formula
281.1204	281.1204	0.0	0.0	15.0	782.1	0.0	C21 H15 N

Elemental Composition Report **Page 1**

Single Mass Analysis
Tolerance = 1000.0 PPM / DBE: min = -5.5, max = 1000.0
Element prediction: Off
Number of isotope peaks used for i-FIT = 3

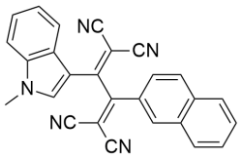

Monoisotopic Mass, Odd and Even Electron Ions
1 formula(e) evaluated with 1 results within limits (all results (up to 1000) for each mass)
Elements Used:
C: 27-27 H: 15-16 N: 5-5
Cagatay Dengiz
32149_20210326_13-02 4 (0.172) Cm (1:13)

1: TOF MS ES+
9.30e+004

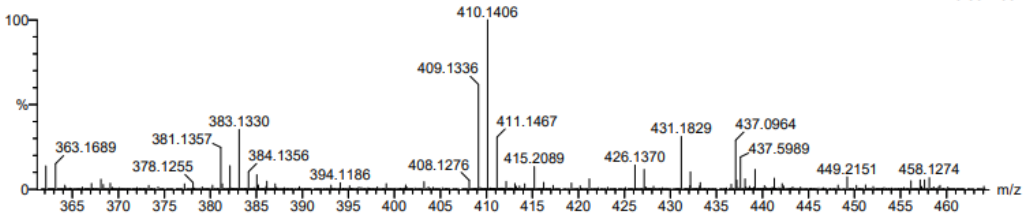

Minimum:				-5.5			
Maximum:		1000.0	1000.0	1000.0			
Mass	Calc. Mass	mDa	PPM	DBE	i-FIT	i-FIT (Norm)	Formula
410.1406	410.1406	0.0	0.0	22.5	469.3	0.0	C27 H16 N5

Elemental Composition Report

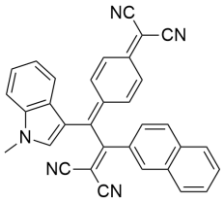

Single Mass Analysis

Tolerance = 1000.0 PPM / DBE: min = -5.5, max = 1000.0
Element prediction: Off
Number of isotope peaks used for i-FIT = 3

Monoisotopic Mass, Even Electron Ions
1 formula(e) evaluated with 1 results within limits (all results (up to 1000) for each mass)
Elements Used:
C: 33-33 H: 19-20 N: 5-5

Cagatay Dengiz
32149_20210326_14-03 4 (0.172) Cm (3:17)

1: TOF MS ES+
3.09e+004

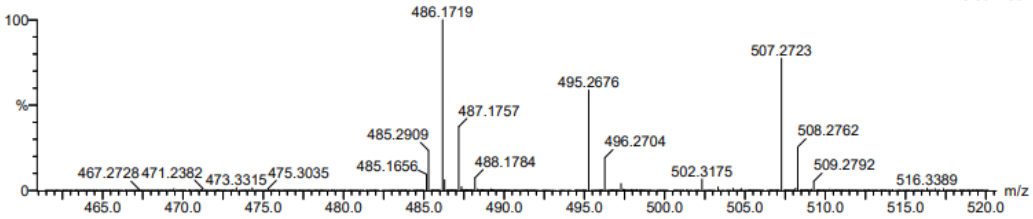

Minimum:				-5.5			
Maximum:		1000.0	1000.0	1000.0			
Mass	Calc. Mass	mDa	PPM	DBE	i-FIT	i-FIT (Norm)	Formula
486.1719	486.1719	0.0	0.0	26.5	368.1	0.0	C33 H20 N5